UNIVERSITY OF OKLAHOMA

GRADUATE COLLEGE

DESIGN AND SYNTHESES OF SUPRAMOLECULAR SCAFFOLDS FOR CATALYSIS AND AQUEOUS MOLECULAR RECOGNITION

A DISSERTATION

SUBMITTED TO THE GRADUATE FACULTY

in partial fulfillment of the requirements for the

Degree of

DOCTOR OF PHILOSOPHY

By

SHEKAR MEKALA
Norman, Oklahoma
2012

DESIGN AND SYNTHESES OF SUPRAMOLECULAR SCAFFOLDS FOR CATALYSIS AND AQUEOUS MOLECULAR RECOGNITION

A DISSERTATION APPROVED FOR THE
DEPARTMENT OF CHEMISTRY AND BIOCHEMISTRY

BY

_____
Dr. Ronald L. Halterman, Chair

_____
Dr. Kenneth M. Nicholas

_____
Dr. Daniel T. Glatzhofer

_____
Dr. Paul F. Cook

_____
Dr. Lloyd A. Bumm

ACKNOWLEDGEMENTS

I would like to thank my graduate advisory committee members for their advice and patience through out my graduate study at the University of Oklahoma. I would like to thank my major Professor and mentor Dr. Ronald L. Halterman for his mentorship, constant financial support, persistent and patient guidance. I would also thank Dr. Steven Foster for his help in Mass Spectrometry Instrument. I would like to thank the present and past members of Dr.Halterman research group, from whom I learned many things. I would like to thank Dr. Hisanori Ueki and Dr. Jason Moore for their valuable guidance and encouragement at the beginning of my graduate study. I would like to thank my parents Chennamma M. Yadav and Anjaiah M. Yadav, and my brothers and sisters for their constant help and support along this journey. Finally I would like to thank all of my friends at the University of Oklahoma for their support and encouragement.

TABLE OF CONTENTS

LIST OF TABLES

LIST OF SCHEMES

LIST OF FIGURES

ABSTRACT

Organic supramolecular systems can be considered as one of the most advanced tools of physical organic chemistry for catalysis. The main aim of the supramolecular model systems for the study of catalytic processes is to explain the observed rate enhancement in terms of reactivity and selectivity of various functional groups. In the last decade, the use of small molecular catalysts become less useful due to their ability in terms of selectivity, reactivity and solubility. Therefore, the use of supramolecular catalysts has become more attractive in the field of organic synthesis and catalysis, especially to perform organic transformations in aqueous media. Since the discovery of picket fence porphyrins by James Collman, the applicability of these molecules in the field of organometallic chemistry and supramolecular chemisty has a high impact in terms of selectivity, reactivity. In this dissertation, we have utilized the Collman's 'picket fense' porphyrin concept to design and synthesize *meso*-tetra(o-alkyl/arylaminphenyl)porphyrins as supramolecualr scaffolds for the dimerization of high molecular weight aldehydes into vicinally functionalized 1,2-diols (pinacols). These vicinal 1,2-diols could also be further derivatized into fuels and value added chemicals. For this process, we have successfully synthesized desired porphyrin scaffolds based on 'Dynamic Exchange Reactions' and investigated their thermal stability to design supramolecular catalyst, but failed to utilize these scaffolds for catalyst design due to their low thermal stability. Therefore, for effective, stable and water soluble catalyst design, we have chosen to take the advantage of stable and preorganized calix[4]arene based scaffolding for the non-

covalent supramolecular catalyst design to perform the pinacol reactions to dimerize cellulose derived oxygenated feed-stocks such as 5-hydroxymethylfurfurals (HMF), into 1,2-diols in aqueous media. To perform this chemical transformations, initially we have successfully synthesized several water soluble calix[4]arene derivatives and studied the molecular recognition of these calix[4]arenes with various guest molecules in aqueous media for non-covalent catalyst design. Efforts are under way for the water-soluble, non-covalent supramolecular catalyst design for the effective pinacol coupling reactions in aqueous media for biofuel applications.

Chapter 1

Supramolecular Catalysis and Molecular Self-Assembly

1.1 Introduction

Today, more than three quarters of world energy is provided by fossil fuels such as coal, oil, and natural gases. Unfortunately, the growing demand for fossil fuel resources comes at a time of diminishing reserves of these non-renewable resources, such that the worldwide reserves of oil are sufficient to supply energy and chemicals for only about another 40 years, causing widening concerns about rising oil prices.[1] Therefore, the only sustainable, renewable source of energy and organic carbon for our industrial society is 'biomass'. Moreover, the production of energy from biomass has the potential to generate lower greenhouse gas emissions compared to the fossil fuels, because the CO_2 released during energy conversion is consumed during subsequent biomass re-growth. It has been reported by the United States department of energy (US DOE) and the US department of agriculture that, by the year 2030, 20% of the transportation fuel and 25% of chemicals will be produced from biomass. While corn-to-ethanol and oil-to-biodiesel have limited capacity to fulfill these goals, the evolution of a broad range of conversion technologies, including enzymatic, catalytic and thermochemical processes for conversion of more abundant ligno-cellulosic biomass into fuels and materials will be critical.

In the recent decade, most of the industrial processes are based on catalytic reactions. Catalysts are utilized in diverse fields ranging from large-scale processes such as petroleum refining, hydro-treatment, production of

ammonia *etc,* and small-scale processes such as synthesis of drugs, and chemical reagents. There fore, catalysis is a key element in the development of technological processes. The development and implementation of new, highly efficient and selective catalysts will stimulate production and contribute to the solution of global problems such as rational exploitation of natural resources and environmental protection. There have been numerous homogeneous and heterogeneous catalysts known up to date, but these catalysts do not always possess high selectivity and reactivity toward some functional groups such as reactants with heteroatoms etc. There fore, some of the catalysts can only be used in mild conditions in order to avoid side reactions.[2]

Supramolecular systems can be considered as new tools of modern physical organic chemistry. 'Supramolecular chemistry' a term introduced by Jean-Marie Lehn is 'Chemistry Beyond the Molecule', that is the chemistry of molecular assemblies using noncovalent bonds. This is the chemistry where molecules are able to self-assemble, self-organize, and self-control into systems and the components are often analogues to biological molecules. It is a highly interdisciplinary field of science covering the chemical, physical, and biological features of chemical species held together and organized by means of intermolecular binding interactions such an hydrogen bonding, electron pair donor-acceptor, cation-π and π-π interactions, electrostatic, and van der waal interactions. Supramolecular chemistry is at the heart of the development of chemistry of complex systems, molecular devices, ensembles and

nanochemistry.[3] Study of catalytic processes using supramolecular model systems aims to explain the observed rate enhancement in terms of structure and mechanism. Catalysis is a longstanding proposed application of supramolecular chemistry and the production of supramolecular systems capable of mimicking the catalytic ability of natural enzymes is one of the ultimate goals of self-assembly research.

In this dissertation, the projects we deal mainly with the 'design and synthesis of supramolecular scaffolds based on *tetra*-(*o*-aminophenyl)porphyrins and calix[4]arenes for catalytic pinacol coupling reactions in water' for effective dimerization of bio-feed stocks into value added chemicals and fuels. This chapter (Chapter one) deals with literature background on a) supramolecular chemistry of metallo porphyrins, molecular recognition, binding properties and catalytic systems. b) Supramolecular catalysis and/or homo/heterodimerization and encapsulation studies of calix[4]arenes in apolar and polar solvents. Chapter two deals with various pinacol-coupling reactions for dimerization of aldehydes in various catalytic conditions ranging from simple asymmetric synthesis to biofuel applications. Chapter three focuses on a) 'dynamic combinatorial chemistry' and exchange reactions focusing on imine exchange reactions, b) synthesis of *meso*-*tetra*-(alkyl/arylamiophenyl)porphyrins and the imine exchange reactions, c) synthesis of *meso*-tetra(pivalyl/benzyl)aminophenyl porphyrins via Schiff base formation and reductive amination. Chapter four mainly deals with a) the

thermal atropisomerization of the substituted *meso-tetra*-(alkyl/arylaminophenyl) porphyrins by VT-NMR (Variable Temperature NMR) spectroscopy, while discussing various methods to calculate energy barriers for thermal atropisomerization in substituted phenylporphyrins, b) methods to control atropisomerization. In the chapter five, the research includes the design and synthesis of various calix[4]arene derivatives as supramolecular scaffolds for encapsulation studies in aqueous media, in which a) literature background on various types of Calix[4]arene based host-guest complexes in aqueous media, b) host-guest complexation studies of calix[4]arene derivatives in water, c) finally, the encapsulation studies of highly water soluble calix[4]arene derivatives with various guest molecules.

1.2 Historical Background of Supramolecular Catalysis of Metalloporphyrins

Metalloporphyrins are remarkable precursors in supramolecular chemistry and the rapid development of this chemistry led to various assemblies possessing of various architectures and properties such as photo, electro and catalytic properties. Metalloporphyrins are one of the cornerstones on which the existence of life is based, and major biochemical, enzymatic, and photochemical functions depend on the special properties of a tetrapyrrolic macrocycle. However, metalloporphyrins are the only molecules having the key elements that require assembly with other elements to form the

supramolecular structure, which is the working device. The rapid development of this new area of chemistry has promoted the understanding of the concepts of design and strategies of self-assembly of structures based on intermolecular interactions to result in natural and synthetic supramolecular complexes of metalloporphyrins.

Synthetic metalloporphyrin complexes are often used as analogues of natural systems found in photosynthesis, oxygen carriers and catalysis.[4] An application of increasing importance is the use of metalloporphyrins as receptors, exploiting their ability to selectively form complexes which can sharply change the spectral properties.[5]

A significant early breakthrough of synthetic porphyrin **1** (**Scheme 1.1**) chemistry would be attributed to Rothemund's synthesis of *meso*-tetraphenyl porphyrin (TPP) in 1939,[6] by the condensation reaction of benzaldehyde with pyrrole in the presence of pyridine in a sealed vessel at 145-155 ^{o}C over 2 days. However, these reaction conditions were harsh and the yields of the TPP products were significantly low ranging from 4-5% only.

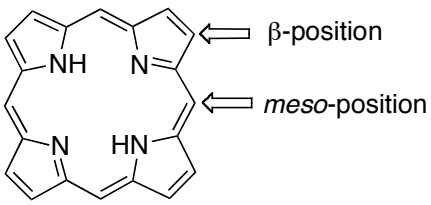

1

Scheme 1.1 Porphyrin **1**

In 1967, Alder and his co-workers reported a more simplified and new reaction method (**scheme 1.2**) which was the 'improved Rothemund's method' by the reaction benzaldehyde **2** and pyrrole **3** in refluxing propionic acid for 30 minutes to give desired porphyrin **4** (TPP) in 20% yield[7]. The Alder-Logo method thus presented has two significant limitations a) harsh reaction conditions limiting the scope of substituents and b) lack of any rational access to porphyrins bearing two or more distinct *meso* substituents. Such methods were insufficient to unlock the tremendous promise of *meso*-substituted porphyrin for use as building blocks in the material chemistry and as tailorable surrogates for naturally occurring porphyrins.

In the early 1980s, Jonathan Lindsey developed a two-step, one flask reaction strategy to overcome the first limitation of the prior method (Alder-Longo method). The approach entailed a) acid-catalyzed condensation of aldehyde **2** and pyrrole **3** to form a porphyrinogen and b) addition of an oxidant to carryout the oxidative dehydrogenation of porphyrinogen to give the desired porphyrin **4** (**scheme 1.3**).[8] Mild conditions identified for the entire process that include reaction at room temperature in a chlorinated solvent containing an acid such as trifluoroaceticacid (TFA) or $BF_3.O(Et)_2$, use of an organic soluble oxidant such as DDQ or *p*-chloranil and dilute concentrations of pyrrole **3** and aldehyde **2** to overcome the olegomerizatin to give cyclic product a porphyrinogen.

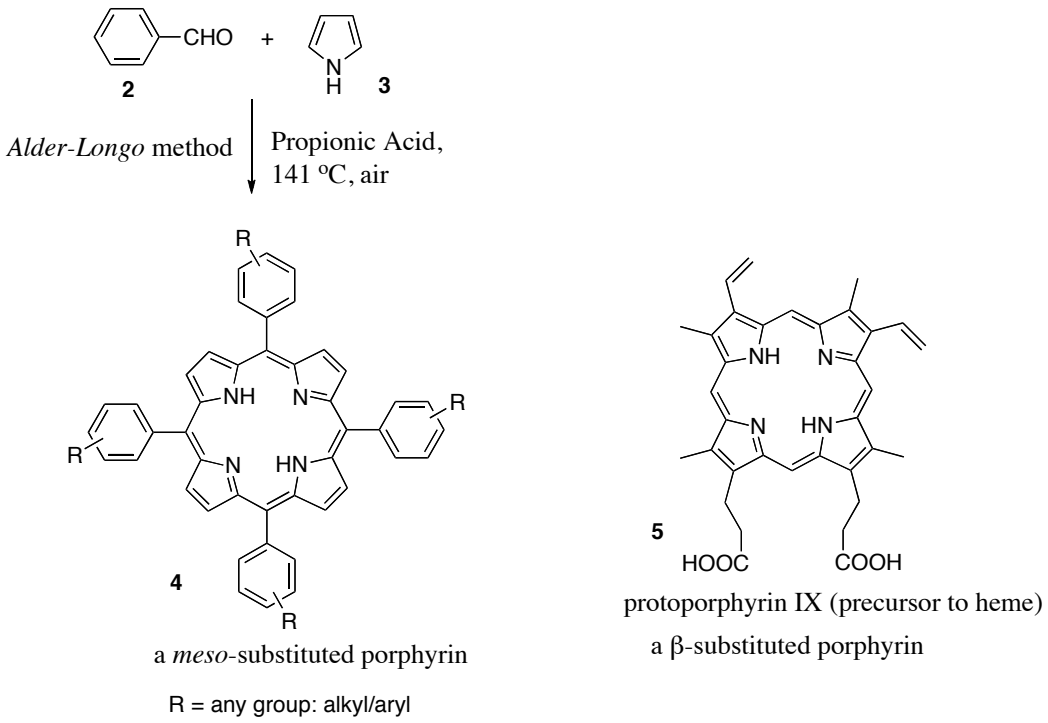

Scheme 1.2 Alder Longo method: a synthetic porphyrin with four identical *meso*-substituents **4**, compared with a naturally occurring β-substituted porphyrin **5**.

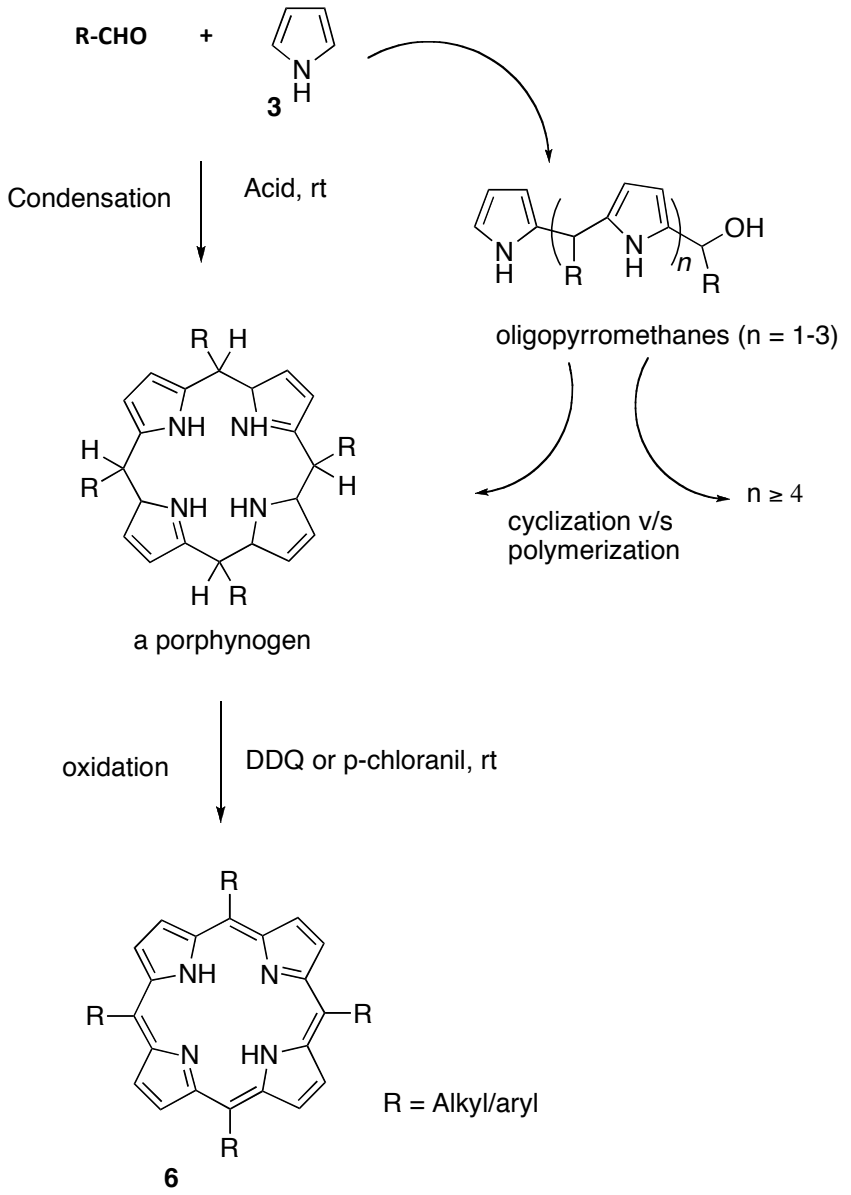

Scheme 1.3 Lindsey Method of Synthesis of Porphyrins **6**

1.2.1 Lindsey's ABCD-porphyrins

In the late 1980s, Lindsey's group embarked on a program to overcome the second limitation of the Alder-Longo method, the inability to prepare unsymmetrical *meso*-substituted porphyrins. Their initial goals focused on obtaining the desired target compounds without reliance on statistical

reactions by using mild conditions and broad scope. But over time, their objectives grew to encompass processes that could be implemented with limited or without column chromatography. Directed routes for constructing porphyrins bearing up to four distinct *meso*-substituents typically synthesized in stepwise manner starting with substituted dipyrromethanes (**7** and **8**) as precursors, then dimerize or couple these substituted fragments into desired *meso*-substituted porphyrinogens **9** followed by the oxidation to give desired tetra-*meso*-substituted porphyrins **10** (**Scheme 1.4**) and this is the latest and widely used methods in porphyrin synthesis.[9]

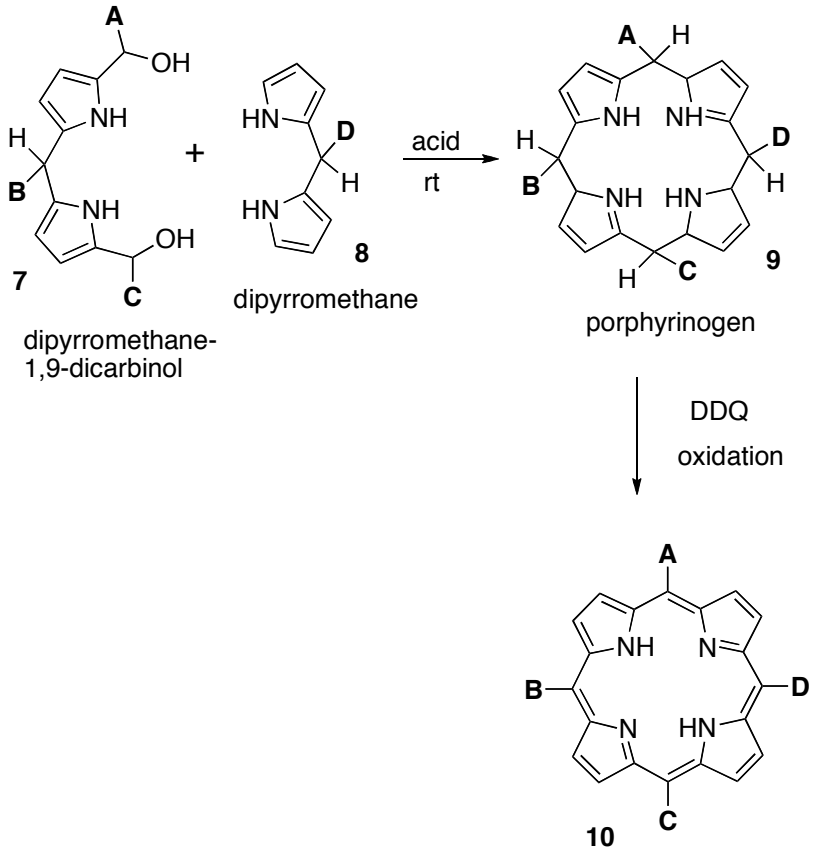

Scheme 1.4 Lindsey's stepwise method for the synthesis of ABCD-porphyrins

1.2.2 Collman's picket fence porphyrins

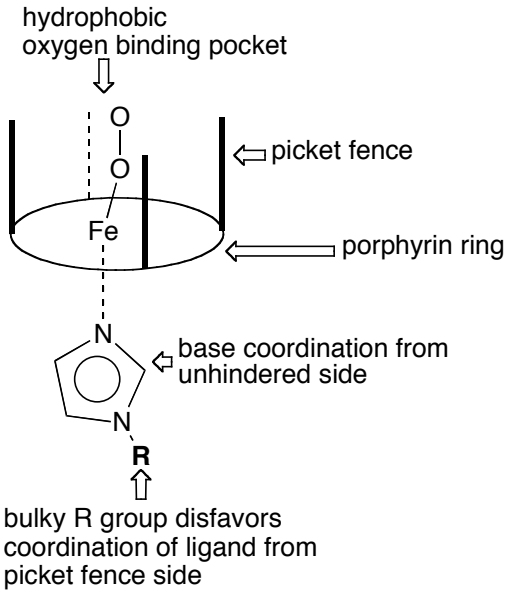

Scheme 1.5 Collman's picket fence porphyrin concept

The concept of picket fence porphyrins was developed by James Collman,[10] in order to favor five coordinations and simultaneously inhibit bimolecular reactions. The concept of these porphyrins was to have great steric bulk on one side of the plane of porphyrin and leaving the other side of the porphyrin unhindered. Employing suitable bulky ligand such as *N*-alkyl imidazole would allow the coordination of the imidazole on the unhindered side of the porphyrin while restraining the bulkier base on the hindered side of the porphyrin which is due to the steric repulsion between substituents on the picket fence and the bulky substituent **R** (**Scheme 1.5**) on the imidazole ligand. Collman developed this concept 'picket fence porphyrin' in order to favor five coordinations and simultaneously inhibit bimolecular reactions,[11] such as synthetic models for oxygen binding hemoproteins. In which the dioxygen can

coordinate to the metal center in the porphyrin only from hydrophobic, picket fence side, but not from the bottom or ligand (imidazole) side of the porphyrin.

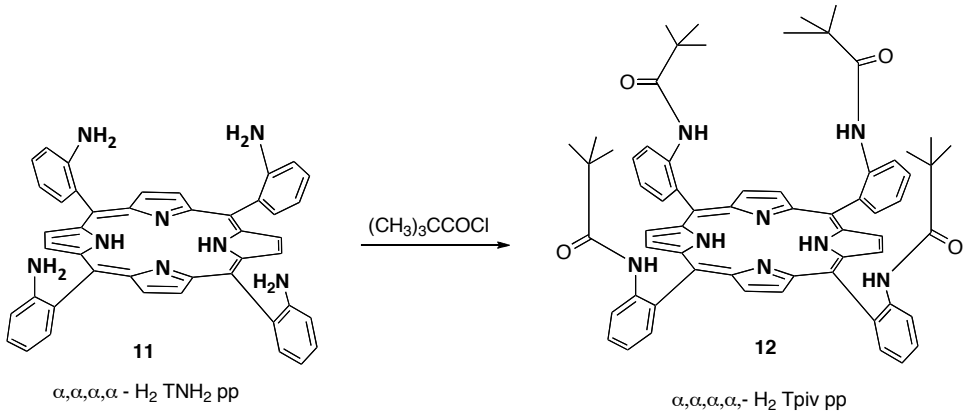

Scheme 1.6 Collman's Picket fence Porphyrin: *meso-tetra*(*o*-pivaloylaminophenyl)porphyrin **12**

By separating the α,α,α,α-atropisomer of *meso-tetra*(*o*-aminophenyl)porphyrin **11** from the mixture of atropisomers (in chapter 3), Collman et al. have synthesized the *meso-tetra*(α,α,α,α-*o*-pivalamidophenyl)porphyrin **12** by treating **11** with pivaloyl chloride (**Scheme 1.6**). This was the first picket-fence porphyrin and has the phenyl group oriented nearly normal to the porphyrin plane, projecting the ortho substituents above or below the plane. The α,α,α,α-atropisomer **12** can be seen to represent the essence of a 'picket-fence porphyrin' based on the pivolyl substituents, which are above the plane of the porphyrin. These porphyrin derivatives (picket-fence porphyrin) have wide range of applications in molecular

recognition and catalysis. This dissertation is mainly of the concept of picket-fence porphyrins. Hence, I would use this term throughout the dissertation.

1.3 Molecular Recognition of Metalloporphyrins

1.3.1. Substrate binding and molecualr recognition

Depending on the porphyrin structure, porphyrin possesses the ability to bind a large variety of substrates. There are large number of supramolecualr architectures based on porphyrin-substrate complexes are used for molecular recognition purposes, as receptors and sensors. The ability of the porphyrins to bind various substrates strongly, these can be used as catalysis in supramolecular approach and also numerous models of enzymes in which the key skeleton is the porphyrin-substrate complex. Simple axial complexes of metalloporphyrins exhibiting one coordination site can be viewed as classical coordination compounds and have been investigated for many years. Supramolecular derivatives, which can be classified as 'complexes with two or more co-ordination sites', were synthesized mainly during the last decade. In the supramolecular architectures of porphyrins, additional interaction sites induce not only an increase of binding constants but also selectivity toward a substrate, therefore porphyrins with multiple binding sites exhibit excellent molecular recognition.

Porphyrins having bulky peripheral substituents on one porphyrin face are called picket-fence porphyrins (**Scheme 1.5**)[12], and these derivatives can be considered as first supramolecualr complexes. The additional binding factors for these compounds are CH-π interactions of aromatic ligands with porphyrin

substituents. The pyridine ligand can bind with zinc metal with non-covalently as well as with C-H groups of the ^{t}Butyl groups for additional CH-π interactions and is the driving force for the ligand to approach to the metal center from top side of the plane of the porphyrin in non polar solvents. (**Scheme 1.7**).[13]

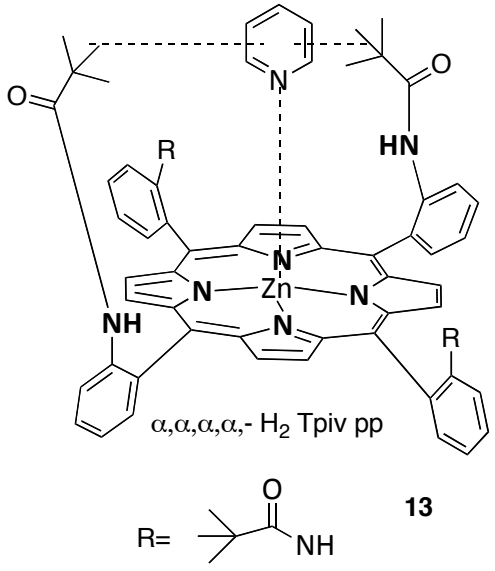

Scheme 1.7 Picket fence porphyrin (α,α,α,α,- H_2 Tpiv pp) **12** binding with pyridine (Host-Guest complex, **13**)

Strapped porphyrins are the systems where two opposite substituents are connected by a bridge defining a 'roof' above the plane of the macrocycle with an intramolecular cavity under this 'roof' and these porphyrins are excellent binders for the molecules able to fit this cavity (**Scheme 1.8**)[14]

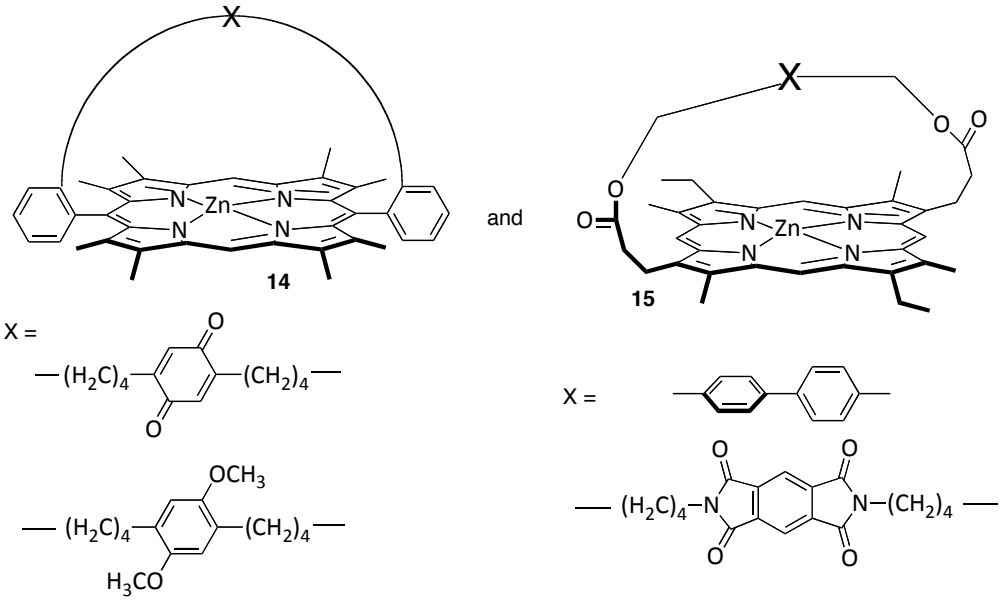

Scheme 1.8 Strapped Porphyrin models (**14** and **15**)

The strapped porphyrin **16** with diazaphenanthrene as a roof forms very stable complexes with imidazole derivatives. The size of these imidazole molecules corresponds perfectly to the size of the host molecule cavity and binding occurs through two sites, that is, via the coordination with Zinc atom and the hydrogen bonding with nitrogen atoms of the imine functionality in the strapped porphyrin moiety (**Scheme 1.9**).[15]

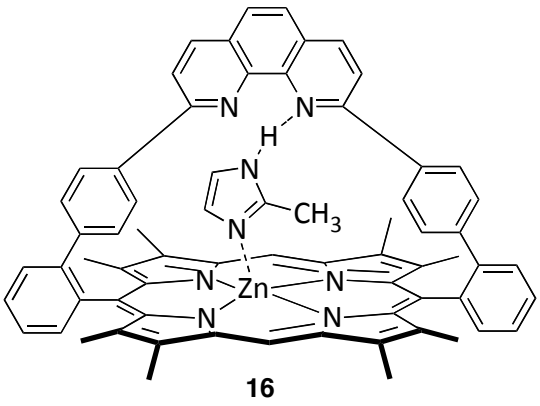

Scheme 1.9 Strapped porphyrin **16** with imidazole derivative as a guest

The main advantage of the above system is having multiple binding sites (two) on the porphyrin as well as on the guest molecule (imidazole derivative), that eventually contribute the increased association constant by two or more orders of magnitude compared with the simple tetraphenylporphyrins.

The another interesting area of porphyrin based supramolecular chemistry is the construction or merging of porphyrins with other type of supramolecules such as calix[4]arenes (**Scheme 1.10**)[16]. These combined supramolecular blocks possesses different topologies as well as electronic properties allows to create molecular receptors. These porphyrin-calixarene based supramolecules can be created by connecting axially located calixarene moieties with porphyrin macrocycles by the aid of flexible functionalities such as methylene bridges. The advantage of these molecules is the length of the linker. By changing the linker, one can control the selectivity of the guest molecule by changing the guest size. The well-defined cavity of the molecule with four bridges (**Scheme 1.10, 18**), has the advantage for the small molecule binding (pyridine and N-methylimidazole etc), while the molecule with two bridges (**Scheme 1.10, 17**) has the advantage for binding of large molecules (4-phenylpyridine). Therefore, the important advantage of this supramolecule is the flexibility of the cavity, which can be modified by changing the bridge size.

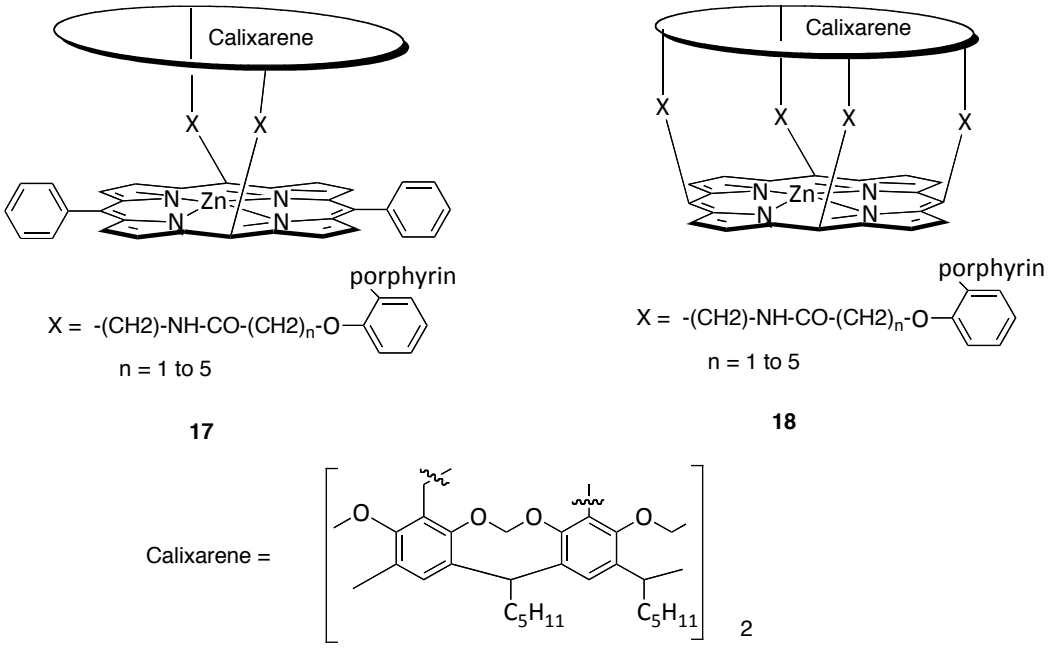

Scheme 1.10 Porphyrin-calixarene (cavitand) complexes **17** and **18**

Another most important area of the Porphyrin based supramolecular architecture is the anion recognition property. Among the various neutral anion receptors reported to date, calix[4]pyrroles appear particularly attractive as a starting point for the design of yet-improved anion selective receptors. They are easy to make, being readily obtained in one step from the acid-catalyzed condensation of pyrrole and acetone, and have been shown to bind various anions in organic media.[17]

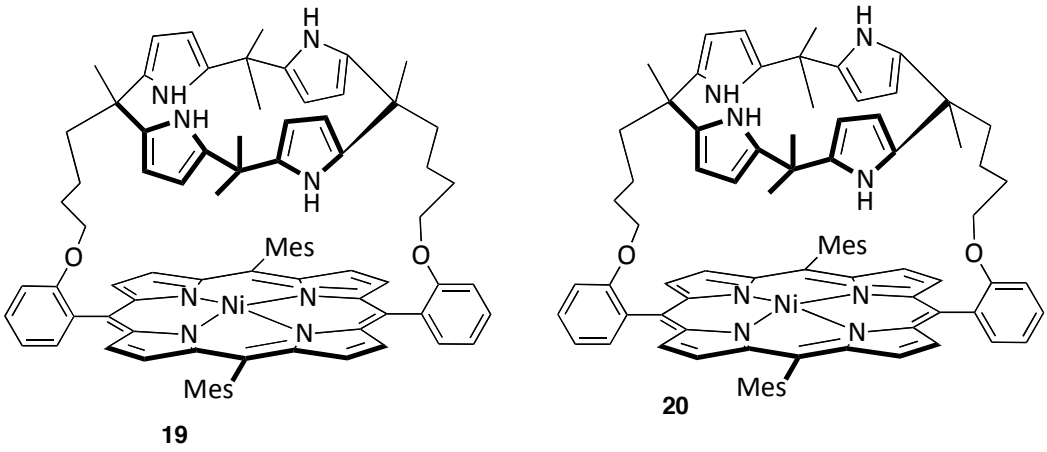

Scheme 1.11 Calixpyrroles **19** and **20**

Since their anion recognition characteristics were first described by Sessler[18] et al. in 1996, various modifications of the calix[4]pyrrole skeleton have been made in an effort to tune the binding characteristics of the parent system.[19] Recently, Lee et al[20] (**scheme 1.10)** have developed a strapped calix[4]pyrrole–metalloporphyrin conjugates as potential hosts for anionic guests. In the synthesis, the condensation unexpectedly resulted in the formation of the two conformational isomers of calix[4]pyrrole-capped porphyrins (**Scheme 1.11**) **19** and **20.** The anion binding studies revealed that only isomer **19** showed strong binding with fluoride anion in organic solvent, and neither isomer showed any appreciable binding with Cl^-, Br^-, and I^-.

1.3.2. Receptor Properties of Metalloporphyrins

1.3.2.1 Metalloporphyrins in chiral recognition

Because of the tunable substituents and rigid skeleton, the metalloporphyrins act as good receptors for selective binding of wide range of substrates. In metalloporphyrin receptors, the strong binding and high selectivity is the result of the combinations of the axial coordination of substrate to a metal cation with additional binding centers at the periphery of the macrocycle. Infinite variety of porphyrin structures and variety of binding elements allow design of receptors for any kind of substrate. The unique properties of the porphyrin chromophore and its ability of complex formation with chiral compounds are also utilized in circular dichroism spectroscopy (CDS) by which the investigation of the absolute configuration of the chiral compounds is made possible (**scheme 1.12**).[21]

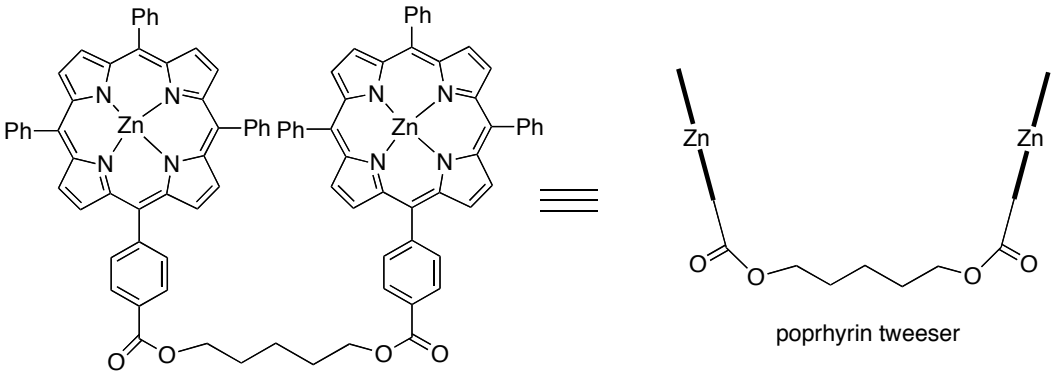

21

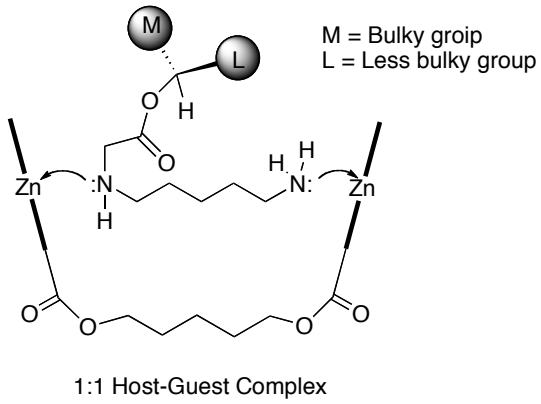

22

Scheme 1.12 porphyrin tweeser **21**, 1:1 H:G complex of the porphyrin tweeser and chiral guest molecule **22**.

1.3.2.2 Metalloporphyrins in anion recognition

In recent years, in the field of molecular recognition, the design and synthesis of increasingly sophisticated molecular receptors for the strong and selective recognition of anionic guests is the topic of great current interest. In 2006, Beer et al.,[22] (**Scheme 1.13**)

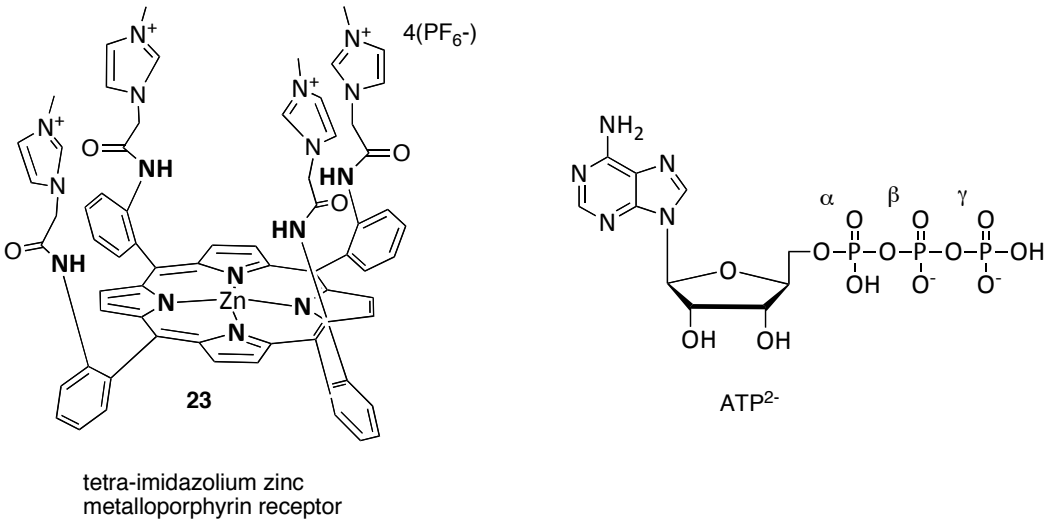

Scheme 1.13 tetra-imidazolium zinc metalloporphyrin receptor **23** and ATP^{2-} as anion.

have reported sulfate selective anion recognition by a novel tetra-imidazolium zinc metalloporphyrin receptor **23**. In which the imidazolium groups have been successfully incorporated into the structure of a 'picket fence' porphyrin molecule to produce a novel tetra-imidazolium zinc metalloporphyrin anion receptor and the results were studied by UV/vis spectroscopic studies and they reveal that the porphyrin receptor is selective for sulfate anions, capable of strongly complexing sulfate in 5% water in DMSO solvent mixture. They have also used cyclic square wave voltametric studies and demonstrated the receptor's ability to sense a variety of anions electrochemically.

In 1997, Burns et al.,[23] (**Scheme 1.14**) have prepared a neutral anion receptors that exhibit selective anion binding and which ultimately lead to the

development of sensors and transport mimics that function in a aqueous environment.

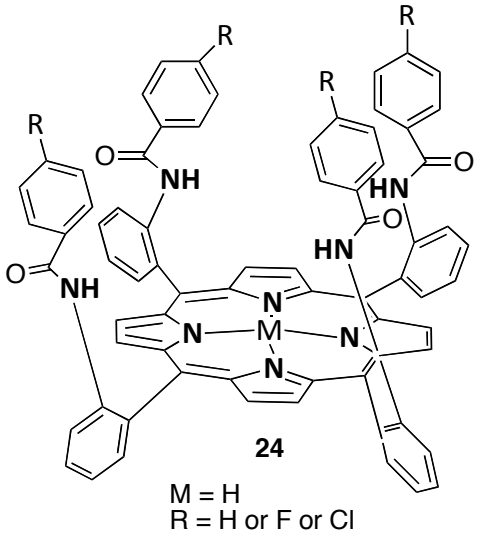

Scheme 1.14 Arylurea porphyrin as an anion receptor **24**.

Porphyrins bearing four arylurea substituents present receptor properties for chloride anion, since the selective binding of anion in a solution of DMSO operates with the binding constant of 105 M^{-1}, and with respect to the binding selectivity toward nitrate and phosphate anions, the binding constants are about 1000 and 280 respectively. Therefore, the design and synthesis of metalloporphyrin based receptors for the recognition of neutral organic molecules in water is an emerging field in the supramolecular chemistry and this concept can be applied for the recognition of biomass derived oxygenated compounds in order to convert them in to value added chemicals and fuels.

1.3.2.3 Catalytic applications of Metalloporphyrins

In recent years, a completely different approach to achieve catalysis using supramolecular strategies have been developed based on the noncovalent interactions. These noncovalent interactions are the main driving force for the rapid formation of bonds in a simple and effective way. Chemists have been employing the reversible interactions (non covalent) to generate the backbones of the supramolecular catalysts by bringing the starting building blocks together. In order to generate or establish a supramolecular assembly for the catalysis, the building blocks must have the desired functional groups for catalysis as well as to bring substrate to the metal center by noncovalent interactions such as hydrogen bonding, π-π interactions, van der walls interactions etc. Moreover, this novel methodology has enabled the synthesis of structurally diverse supramolecualr ligands compared to the use of standard covalent chemistry. Catalysts based on metalloporphyrins are widely used in photochemical processes,[24] polymer chemistry,[25] and the energy conversion[26] etc. Reek, van Leeuwen and coworkers[27] have developed the use of a nitrogen donor groups that binds to Zn(II)-porphyrins non-covalently to construct a library of chiral supramolecualr phosphorous-containing bidentate ligands for asymmetric catalysis (**Scheme 1.14**). In their pioneering work, they have developed a porphyrin based supramolecular catalyst in which the constituent units of the final entity are assembled around the template molecule. The supramolecular catalyst **25** (**Scheme 1.15**) was generated by introducing two pyridine-phosphite units onto a bis-Zn(II)porphyrin template and the preferential binding of the Zn-porphyrin to the pyridine nitrogen over the

phosphorous was the crucial and allowed for generation of the supramolecular catalyst with free phosphite groups that could bind with a transition metal [Rh] for catalytic reactions.

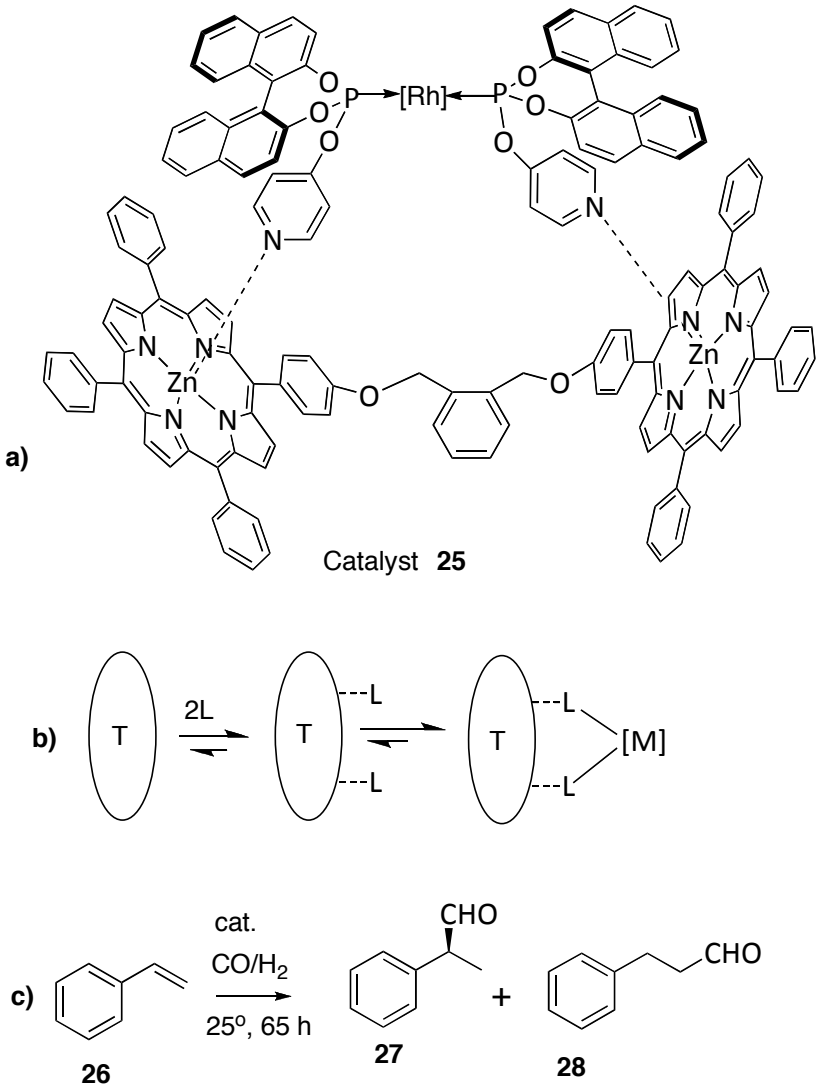

Scheme 1.15 Supramoelcualr catalyst 25. T = Template; a) Transition metal Rh-catalysts formed by self-assembly; b) Schematic representation of self-assembly process: c) Hydroformylation of sturene **26** with supramolecular Rh-catalyst[28].

They have used this catalyst for the study of hydroformylation of 1-octene and styrene. The supramolecular complex showed a slightly lower catalytic activity than that of the complex based on the analogue monodentate ligand, but exhibited much more higher selectivity for the linear products than that of branched products and in terms of enantioselectivity, this catalyst showed a little better selectivity than the monodentate counterpart for the hydroformylation of styrene (33% ee).

In 2010, Fackler et al,[29] have developed a Chiral Ruthenium porphyrin based supramolecular catalyst for hydrogen bond mediated enantio- and diastereoselective epoxidation reactions. A chiral epoxidation catalyst based on a tricyclic octahydro-1H-4,7-methanoisoindol-1-one scaffold (**Scheme 1.16**) was synthesized and in which a hydrogen bonding site and the catalytically active ruthenium center are spatially separated. It was shown that epoxidation reactions in such a supramolecular catalyst occur with high enantio- and regioselectivity because the hydrogen bonds expose the substrate to the ruthenium porphyrin complex with a clear conformational preference. The epoxidation of 3-vinylquinolone **29** proceeded in 71% yield and up to 95% ee.

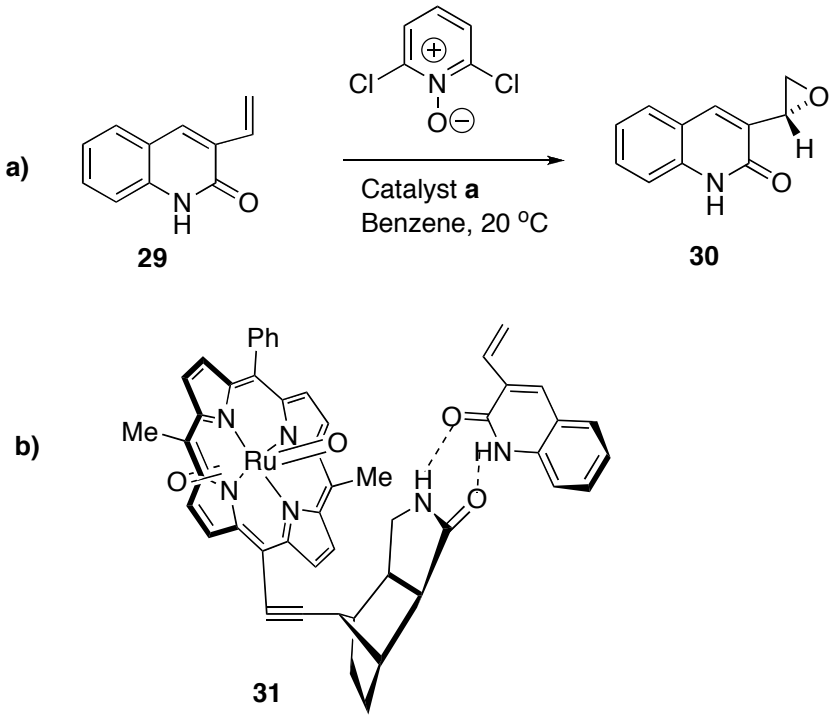

Scheme 1.16 a) Epoxidation of **29** with 'Ru' porphyrin catalyst; b) Supramolecular intermediate **31**

Therefore, the development of such supramolecular catalysts based on porphyrins is one of the most important and emerging fields in the field of catalysis for the conversion of higher molecular weight compounds into appropriate functionality for biofuel and energy based applications.

1.4 Historical background of Calixarene chemistry

Calixarene is a macrocyclic or cyclic oligomer based on hydroxyalkylation product of a phenol and aldehyde[30]. These compounds are composed of phenolic units connected by methylene bridges to form a hydrophobic cavity that is capable of forming inclusion complexes with a variety of molecules. The word calixarene is derived from words 'calix' and 'arene' because of these types of molecules, a vase refers to the calix or cup and the word arene refers to the aromatic building block.

In 1942, Zinke and Ziegler[31] reported that the *p*-tert-butylphenol and formaldehyde react under basic (sodium hydroxide) conditions in linseed oil as a solvent to form a cyclic tetramer, then after 4 years, another paper stating that the reaction is general and works for *p*-phenylphenols[32]. In the late 1970's, David C. Gutsche's pioneering work led to the renewed interest in the field of phenol and aldehyde condensation products and these products are called calixarenes.[33]

Calixarenes have been synthesized in different sizes based on the number of phenolic units connected to the methylene bridge in the macrocycle. Calixarenes can be named by placing the number in the bracket between calix and arene. For example: in the name calix[n]arene, the letter 'n' represents the number of phenolic units connected to the methylene bridge in the macromolecule (**Scheme 1.17**). These calixarenes possess a well defined cavity with the more polar groups in the lower rim and nonpolar groups in the upper rim, therefore these can be selectively derivatized at lower and upper rims with

appropriate functional groups in order to design substrate selective compounds capable of forming stable inclusion complexes in polar and nonpolar solvents.

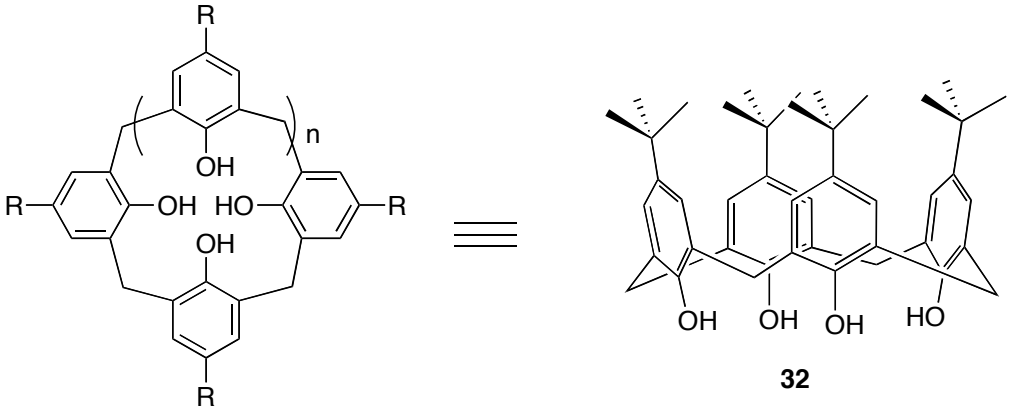

n = 4 and R = *t*-butyl, then
the name is *p*-*t*-butyl Calix[4]arene **32**

Scheme 1.17 Representation of Calix[n]arene (left) and *p*-^{t}butyl Calix[4]arene **32**.

In a calixarene, a distinct cylindrical shaped cavity is formed by the phenolic groups linked by methylene units, in which the wider side is called upper rim and the narrower side is called lower rim.[34] Calix[n]arenes with n = 3 to 20 are known, but the majority of studies deal with only three classes of calixarenes a) calix[4]arene, b) Calix[6]arene and c) Calix[8]arene and the cavity size of the Calix[4]arene, Calix[6]arene and Calix[8]arene are 3.0, 7.6 and 11.6 Å respectively,[35] and the most popular and widely used calix[n]arene in the supramolecular chemistry is the Calix[4]arene, because of it's size and well defined cavity size are compatible for inclusion of wide range of small molecules for host-guest complexation studies as well as for encapsulation studies. Since this dissertation is mainly based on the calix[4]arene derivatives, therefore, I would emphesize and/or discuss only on calix[4]arene derivatives

and their use as receptors and in sensory applications.

1.4.1 Receptor propeties of calix[4]arenes

In biochemistry, hydrogen bonding is one of the most important interactions of all noncovalent bonds,[36] and they play an essential role in the formation of biological molecules such as the globular proteins and DNA double helix and also in the mechanism of the enzyme-substrate recognition and the formation of the hydrogen bonds as a driving force for the molecular recognition has also been widely used in the artificial receptors.[37] In supramolecualr chemistry, molecular recognition of neutral molecules with calix[4]arene derivatives is also a subject of special attention. In late 1990's the calix[4]arene chemistry was mainly based on the inclusion complexes in solid state, but in recent years, the scientists have focused on the development of calix[4]arene based complexation in polar solvents and aqueous media.[38] Several hydrogen bonding calix[4]arene derivative have been decribed, but some of them tend to form homodimer (self-association). To overcome this problem, in 1998, Stibor et al. have specculated that, the immersion of H-bond active groups into a large cavity should disfavor the self-association and favor the binding of substrate in apolar solvents such as CCl4.. Based on this idea, they have designed and synthesized several calix[4]arene receptors for the host-guest complexation study[39] (**Scheme 1.18**).

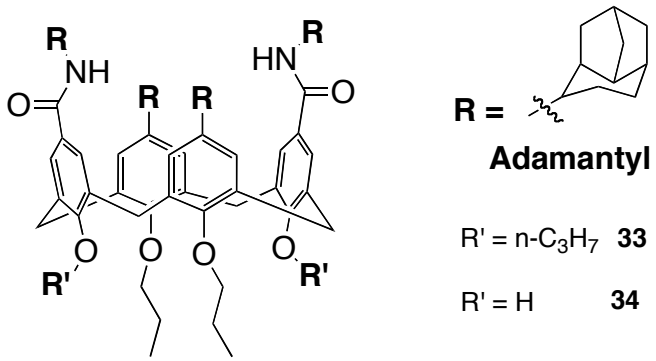

Scheme 1.18 Adamantane based calix[4]arene receptors

According to Stibor's concept, the receptor is made of calix[4]arene framework, a hydrogen bonding group and a bulky hydrocarbon moiety. The fixed cone conformation of the calix[4]arene predetermines the shape and the coformational mobility while the substitution at the lower rim can changes the conformational features. The complexation studies were performed in apolar solvent (CCl_4) with water as guests using both calix[4]arenes **33** and **34** in the **Scheme 1.18**. Compound '**33**' forms strong complex with water and the binding was confirmed by NOE difference experiment, in which they irradiated protons of water and monitored the aromatic protons of the directly attached adamantyl groups. The downfield shift of the amide protons indicate the formation of the hydrogen bonding with water molecule in the cavity. In the case of compound 'b' due to the hydrogen bonding at the lower rim, that changes the conformation of the calixarene and adopts a pinched cone conformation. Therefore, the calix[4]arene **34** has no affinity towards water and by using this result, one can tune the property of the calix[4]arene for effective binding of various substrates.

In 2006, Zhao et al,[40] published a similar idea of a calix[4]arene based amphiphilic molecular basket, which is sensitive to both solvent and UV irradiation. They have synthesized a calix[4]arene based molecular basket by linking four cholate units to a cone-shaped calix[4]arene scaffold through azobenzene spacer. They have been interested to construct a conformationally controllable foldamers[41] and nonfoldamers[42] by using cholic acid as a building block. The 'molecular basket' that can reversibly switch between a micelle-like conformation in polar environment and reversed-micelle like conformation in non-polar environments. They have studied the guest binding properties of the calix[4]arene **35** with various guest **36**, **37** and **38** etc**,** in polar and non polar solvents (**Scheme 1.19**).

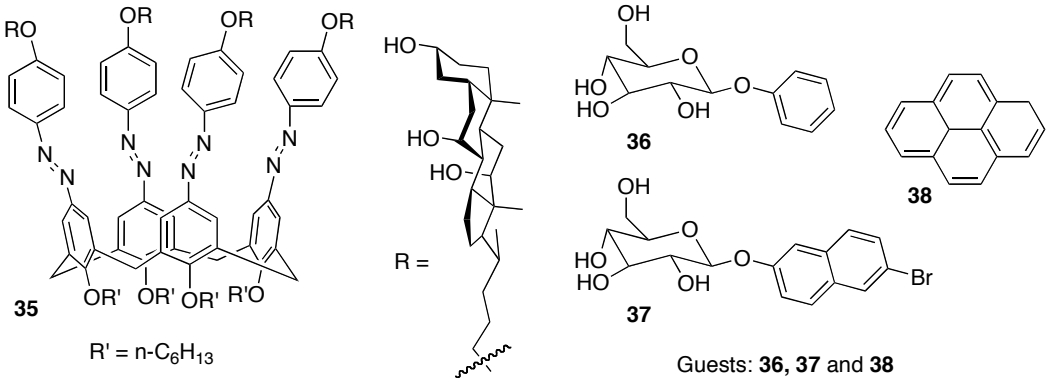

Scheme 1.19 Zhao's Amphiphilic molecular basket **35**

The guest binding properties and the conformational properties of calix[4]arene **35** was studied with guests **36**, **37**, and **38** in non-polar and polar solvents and results were analyzed by ^{1}H NMR spectroscopy. In a non-polar mixture 5% of CD_3OD/CCl_4, the host, **35,** could bind the guest, **36** (β-D-

glucopyranoside) with an association constant (K_a) of ~380 M^{-1} and the binding was confirmed by the stoichiometry of the Job's plot. They have observed high binding constant (K_a = ~ 700 M^{-1}) for guest **37**, which may be due to the extra aromatic ring than that of guest **36**. Therefore the addirional π-π interactions with calix[4]arene favor the high binding constant for guest **36**. Pyrene **37** was found to be the best guest for micelle-like conformation in polar solvent[43](CD_3OD) with an association constant (K_a) of ~ 5 - 10 M^{-1}, and which is evidenced by the fact that, in polar solvent, the association is favored by the hydrophobic nature of the calix[4]arene cavity adopting micelle-like conformation. Therefore, one can conclude that, the change in the conformation of the calix[4]arene **35** was based on the fact that of the change in the polarity of the solvent as well as the hydrophobic and/or hydrophilic nature of the guests. In addition to the above two findings, they have also studied the *trans-cis* isomerization of the diazo groups in the calix[4]arene **35** upon irradiation of UV light at 350 nm. Diazocalix[4]arene **35** displayed a π-π* transition near 350 nm and a very weak n-π* transition at 450 nm in UV spectrum. With irradiation by 360 nm UV light for about 5 min, the π-π* band lost about 405 and the n-π* band grow stronger and this is the evidence for the *trans-cis* isomerization of diaazocalix[4]arene **35** in UV light. Hence, one can conclude that, these calix[4]arene baskets can be used for host-guest complexation studies as well as for drug delivery systems in polar and non-polar solvents.

1.4.2 Homo and heterodimerization studies of calix[4]arenes

The design and synthesis of organic compounds that form defined structures through a noncovalent (hydrogen bonding, pi-pi interactions, van der wal interactions etc.) association is most important for the development of new molecules for information storage, catalysis, molecular recognition, sensing, molecular transport and self assembly of the supramolecular structures. In late 1990's, the self assembly of organic compounds in apolar solvents was less common until Rebek's work[44] on synthesis and self-assembly of calix[4]arene derivatives in apolar (Benzene-d_6, Toluene-d_8) solvents. In their work, they have designed and synthesized a tetraurea calix[4]arene derivative **39** to reversibly dimerize to form an egg shaped enclosure. A circular array of eight-hydrogen bonded interactions in self-assembly were provided by four self-associating tetra-urea functionalities. The dimerization was confirmed by ^{1}H NMR and mass spectrometry studies and these dimers are capable of encapsulating small molecules such as benzene and chloroform.

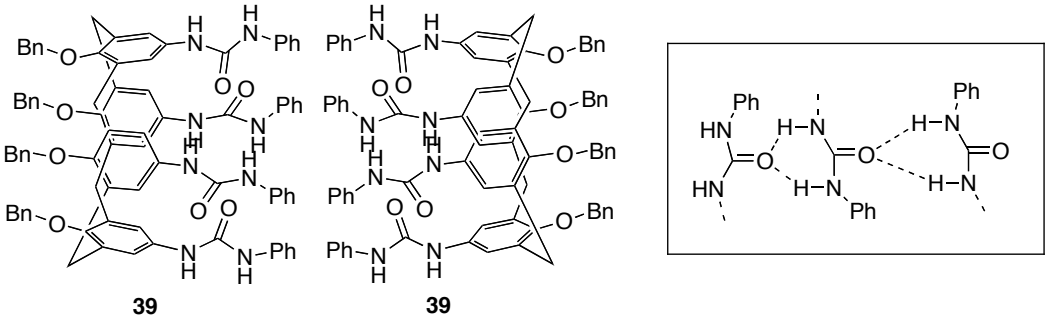

39 **39**

Scheme 1.20 Rebek's Homodimer [**1•1**] of **39** (Bn = Benzyl). Schematic representation of hydrogen bonding in dimmer (right)

After Rebek's paper, there are many examples have been reported based on homodimerization in aprotic solvents, but very few papers on

homodimerization in polar solvents were reported[45] until Shuker's work on homodimerization in polar protic solvents was published in 2002. The idea is mainly based on the design of systems capable of association in polar solvents, especially the development of systems that will be compatible with biological environment and applications in drug transport, delivery, biocatalysis, binding and detection of biomolecules. Calix[4]arenes substituted aryl or peptidyl ureas have been studied extensively for their dimeriztion in apolar solvents, but addition of little polar protic solvents, the dimer dissociates into monomers. Therefore, they have developed a new class of tetrapeptido calix[4]arenes (**Scheme 1.21**, **40**) in which the amino acids are attached to the upper rim through the carboxyl termini and they are interested in this new class of peptidocalixarene, both in their ability to dimerize and bind to small molecules, for application to molecular recognition and catalysis.

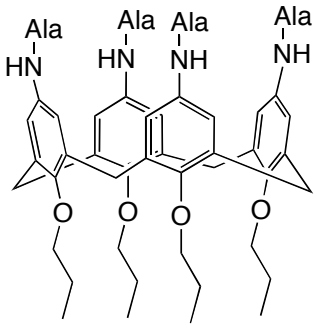

40

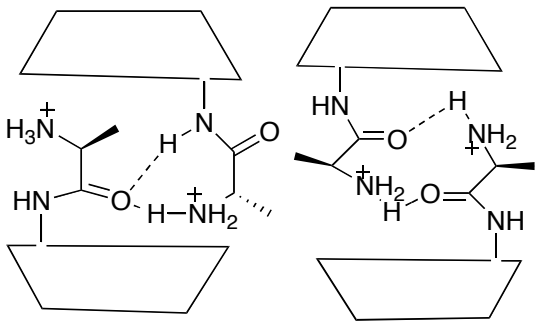

Hydrogen bonding in dimer

Scheme 1.21 Shuker's Alanino calix[4]arene **40**. Schemetic representation of dimerization by hydrogen bonding in polar solvent (MeOH-d_4) (right).

The dimerization and binding properties of **40** were investigated by ^{1}H

NMR spectroscopy, the alanineclixrene was dissolved in MeOD containing 4% D_2O. The resonance of alinine methyl protons shifted upon dilution and confirmed the dimerization by ^1H NMR, and mass spectrometry confirms the multiple charged species, which are the result of protonation of amines. The dimerization (**Scheme 1.21**) or association constants were calculated by dilution experiment by diluting 10 mM of calixarene in 24:1 (MeOD:D_2O) to a final concentration of 0.05 mM and monitored the change in chemical shift of alanine methyl protons and association constant was found to be 2.9 x 10^4 M^{-1}, which is the higher than the K_a value reported for peptidylureidocalixarene in apolar solvent.[46] The preparation of a peptidocalixarene that associates in polar solvent opened new doors for the use of calix[4]arenes for molecular recognition in biologically relevant environments.

In 2006, Shuker et al,[47] published another paper on heterodimerization studies of calixarene derivatives in polar solvents. The dimerization is favored by the increased bond strength of ionic bonds over hydrogen bonds, and they prepared several calix[4]arene derivatives (C-linked alaninocalix[4]arene **41**, N-linked alaninocalix[4]arene **44**, anilino calix[4]arene **42**, carboxy calix[4]arene **43**, carboxyphenyl calix[4]arene **45**, amidino calix[4]arene **46**) that utilize ionic interactions to form heterodimers in polar solvents (**Scheme 1.22**). The self assembly of these derivatized calix[4]arenes into heterodimers was studied by ^1H NMR in DMSO-d_6 or CD_3OD with 5% aqueous phosphate buffer. The dimerization of these derivatives is attributed to the larger dfference in pK_a's of

protonated amine and carboxylic acid groups of calix[4]arenes (**41** to **46**). The monomers with the largest pK_a difference, N-linked and C-linked alanyl calix[4]arene, form the tightest binding heterodimer (**41:44**, Ka = 5040 M-1) followed by **41:45** and **41:43**. There is no dimerization in any of the other combinations because of the low pK_a difference between carboxylic acid derivative and protonated amine derivative. The addition of phenyl spacer to the calix[4]arene scaffold increases the size of the heterodimer with little effect on its abilty to dimerize and the heterodimers were analyzed by job's plot and the maximum value in x-axis is 0.5, which indicates the assembly of supramolecular structure with a 1:1 monomer ratio. Therefore, this idea can be used to design of heterodimers in aqueous media for biological applications at physiological conditions as well as for encapsulation of guests for biosensor applications.

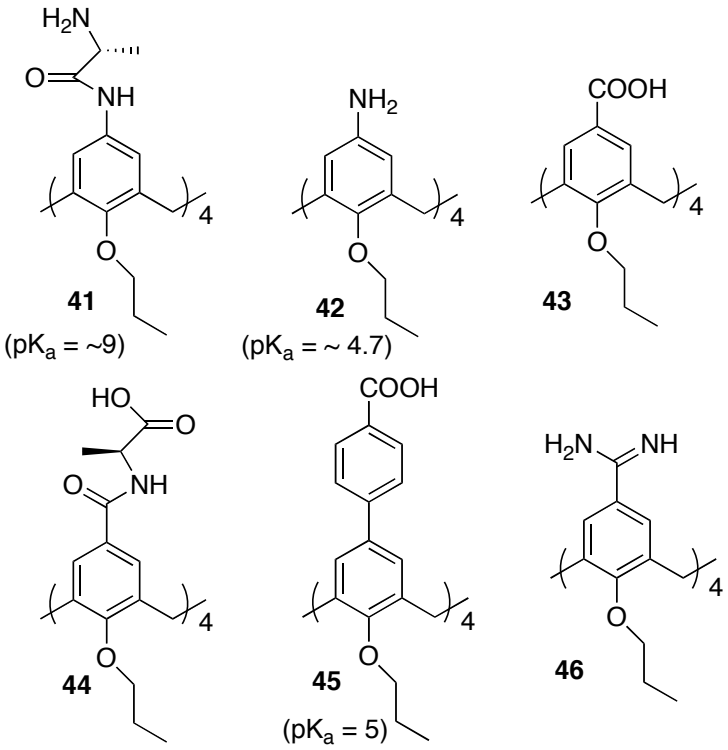

Dimer	K_a	Solvent	pH
41:44	5040	DMSO-d_6 / 5% buffer,	6.5
41:45	4410	DMSO-d_6 / 5% buffer,	6.5
41:43	1200	DMSO-d_6 / 5% buffer,	6.5

Scheme 1.22 Calix[4]arene derivatives (**41** to **46**) for heterodimerization studies in polar solvents (DMSO-d_6 with 5% phosphate buffer). Association constants for dimerization are given in the table.

1.4.3 Encapsulation studies of calix[4]arenes

Calix[4]arene tetraurea capsules are the most extensively studied molecular capsules in early 1990's, since their invension by Rebek[48] and Bohmer.[49] The architecture of these capsules comprises the bowl-shaped curvature of the calix[4]arene monomer in the cone conformation and the four self complementary ureas on the upper rim. The formation of dimeric assembly is the basis of hydrogen donor and acceptor properties of the

functional groups attached to the upper rim. There are a total of 16 intermolecular hydrogen bonds possible in a dimeric tetraurea calix[4]arene capsule (**Scheme 1.19**) with a diameter of ~7 $Å^3$ and the interior volume of ~200 $Å^3$ and these can accommodate benzene and chloroform size of molecules in apolar solvents. In 2000, Rebek et al.[50] reported a second generation of the tetraurea calix[4]arene capsules with expanded cavities (with additional benzene ring) for guest encapsulation in apolar solvents (**Scheme 1.23**).

They have synthesized the calixarene monomer **47** in five steps starting with tetrabromo tetrabenzyloxy calix[4]arene (not shown) by Gutsche's procedure.[51]

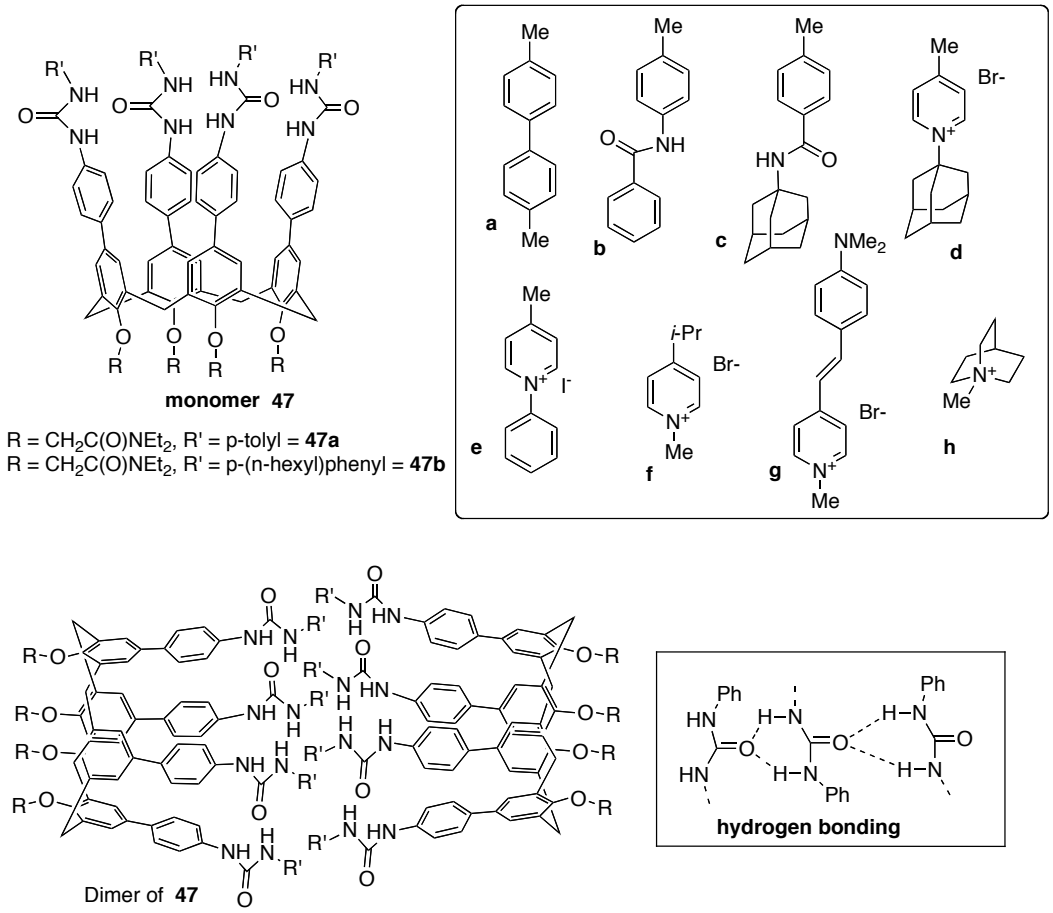

Scheme 1.23 Rebek's second-generation tetraurea capsule (dimmer **47**) and monomer **47**. Hydrogen bonding in the capsule (bottom box), guests (**a** to **h**) used for encapsulation studies (top box).

The capsule formation was monitored by ^{1}H NMR in CD_2Cl_2 by following the downfield shift of the NH protons. The dimerization also confirmed by the mixed dimmer of **47a** and **47b**, in which the appearance of new set of NH resonances in ^{1}H NMR measurements, and also confirmed by ESI-MS and the dimerization constant value was beyond the NMR limits (>10^5 M^{-1}). The egg-shaped cavity that results has the volume estimated at ~400 Å and was the first largest capsule synthesized in early 2000's. The encapsulation studies by various neutral and flat guests (**a, b, and c**) failed but charged guests

(**d-h**) showed strong binding and the binding constants ranged from 5.6 x10^3 to 1.9 x 10^5 M^{-1}, and the stoichiometry was confirmed by Job's plot and association constants were calculated by spread sheet software. Therefore, these large sized capsules could be further tuned for encapsulation of neutral guests by changing the functional groups at upper rim of the calix[4]arene.

In 2002, Reinhoudt et al,[52] have reported a novel type of capsule resulting from the self-association between oppositely charged complementary building blocks in MeOH/H_2O.They observed the dimerization based on the interaction between tetraamidinium calix[4]arenes **48a - 48d** and tetrasulfonato calix[4]arene **49** (**Scheme 1.24**).

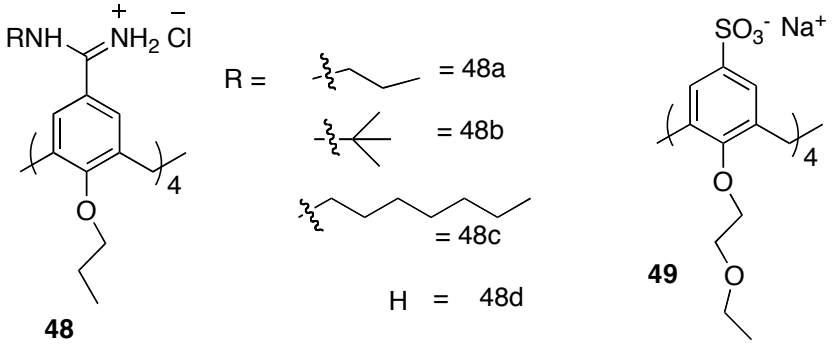

Scheme 1.24 Reinhoudt's calix[4]arene derivatives (**48** and **49**) for encapsulation

The 1:1 assembly was evidenced by ^{1}H NMR, ESI-MS, and ITC (Isothermal Calorimetry Titrations). The association constants were in the range of 10^6 M^{-1} and the association process is fast on NMR time scale and strongly entropy driven. The system **48a•49** shows strong binding affinity toward acetylcholine, tetramethylammonium, and N-methylquinuclidinium cations. This is the

example of guest encapsulation in polar protic solvents.

Kraft et al., have published series of articles[53] on 'self-assembly of molecular capsules in polar protic solvents', based on the concept that, nature often employ a cooperative combination of multiple electrostatic interactions between arginine or lysine residues and aspartates or glutamates on the neighboring subunits of virus particles (self assembly of tobacco mosaic virus). Their idea was a modular system of complementary half-spheres that relies on strong salt bridges in a self-reinforcing manner. Initially they focused on the C_{3v}-symmetric building blocks for the generation of 1:1 assemblies and then they have designed more rigid and highly preorganized[54] half-spheres from calix[4]arene derivatives **50 - 55** (**Scheme 1.25**). These calix[4]arenes with

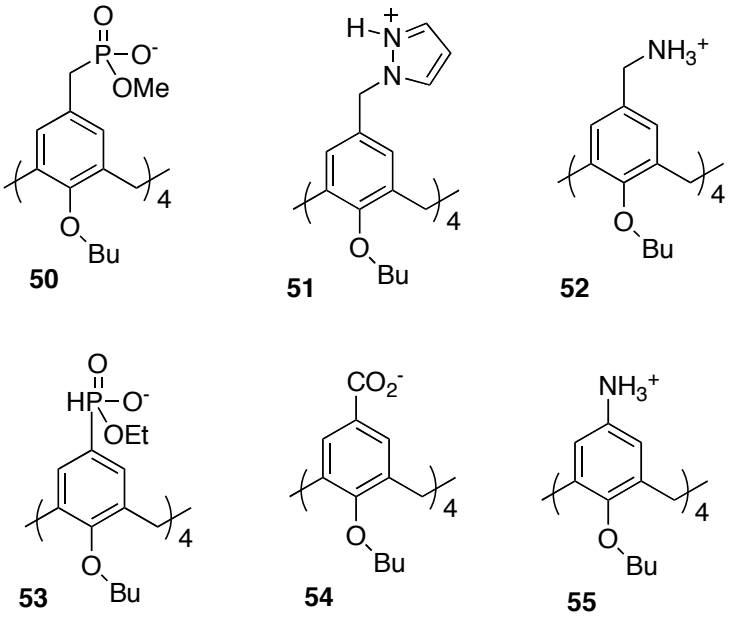

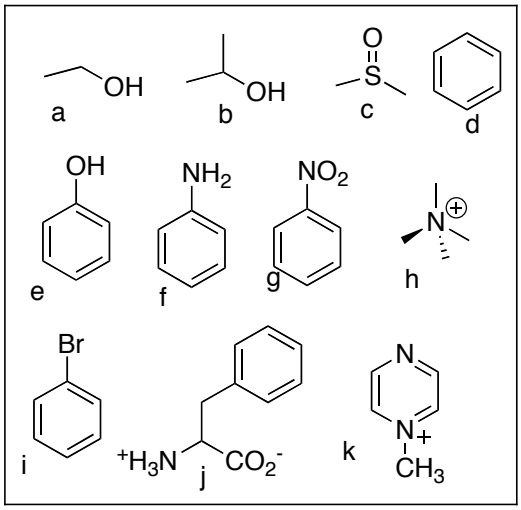

Scheme 1.25 Kraft's Calix[4]arene derivatives **50** - **55** for encapsulation studies in polar protic solvents (top), Guests used for encapsulation studies in Kraft's capsules (bottom).

four anionic groups on the upper rim can form a discrete 1:1 complexes with the complementary calix[4]arene derivatives bearing four cationic groups at the upper rim and each cation is bound by two anions and *vice versa* in a mutual chelate arrangement, reinforced by a network of ionic hydrogen bonds. The formation of highly stable capsule-like assemblies even in polar protic solvents (methanol and water) is due to the multiple electrostatic interactions between complementary calix[4]arenes. The cavity size in these capsules is around 170-230 Å and that is principle large enough for guest encapsulation. The formation of ball shaped complexes from calix[4]arene building blocks was studied with Job's plot, NMR titration, NOESY, and variable temperature experiments and ESI-MS measurements. The highest association constant $1x10^3$ M^{-1} between capsule (**53** •**55**) and guest **J** (phenyl alanine), and 500 M^{-1} for guest **h**. These results clearly indicate the encapsulation is truly based on ionic interactions

between host (capsule) and guests, and hydrophobic character of the capsule interior and appropriate size of the guest molecule that has size equal to the cavity size of the capsule.

In addition to the above examples on heterodimerization and encapsulation studies of various calix[4]arene based capsules in polar protic solvents have been studied recently ranging from the tetraurea benzyl calix[4]pyrroles and tetraurea tolyl calix[4]arene to afford unprecedented hybrid dimeric capsules in polar solvents[55] and the use of tetraurea calix[4]arenes with sulfur functionality[56] used for homo (in apolar sovents) and hetero (polar solvents) as well as their self assembly on gold suface (self assembled momolayers SAMs). The self-assembly process and the stability of SAMs formed by capsules filled with ferrocenium cations in electrolyte solutions were tested with surface plasmon spectroscopy. The inclusion of guests, such as dichloromethane or ferrocenium, in the immobilized capsules were confirmed by classical surface plasmon spectroscopy, gold nanoparticle absorption spectroscopy and time-of flight secondary ion mass spectrometry (ToF-SIMS). The film stability and quality was tested by cyclic voltammetry.

1.5 Conclusion

In the last decade, the use of small molecular catalysts become less useful due to their ability in terms of selectivity, reactivity and solubility. Therefore the use of supramolecular catalysts has become more attractive in the field of organic synthesis and catalysis, especially to perform organic transformations in aqueous media. Since the discovery of picket fence

porphyrins by James Collman, the applicability of these molecules in the field of organometallic chemistry and supramolecular chemisty has a high impact in terms of selectivity, reactivity. These can be synthesized easily with inexpensive starting materials and also derivatized easily. The shape of the picket fence porphyrins could allow to tune the scaffold with different substituents in order for effective binding with various substrates and to perform chemical transformations effectively in polar and aqueous media.

The hydrophobic effects can bring organic molecules together in aqueous media, because of their poor solubility nature in water. To introduce or design a supramolecualr scaffold with high hydrophobic cavity or groups capable to bring variety of substrates towards its own cavity is one of the most emerging field in supramolecualr chemistry. Calix[4]arenes are the best organic components with above all characteristics can be used as supramolecualr scaffolds for molecular recognition and catalysis.

But the use of picket-fence porphyrins and calix[4]arenes as supramolecualr scaffolds or catalysts in aqueous media is still in undeveloped area of organic chemistry. Therefore, the development of ideal, water-soluble supramolecular scaffolds for molecular self-assembly and catalysis, remains a driving force in the field of catalysis. In this dissertation, we are taking an opportunity to develop a high efficient porhyrin and calix[4]arene based supramolecualr scaffolds for catalytic pinaocl coupling reactions for biofuel applications as well as for molecular recognition and encapsulation studies in aqueous media.

1.6 References

1. Chheda, J. N.; Huber, G. W.; Dumesic, J. A. Liquid-Phase Catalytic Processing of Biomass-Derived Oxygenated Hydrocarbons to Fuels and Chemicals. *Angew. Chem. Int. Ed.* **2007**, *46*, 7164 -7183.

2. Karakhanov, E. A.; Maksimov, A. L.; Runova, E. A. Design of supramolecular metal complex catalytic systems for organic and petrochemical synthesis *Russian Chemical Reviews*, **2005**, *74*, 97-111.

3. Lehn, J.-M, Supramolecular Chemistry, *Science,* **1993**, *260*, 1762-1763.

4. Biochemistry and Binding: Activation of Small Molecules. The Porphyrin Handbook; Kadish, K. M., Smith, K. M., Guilard, R., Eds.; Academic Press: San Diego, CA, **2000**; Vol. *4*.

5. Vicente, M. G. H.; Jaquinod, L.; Smith, K. M. Oligomeric Porphyrin Arrays, *Chem. Commun.* **1999**, *6*, 1771–1782. Hamilton, A.; Lehn, J. M.; Sessler, J. L. Coreceptor molecules. Synthesis of metalloreceptors containing porphyrin subunits and formation of mixed substrate supermolecules by binding of organic substrates and of metal ions

J. Am. Chem. Soc. **1986**, *108*, 5158–5167.

6. Rothemund. P. A New Porphyrin Synthesis. The Synthesis of Porphyrin, *J. Am. Chem. Soc*, **1939***, 58*, 625–627.

7. A. D. Adler, F. R. Longo, J. D. Finarelli, J. Goldmacher, J. Assour and L. Korsakoff, A simplified Synthesis of meso-tetraphenylporphine, *J. Org. Chem*, **1967**, *32*, 476–476.

8. Lindsey, J. S. The Synthesis of *meso*-substituted Porphyrins. In Metalloporphyrins Catalyzed Oxidations; Montanari, F., Casella, L., Eds.; Kluwer Academic Publishers: Dordrecht, The Netherlands, **1994**; pp 49-86.

9. Lee, C.-H.; Li, F.; Iwamoto, K.; Dadok, J.; Bothner-By, A. A.; Lindsey, J. S. Synthetic Approaches to Regioisomerically Pure Porphyrins Bearing Four Different meso- Substituents. *Tetrahedron* **1995**, *51*, 11645–11672.

10. Collman, J. P.; Gagne, R. R.; Reed, R. Halbert, T. R.; Lang, G.; Robinson, W. T. Picket fence porphyrins. Synthetic models for oxygen binding hemoproteins, *J. Am. Chem. Soc*., **1975**, *97*, 1427–1439.

11. Traylor, T.G.; Diekmann, H.; Chang, C. K. Cyclophane Porphirin, *J. Am. Chem. Soc*, **1971**, *93*, 4068-4070.

12. Collman, J. P.; Gagne, R. R.; Reed, R.; Halbert, T. R.; Lang, G.; Robinson, W. T. Picket fence porphyrins. Synthetic models for oxygen binding hemoproteins, *J. Am. Chem. Soc*., **1975**, *97*, 1427–1439.

13. Imai, H.; Kyuno, E. Base Binding to Zinc Picket Fence Porphyrins. Attractive Intramolecular Interactions in Organic Solvents, *Inorg. Chem*. **1990**, *29*, 2416– 2422.

14. Weiser, J. and Staab, H. A. A new benzoquinone-bridged porphyrin, *Tetrahedron Lett*. **1985**, *26*, 6059– 6062. Anderson, H. L., Hunter, C. A.,

Meah, M. N. and Sanders, J. K. M. Thermodynamics of induced-fit binding inside polymacrocyclic porphyrin hosts, *J. Am. Chem. Soc.* **1990**, *112*, 5780–5789.

15. Giraudeau, A.; Gisselbrecht, J. P.; Gross, M.; Weiss, J. Phenanthroline-assisted metallation of a porphyrin: copper and silver mixed valence homodinuclear complexes, *J. Chem. Soc., Chem. Commun.* **1993**, 1103– 1105, Froidevaux, J.; Ochsenbein, P.; Bonin, M.; Schenk, K.; Maltese, P.; Gisselbrecht, J.-P.; Weiss, J. Side Selection of the Fifth Coordinate with a Single Strapped Zinc(II) Porphyrin Host: Full Characterization of Two Imidazole Complexes, *J. Am. Chem. Soc.* **1997**, *119*, 12362– 12363.

16. Middel, O., Verboom, W. and Reinhoudt, D. N. Cavitand Zn(II)–Porphyrin Capsules with High Affinities for Pyridines and *N*-Methylimidazole, *J. Org. Chem.* **2001**, *66*, 3998– 4005.

17. Gale, P. A.; Sessler, J. L.; Kral, V.; Lynch, V. Calix[4]pyrroles: Old Yet New Anion-Binding Agents, *J. Am. Chem. Soc.* **1996**, *118*, 5140–5141, Sessler, J. L.; Anzenbacher Jr. P.; Miyaji, H.; Jursikova, K.; Bleasdale, E. R.; Gale, P. A. Modified Calix[4]pyrroles, *Ind. Eng. Chem. Res.* **2000**, *39*, 3471–3478, Gale, P. A.; Anzenbacher, P., Jr.; Sessler, J. L. Calix[4]pyrroles II, *Coord. Chem. Rev.* **2001**, *222*, 57–102.

18. Gale, P. A.; Sessler, J. L.; Kral, V.; Lynch, V. Calix[4]pyrroles: Old yet new anion-binding agents, *J. Am. Chem. Soc.* **1996.** *118*, 5140.

19. Beer, P. D.; Gale, P. A. Anion Recognition and Sensing: The State of the Art and Future Perspectives, *Angew. Chem., Int. Ed.* **2001**, *40*, 486-516,

Schmidtchen, F. P.; Berger, M. Artificial Organic Host Molecules for Anions, *Chem. Rev*. **1997**, *97*, 1609–1646.

20. Panda, P. K.; Lee, C.-H. Calix[4]pyrrole-Capped Metalloporphyrins as Ditopic Receptor Models for Anions, *Org. Lett*. **2004**, *6*, 671– 674.

21. Matile, S.; Berova, N.; Nakanishi, K. Exciton coupled circular dichroic studies of self-assembled brevetoxin-porphyrin conjugates in lipid bilayers and polar solvents, *Chem. Biol*. **1996**, *3*, 379– 392, Huang, X., Rickman, B. H., Borhan, B., Berova, N. and Nakanishi, K. Zinc Porphyrin Tweezer in Host–Guest Complexation: Determination of Absolute Configurations of Diamines, Amino Acids, and Amino Alcohols by Circular Dichroism, *J. Am. Chem. Soc*. **1998**, *120*, 6185– 6186.

22. Cormode, D. P.; Murray, S. S.; Cowley, A. R.; and Beer, P. D. Sulfate selective anion recognition by a novel tetra-imidazolium zinc metalloporphyrin receptor, *Dalton Trans*, 2006, 5135-5140.

23. Jagessar, R. C.; Burns, D. H. *Chem. Commun*. **1997**, 1685–1686.

24. Metalloporphyrins in Catalytic Oxidations; Sheldon, R. A., Ed.; Marcel Dekker, Inc.: New York, **1994**.

25. Ptaszek, M.; Yao, Z.; Savithri, D.; Boyle, P. D.; Lindsey, J. S. Synthesis and structural properties of porphyrin analogues of bacteriochlorophyll *c*, *Tetrahedron*, **2007**, *63*, 12629– 12638.

26. Esswein, A. J.; Nocera, D. G. Hydrogen Production by Molecular Photocatalysis, *Chem. Rev*. **2007**, *107*, 4022– 4047.

27. Slagt, V. F.; Röder, M.; Kamer, P. C. J.; van Leeuwen, P. W. N. M.; Reek, J. N. H. Supraphos: A Supramolecular Strategy To Prepare Bidentate Ligands, *J. Am. Chem. Soc.*, **2004**, *126*, 4056–4057.

28. Slagt, V. F.; Röder, M.; Kamer, P. C. J.; van Leeuwen, P. W. N. M.; Reek, J. N. H. Supraphos: A Supramolecular Strategy To Prepare Bidentate Ligands, *J. Am. Chem. Soc.*, **2004**, *126*, 4056–4057.

29. Fackler P.; Berthold, C.; Voss, F.; Bach, T. Hydrogen-Bond-Mediated Enantio- and Regioselectivity in a Ru-Catalyzed Epoxidation Reaction, *J. Am. Chem. Soc.*, 2010, *132*, 15911–15913.

30. Gutsche, C. D. **1989**. *Calixarenes*. Cambridge: Royal Society of Chemistry.

31. Zinke, A.; Ziegler, E. *Chem. Ber.* **1944**, 774, 264.

32. Zinke, A.; Zigeuner, G.; Hossinger, K.; Hoffmann, G. *Monatsh.* **1948**, *79*, 438.

33. Gutsche, C.D.; Dhawan, B.; No, K. H.; Muthukrishnan, R. Calixarenes. 4. The synthesis, characterization, and properties of the calixarenes from p-tert-butylphenol, *J. Am. Chem. Soc.* **1981**, *103*, 3782-3792.

34. Gutsche, C.D. Calicarenes, *Acc. Chem. Res.*, **1983**, *16*, 161.

35. Stewart, D.R.; Gutsche, C.D. Isolation, Characterization, and Conformational Characteristics of *p-tert*-Butylcalix[9–20]arenes, *J. Am. Chem. Soc.*, 1999, *121*, 4136, Gutsche, C.D. Calixarenes. The Royal Society of Chemistry (Ed.: J.F. Stoddart), Cambridge, 1989.

36. Jeffrey, G. A.; Saenger, W. *Hydrogen Bonding in Biological Structures*; Springer: Berlin, **1991**.

37. Hamilton, A. D. In *Advances in Supramolecular Chemistry*; Gokel, G. W., Ed.; JAI Press Inc.: London, **1990**; Vol. *1*, pp 1–64, van Doorn, A. R.; Verboom, W.; Reinhoudt, D. N. In *Advances in Supramolecular Chemistry*; Gokel, G. W., Ed.; JAI Press Inc.: London, **1993**; Vol. *3*, pp 169–206.

38. Andreetti, G. D.; Ugozzoli, F. In Calixarenes: A Versatile Class of Macrocyclic Compounds; Vincens, J., Boehmer, V., Eds.; Kluwer Academic: Dordrecht, pp 87–123, Smirnov, S.; Sidorov, V.; Pinkhassik, E.; Havlíček, J.; Stibor, I. Complexes of p-tert-butylcalix[4]arene derivatives with neutral molecules. Structures and stabilities, *Supramol. Chem.* **1997**, *8*, 187–196.

39. Pinkhassik, E.; Sidorov, V.; Stibor. I. Calix[4]arene-Based Receptors with Hydrogen-Bonding Groups Immersed into a Large Cavity, *J. Org. Chem.*, **1998**, *63*, 9644–9651.

40. Ryu, E-H.; Zhao, Y. An Amphiphilic Molecular Basket Sensitive to Both Solvent Changes and UV Irradiation, *J. Org. Chem.* **2006**, *71*, 9491-9494.

41. Zhao, Y.; Zhong, Z. Detection of Hg^{2+} in Aqueous Solutions with a Foldamer-Based Fluorescent Sensor Modulated by Surfactant Micelles, *Org. Lett.* **2006**, *8*, 4715–4717. 42. Ryu, E.-H.; Jie, Y.; Zhong, Z.; Zhao, Y. Solvent-Induced Amphiphilic Molecular Baskets: Unimolecular Reversed Micelles with Different Size, Shape, and Flexibility, *J. Org. Chem.* **2006**, *71*, 7205–7213.

43. Zhao, Y.; Ryu, E.-H. Solvent-Tunable Binding of Hydrophilic and Hydrophobic Guests by Amphiphilic Molecular Baskets, *J. Org. Chem.* **2005**, *70*, 7585–7591.

44. Shimizu, K. D.; Rebek. Jr, J. Synthesis and assembly of self-complementary calix[4]arenes, *Proc. Natl. Acad. Sci. USA,* **1995**, *92*, 12403-12407.

45. Prins, L. J.; Reinhoudt, D. N.; Timmerman, P. Noncovalent Synthesis Using Hydrogen Bonding, *Angew. Chem., Int. Ed.* **2001**, *40*, 2382–2426, Hirschberg, J. H. K. K.; Brunsveld, L.; Ramzi, A.; Vekemans, J. A. J. M.; Sijbesma, R. P.; Meijer, E. W. Helical self-assembled polymers from cooperative stacking of hydrogen-bonded pairs, *Nature*. **2000**, *407*, 167–170.

46. Rinco´n, A. M.; Prados, P.; de Mendoza, J. A Calix[4]arene Ureidopeptide Dimer Self-Assembled through Two Superposed Hydrogen Bond Arrays, *J. Am. Chem. Soc*. **2001**,*123*, 3493-3498.

47. Sasine, J. S.; Brewster, R. E.; Caran, K. L.; Bentley, A. M.; Shuker, S. B. Heterodimerization Studies of Calix[4]arene Derivatives in Polar Solvents, *Org. Lett*., **2006**, *8*, 2913–2915.

48. Shimizu, K. D.; Rebek. Jr, J. Synthesis and assembly of self-complementary calix[4]arenes, *Proc. Natl. Acad. Sci. USA,* **1995**, *92*, 12403-12407, Hamann, B. C.; Shimizu, K. D.; Rebek, J., Jr. Reversible Encapsulation of Guest Molecules in a Calixarene Dimer, *Angew. Chem. Int. Ed,* **1996**, *35*, 1326–1329.

49. Mogck, O.; Böhmer, V.; Vogt, W. Hydrogen bonded homo- and heterodimers of tetra urea derivatives of calix[4]arenes Tetrahedron **1996**, *52*, 8489–8496. Mogck, O.; Paulus, E. F.; Böhmer, V.; Thondorf, I.; Vogt, W. Hydrogen-bonded dimers of tetraurea calix[4]arenes: unambiguous proof by single crystal X-ray analysis, Chem. Commun. **1996**, 2533–2534.

50. Cho, Y. L.; Rudkevich, D. M.; Julius Rebek, J. Jr. Expanded Calix[4]arene Tetraurea Capsules, *J. Am. Chem. Soc*, **2000**, *122*, 9868–9869.

51. Gutsche, C. D.; Pagoria, P. F. Calixarenes. 16. Functionalized calixarenes: the direct substitution route, *J. Org. Chem.* **1985**, *50*, 5795-5802.

52. Corbellini, F.; Fiammengo, R.; Timmerman, P.; Crego-Calama, M.; Versluis, K.; Heck, A. J. R.; Luyten, I.; Reinhoudt, D. N. Guest Encapsulation and Self-Assembly of Molecular Capsules in Polar Solvents via Multiple Ionic Interactions, *J. Am. Chem. Soc*., 2002, *124*, 6569–6575.

53. Grawe, T.; Schrader, T.; Gurrath, M.; Kraft, A.; Osterod, F. Self-Organization of Spheroidal Molecular Assemblies in Polar Solvents, *Org. Lett*. 2000, *2*, 29–32, Grawe, T.; Schrader, T.; Kraft, A. Self-Assembly of Ball-Shaped Molecular Complexes in Water, *J. Org. Chem*. 2002, *67*, 3755–3763.

54. Zadmard, R.; Schrader, T.; Grawe, T.; Kraft, A. Self-Assembly of Molecular Capsules in Polar Solvents, *Org. Lett*. 2002, *4*, 1687–1690. Zadmard, R.; Junkers, M.; Schrader, T.; Grawe, T.; Kraft, A. Capsule-like Assemblies in Polar Solvents, *J. Org. Chem*., 2003, *68*, 6511–6521.

55. Chas, M.; Gil-Ramírez, G.; Ballester, P. Exclusive Self-Assembly of a Polar Dimeric Capsule between Tetraurea Calix[4]pyrrole and Tetraurea Calix[4]arene, *Org. Lett.* 2011, *13*, 3402–3405.

56. Xu, S.; Podoprygorina, G.; Volker Böhmer, V.; Ding, Z.; Rooney, P.; Rangan, C.; Mittle, S. Tetraurea calix[4]arenes with sulfur functions: synthesis, dimerization to capsules, and self-assembly on gold, *Org. Biomol. Chem.*, **2007**, 5, 558-568.

Chapter 2

Pinacol Coupling Reactions and Applications

2.1 Introduction

The Pinacol coupling reaction is one of the most important and useful reactions in organic chemistry for construction of carbon-carbon bonds. In a pinacol coupling reaction, carbon-carbon covalent bond is formed between the carbonyl groups of aldehydes or ketones in the presence of a metal reductant is a radical process and the products formed are called 'Pinacol' products **56** (**Scheme 2.1**). The reductive dimerization of carbonyl compounds is a useful synthetic method for constructing vicinally functionalized carbon-carbon bonds. One electron transfer from a metal to a carbonyl function generates the corresponding ketyl radical, which can dimerize to give either *dl* and/or *meso* isomers of 1,2-diols.

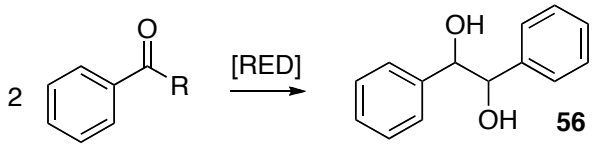

Scheme 2.1 Pinacol product (vicinal diol)

In organic chemistry, the method for the generation of anionic or cationic radicals is one electron reduction or oxidation of organic compounds. These are the most important methods used in the process of generation of radical reactions. Redox properties of transition metals can be utilized for an efficient one-electron reduction or oxidation.[57] In particular, transition metals

including titanium, vanadium and magnesium have been of synthetic potential in terms of redox properties. The synthetic limitation arises from the use of stoichiometric amounts or excess of metallic reductants or oxidants in order to complete the catalytic cycle, and it is difficult to construct such catalytic cycles. Therefore, a catalytic cycle should be constructed to avoid the use of such expensive and excess amounts of toxic metallic reagents.

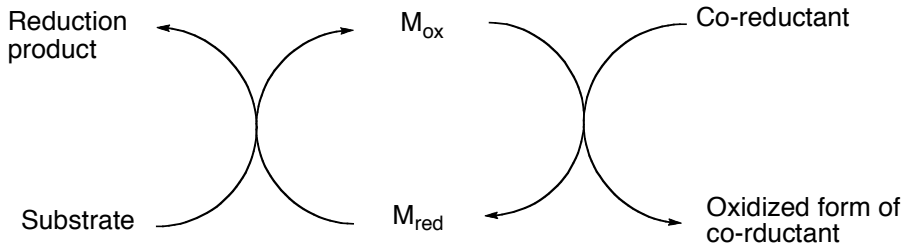

Scheme 2.2 Catalytic cycle with metal co-reductant

A co-reductant can also be used in the formation of a reversible redox cycle for one-electron reduction as shown in **Scheme 2.2**. In addition to the above process, the electron transfer process can also be enhanced by either introducing a ligand on to the metal in order to increase the bulkiness on the metal for effective interaction with substrate or by introducing Lewis acid activation of substrate towards efficient electron transfer process. Therefore it is important to select stoichiometric co-reductants or co-oxidants for the reversible cycle of catalyst, in which the metal co-reductant is converted to the corresponding metal salt in higher oxidation state, which may act as a Lewis acid for activation. There fore taking these interactions into account, the required catalytic system can be constructed in terms of reactivity and

selectivity for the selective methods in synthetic radical reactions.

2.2.1 Catalytic systems for Pinacol Coupling Reactions in organic solvents

In 1988, Sharpless and Jacobsen[58] developed a complementary route to 1,2-diols for the construction of vicinally functionalized carbon-carbon bonds by the ligand-accelerated, osmium-catalyzed asymmetric dihydroxylation of olefins **57** (**Scheme 2.3**) 'acetone and water' solvent system.

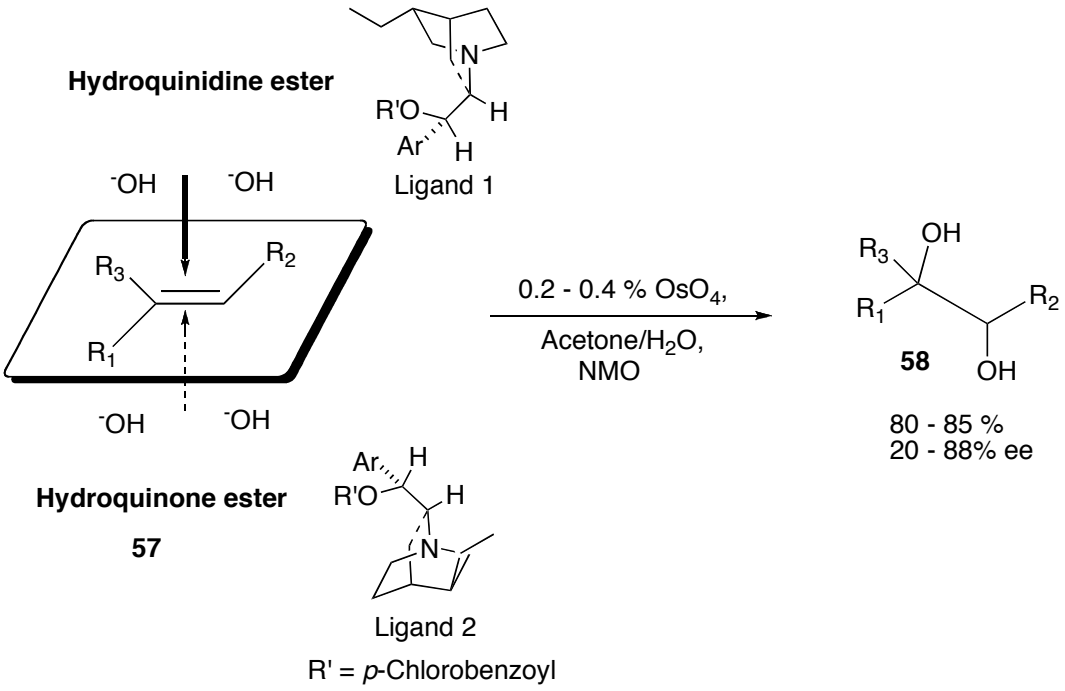

Scheme 2.3 Ligand accelerated ssymmetric dihydroxylation, *'a complementary route to 1,2-diols'*.

In this method they have achieved substantially improved rates and turnover numbers as well as useful levels of asymmetric induction (**Table 2.1**), and the use of water and acetone mixture as a solvent system, but the draw back for this method is the use of toxic and expensive metals for catalysis. The main important features of this method include a) unlike asymmetric

epoxidation and hydrogenation, it requires no directing functional group; 2) because of the ligand acceleration phenomenon, very little amount of osmium catalyst (0.2 - 0.4 mol %) required; 3) easily available and easily recoverable cinchona alkaloids (quinine and quinidine) as ligands; 4) reagents are insensitive to air and water and work better under high concentration conditions.

entry	Olefine (57) 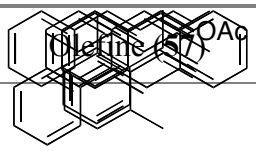	Ligand, % ee, config. of diol (**58**)
1		**1**, 62, R-(-) **2**, 53.6, S-(+)
2		**1**, 65, R,R-(-) **2**, 55.4, S,S-(+)
3		**1**, 33, R-(-)
4		**1**, 46, R-(+)
5		**1**, 76, R,R-(+)
6		**1**, 65, (-)
7		**1**, 20, R,R-(+)
8		**1**, 88, R,R-(+) **2**, 75.5, S,S-(-)

Table 2.1 Substrate scope in Asymmetric dihydroxylation by ligands **1** and **2**.

In order to make the pinacol coupling reactions successful, more efficient, less toxic and using inexpensitve starting materials, catalysts, and for

the stoichiometric reductive dimerization, low-valent metals such as aluminum, titanium, vanadium, zinc, and samarium compounds have been employed conveniently.[59] The pinacol coupling reactions using $TiCl_3$/Zn-Cu and $[VCl_3(THF)_6]_2[Zn_2Cl_6]$ have been employed successfully for the synthesis of paclitaxel and C_2-symmetrical HIV protease inhibitors respectively.[60] To synthesize such complicated molecules, efficient control of the stereochemistry in the coupling reactions is of importance in addition to the construction of a catalytic cycle of low-valent metals.

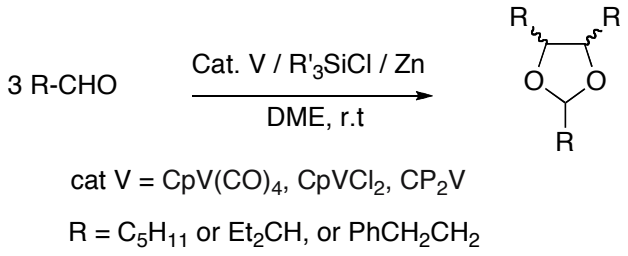

Scheme 2.4 a novel catalytic system for one electron reduction: Low valent Vanadium catalyzed Pinacol coupling of aldehydes

First time, in 1996, Hirao et al,[61] have developed a diastereoselective pinacol coupling reaction using ternary catalytic system consisting of a metallic catalyst, a chlorosilane, and a stoichiometric co-reductant (**Scheme 2.4**). The homocoupling of aliphatic aldehydes is catalyzed by $CpV(CO)_4$, $CpVCl_2$ and CP_2V in the presence of a chlorosilane and Zn in DMF to give the 1,3-dioxolanes via the coupling and acetalizaion. A vanadium catalyst is essential although the combination of Zn and Me_3SiCl is capable of reductive dimerization of aldehydes. The catalytic cycle is completed by the addition of stoichiometric amount of Zn metal as a co-reductant and chlorosilane to

regenerate the metal. Highest diastereoselectivity was observed with for the aldehyde where the substituent R is $PhCH_2CH_2$. The main advantage of the catalytic system is the use of low valent Vanadium metal and low temperature reactions, but the use of stoichiometric amount of co-reductant, use of aprotic solvent is somewhat disadvantage for this method.

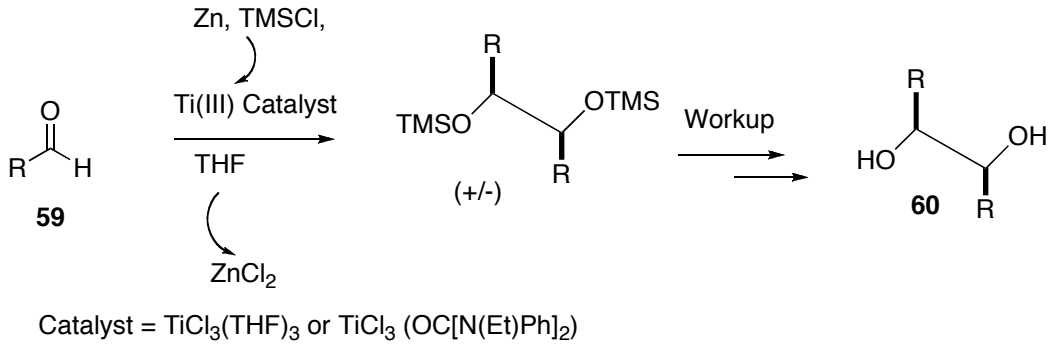

Scheme 2.5 Ligand modified catalysis for McMurrey pinacol coupling reaction

In 1998, Hirao et al, have reported the Ti(III) catalyzed highly diastereoselective pinacol coupling reaction for the formation of DL-1,2-diols using THF as a solvent instead of DME (**scheme 2.5**).[62] In this, approach they have observed the formation of only DL-1,2-diols from secondary aliphatic aldehydes without formation of any olefinic products and 1,3-dioxalones. They have also observed the decrease in the yield and diastereoselcetivity at elevated temperatures. The diastereoselctivity depends on chlorosilanes and is enhanced by using $PhMe_2SiCl$ in place of Me_3SiCl. Diastereoselctivitie and % yield of the products summarized in **Table 2.2**. The main disadvantage of the method is the use of stoichiometric amount of coreductant and aprotic organic solvent.

entry	substrate **59**	% yield	*dl*:meso **60**
1	C_6H_5CHO	90	69:31
2	p-BrC_6H_4CHO	95	55:45
3	$C_6H_{11}CHO$	85	83:17
4	$PhCH_2CH_2CHO$	79	74:26
5	Me_2CHCH_2CHO	76	67:33
6	$C_6H_5COCH_3$	67	67:33
7	2-$C_{10}H_7COCH_3$	84	62:38

Table 2.2 Ti(III) Catalyzed pinacol coupling of aldehydes and ketones

In 1999, Hirao et al, (**Scheme 2.6**)[63] have reported another important

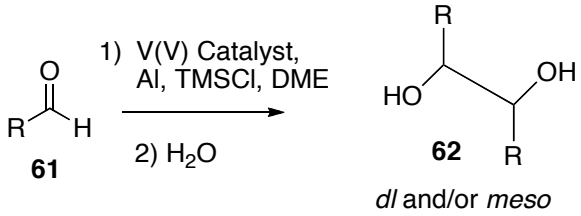

Scheme 2.6 V(V) catalyzed stereoselective coipling of benzaldehyde derivatives

highly diastereoselective catalytic pinacol coupling reaction of benzaldehyde derivatives in presence of vanadium metal, chlorosilane and aluminum metal as a co-reductant in DME solvent. They have investigated various vanadium catalysts VCl_3, Cp_2VCl_2, $VOCl_3$ etc, in presence of Mn or Mg or Zn or Al as co-reductant along with TMSCl in THF or DME solvent.

entry	R **61**	% yield	*dl*/*meso* **62**
1	C_6H_5	68	>95/5
2	p-MeC_6H_4	62	>95/5
3	p-ClC_6H_4	89	>95/5
4	p-$MeOC_6H_4$	49	90/10
5	m-ClC_6H_4	77	>95/5
6	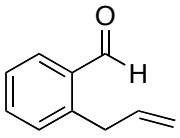	84	>95/5

Table 2.3 Pinacol coupling of various benzaldehyde derivatives in presence of 5 mol% of V(V) (for 3.3 mmol benzaldehyde), TMSCl (6.6 mmol) , Al (6.6 mmol) and DME (10 ml) as solvent, at 50 ^{o}C, 24 h.

The oxovanadium $VOCl_3$, which is widely accepted as a one-electron oxidant, was found to catalyze a highly selective pinacol coupling of benzaldehyde in the presence of Al powder and Me_3SiCl. This result suggests that an active low-valent vanadium species may be generated in situ through reduction of the oxovanadium(V) with Al. The diastereoselectivity was improved under the optimized conditions, and this system was successfully applied to a variety of aromatic aldehydes to produce the corresponding 1,2-diols in good yields with excellent selectivity, as summarized in **Table 2.3**. The stereoselectivity for the formation of diols can be explained by the **Scheme 2.7.** In which a cyclic intermediate is suggested to favor the formation of the *dl*-isomer. On the other hand, an acyclic intermediate is proposed to give *meso*-

selectivity.

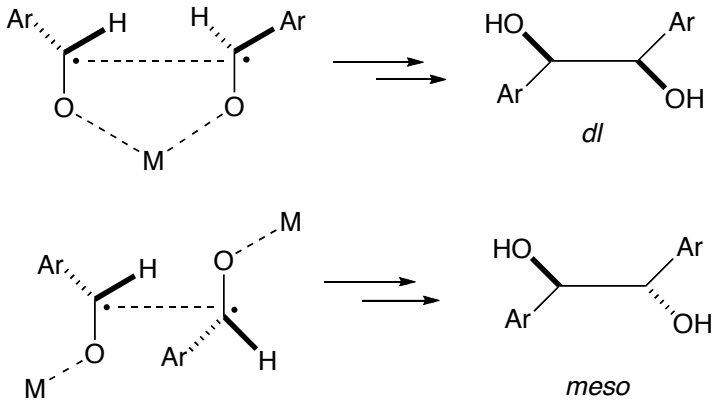

Where M = Metal, Ar = Phenyl derivative

Scheme 2.7 Schemetic representation of diastereoselectivity in pinacol coupling reaction catalyzed by V(V) metal in presence of Al as co- reductant

For enantioselective pinacol coupling reactions, in 2000, Halterman et al,[64] reported a catalytic system based on chiral titanocene dichloride catalysts. They have synthesized chiral titanocene complexes of bis(indenyl) **63** and bis(tetrahydroindenyl) **64** compounds (**Scheme 2.8**) and investigated the enantioselectivities for the pinacol coupling reactions of benzaldehyde.

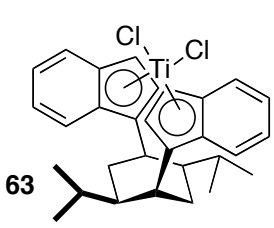

bis(indenyl)titanium dichloride

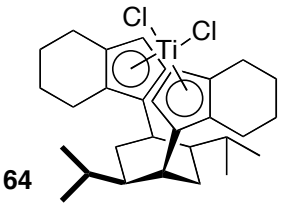

bis(tetrahydroindenyl)
titanium dichloride

Scheme 2.8 Titanocene catalysts for enantioselective pinacol coupling reaction of benzaldehyde

When the pinacol coupling is run using manganese metal as the stoichiometric reductant and TMSCl in THF at room temperature, it was catalytic in titanocene dichloride producing a mixture of unreacted aldehyde and *meso*- and *dl*-silyl ethers (**Scheme 2.9**). The silyl ethers were desilylated using tetrabutylammonium fluoride to give a *meso/dl* mixture of diols and the enantiomeric purity of these diols were analyzed by chiral HPLC. The bis(indenyl) **63** complex was slightly more selective for the dl isomer (4.6:1, 0 % ee) than was the bis(tetrahydroindenyl) **64** complex (3.4:1,), but only the bis(tetrahydroindenyl) complex produced enantiomerically enriched diol (32% ee), therefore one can postulate that the tetrahydroindenyl ligand provides more steric hindrance in the vicinity of the active site than does the indenyl ligand. This method provies some extent of enatioselectivity but there are some drawbacks in this method that the use of excess of Mn and TMSCl and low % yield of pinacol products (1:3 and 1:4 ratios of product: benzaldehyde for bis(indenyl and bis(tetrahydroindenyl) complexes respectively).

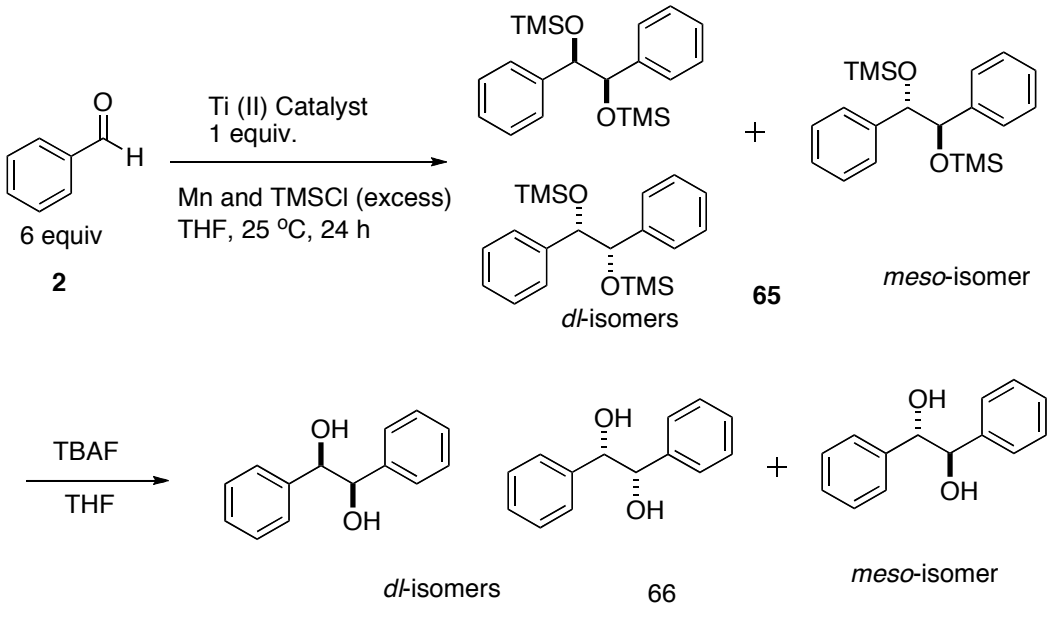

Scheme 2.9 Enantioselectivity in pinacol coupling reactions by Titanocene complexes in THF solvent at room temperature

So far, highest enantioselcetivities in pinacol coupling reactions were achieved by the use of titanium-catalyzed enantioselective coupling reaction of aromatic aldehydes using chiral salen lignads. By this method, high yields and highest enantioselectivities up to 91% were achieved.[65]

2.2.2 Catalytic systems for Pinacol coupling reactions in water

In recent years organic reactions in water or aqueous media has attracted great interest in organic synthesis from the vantage points of its cost, safety, and environmental concern. Therefore, the development of an efficient synthetic methodology to form a carbon-carbon bond in water or aqueous media has attracted great interest in synthetic organic chemists. On the basis of the importance of the pinacol coupling reactions in water, there have been some reports on the pinacol reactions in aqueous media, but these protocols require a stoichiometric metallic reductant with an acid or base activator, or a stoichiometric metallic reductant generated by treatment with a metallic co-reductant.[66]

In 2005, Hirao et al, have successfully developed a catalytic pinacol coupling for the first time using a ternary catalytic system consisting of a vanadium catalyst, a metallic co-reductant and a chlorosilane to recycle the catalyst.[67]

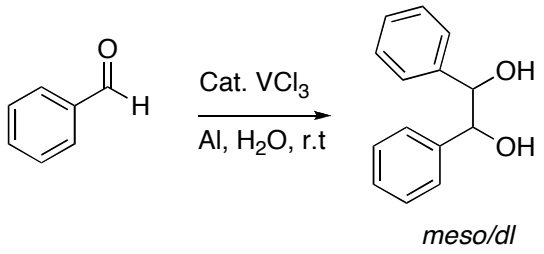

Scheme 2.10 Binary catalytic system for pinacol coupling reaction using VCl_3 catalyst in presence of Al as a co-reductant in water

Based on this idea, In 2005, they developed a binary catalytic system consisting of metal catalyst, and a metallic co-reductant in water (**Scheme 2.10**).[68] The catalytic cycle for the binary system is in **Scheme 2.11**, in which the metal reduce the aldehyde to form dimerized product (pinacol), then the oxidized metal can be reduced back by metallic co-reductant in water without addition of chlorosilane.

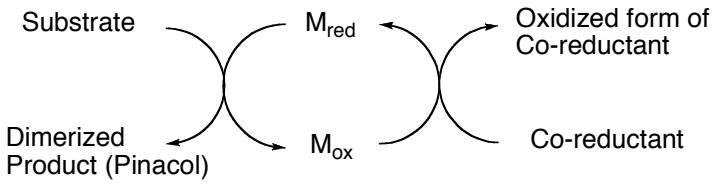

Scheme 2.11 Catalytic cycle in binary catalyst system

Using vanadium salts as a stoichiometric promoter, they first studied the effect of metallic co-reductants (Zn, Mg, Mn and Al) and solvent on the pinacol coupling reaction of benzaldehyde. They found that the combination of VCl_3 and Al was found to be a more efficient system to promote the pinacol coupling in water and there is no effect in the catalytic reactivity by the

addition of additives such as ethylene glycol, and α or β cyclodextrines.

The best catalytic system found to be the use of 0.33 mmol of VCl_3 in presence of Al as a co-reductant in water at room temperature (**Scheme 2.12**) and the results are summarized in the **Table 2.4**. It is note worthy to say that the catalytic pinacol coupling reaction successfully proceeded in water even in the absence of chlorosilane. It is in sharp contrast to the reaction in organic solvent,

entry	substrate	Metallic coreductant	solvent	time (days)	Isolated yield (pinacol product)	*dl*/*meso*
1	PhCHO	Zn	H_2O	3	75	51/49
2	PhCHO	Al	H_2O	3	92	56/44
3	3-ClPhCHO	Al	H_2O	4	79	45/55
4	4-MePhCHO	Al	H_2O	4	84	62/38
5	2-ClPhCHO	Al	H_2O	4	62	42/58
6	2-BrPhCHO	Al	H_2O	5	53	56/44
7	4-ClPhCHO	Al	H_2O	3.5	68	54/46
8	4MeOPhCHO	Al	H_2O	4	51	59/41
9	2furaldehyde	Al	H_2O	3	62	71/29
10	$PhCOCH_3$	Al	H_2O	3	0	-
11	PhCHO	Al	H_2O	3	65	59/41
12	3-ClPhCHO	Al	H_2O	3	66	50/50

13	4-MePhCHO	Al	H_2O	4	59	62/38

Table 2.4 Cat. VCl_3/Al Catalyzed pinacol coupling reaction of various benzaldehyde derivatives in water

which requires a chlorosilane as an additive and Al found to be the best over Zn as a co-reductant.Various aromatic aldehydes underwent the reductive coupling with this catalytic system in water to give moderate to good yields and little high

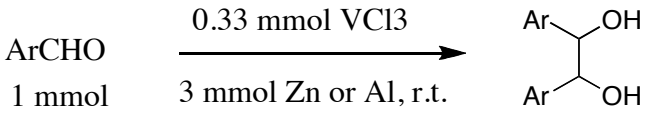

Scheme 2.12 Binary catalytic system for pinacol coupling reactions in water

dl selectivity was observed for the aromatic aldehydes bearing an electron-donating group. Therefore this method is synthetically versatile for the carbon-carbon bond formation reactions in water.

2.3 $CrCl_2$ catalyzed pinacol coupling of benzaldehyde in water[69]

2.3.1 Improved catalytic system

This work was published in a full paper in the Tetrahedron Letters.[69] Binary catalytic system developed by Hirao et al,[70] consisting of metal catalyst, and a metallic co-reductant in water has some disadvantage of using stoichiometric amounts of co-reductant and longer reaction times etc. Therefore, we have initiated an investigation of chromium salts as effective catalysts for dimerization of benzaldehyde in aqueous media, in order to extend the scope of reductive coupling reactions in water (**Scheme 2.13**).

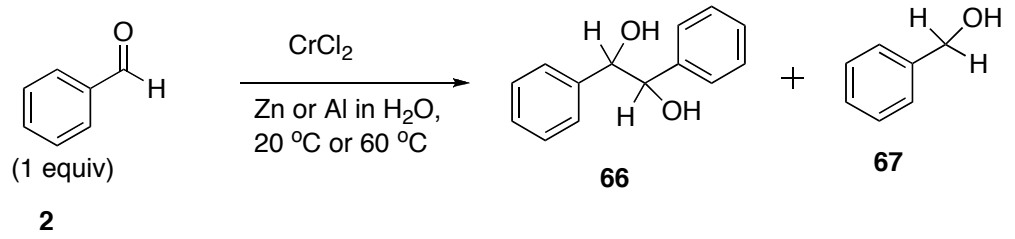

Scheme 2.13 $CrCl_2$ catalyzed pinacol coupling of benzaldehyde in water in the presence of Zn^0 or Al^0.

Since the chromium catalysts have been effectively used in ternary catalytic system for dimerization reactions in aprotic solvents and a very good variety of low valent chromium-ligand complexes are known. Therefore, the initial thought was likely that, we could attach appropriate chromium species to heterogenous supports. The main advantage of the use of heterogeneous catalysts in aqueous media would facilitate the removal of the catalyst and potentially improve the cost efficiency and environmeltal impact of chromium in pinacol coupling reactions.

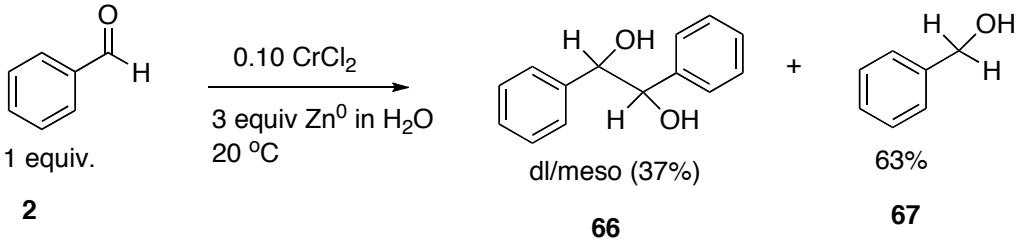

Scheme 2.14. Pinacol coupling of benzaldehyde by Cr(II)/Zn(0) catalyst system in water.

Initially we have examined the reductive coupling of benzaldehyde **2** (0.25 M) in water with the use of 10 mol% $CrCl_2$ and excess amount of Zinc-

dust at ~ 20 ºC. We were gratified to observe the formation of diol **66** in a product ratio of 37% in a *dl*-/*meso* diastereomeric ratio of 0.7:1 along with the direct reduction product benzyl alcohol **67** in about 63% of product ratio (**Scheme 2.14**), and also some unreacted benzaldehyde (recovered). The formation of dimerized product and the diastereoemric ratios, as well as the formation of benzylalcohol was monitored and confirmed by ^{1}H NMR spectroscopy. The ^{1}H NMR spectrum of reaction mixture is shown in **Figure 2.1** and in which the d*l*-1 (**66**) and *meso*-1 (**66**) product signals for the benzylic CH groups of dimerized product are very well separated. But the benzylic methylene proton signal of the benzyl alcohol **67** is quite close to the *meso*-1 (**66**), and is partially overlapped. Therefore giving some uncertainity in determining the product ratios.

According to the catalytic cycle depicted in the **Scheme 2.15**, chromium(II) can initially reduce the aldehyde (step a) to form radical intermediate **68.** The reactive carbon site in **68** can combine with a second aldehyde unit (either before or after its reduction) as in step b to form coupled product **69**. Hydrolysis to release the 1,2-diol and reduction of the chromium species back to a lower valent metal as in step c completes the desired catalytic cycle.

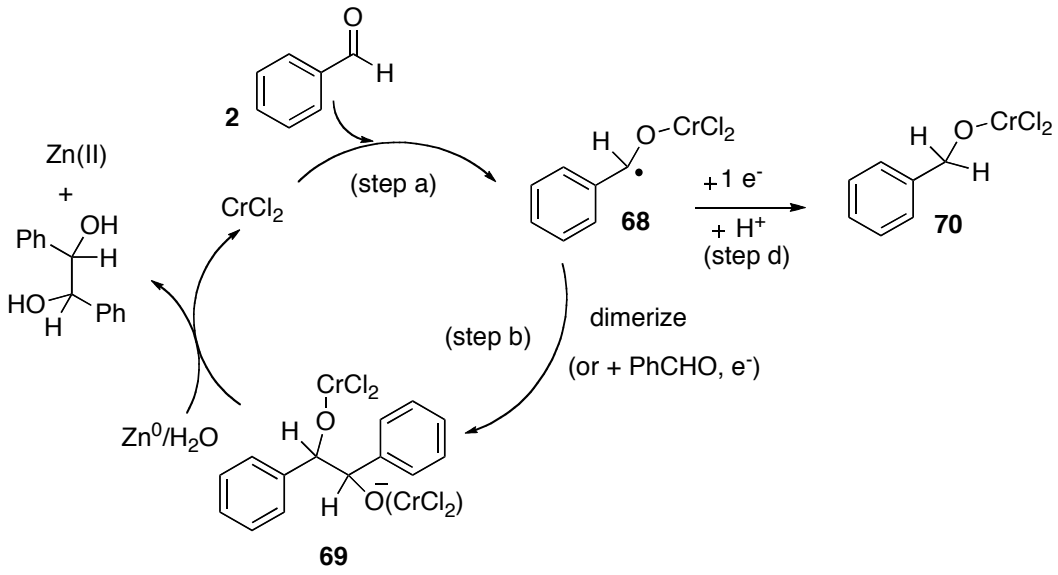

Scheme 2.15 Catalytic cycle for Cr(II)/Zn(0)-catalyzed pinacol reaction with competitive benzaldehyde reduction.

However, intermediate **68** can be further reduced by a second electron from a co-ordinated chromium (III) or by an electron from an external metal as in step d. This competitive side reaction can lead to the formation of the undesired reduced benzyl alkoxide **70** that can hydrolize to form benzyl alcohol **67**. Then, the effects of varying the concentration of the reacting species, the ratio of catalyst, the temperature and the stoichiometric reductant on the formation of the desired 1,2-diol product were studied. The results are summarized in the Table **2.5a**.

In control reactions with no chromium catalyst present neither reduction nor pinacol coupling products were observed in the presence of Zn-dust (entries 1 and 2). During the standard reaction time of 20 h the reactions consumed nearly all benzaldehyde at 20 °C or at 60 °C in the presence of Zn-dust (entries 3–8) when the starting benzaldehyde concentration was 0.25 M in

water. The reactions proceeded to complete consumption of benzaldehyde at 20 °C, when the concentration of the reagents and catalyst were increased fivefold (compare entries 9–11 with 3–5). In the presence of Al as the stoichiometric reductant, only the reaction at 60 °C was effective (**entries 12 and 13**). We have also noted that the observation of the incomplete reactions were due to the improper or not enough stirring of the reaction mixtures. We have also observed that, the formation of benzyl alcohol, in terms of the chemical selectivity for the dimerization versus benzylalcohol formation is always major product in all cases. Under most conditions, the ratio of dimerized product (pinacol) to benzyl alcohol is about 1:1 to 1:2. Lower selectivity for the pinacol product was observed at elevated temperatures and higher ratio of starting chromium catalyst loadings. The diastereoselectivity of the pinacol coupling reaction for *dl*-1 (**66**) versus *meso*-1 (**66**) is 0.6:1 to 1:1 (**Table 2.5b**). Therefore, this catalytic system is somewhat diastereoselcetive in favor of meso-product formation. We have also observed the stereoselectivity in terms of metal co-reductan. In which, the use of aluminum versus zinc at stoichiometric amounts gave the same stereoselectivity.

Entry	$CrCl_2$[a]	[PhCHO]	Metal Reductant[b]	Temp	Recovered PhCHO
1	0	0.25 M	3 equiv Zc	20 °C	100%
2	0	0.25 M	3 equiv Zc	60 °C	100%
3	5	0.25 M	3 equiv Zn	20 °C	ca. 5%
4	10	0.25 M	3 equiv Zn	20 °C	ca. 5%
5	25	0.25 M	3 equiv Zn	20 °C	ca. 5%
6	5	0.25 M	3 equiv Zn	60 °C	ca. 5%
7	10	0.25 M	3 equiv Zn	60 °C	ca. 5%
8	25	0.25 M	3 equiv Zn	60 °C	ca. 5%
9	5	1.25 M	3 equiv Zn	20 °C	<1%
10	10	1.25 M	3 equiv Zn	20 °C	<1%
11	25	1.25 M	3 equiv Zn	20 °C	<1%
12	10	0.25 M	3 equiv Al	20 °C	90%
13	10	0.25 M	3 equiv Al	60 °C	ca. 5%

Entry	% dl-1[c] (66)	% meso-1 (66)	% 67 ($PhCH_2OH$)	dl-/meso-	66/67
1	0	0	0	--	--
2	0	0	0	--	--
3	18	23	59	0.8	0.6
4	14	23	63	0.6	0.7
5	25	28	27	0.9	0.8
6	19	20	61	1.0	0.7
7	20	23	57	0.9	0.8
8	6	11	83	0.6	0.2
9	15	18	67	0.8	0.5
10	14	19	67	0.7	0.5
11	21	23	56	0.9	0.8
12	n.d.	n.d.	n.d.	n.d.	n.d.
13	22	25	53	0.9	0.9

Table 2.5a (top) and 2.5b (bottom). a = Mole% of $CrCl_2$ relative to benzaldehyde, b = equivalent of metal reductant relative to benzaldehyde. c = percentages of products as relative product abundance in ^1H NMR spectrum.

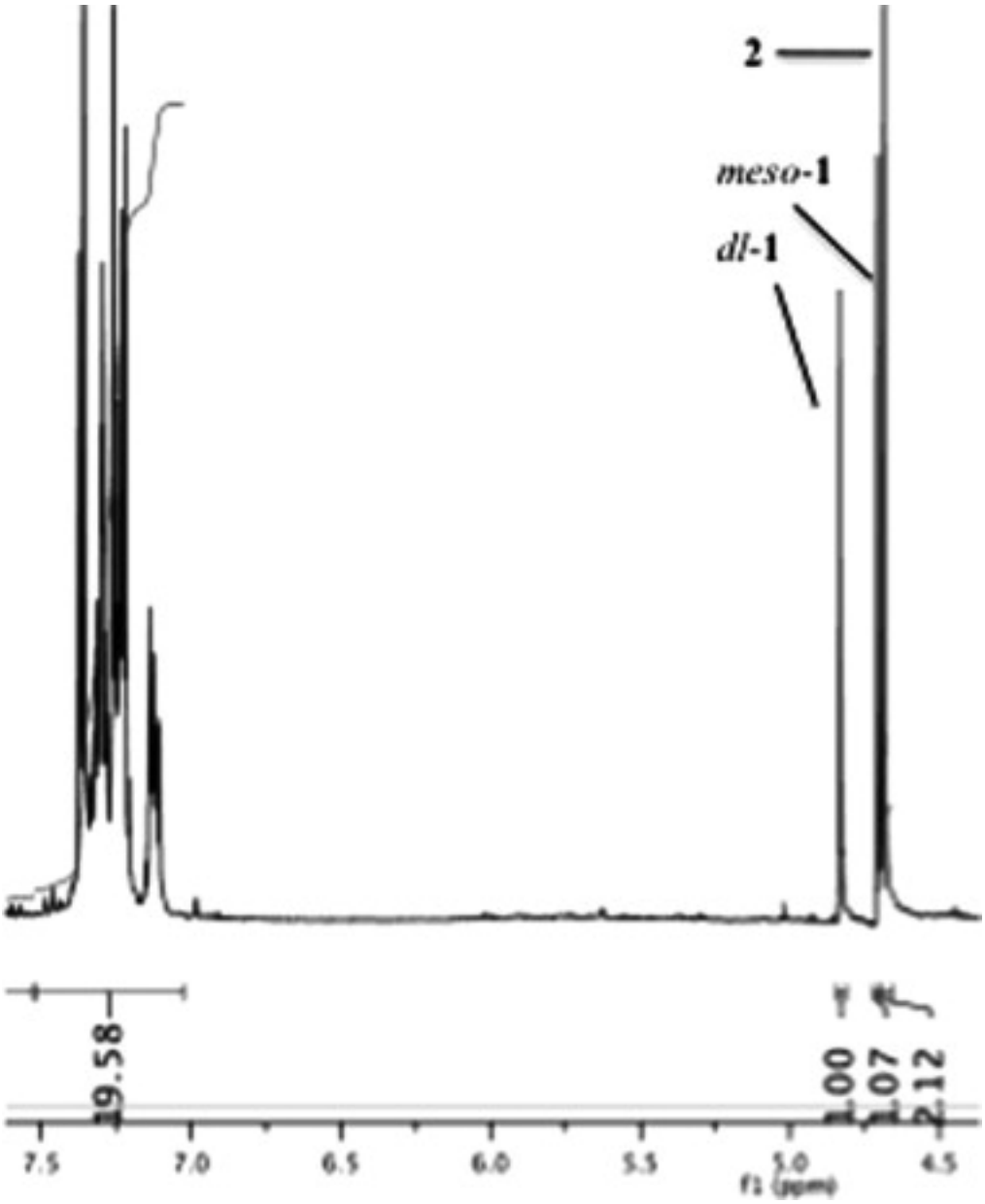

Figure 2.1 Figure 3. ^{1}H NMR spectrum of pinacol reaction mixture (where *dl*-1, *meso*-1 = **66** and 2 = **67**).[69]

2.4 Use of Pinacol Coupling Reactions in Biofuel Applications

Throughout most of the human history, renewable biomass resources have been the primary industrial and consumer feedstocks.[71] With advances in conversion technology, plentiful biomass resources have the potential to regain

their central position as feedstocks for civilization, particularly as renewable carbon sources for transportation fuels and chemicals. A hexose dehydration product (**Scheme 2.16**), the platform chemical 5-hydroxymethylfurfural (HMF), will be a key player in the biobased renaissance. This six-carbon analogue of commodity chemicals like terephthalic acid and hexamethylenediamine can be converted by straightforward methods into a variety of useful acids, aldehydes, alcohols, and amines, as well as the promising fuel 2,5- dimethylfuran (DMF). The conversion of biomass-derived oxygenates to fuels and chemicals involves the combination and/or coupling of various type of reactions, including hydrolysis, dehydration, reforming, C-C hydrogenolysis, hydrogenation, aldol condensation and selective oxidation reactions.[72]

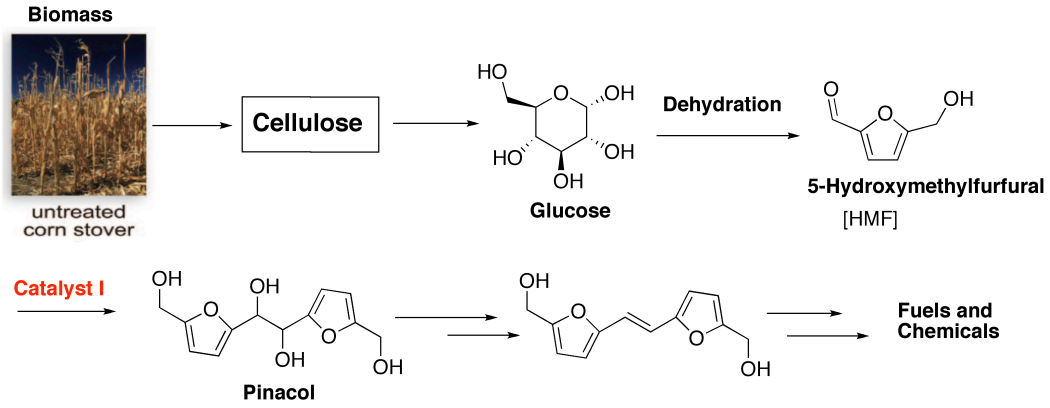

Scheme 2.16 Schematic representaion of conversion of biomass into value added chmicals and fuels.[73]

The development of a new catalytic system that converts the 5-hydroxymethylfurfural (HMF) and its derivatives into larger molecules (1,2-diols) is one of the important and challenging processes in organic synthesis

and catalysis. The resulting 1,2-diols could also be further converted into fuels and chemicals by various methods such as deoxydehydration to give unsaturated compounds that could further be converted into saturated high molecular weight hydrocarbons that would be more valuable as fuels. Therefore, to achieve the goal of dimerization of 5-hydroxymethylfurfural (HMF) and similar compounds, we are investigating to find best catalytic system for the dimerization in water (Halterman et al., *Tetrahedron letters*, 2009). Initially we have reported a binary catalytic system for the dimerization of benzaldehyde in water while investigating to synthesize a supramolecular catalyst for the dimerization in water.

2.5 Conclusion

We have shown that chromium salts will catalyze the pinacol coupling of benzaldehyde in water in the presence of zinc or aluminum as terminal reductants. Gratifyingly, the best pinacol/benzyl alcohol ratios were obtained with the lowest chromium catalyst ratios. It was still disappointing that the benzyl alcohol reduction product was in each case the major product of the reaction. Given this promising entry into a catalytic coupling reaction in water, we are next pursuing the reactivity of different ligand systems on chromium to see if the changes in the metal ligation can lead to more selectivity for the coupling reaction. We also plan to extend our investigation to include the coupling of different aromatic as well as aliphatic aldehydes.

However, to achieve the dimerization of high molecular weight

aldehydes (HMF in **Scheme 2.17**) into 1,2-diols using less expensive and environmentally free catalytic system is still a challenging tosk in the field of catalysis. Therefore, design of supramolecular catalysts (**Catalyst 1** in **Scheme 2.17**) that are water-soluble and bind the substrates effectively by hydrophobic and noncovalent interactions could be the best way to improve the productivity of dimerized products from readily available starting materials such as bio-feed stocks.

2.6 Experimental procedure[69]

A suspension of zinc powder (3.0 mmol, 196 mg) and $CrCl_2$ (0.10 mmol, 12.3 mg) in water (4 mL) was stirred at 20 °C for about 5 min under a nitrogen atmosphere. Distilled benzaldehyde **2** (1.0 mmol, 100 μL) was added to the mixture which was then stirred vigorously for 20 h. (For the heated reactions, the reaction flask was placed in a silicon oil bath at 60 °C immediately following the addition of the benzaldehyde.) The reactions were quenched with 1 N HCl (5 mL), additional water (4 mL) was added, and the mixture was extracted with ether (3 × 20 mL). The combined organic layers were dried with magnesium sulfate and filtered. The filtrate was concentrated under reduced pressure to give the crude product mixture (ca. 90% mass recovery), which was analyzed by ^{1}H NMR spectroscopy in $CDCl_3$. The diagnostic benzylic hydrogen signals for *meso*-**1 (66)** at 4.84 ppm, *dl*-**1 (66)** at 4.72 ppm, and benzyl alcohol at 4.67 ppm were used in conjunction with the

total aromatic region 7.1–7.35 ppm to calculate product ratios.

2.7 References

57. Hirao, T. Catalytic Reductive Coupling of Carbonyl Compounds- The Pinacol coupling reaction and beyond. *Top. Curr. Chem*, **2007**, *279*, 53-75.

58. Kozikowski, A. P.; Wu, J. P.; Shibuya, M.; Floss, H. G. Probing ergot alkaloid biosynthesis: identification of advanced intermediates along the biosynthetic pathway, *J. Am. Chem. Soc*. **1988**, *110*, 1970-1971.

59. Nicolaou, K.C.; Liu, J-J.; Yang, Z.; Ueno, H.; Guy, R.K.; Sorensen, E. J.; Claiborne, C. F.; Hwang, C-K.; Nakada, M.; Nantermet, P. G. Total Synthesis of taxol. 2. Construction of A and C ring intermediates and initial attempts to construct the ABC ring system, *J. Am. Chem. Soc*. **1995**, *117*, 634-644; Kammermeier, B.; Beck, G.; Holla, W.; Jacobi, D.; Napierski, B.; Jendralla, H. Vanadium(II)- and Niobium(III)-Induced, Diastereoselective Pinacol Coupling of Peptide Aldehydes to Give a *C*2-Symmetrical HIV Protease Inhibitor, *Chem. Eur. J*. **1996**, *2*, 307-315.

60. Park, J.; Pedersen, S. F. A stereospecific synthesis of 3,3-disubstituted allylic alcohols. The intermolecular pinacol cross-coupling reaction between α,α-disubstituted-α-(diphenylphosphinoyl)acetaldehydes [$Ph_2P(O)CR1R_2CHO$] and saturated aldehyde, *J. Org. Chem*. **1990**, *55*, 5924 – 5926; Konradi, A.W.; Kemp, S. J.; Pedersen, S. F. Pinacol Cross Coupling of 2-[N-(Alkoxycarbonyl)amino] Aldehydes and Aliphatic Aldehydes by

$[V_2Cl_3(THF)_6]_2[Zn_2Cl_6]$. Synthesis of syn, syn-3-[N-(Alkoxycarbonyl)amino] 1,2-Diols, *J. Am. Chem. Soc*, **1994**, *116*, 1316-1323.

61. Hirao, T.; Hasegawa, T.; Muguruma, Y.; Ykeda, I. A Novel Catalytic System for One-Electron Reduction. Low Valent Vanadium-Catalyzed Coupling of Aldehydes, *J. Org. Chem*. **1996**, *61,* 366-367.

62. Hirao, T.; Asahara, M.; Muguruma, Y.; Ogawa, A. Ligand-Modified Catalysts for the McMurry Pinacol Reaction, *J. Org. Chem*. **1998**, *62*, 4566-4567.

63. Hirao, T.; Hatano, B.; Imamoto, Y.; Ogawa, A. A Catalytic System Consisting of Vanadium, Chlorosilane, and Aluminum Metal in the Stereoselective Pinacol Coupling Reaction of Benzaldehyde Derivatives, *J. Org. Chem*. **1999**, *64*, 7665-7667.

64. Halterman, R. L.; Zhu, C.; Chen, Z.; Dunlap, M. S.; Khan, M. A.; Nicholas, K. M. Preparation of [2,5-Diisopropylcyclohexane-1,4- bis(indenyl)]titanium Dichloride and [2,5-Diisopropylcyclohexane-1,4-bis(tetrahydroindenyl)]-titanium Dichloride and Their Comparison as Catalysts for the Enantioselective Pinacol Coupling of Benzaldehyde, *Organometallics*, **2000**, *19*, 3824-3829.

65. Bensari, A.; Renaud, J-L.; Riant, O. Enantioselective Pinacol Coupling of Aldehydes Mediated and Catalyzed by Chiral Titanium Complexes, *Org Lett*, **2001**, *3*, 3863-3865.

66. Matsukawa, S.; Hinakubo, Y. Samarium(II)-Mediated Pinacol Coupling in Water: Occurrence of Unexpected Disproportionation and Action of Low-Valent Samarium as an Active Species, *Org. Lett*. **2003**, *5*, 1221 – 1223,

Mecarova, M.; Toma, S. Optimization of pinacol coupling in aqueous media, *Green Chem.* **1999**, *1*, 257.

67. Hirao, T.; Ogawa, A.; Asahara, M.; Muguruma, Y.; Sakurai, H. *dl*-Selective Pinacol-type Coupling Using Zinc, Chlorosialne, and Catalytic Amounts of Cp_2VCl_2; *dl*-1,2-(1,2-Ethanediol,1,2-dicyclohexyl-), , *Org. Synth.* **2005**, *8*, 26.

68. Xu, X.; Hirao, T. Vanadium-Catalyzed Pinacol Coupling Reaction in Water *J. Org. Chem.* 2**005**, *70*, 8594-8596.

69. Halterman, R.L.; Porterfield, J. P.; Mekala, S. Chromium-catalyzed pinacol coupling of benzaldehyde in water *Tetrahedron Letters*, **2009**, *50*, 7172-7174.

70. Xu, X.; Hirao, T. *J.* Vanadium-Catalyzed Pinacol Coupling Reaction in Water, *Org. Chem.* **2005**, *70*, 8594-8596.

71. Binder, J. B.; Raines, R. T. Simple Chemical Transformation of Lignocellulosic Biomass into Furans for Fuels and Chemicals, *J. Am. Chem. Soc.* **2009,** *131*, 1979–1985.

72. Binder, J. B.; Raines, R. T. Simple Chemical Transformation of Lignocellulosic Biomass into Furans for Fuels and Chemicals, *J. Am. Chem. Soc.* **2009**, *131*, 1979–1985.

73. Chheda, J. N.; Huber, G. W.; Dsumesic, J. A. Liquid-Phase Catalytic Processing of Biomass-Derived Oxygenated Hydrocarbons to Fuels and Chemicals, *Angew. Chem. Int Ed.* **2007**, *46,* 7164.

CHAPTER 3

Dynamic Combinatorial Chemistry for *meso*-Tetra (*o*-aminophenyl)porphyrins: a supramoelcualr catalyst design

3.1 Introduction to Dynamic Combinatorial Chemistry (DCC)

Dynamic combinatorial chemistry (DCC) is defined as combinatorial chemistry under thermodynamic control, that is, in a dynamic combinatorial library (DCL), all constituents are in equilibrium.[74] The dynamic combinatorial library requires the interconversion of library members into one another through a reversible chemical processes through covalent or non-covalent interactions. The composition of the library is determined by the thermodynamic stability of each of the library members under given conditions such as temperature, pressure, light and electric or magnetic fields or a template. The structures that have the most favorable internal non-covalent interactions will be stabilized and formed in preference of those library members that lack such stabilization, which means that the application of an external stimulus to the library members may shift the equilibrium to favor a specific product or a building block. This may be due to the interactions between the template and a member of the library.

If a template preferentially removes a product form the library, then the library will respond to the perturbation in the position of the equilibrium by producing more of that product, this concept is termed as amplification in the Dynamic Combinatorial Chemistry (**Scheme 3.1**).[75] Therefore, the Dynamic Combinatorial Chemistry (DCC) is one of the most powerful and emerging

techniques in the field of organic chemistry for the discovery of molecules with specific functional characteristics, such as receptors, inhibitors, drugs and catalysts.

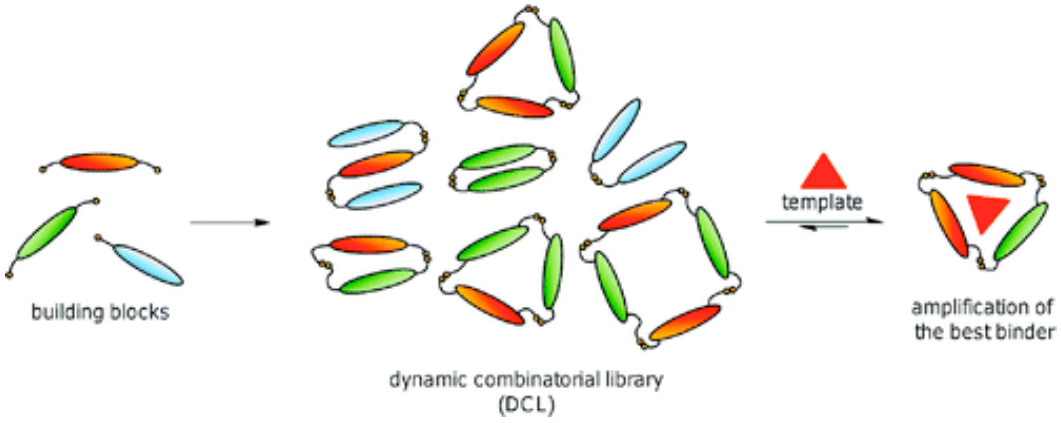

Scheme 3.1 Schematic representation of a dynamic combinatorial library and amplification of the best binder in the presence of a template.[76]

During the past decade, Dynamic Combinatorial Chemistry (DCC) has been established as a component to combinatorial synthesis for the identification of biologically or catalytically active small molecule ligands in drug discovery and receptor design as well as in catalysis.[77] In a combinatorial library, the reactions were set by introducing complementary building blocks bearing structural units or functional groups known to selectively interact with the target receptor in a particular spacial arrangement. Whereas in combinatorial synthesis a large number of structurally different compounds are statistically synthesized based on irreversible reactions. In the combinatorial synthesis, the concept 'molecular evolution' allows the selective formation of

the compound with the most favorable interaction with the receptor as the major product in an equilibrium mixture of compounds. The identification of an active compound in the compound libraries obtained by the combinatorial synthesis is a tedious, laborious and time-consuming process, whereas in the dynamic combinatorial libraries (DCCs), the act of forming only one or a few predominant compounds from all of the theoretically possible combinations of reagents (called as a virtual library by J.M-Lehn) considerably facilitates the identification and isolation form the compound mixture.[78]. Therefore, the Dynamic Combinatorial Chemistry is the more powerful and emerging methodology in organic synthesis and catalyst development.

3.2 Exchange reactions in Dynamic Combinatorial Chemistry (DCC)

Reversible reaction is the key feature of the dynamic combinatorial chemistry that mediates exchange of the building blocks between the different library members. The main requirements for the reversible reactions in dynamic combinatorial chemistry are a) it must be reversible; b) the equilibration and the selection ideally occur simultaneously, therefore the reversible reaction needs to be compatible with the experimental conditions of the selection process; c) reaction conditions needs to be mild; d) it needs to guarantee the solubility of all the library members at equilibrium because any insoluble or insufficient soluble material will disrupt the equilibrium; e) it should be possible to turn off the reaction so as to kinetically 'freeze' the selected library members enabling their isolation and handling; f) all library

members should be isoenergetic in order to prevent the production of reaction mixtures.

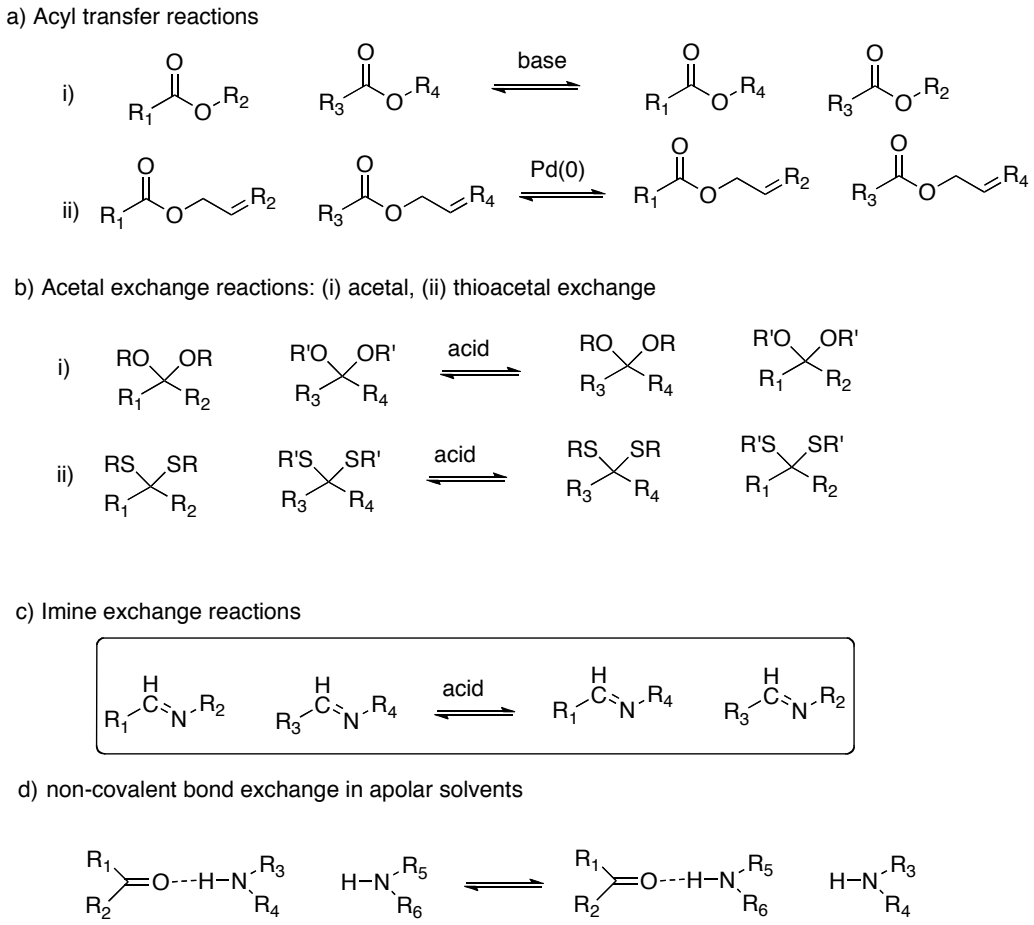

Scheme 3.2 Reversible reactions most often used in Dynamic Combinatorial Chemistry

Three main types of bonds have been used to date in reversible reactions[79] a) non-covalent (hydrogen bonds), b) covalent bonds and c) coordination bonds. The list of reversible covalent bond reactions for DCL is somewhat short, which include imine exchange, acyl transfer related, acetyl transfer related and other type of exchanges such as disulfide exchange reactions (**Scheme 3.2**). Although these reactions by no means represent the

entire possible range of available exchange reactions for DCL, but they constitute the predominance in the literature of DCL chemistry.

Among the mentioned series of possible reactions, the formation of imines by reaction of carbonyl compounds with amine derivatives in an aqueous environment[80] is one of the most widely used examples of dynamic combinatorial library set-up by covalent bond formation. Generally, acid catalyzed, pH- and temperature dependent reactions proceed upon loss of water molecule. For preparative purposes water has to be removed from the system in order for the reaction to proceed forward. Furthermore, in aqueous media the reaction is reversible and reaches equilibrium. In terms of formation of DCLs, the formation of imines (Schiff bases) has several practical advantages. The most important point is, it tolerates a broad variety of substituents allowing the generation of DCLs with a broad structural diversity. The other advantage is, the relative rate of the product formation and the position of the equilibrium depend on the pH, which can be generally adjusted to a given value. Finally, once the mixture has equilibrated, the imine double bond can be reduced, which disrupts the equilibrium and allows the isolation and characterization of individual compounds.

3.3 Multiple exchange reactions in Dynamic Combinatorial Chemistry

There are some advantages for the DCL having more than one exchange reaction, but also brings with it some additional complications in addressing the chemistries independently. The possibility arises for an

evolutionary approach of an orthogonal library, when multiple exchange processes are used is: each reversible chemistry can carry its own dimension in structural space, and these dimensions can be explored alternatingly, keeping one dimension constant which means the exchange process is switched off, while exploring the other process switched on and vice versa. The other advantage of the DCL with multiple exchange processes is the extension of the diversity within the libraries, since multiple linkages hold the building blocks together.

So far, there are only three examples on orthogonal libraries reported by a) Lehn et. al.,[81a] b) Leclaire et. al,[81b] and c) Furlan et. al.,[81c] to address the properties of multiple exchange reactions in a given DCL, which means each reversible reaction used can be activated under different conditions, such setup allows the manipulation of the reactions in a sequential order. In Lehn's orthogonal library (**Scheme 3.3**), the first process is the formation of cobalt complexes with terpyridine-based ligands, and the second is imine formation with aldehyde substituents on the terpyridine moities. The first exchange process is the metal-ligand exchange, which can be stopped by oxidation of Co(II) to Co(III) complex. The second process is the imine exchange reaction, which can be activated by lowering the pH to below 3.0 and heating to 60 ^{o}C in the presence of different pool of amines.

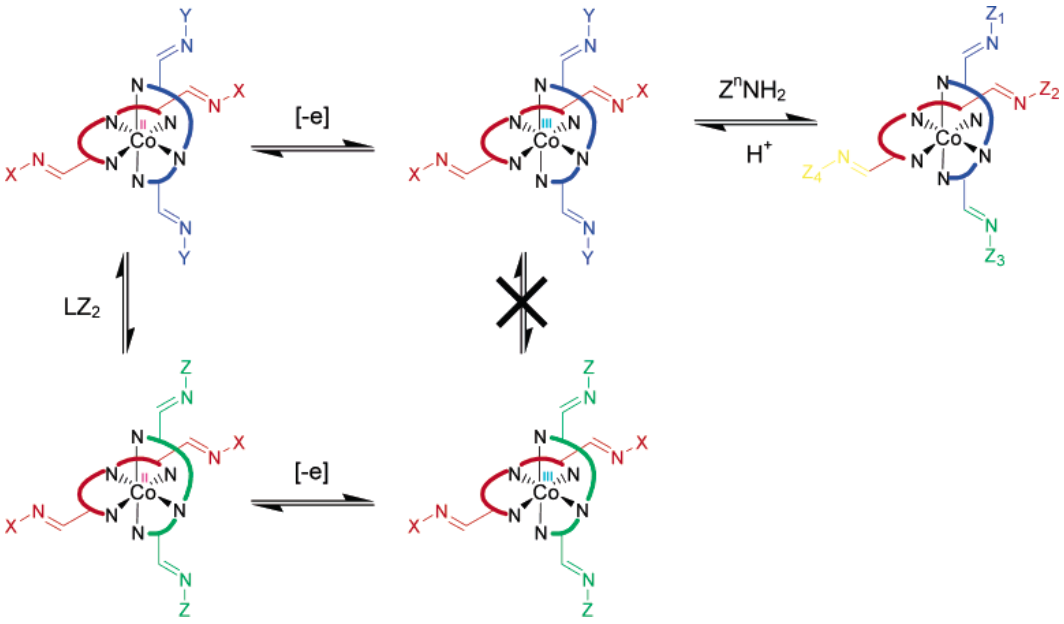

Scheme 3.3 First example of *Orthogonal* Exchange Processes in Dynamic Combinatorial Chemistry in 30% Acetonitrile/water at pH 7.0, by J-M. Lehn.[82]

Based on a) the improved catalytic system for pinacol coupling reactions in water reported by us,[69] b) the process of imine exchange reactions in Dynamic Combinatorial Libraries and c) orthogonal exchange process, we have initiated to develop a highly efficient and novel supramolecular catalyst for an effective and stereoselective pinacol coupling reactions for the dimerization of biomass derived oxygenated feed-stocks such as 5-hydroxymethylfurfural (HMF) and its derivatives to larger molecules, that could be further converted into valuable fuels and chemicals.

3.4 Design of improved catalytic system ('Catch and Release'): a supramolecular approach

To synthesize a metalloporphyrin catalyst (**E**) (**Scheme 3.4**), we came up with the idea of taking advantage of the dpreorganized structure of metallo

α_4-*meso*- tetra(aminophenyl)porphyrin **A** to form a pinacolate complex **B** with preformed ethylene glycol derivative (pinacol), in which all the amino groups are located at the same side (above the plane) of the porphyrin moiety. Then we plan to introduce a pool of different aldehydes (aliphatic and aromatic aldehyde derivatives) in a given reaction condition for imine formation. In the presence of various aldehydes, there is a possibility of forming the most stable imine **C**, based on the imine stability and the interaction of aldehyde groups with **R** groups on pinacolate complex.

The resulting compound **C** can be freezed by the addition of 4 Å molecular sieves to remove water in order to stop the equilibrium followed by the reduction of imine with reducing agent such as $NaBH_3CN$ to give compound **D**. This compound can be analysed by HRMS and the scaffold **E** can be synthesized in a stepwise manner in large scale. To achieve this goal we have synthesized model compounds of **E** (without metal) and investigated their stability in terms of thermal atropisomerism at elevated temperatures. In this chapter, I will discuss the synthesis of porphyrin model compounds based on imine exchange reactions for the scaffold synthesis.

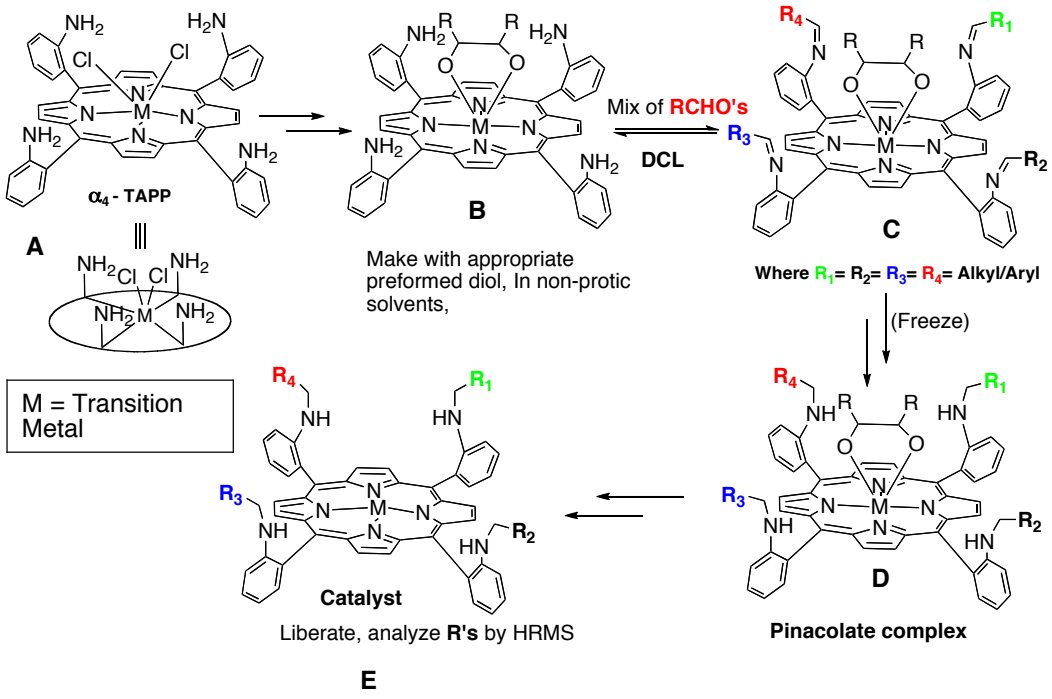

Scheme 3.4 Schematic representation of catalyst design by Dynamic Combinatorial Library approach

3.5 Synthesis of *tetra*[*o*-(benzyl/pivalyl)aminophenyl]porphyrins: Model compounds for supramolecular scaffold

3.5.1 Synthesis of meso- t*etrakis*(*o*-aminophenyl)porphyrin 6, α_4 – TAPP:

For the investigation of porphyrin scaffold for pinacol coupling reactions, first we have synthesized the core porpyrin molecule *meso*-t*etrakis*(*o*-aminophenyl)porphyrin **74** following literature procedures of Collmann et al.[83] by dissolving *p*-nitrobenzaldehyde **71** in refluxing glacial acetic acid and then slowly addition of freshly distilled pyrrole **3** to the boiling solution followed by the addition of chloroform to give the purple crystalline

product of *meso-Tetra*(*o*-nitrophenyl)porphyrin $H_2T_{NO2}PP$ **72** in *ca*. 12-13% yield. Then the reduction of nitro groups of **72** into amines were carried out by $SnCl_2 \cdot 2H_2O$ in conc HCl followed by quick heating of reaction mixture to 65-70 oC for 25 min, then neutralization with concentrated aqueous ammonia to give the purple solid of *meso*-tetra(*o*-aminophenyl)porphyrin $H_2T_{NH2}PP$ **73** in *ca*. 90% yield as reported in the literature.

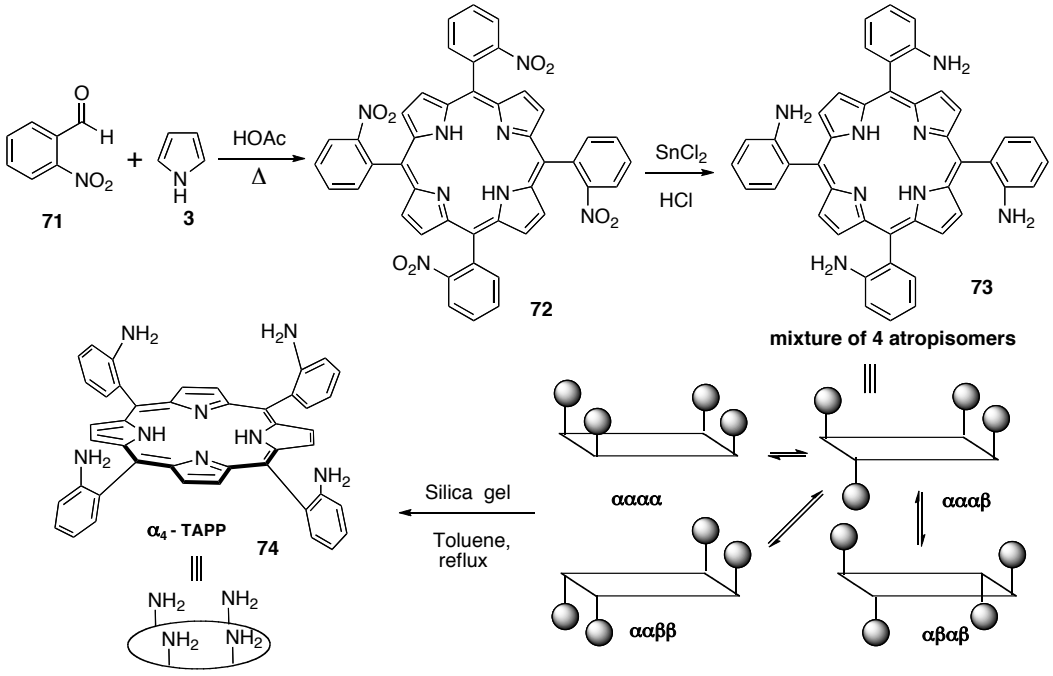

Scheme 3.5 Synthesis of **α_4-***meso-tetra*(*o*-aminophenyl)porphyrin $H_2T_{NH2}PP$

The resulting *meso-tetra*(*o*-aminophenyl)porphyrin $H_2T_{NH2}PP$ **73** exists in the isomeric mixture with the ratio of 1:2:4:1. Based on R_f value and relative amounts of individual isomers on TLC (Thin Layer Chromatography). These isomers were assigned as α,β,α,β-, α,α,β,β-, α,α,α,β-, α,α,α,α-, with most polar isomer α,α,α,α- moving slowly on TLC.

By using Lindsey's method of atropisomerization[84], we were able to isolate increased yield of desired isomer α,α,α,α- by equilibria displacement on binding to silicagel. In which we have refluxed equilibrium mixture of atropisomers **73** in silicagel and benzene as solvent for 20 h then separation by column chromatography to yield the desired atropisomer **74** in 60-70% yield as purple solid.

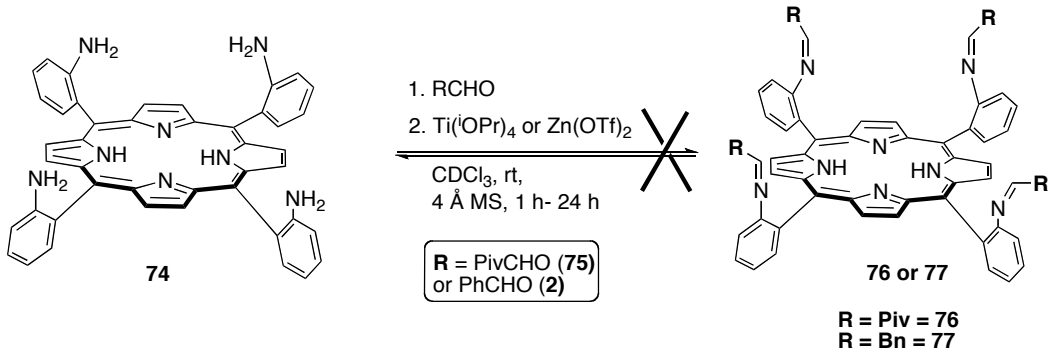

Scheme 3.6 Synthesis of porphyrin Schiff base **76** or **77**

Before embarking into the dynamic combinatorial approach, we have tried to investigate the synthesis of Schiff base (CH=N, imine) between α,α,α,α-*meso*-tetra(*o*-aminophenyl)porphyrin ($H_2T_{NH2}PP$) **74** and pivaldehyde **75** or benzaldehyde **2** (4.0 – 10.0 equiv) individually to give the tetra-imine derivative of **76** or **77**. Initial attempts to synthesize the compound **76** or **77** in presence of $Ti(^iOPr)_4$ as a Lewis acid catalyst in $CDCl_3$ solvent at room temperature and monitored (1- 24 h) by ^1H NMR on 400 MHz instrument for 1 – 24 hrs period.[85] But, there was no desired product of **76** or **77** by ^1H NMR, even with the addition of 4° MS to absorb water in the system and to push the equilibrium forward. The main observation was the formation of some

precipitate after 30 min, in the reaction vial or NMR sample tube. Which may be due to the poor solubility of the intermediate imine (mono or di or tri imine of **76** or **77**). Then we have tried to use different Lewis acid catalyst i.e $Zn(OTf)_2$ with the same reaction conditions as mentioned above. But, still there was no product formation by ^1H NMR. Therefore, finally ran the reaction at elevated temperature in the presence of 4° MS, and we observed still no imine product formation.

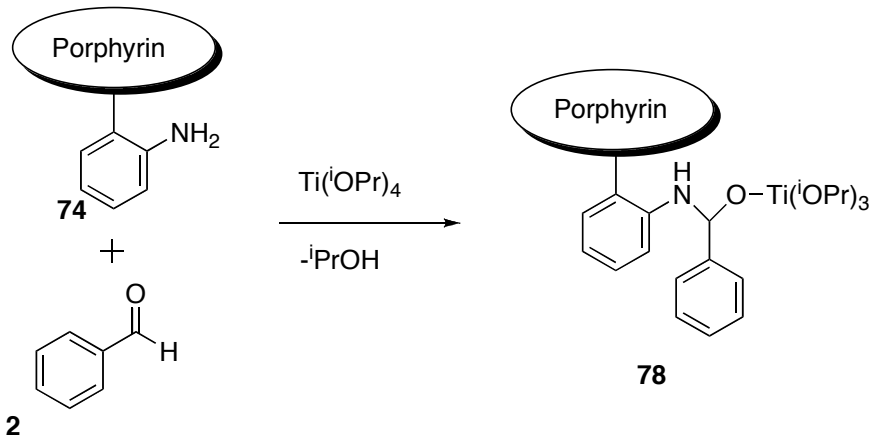

Scheme 3.7 Lewis acid effect in the Schiff base formation

Finally, we have tried with $Ti(^iOPr)_4$ (4.0 equiv) as Lewis acid catalyst in toluene solvent in reflux conditions under argon atmosphere for overnight. Unfortunately, there were no desired products observed either by mass spectrometry or ^1H NMR analyses. From the above measurements and observations, I can conclude that the imine formation in the above compounds is difficult, because of the Ti-O bond is more stronger (~ 90 kcal/mol, 1.95 A°)[86] than C-N bond (73 kcal/mol) and this suggests that an iminium species is,

at most, a transient intermediate in this reaction. In one possible mechanism, the stable complex **78** is formed and which then is reduced either directly or via a transient iminium species. Moreover, the precipitation observed in the reaction was may be due to the poor solubility of the intermediate complex **78** or because of some impurities such as benzoic acid in the benzaldehyde may be interacting with amine of the porphyrin to form ammonium salt, which is insoluble in organic solvents. Based on the above observations I can conclude that the imine formation in the porphyrin system was not happened, therefore we moved onto next step to find better reaction conditions for Porphyrin-Schiff base synthesis.

The synthesis of meso - tetrakis(*o*-pivalylaminophenyl)porphyrin **79** **(Scheme 3.8)** and meso - tetrakis(*o*-benzylaminophenyl) porphyrin **80** **(Scheme 3.9)** were achieved from common starting material meso - tetrakis(*o* - aminophenyl)porphyrin (α,α,α,α-TAPP) **74** by the use of Lindsey's literature procedure.[87] In which α,α,α,α-TAPP (0.5 mM) **74** and excess (100.0 eq) Pivalaldehyde **75** (for **79**), (100 eq) benzaldehyde **2** (for **80**) were condensed in dry CH_3CN containing 10% dimethyl acetamide (5×10^{-4} M) at room temperature in the presence of 4.0 equiv of trifluoroacetic acid (TFA). Schiff base formation of **76** and **77** were monitored by ESI-MS in dichloromethane solvent in order to minimize aggregation (in chloroform), and some unwanted reactions (acetonitrile) during the mass analysis in mass spectrometry.

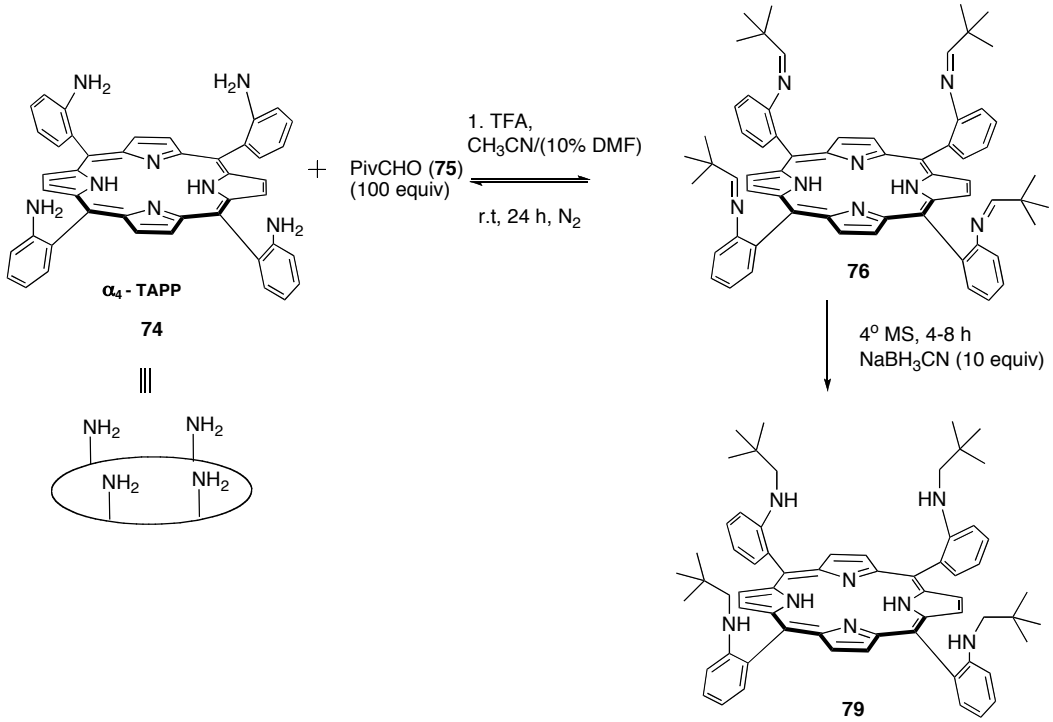

Scheme 3.8 Synthesis of *meso-tetrakis*(*o*-pivalylaminophenyl) porphyrin **79** *via* Schiff base formation

The desired compounds **79**, and **80** were achieved by selective reduction of Schiff bases **76** and **77** into pivalyl, and benzyl aniline derivatives **79** and **80** respectively. The reduced products were obtained by freezing the reaction mixture with addition of 4° MS and stirred for 4-5 hrs, then a total of 10.0 equiv of $NaBH_3CN$ (in 2 ml of CH_3CN) was added after 28 hrs of reaction), and the level of acidity is maintained with addition of extra trifluoroacetic acid (TFA). The *meso*-Tetra-(*o*-alkyl/aryl aminophnyl)porphyrins **79** and **80** were isolated by column chromatography (Basic Alumina, 350:1 CH_2Cl_2:MeOH), followed by the preparative TLC with (20:1 Hex : Ethyl ether), the top spot was collected and analyzed by mass spectrometry, and ^1H NMR in $CDCl_3$. The imine formation of **76** and **77** were

analyzed by ESI-MS, and reduced products **79** and **80** were analyzed by ESI-MS and ^{1}H NMR spectroscopy. The m/z 947.58 [M+H], and 1027.32 [M+H] indicate the formation of **76** and **77** respectively. The m/z of 955.66 [M+H] and 1057.44 [M+Na] indicate the formation of **79** and **80** reduced products.

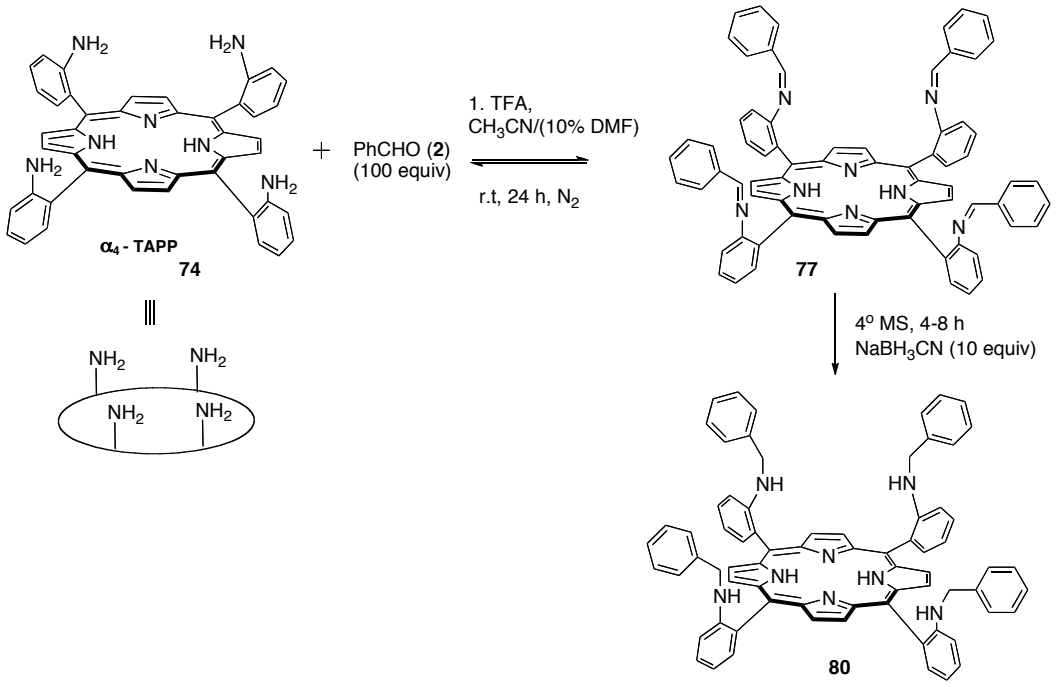

Scheme 3.9 Synthesis of *meso - tetrakis*(*o*-benzylaminophenyl) porphyrin **80** *via* Schiff base formation

The intermediate Schiff bases **76** and **77** are the result of an independent second-order intermolecular reaction, and Schiff base (imine) hydrolysis is a stoichiometric second-order reaction. Thus, the number of molecules remains same in the **76** and **77** condensations, and these are entropically disadvantageous if we use equimolar amounts of porphyrin and aldehydes. Thus, excess (100 folds) of aldehyde is necessary to achieve significant condensation to **76** or **77**. Since the imine formation is reversible,

synthesis is generally carried out by driving C=N bond formation to completion through the removal of water using 4 A° molecular sieves, or using azeotropic distillation,[88] in-addition to the entropically favored driving force.

3.6 Dynamic imine exchange reactions in α,α,α,α-*meso-tetra*(*o*-aminophenyl)porphyrin $H_2T_{NH2}PP$ 74

Based on the above results of synthesis of compounds **76** and **77**, we have moved onto investigate the dynamic imine exchange between porphyrin **74** and aldehydes. For initial measurements, we have chosen to use the same aldehydes (pivaldehyde) **75** and (Benzaldehyde) **2** for exchange reactions. The main reasons of choosing pivaldehyde and benzaldehyde are: a) to compare the reactivity of aliphatic *verses* aromatic aldehydes b) cheap and commercially available c) both are soluble in the given reaction conditions etc.

First we have studied the imine exchange reactions between porphyrin **74** and aldehydes **75** and **2** in the following four ways:

1. First, add PhCHO (50.0 equiv) to the reaction flask containing porphyrin **74** (7.42×10^{-3} mmol) in dry actonitrile (5 mL) containing 10%DMF and equilibrate for 24 h, then add PivCHO (50.0 equiv) and equilibrate another 24 h. After approximately 48 h, freeze the reaction by adding 4A° MS, and then reduce the imine with $NaBH_3CN$ to give mixture of tetraamines of porphyrin **74**. The formation of imine intermediates as well as reduced products were monitored by ESI-MS of the crude reaction mixture. For imine formation: $T_i(Ph)_4$ 1027.32 [M+H] and 1049.31 [M+Na], $T_i(Ph)_3(Piv)_1$ 1007.35 [M+H]

and 1029.32 [M+Na], $T_i(Ph)_2(Piv)_2$ 987.36 [M+H] and 1009.33 [M+Na], indicate the formation of compounds **77**, **81** and **82** (**Scheme 3.10**). For amines: $T_a(Ph)_4$ 1035.67[M+H] and 1057.67[m+Na], $T_a(Ph)_3(Piv)_1$ 1015.69 [M+H] and 1037.67 [M+Na], $T_a(Ph)_2(Piv)_2$, 995 [M+H] indicate the formation amines **80**, **84** and **85** (Scheme 3.11).

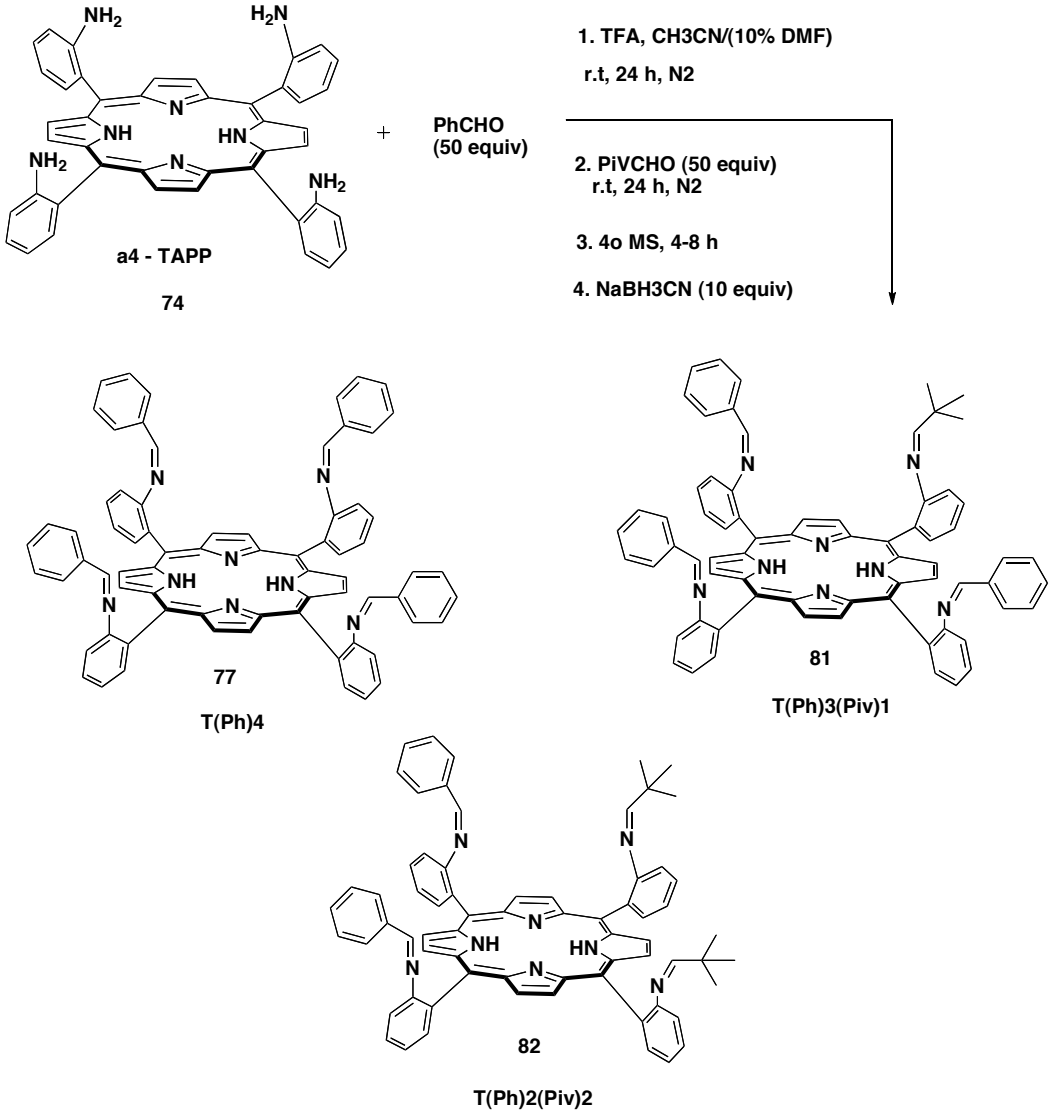

Scheme 3.10 Dynamic exchange reaction between porphyrin **74** and a) Benzaldehydes **2** and b) Pivaldehyde **75**.

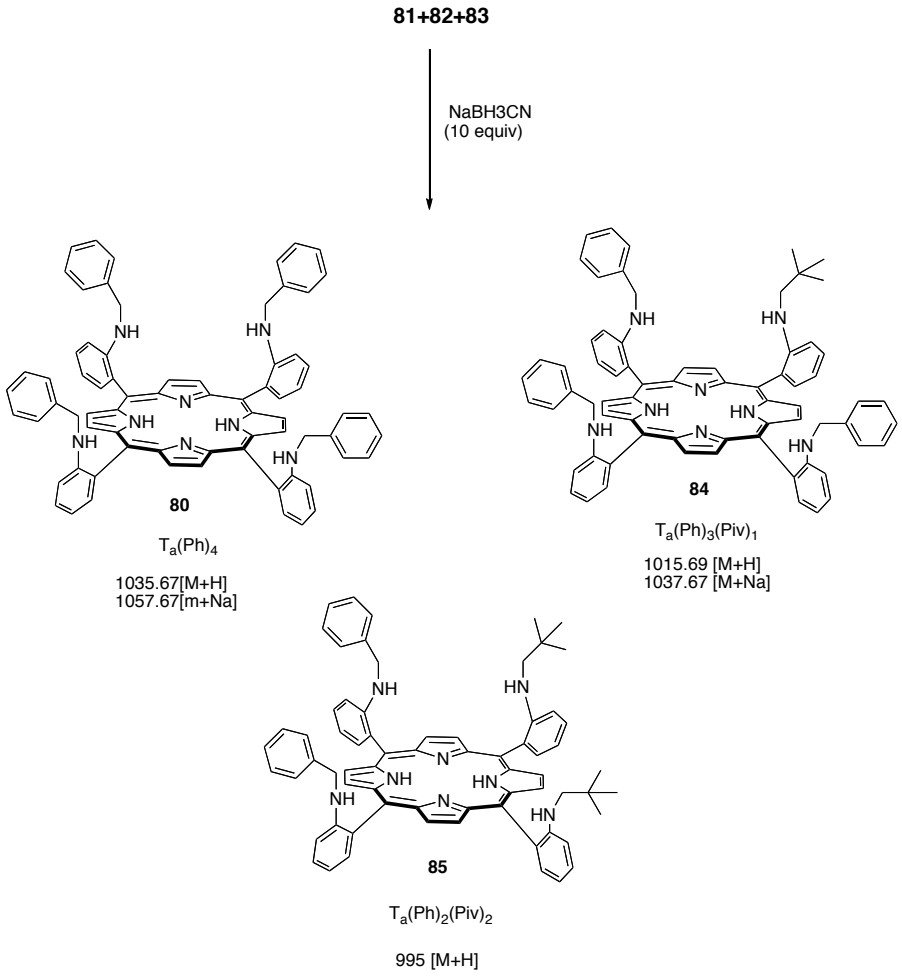

Scheme 3.11 Reduction of mixture of imines (**77, 81** and **82**) with $NaBH_3CN$

2. First added pivaldehyde **75**, after 24 hrs of equilibration, added benzaldehyde **2**. For imine formation: $T_i(Ph)_4$ 1049.23 [M+Na], $T_i(Ph)_3(Piv)_1$ 1007.35 [M+H] and 1029.28 [M+Na], $T_i(Ph)_2(Piv)_2$ 987.32 [M+H] and 1009.33 [M+Na], indicate the formation of compounds **77**, **81** and **82** (**Scheme 3.12**). For amines: $T_a(Ph)_4$ 1035.71[M+H] and 1057.75[m+Na], $T_a(Ph)_3(Piv)_1$ 1015.69 [M+H] and 1037.67 [M+Na], indicate the formation amines **80**, **84** (**Scheme 3.13**).

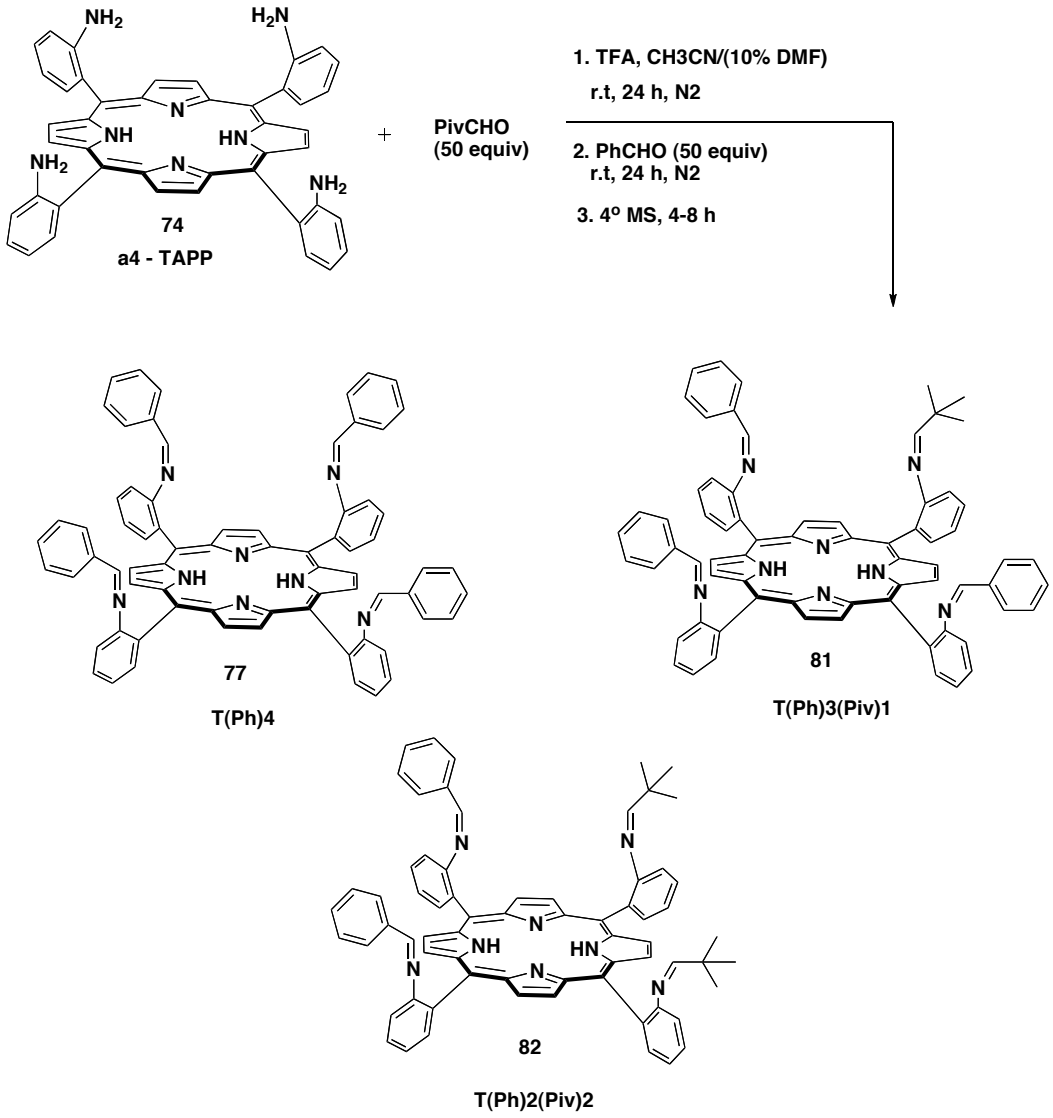

Scheme 3.12 Dynamic exchange reaction between porphyrin **74** and a) Pivaldehydes **75** and b) Benzaldehyde **2**

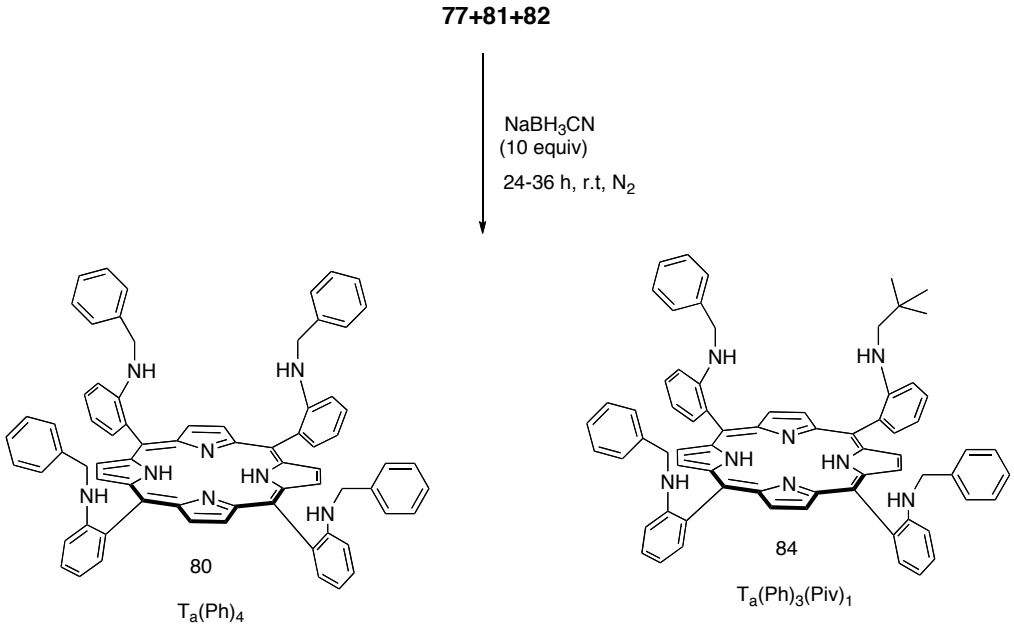

Scheme 3.13 Reduction of mixture of imines (**77, 81** and **82**) with $NaBH_3CN$

3. Added 50.0 equiv of each aldehyde **75** and **2** together, and equilibrated for 24 h. The ESI-MS analysis shows that the formation of imines: $T_i(Ph)_4$ 1049.27 (**77**) [M+Na], $T_i(Ph)_3(Piv)_1$ 1030.33 [M+H] (**81**) and 1029.28 [M+Na], $T_i(Ph)_2(Piv)_2$ 1009.40 [M+Na] (**82**). For amine: $T_a(Ph)_4$ 1035.63[M+H], $T_a(Ph)_3(Piv)_1$ 1015.69 [M+H] and 1037.71 [M+Na], $T_a(Ph)_2(Piv)_2$ 995.69 [M+H] indicate the formation amines **80**, **84** and **85** (**Scheme 3.15**). Since the reduction looks somehow incomplete, therefore we compared this result with a control experiment, in which both the aldehydes added together at the beginning and equilibrated for 24 h, then reduced with $NaBH_3CN$ and analyzed reduced products by ESI-MS. The ESI-MS shows that: m/z 1035.54 [M+H] and 1057.45 [M+Na] for $T_i(Ph)_4$, 1015.54 [M+H] and 1037.50 [M+Na] for

$T_a(Ph)_3(Piv)_1$, and 995.58 [M+H] for $T_a(Ph)_2(Piv)_2$, indicate the reducton occurred via Schiff base formation.

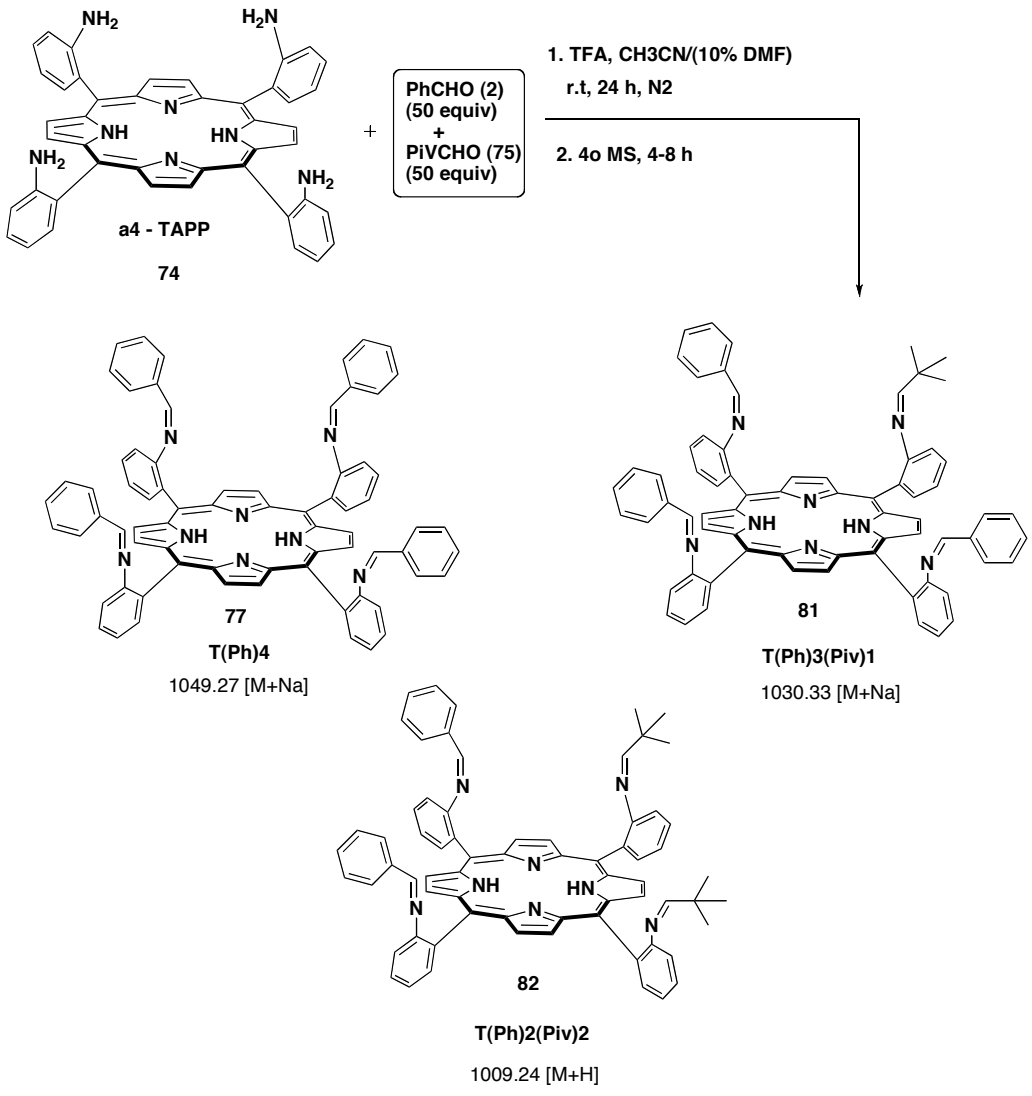

Scheme 3.14 Dynamic exchange reaction between porphyrin **74** and a) Pivaldehydes **75** + Benzaldehyde **2,** when added 50.0 equiv of each together.

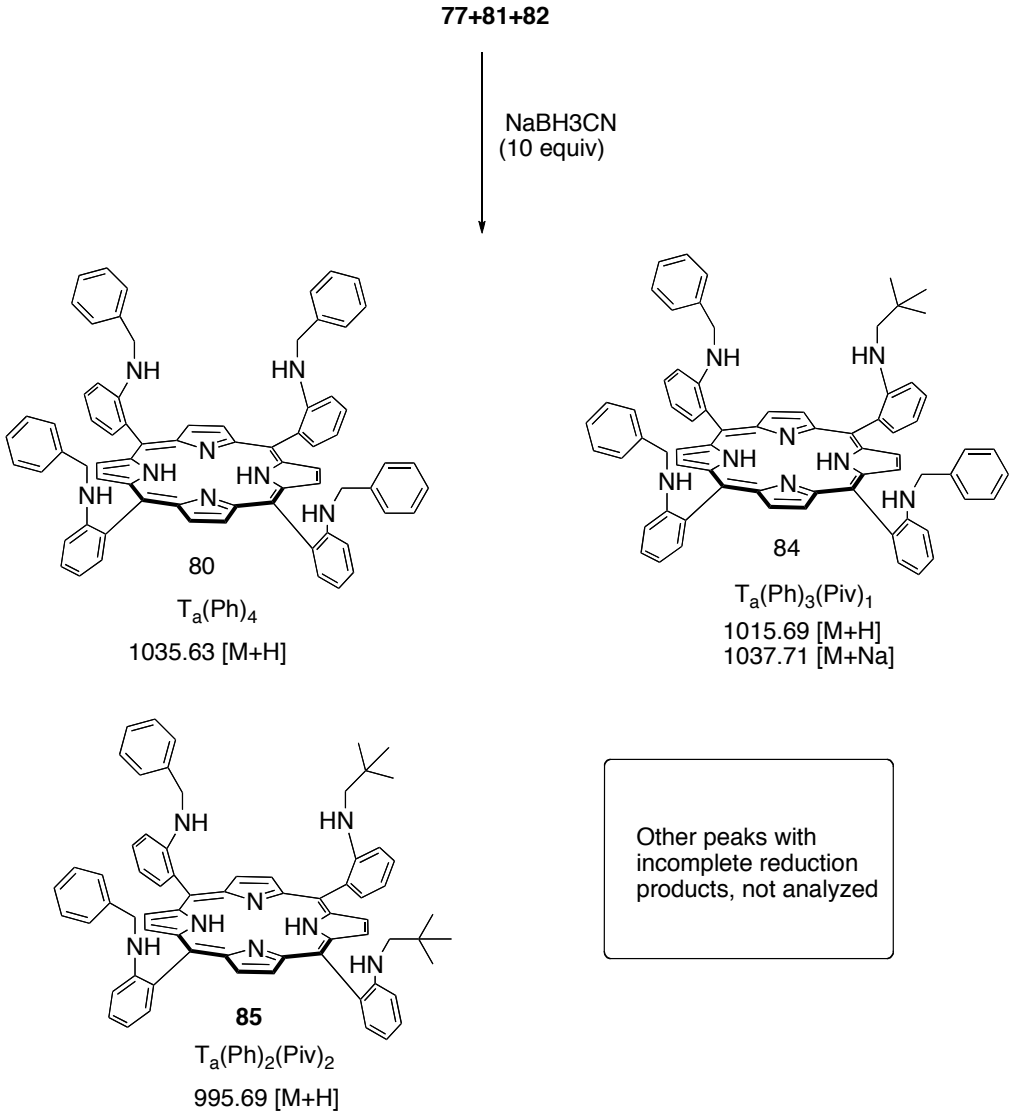

Scheme 3.15 Reduction of mixture of imines (**77, 81** and **82**) with $NaBH_3CN$

4. Finally, we have tried to add excess amount of benzaldehyde than pivaldehyde. In which, added 50.0 equiv of pivaldehyde and equilibrated for 24 h, then transferred ~ 2 ml of crude (from 10 ml of reaction mixture) in to a different round bottomed flask and reduced with $NaBH_3CN$. The ESI-MS shows the formation of compound **79**, m/z 955.57 [M+H]. Then, to the left over 8 ml of reaction mixture was added 50.0 equiv (relative to initial

concentration of porphyrin) of benzaldehyde and equilibrated for 24 h, then reduced with $NaBH_3CN$. ESI-MS shows the formation of only two compound **80** and **81** with m/z 1035.5 [M+H] and 1015.57 [M+H] respectively. This result correlates to the reactivity difference between benzaldehyde and pivaldehyde in terms of imine formation.

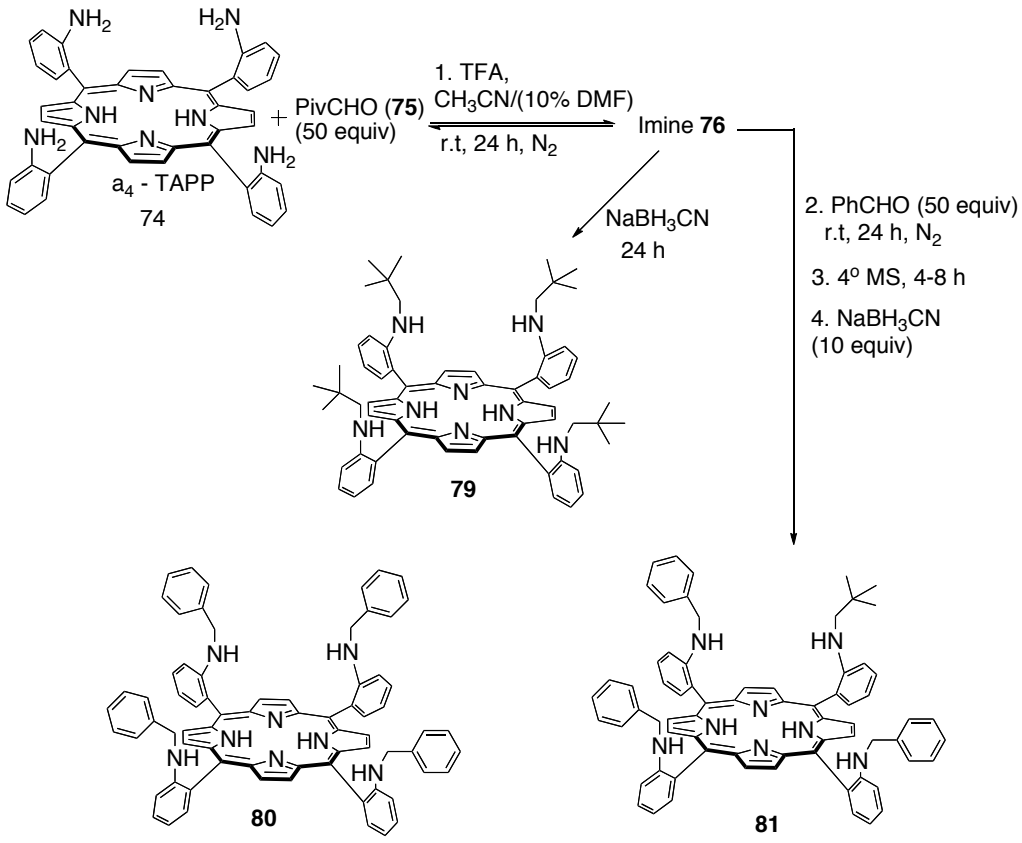

Scheme 3.16 Dynamic exchange reaction between porphyrin **74** and a) Pivaldehydes **75** (50.0 equiv) and b) Benzaldehyde **2** (excess, > 50.0 equiv)

Exp	[**74**] mM	**75** (equiv)	**2** (equiv)	TFA[a] (equiv)	$NaBH_3CN$ (equiv)	Imines	Amines
1	3.0 mM	50.0	50.0	4.0 + 4.0	10.0	$T_i(Ph)_4$ $T_i(Ph)_3(Piv)_1$ $T_i(Ph)_2(Piv)_2$	$T_a(Ph)_4$ $T_a(Ph)_3(Piv)_1$ $T_a(Ph)_2(Piv)_2$
2	3.0 mM	50.0	50.0	4.0 + 4.0	10.0	$T_a(Ph)_4$, $T_a(Ph)_3(Piv)_1$, $T_a(Ph)_2(Piv)_2$	$T_a(Ph)_4$ $T_a(Ph)_3(Piv)_1$
3	3.0 mM	50.0	50.0	4.0 + 4.0	10.0	$T_i(Ph)_4$ $T_i(Ph)_3(Piv)_1$ $T_i(Ph)_2(Piv)_2$	$T_a(Ph)_4$ $T_a(Ph)_3(Piv)_1$ $T_a(Ph)_2(Piv)_2$
4	3.0 mM	50.0	> 50.0	4.0 + 5.0	10.0	-NA-	$T_a(Ph)_4$ $T_a(Ph)_3(Piv)_1$

a = 4.0 equiv of TFA added first for imine formation, and another 4.0 equiv added during reduction step; NA = Not analyzed; Exp#1: Add 50.0 equiv of 8. After 24 h, add 50.0 equiv of 7; Exp#2: Add 50.0 equiv of 7, after 24 h, add 50.0 equiv of 8; Exp#3: Add 50.0 equiv of 7 and 50.0 equiv of 8 together at the beginning; Exp#4: Add 50.0 equiv of 7. After 24 h, add excess (>50.0 equiv) of 8.

Table 3.1 Study of exchange reactions between porphyrin **74** and aldehydes **75** and **2**.

3.7 Discussion

The dynamic exchange reactions between porphyrin **74** and aldehydes **75**, **2** were studied in acetonitrile and 10% dimethyl acetamide (DMA) solvent system at room temperature in presence of trifluoroacetic (TFA) acid. The above experiments (1 to 4) gave a clear evidence for the formation of porphyrin–schiff bases in equilibrium conditions at room temperature. The imine formation was not observed in the absence of TFA as well as in lower concentration of aldehydes (incomplete reaction). Moreover, the co-solvent, dimethyl acetamide is necessary for the reaction in order to improve the solubility of imine intermediates. The results for the imine exchange reactions as well as final reduced products are summarized in the **Table 3.1**. These results indicate the formation of tetraimine $T_i(Ph)_4$ **77,** is the predominant product in all cases. The main reason is, the reactivity difference between

pivaldehyde verses banzaldehyde towards porphyrin **74**. **Scheme 3.17** shows that the energy gap of LUMO of the benzaldehyde and HOMO of porphyrin **74** is low, therefore the interaction is more predominant in this case. But, in the case of pivaldehyde **75** and porphyrin **74** is opposite, which means the HOMO-LUMO gap of electrophile and nucleophile is high, therefore the interaction is less. Hence, the predominant product is **77,** in all four cases (Table 3.1). Formation of other imine products (**81** and **82**) are the evidence for the dynamic imine exchange reactions in equilibrium conditions and the reduced amine products (**80**, **81** and **82**) are the basis for new investigations in dynamic combinatorial chemistry for supramolecualr catalyst design.

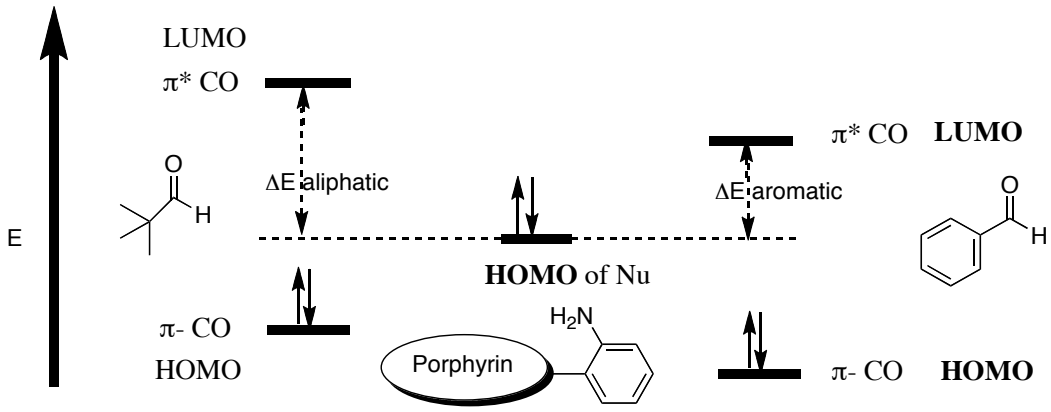

Scheme 3.17 Orbital energy diagram for the reactivity of pivaldehyde **75** versus Benzaldehyde **2** with Porphyrin **74**

3.8 Conclusion

We have successfully synthesized porphyrin model compounds as scaffolds for supramolecualr catalyst for pinacol coupling reactions based on dynamic exchange reactions, and demonstrated the exchange between low

reactive aldehyde (aliphatic) verses high reactive aldehyde (aromatic) towards porphyrin **74**. The reduced products are the evidence for the exchange reactions and basis for the scaffold design for porphyrin based supramolecular catalyst type **E** (**Scheme 3.4**).

3.9 Experimenal Section

Materials and general procedures

All Solvents were purchased from Acros and Aldrich. Acetonitrile was distilled from CaH_2, and Dimethyl acetamide (DMA) was distilled from BaO just before its use by using known procedure from the book. Benzaldehyde was distilled just before use and pivaldehyde was used as received from Acros.

Low-resolution mass analyses were done using a Micromass/Waters QTOF-1 (Bedford, MA) equipped with an electrospray ionization source in positive ion mode. Nitrogen gas was used as a nebulizing and drying gas with capillary voltage 3.0 kV, cone volatage ramp 10-85 V, source block temperature 120ºC, desolvation temperature 150ºC, and desolvation flow rate 200 L/hr. Data was collected and analyzed using Mass Lynz (4.0, SP1., 2003). High resolution mass analyses were done using an Agilent 6538 UHD Accurate Mass QTOF (POS, CA) esquipped with an electrospray ionization source in positive ion mode. Nitrogen gas was used as a nebulizing and drying gas with the drying gas temperature of 325ºC and 10 L/min flow rate. Fragmentor volatge was 160V and capillary voltage of 3500V. Data was collected with Mass Hunter

Acquitition (B.04.00, 2011) and analyzed with Mass Hunter Qualitative (B.04.00, 2011).

3.9.1 Syntheses compounds 73 and 74

5,10,15,20-*tetrakis*(2-aminophenyl)porphyrin (H_2TAPP) **73** was synthesized *via* the method of Collman,[83] and the α,α,α,α-atrop isomer **74** was isolated *via* Lindsey's atropisomerization procedure.[84]

3.9.2 Synthesis of Compounds 79 and 80 *via* Schiff base formation

20 mg of αααα-TAPP **74** (0.0296 mmol) was dissolved in dry acetonitrile/10% DMA (20 mL) to which was added 100.0 equiv of Pivaldehyde **75**, 4.0 equiv of TFA. Then the reaction mixture was stirred at room temperature under nitrogen for 24-36 h and the formation of compound **76** was monitored by ESI-MS (($C_{64}H_{66}N_8$), $(M+Na)^+$ 969.57(100%), calcd mol wt 969.53). Then 5.0 - 10.0 equiv of $NaBH_3CN$ in DMA, 4.0 equiv of TFA in DMA were added periodically for 2 h duration then the reaction mixture was stirred at room temperature under nitrogen for 24 h. Then the reaction mixture was quenched by addition of 10 ml of dichloromethane, ~10 µl of Hunig's base. The dichloromethane portion was washed with water (3x10 ml) and dried over anhydrous Na_2SO_4. After evaporating the solvent at room temperature under vacuum, the resulting crude was purified by silica gel column using $CHCl_3$:Hexane (1:3) eluent system. The desired compound **79** (90%) was collected first as a dark brown colored band leaving a small amount of colored

material at the top of the column. Compounds **77** and **80** were synthesized with the same procudure as above and final products were analyzed by ESI-MS and ^{1}H NMR spectroscopy.

3.9.3 ESI-MS of 76: ($C_{64}H_{66}N_8$), $(M+H)^+$ 947.60 (100%), calcd mol wt 946.54

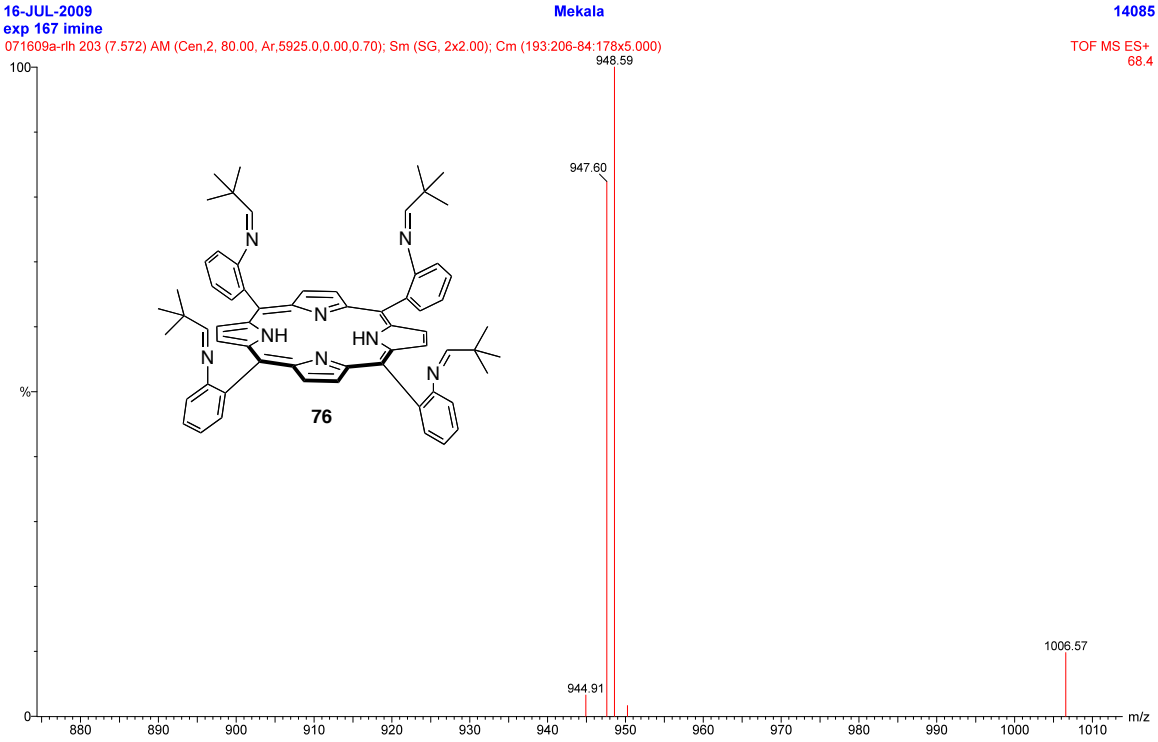

Figure 3.1 ESI-MS spectrum of **76**

3.9.4 ESI-MS of 77: ($C_{72}H_{50}N_8$), $(M+H)^+$ 1027.32 (100%), calcd mol wt 1026.42

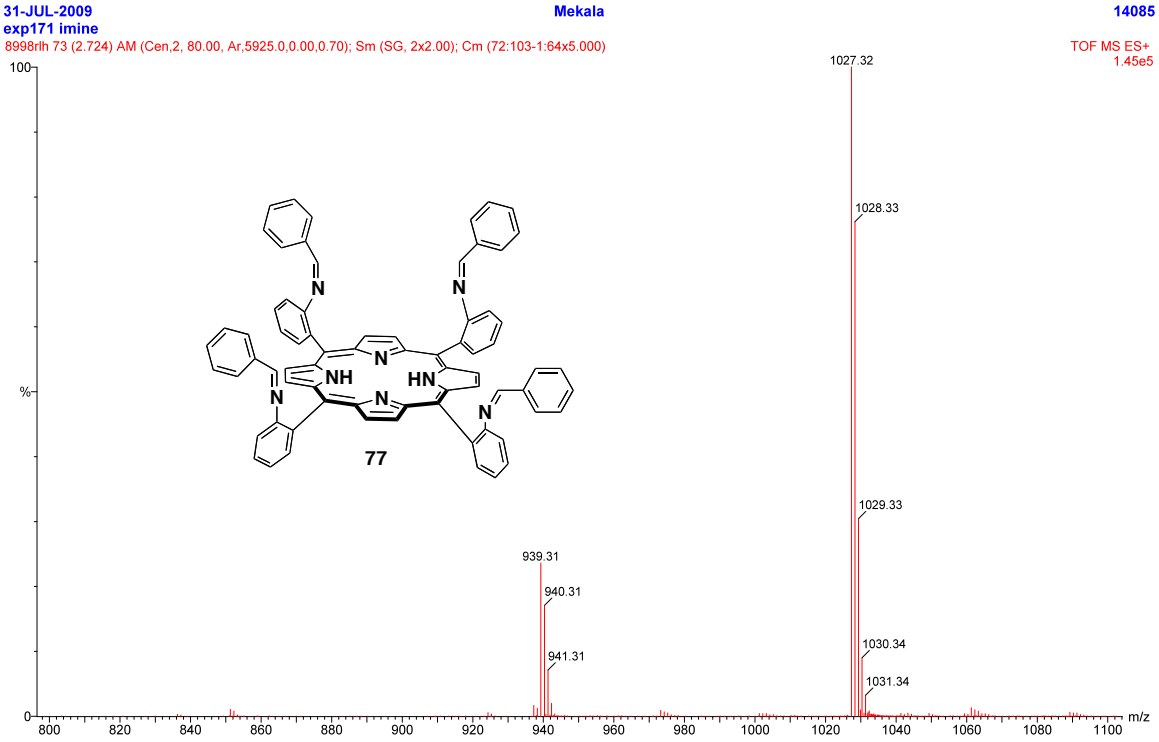

Figure 3.2 ESI-MS spectrum of compound **77**

3.9.5 ^{1}H, ^{13}C NMR and ESI-MS **of 79:** H^1 NMR ($CDCl_3$): 8.90 (8H, s, β -pyrrol H), 7.88 (4H, d, *J* =7.2 Hz, porphyrin PhH), 7.65 (4H, t, *J* = 8.4 Hz, porphyrin PhH), 7.14 (4H, d, *J* =8.4Hz, porphyrin PhH), 7.04 (4H, t, *J* =7.2 Hz, porphyrin PhH), 3.60 (4H, d, *J* =8.4 Hz, PhNH), 2.90 (8H, t, *J* =6.4 Hz, CH_2), 0.40 (36H, s, CH_3); ^{13}C NMR ($CDCl_3$, 500 MHz): δ = 149.1, 149.0, 135.6, 135.5, 129.8, 126.2, 116.0, 115.8, 110.4, 55.7, 27.5, 25.1; ESI-MS: Exact mass:

($C_{64}H_{74}N_8$), $(M+H)^+$ 955.6071(100%), calcd mol wt 954.60

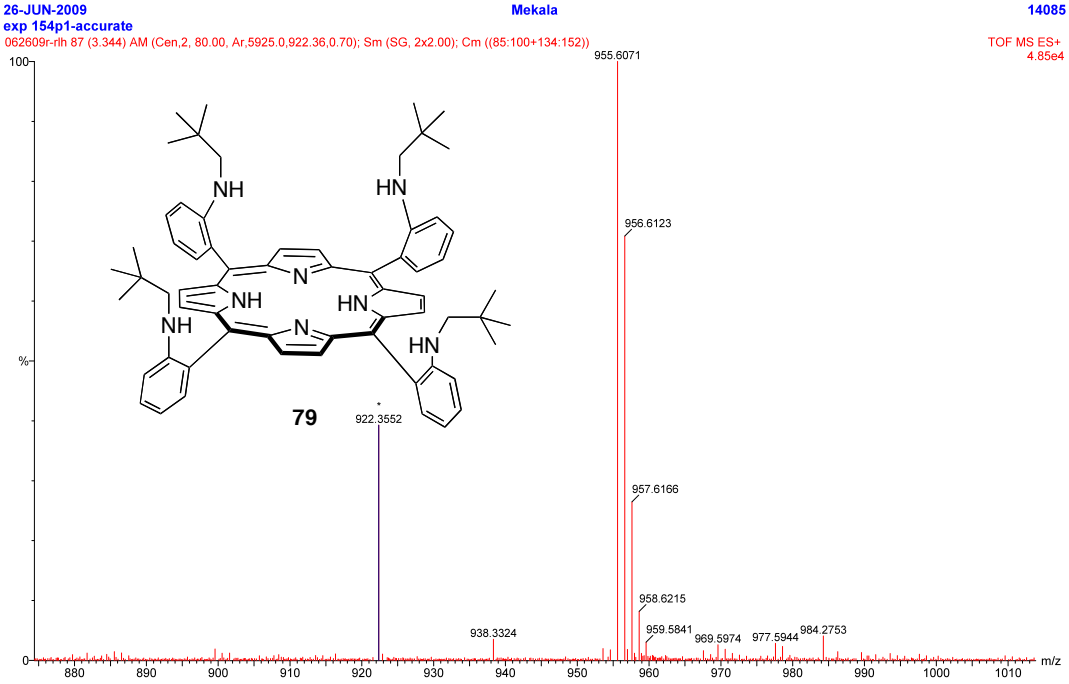

Figure 3.3 ESI-MS spectrum of **79**

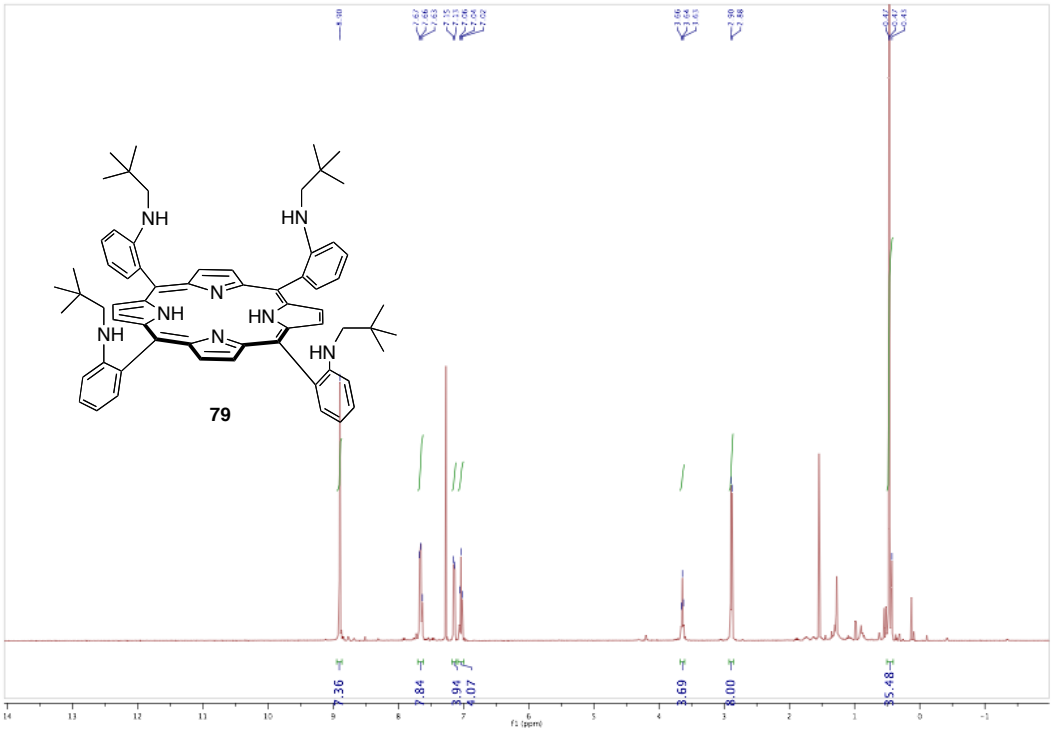

Figure 3.4 ^{1}H NMR spectrum of **79**

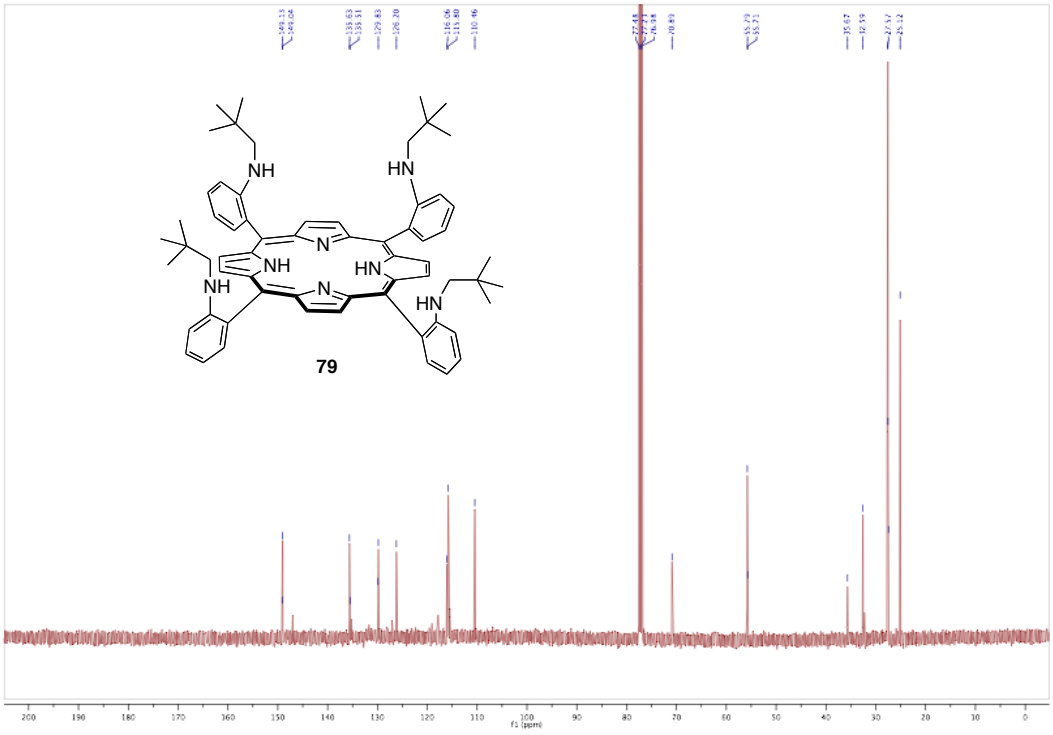

Figure 3.5 ^{13}C NMR spectrum of **79**

3.9.6 ^{1}H, ^{13}C NMR and ESI-MS **of 80**. ^{1}H NMR ($CDCl_3$): 8.90 (8H, s, β-pyrrrole-H), 7.88 (4H, d, *J* =7.2 Hz, porphyrin PhH), 7.62 (4H, t, *J* = 8.4 Hz, porphyrin PhH), 7.14 (4H, t, *J* = 7.2 Hz, porphyrin PhH), 6.9 (24H, m, porphyrin PhH, PhH), 4.16 (8H, d, *J* = 5.6 Hz, CH2), 3.64 (4H, t, *J* = 6.0 Hz, PhNH); ^{13}C NMR ($CDCl_3$, 500 MHz): δ = 148.4, 148.3, 139.3, 139.2, 134.7, 128.4, 126.98, 126.97, 126.96, 116.6, 116.5, 115.7, 111.1, 48.1; ESI-MS: Exact mass: ($C_{72}H_{58}N_8$), $(M+H)^+$ 1035.4966(100%), calcd mol wt 1034.48

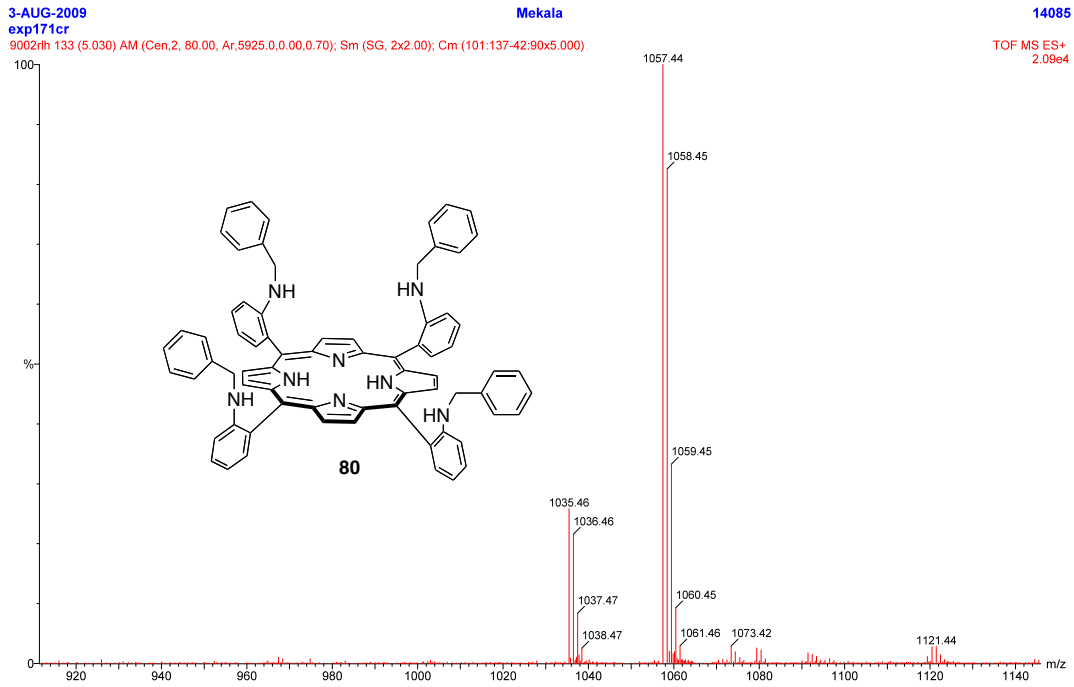

Figure 3.6 ESI-MS spectrum of **80**

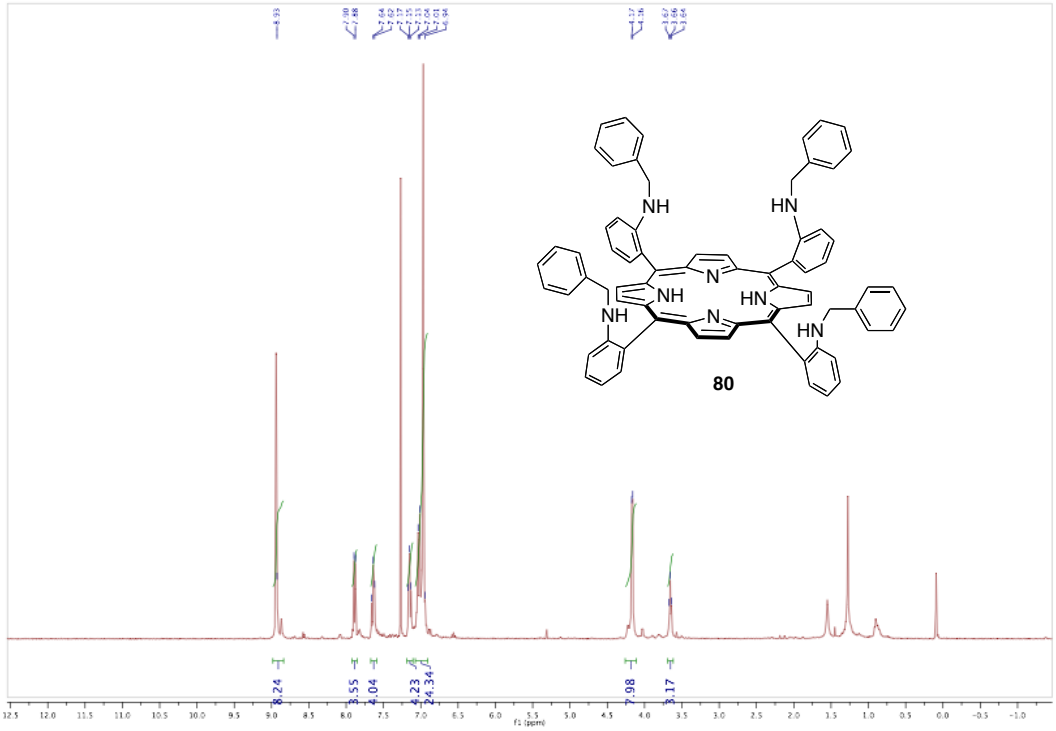

Figure 3.7 ^{1}H NMR spectrum of **80**

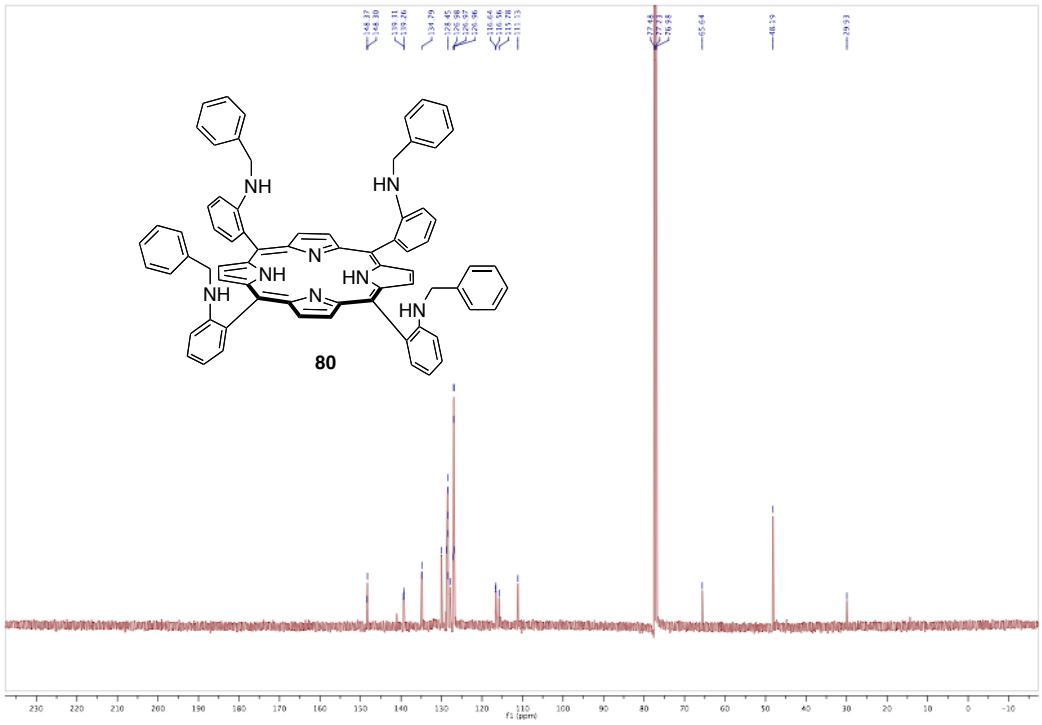

Figure 3.8 ^{13}C NMR spectrum of **80**

3.9.7 Dynamic exchange reactions

Exp#1: 5.0 mg ($7.4*10^{-3}$ mmol) of **74** was dissolved in 5 mL of dry CH_3CN/10%DMA and added 4.0 equiv of trifluoroacetic acid (TFA) and 50.0 equiv of freshly distilled benzaldehyde and stirred for 24 h at room temperature under nitrogen. Then added 50.0 equiv (0.04 mL) of pivaldehyde and stirred another 24 h at room temperature under nitrogen, then added 4 Å MS and stirred for 4 h and crude imine was analyzed by mass spectrometry. Then added 10.0 equiv of $NaBH_3CN$ and 4.0 equiv of TFA and stirred for another 24-36 h at room temperature under nitrogen and the resulting amines were analyzed by ESI-MS for the crude product. For imine formation: $T_i(Ph)_4$ 1027.32 [M+H] and 1049.31 [M+Na], $T_i(Ph)_3(Piv)_1$ 1007.35 [M+H] and

1029.32 [M+Na], $T_i(Ph)_2(Piv)_2$ 987.36 [M+H] and 1009.33 [M+Na], indicate the formation of compounds **77**, **81** and **82** (Scheme 3.10). For amines: $T_a(Ph)_4$ 1035.67[M+H] and 1057.67[m+Na], $T_a(Ph)_3(Piv)_1$ 1015.69 [M+H] and 1037.67 [M+Na], $T_a(Ph)_2(Piv)_2$, 995 [M+H] indicate the formation amines **80**, **84** and **85** (Scheme 3.11).

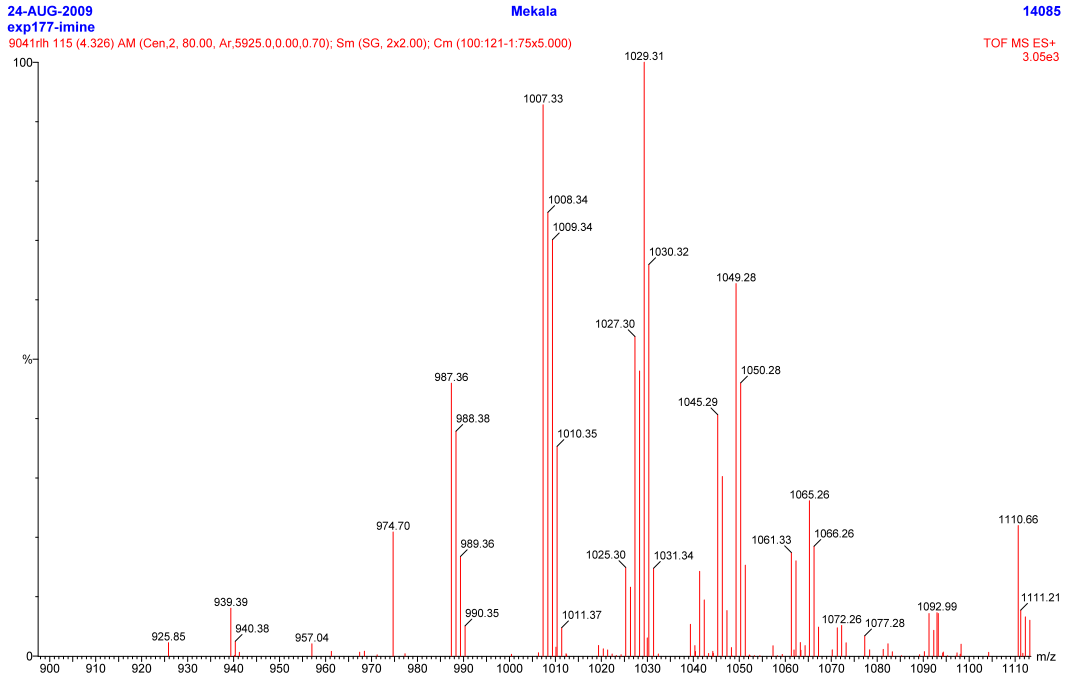

Figure 3.9 ESI-MS spectrum for exp#1 (imine)

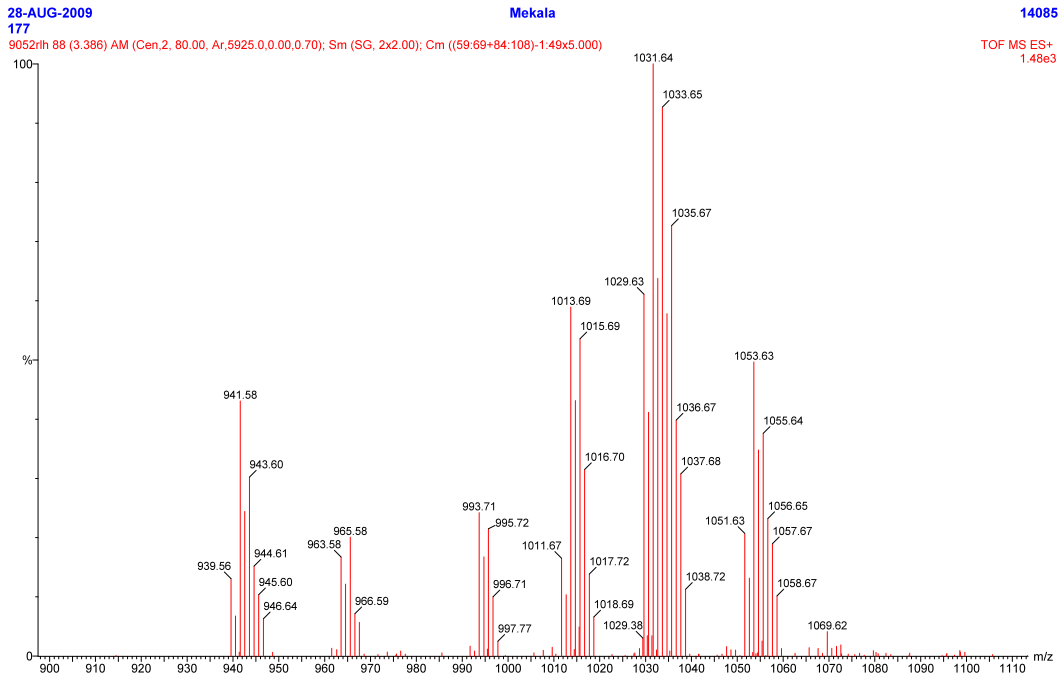

Figure 3.10 ESI-MS spectrum for exp#1 (amine)

Exp#2: 5.0 mg ($7.4*10^{-3}$ mmol) of **74** was dissolved in 5 mL of dry CH_3CN/10%DMA and added 4.0 equiv of trifluoroacetic acid (TFA) and 50.0 equiv of pivaldehyde and stirred for 24 h at room temperature under nitrogen. Then added 50.0 equiv (0.04 mL) of freshly distilled benzaldehyde and stirred another 24 h at room temperature under nitrogen, then added 4° MS and stirred for 4 h and crude imine was analyzed by mass spectrometry. Then added 10.0 equiv of $NaBH_3CN$ and 4.0 equiv of TFA and stirred for another 24-36 h at room temperature under nitrogen and the resulting amines were analyzed by ESI-MS f the crude product. For imine formation: $T_i(Ph)_4$ 1049.23 [M+Na], $T_i(Ph)_3(Piv)_1$ 1007.35 [M+H] and 1029.28 [M+Na], $T_i(Ph)_2(Piv)_2$ 987.32 [M+H] and 1009.33 [M+Na], indicate the formation of compounds **77**, **81** and

82 (Scheme 3.12). For amines: $T_a(Ph)_4$ 1035.71[M+H] and 1057.75[m+Na], $T_a(Ph)_3(Piv)_1$ 1015.69 [M+H] and 1037.67 [M+Na], indicate the formation amines **80**, **84** (Scheme 3.13).

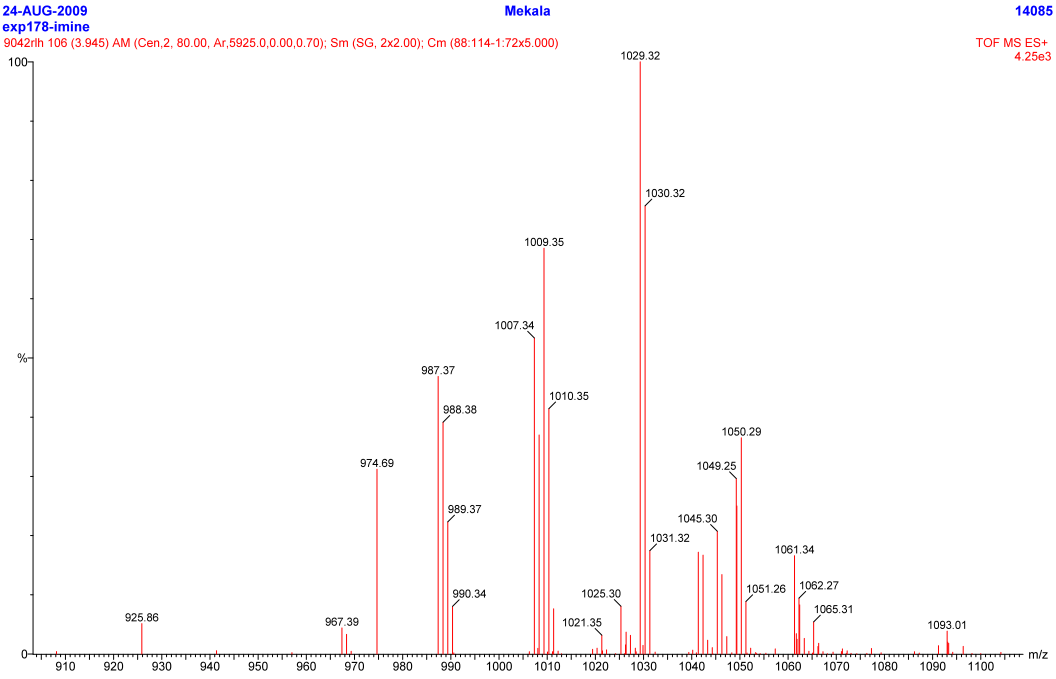

Figure 3.11 ESI-MS spectrum for exp#2 (imine)

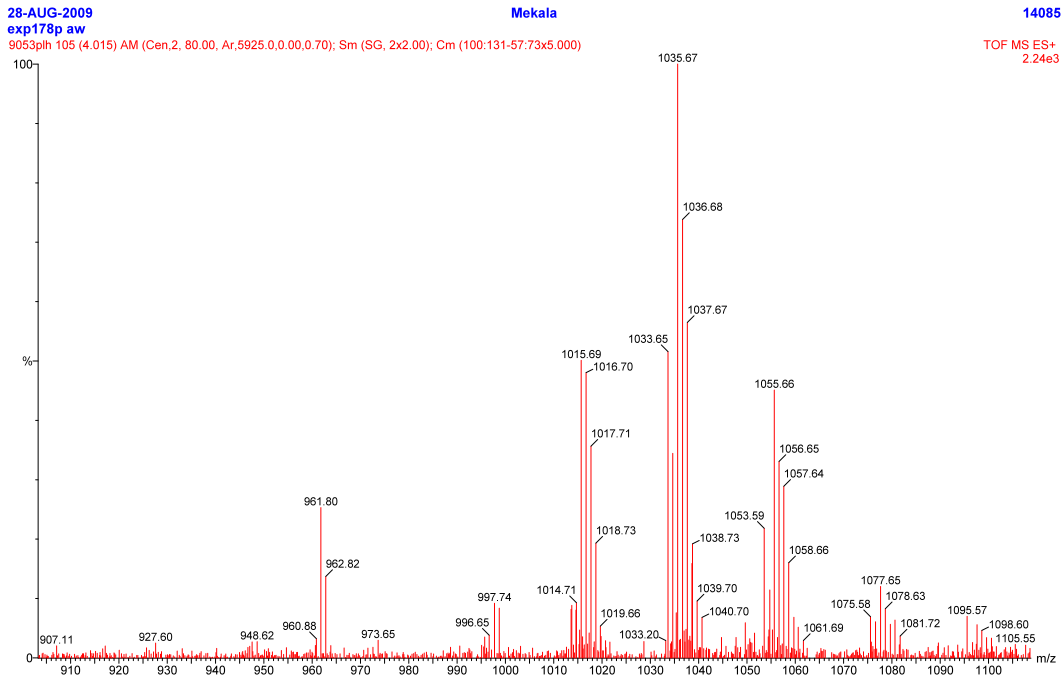

Figure 3.12 ESI-MS spectrum for exp#2 (amine)

Exp#3: 5.0 mg ($7.4*10^{-3}$ mmol) of **74** was dissolved in 5 mL of dry CH_3CN/10%DMA and added 4.0 equiv of trifluoroacetic acid (TFA) and 50.0 equiv of pivaldehyde and 50.0 equiv of benzaldehdye added together at the beginning and stirred for 24 h at room temperature under nitrogen, then added 4 Å MS and stirred for 4 h and crude imines were analyzed by mass spectrometry. Then added 10 equiv of $NaBH_3CN$ and 4.0 equiv of TFA and stirred for another 24-36 h at room temperature under nitrogen and the resulting amines were analyzed by ESI-MS for the crude product. The ESI-MS shows that: m/z 1035.54 [M+H] and 1057.45 [M+Na] for $T_a(Ph)_4$, 1015.54 [M+H] and 1037.50 [M+Na] for $T_a(Ph)_3(Piv)_1$, and 995.58 [M+H] for

$T_a(Ph)_2(Piv)_2$, indicate the formation of desired products **80**, **84** and **85** and the reducton occurred via Schiff base formation.

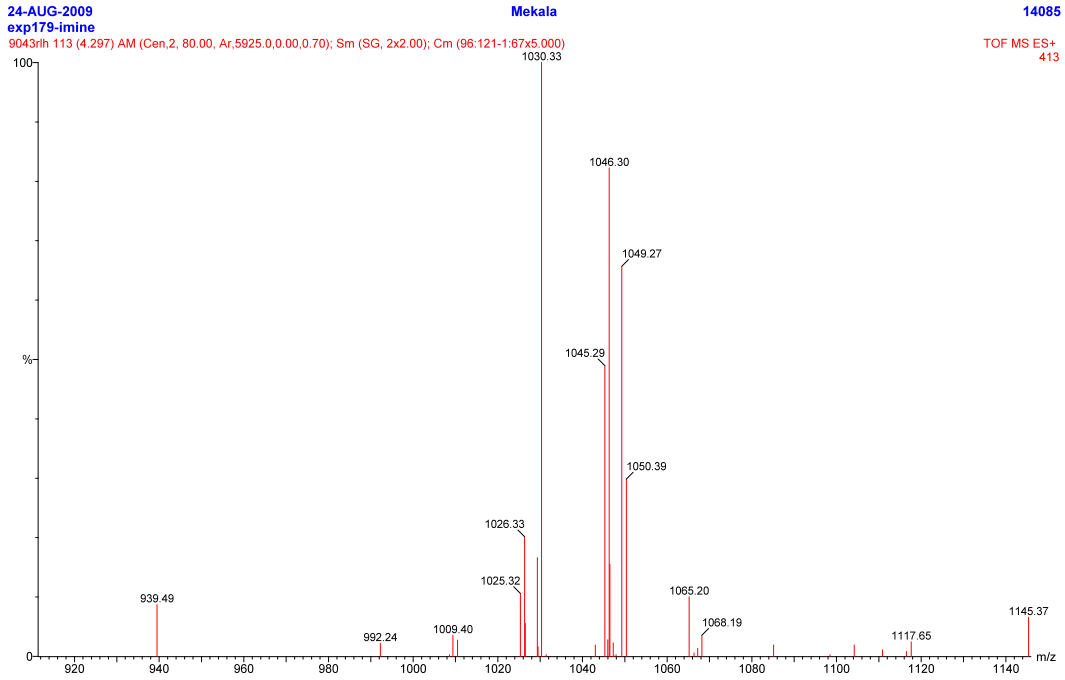

Figure 3.13 ESI-MS spectrum for exp#3 (imine)

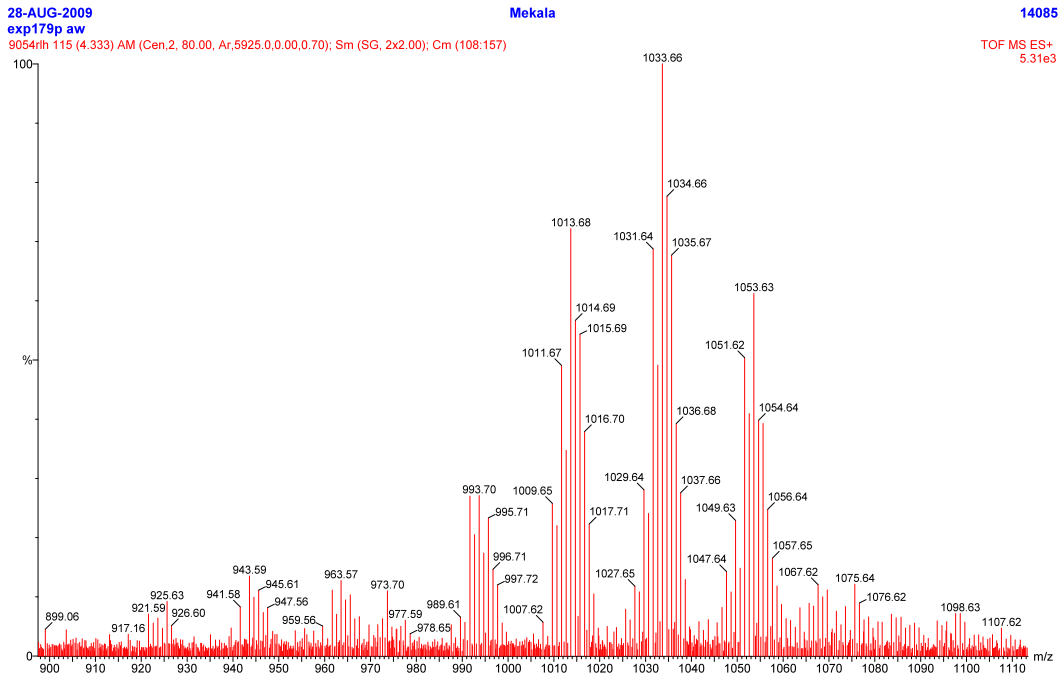

Figure 3.14 ESI-MS spectrum for exp#3 (amine)

Exp#4: 5.0 mg ($7.4*10^{-3}$ mmol) of **74** was dissolved in 5 mL of dry CH_3CN/10%DMA and added 4.0 equiv of trifluoroacetic acid (TFA) and 50.0 equiv of pivaldehyde and stirred for 24 h at room temperature under nitrogen. (The imine formation was monitored by removing 2 ml of crude into a separate small round bottomed flask and reduced with $NaBH_3CN$ and analyzed the amine product by ESI-MS). To the reaction flask, added 50.0 equiv (relative to starting concentration of **74** before romoving 2 ml crude into a separate flask) (0.04 mL) of freshly distilled benzaldehyde and stirred another 24 h at room temperature under nitrogen, then added 4 Å MS and stirred for 4 h and crude imine was analyzed by mass spectrometry. Then added 10 equiv of $NaBH_3CN$ and 4.0 equiv of TFA and stirred for another 24-36 h at room temperature

under nitrogen and the resulting amines were analyzed by ESI-MS. The ESI-MS shows the formation of compound **79**, m/z 955.57 [M+H]. For amine formation: ESI-MS shows the formation of only two compound **80** and **84** with m/z 1057.42 [M+H] and 1049.94 [M+H] respectively.

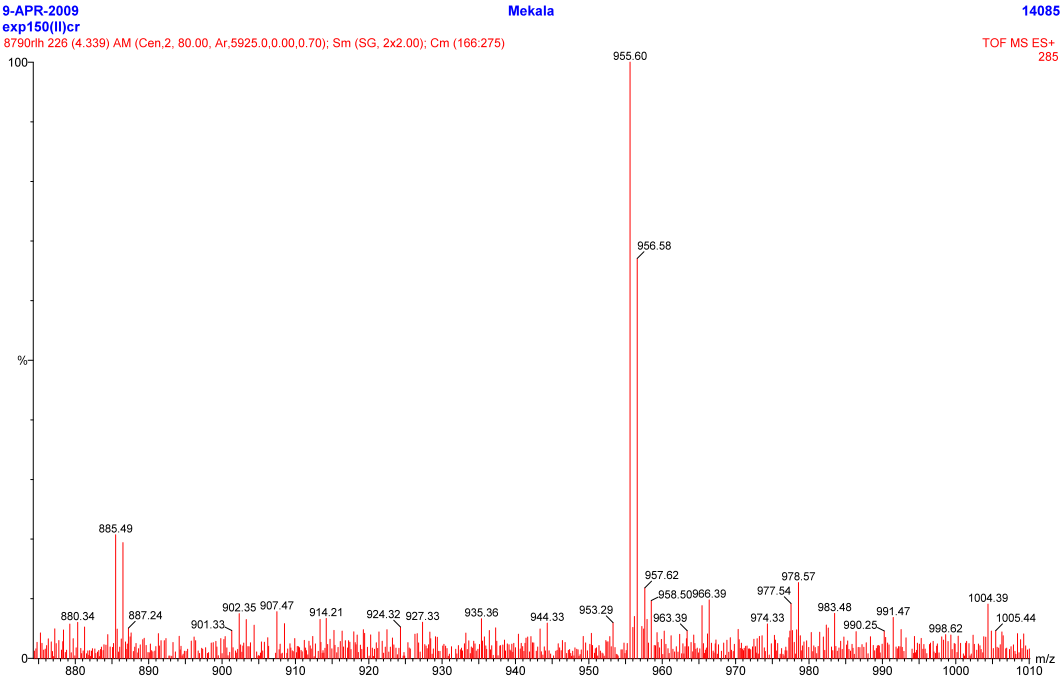

Figure 3.15 ESI-MS spectrum for exp#4 (imine)

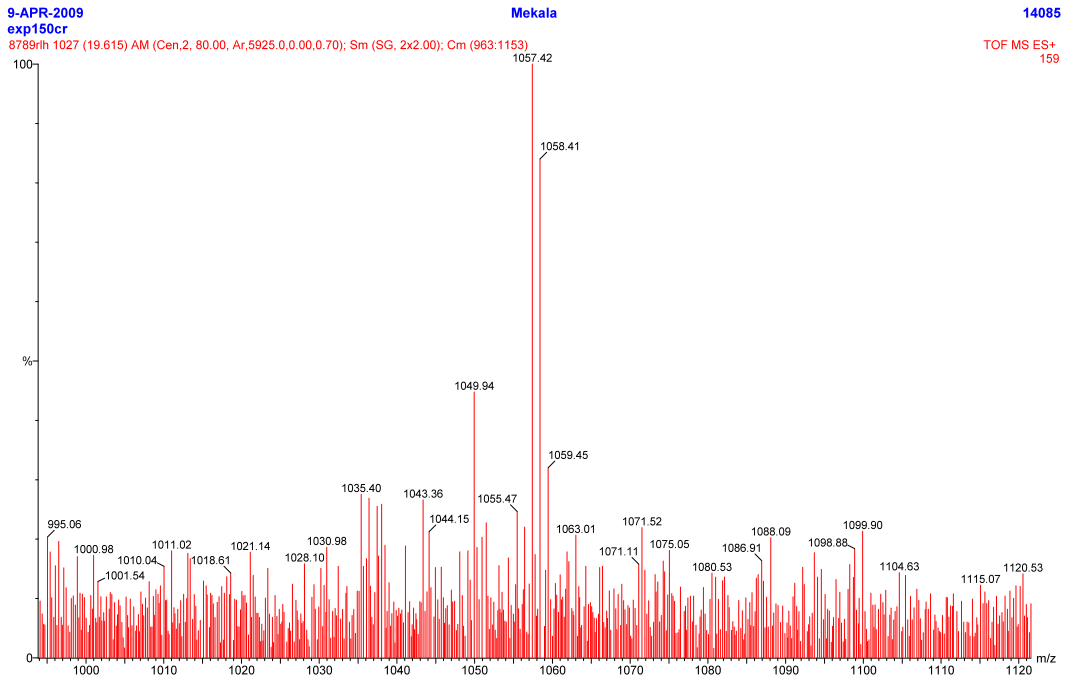

Figure 3.16 ESI-MS spectrum for exp#4 (amine)

3.10 References

74. Corbett, P.T.; Leclaire, J.; Vial, L.; West, K. R.; Wietor, J-L.; Sanders, J. K. M.; Otto, S. Dynamic Combinatorial Chemistry, *Chem. Rev.*, **2006**, *106*, 3652–3711.

75. Cougnon, F. B. L.; Sanders, J. K. M. Evolution of Dynamic Combinatorial Chemistry, *Acc. Chem. Res.* **2011**, ASAP.

76. Cougnon, F. B. L.; Sanders, J. K. M. Evolution of Dynamic Combinatorial Chemistry, Acc. Chem. Res. 2011, ASAP.

77. Hermann, A. Dynamic mixtures and combinatorial libraries: imines as probes for molecular evolution at the interface between chemistry and biology, *Org. Biomol. Chem,* **2009**, *7*, 3195-3204.

78. a) Eliseev, A.V.; Lehn, J.-M. Curr. Top. Microbiol. Immunol, **1999**, *243*, 159–172; (b) Cousins, G. R. L.; Poulsen, S. –A.; Sanders, K. K. M. Molecular evolution: dynamic combinatorial libraries, autocatalytic networks and the quest for molecular function Curr. Opin. Chem. Biol, **2000**, *4*, 270–279; (c) S. Ladame, S. Dynamic combinatorial chemistry: on the road to fulfilling the promise, *Org. Biomol. Chem.,* **2008***, 6*, 219–226.

79. Corbett, P.T.; Leclaire, J.; Vial, L.; West, K. R.; Wietor, J-L.; Sanders, J. K. M.; Otto, S. Dynamic Combinatorial Chemistry, *Chem. Rev.*, **2006**, *106*, 3652–3711. Cougnon, F. B. L.; Sanders, J. K. M. Evolution of Dynamic Combinatorial Chemistry, *Acc. Chem. Res.* **2011**, ASAP.

80. Layer, R. W. The Chemistry of Imines, *Chem. Rev*, **1963**, *63*, 489 – 510.

81. a) Goral, V.; Nelen, M. I.; Eliseev, A. V.; Lehn, J.-M. Double-level "orthogonal" dynamic combinatorial libraries on transition metal template, *Proc. Natl. Acad. Sci. U.S.A.* **2001**, *98*, 1347; b) Leclaire, J.; Vial, L.; Otto, S.; Sanders, J. K. M. Expanding diversity in dynamic combinatorial libraries: simultaneous exchange of disulfide and thioester linkages, *Chem. Commun.* **2005,** 1959 - 1961; c) Escalante, A. M.; Gastón Orrillo, A.; Furlan, R. L. E. Simultaneous and Orthogonal Covalent Exchange Processes in Dynamic Combinatorial Libraries, *J. Comb. Chem.* **2010**, *12*, 410–413.

82. Goral, V.; Nelen, M. I.; Eliseev, A. V.; Lehn, J.-M. Double-level "orthogonal" dynamic combinatorial libraries on transition metal template *Proc. Natl. Acad. Sci. U.S.A.* **2001**, *98*, 1347.

83. Collman, J. P.; Gagne, R. R.; Reed, C.; Halbert, T. R.; Lang, G Robinson, W. T. Picket fence porphyrins. Synthetic models for oxygen binding hemoproteins, *J. Am. Chem. Soc.* **1975**, *97*, 1427.

84. Jonathan Lindsey. Increased yield of a desired isomer by equilibriums displacement on binding to silica gel, applied to *meso*-tetrakis(*o*-aminophenyl)porphyrin, *J. Org. Chem.* **1980**, *45,* 5215.

85. Mattson, R. J.; Pham, K. M.; Leuck, D. J.; Cowen, K. A. An improved method for reductive alkylation of amines using titanium(IV) isopropoxide and sodium cyanoborohydride, *J. Org. Chem.*, **1990**, *55*, 2552–2554.

86. Huang, K. W.; Waymouth, R. M. Coordination Chemistry of Stable Radicals: Homolysis of a Titanium–Oxygen Bond, *J. Am. Chem. Soc.*, **2002**, *124*, 8200–8201.

87. Lindsey, J. L.; Mauzerall, D. C. Synthesis of a cofacial porphyrin-quinone via entropically favored macropolycyclization, *J. Am. Chem. Soc.* **1982**, *104*, 4498-4500.

88. Moffett, R. B.; Hoehn, W. M. Analgesics. II. The Grignard Reaction with Schiff Bases, *J. Am. Chem. Soc.* **1947**, *69*, 1792 - 1794, Freifelder, M. Selective Hydrogenolysis. Dehalogenation in the Presence of N-Benzyl Linkage, *J. Org. Chem.* **1966**, *31*, 3875.

Chapter 4

Thermal Atropisomerization of *meso*-tetrakis[2-(N-neopentylamino or N-benzylamino)phenyl]-porphyrins

4.1 Introduction

The stereoselective synthesis of compounds containing one or more stereogenic centers has emerged as one of the most important fields in chemistry, ever since the first resolution of tartaric acid by Louis Pasteur in 1848.[89] Numerous excellent diastereo- and enantioselective procedures have been developed which belong nowadays to the standard repertoire of synthetic chemistry.[90] Axial chirality, by contrast, as a stereogenic element in rotationally hindered biaryl compounds of natural and synthetic origin, has often been overlooked or treated as an "academic curiosity". This, however, has changed with the recognition that the configuration at a biaryl axis can be a decisive factor in governing the pharmacological properties of a bioactive compound and that axial chirality is the fundamental basis for useful reagents and catalysts in asymmetric synthesis.[91] Axially chiral biarylic auxiliaries and catalysts exhibit excellent chirality transfer properties and example for axially chiral biaryl molecues are given in the **Scheme 4.1**.

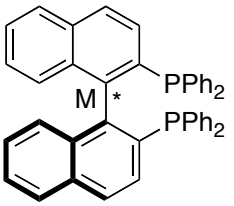

binap

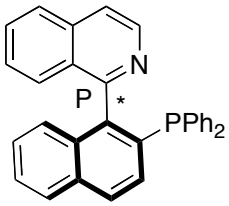

quinap

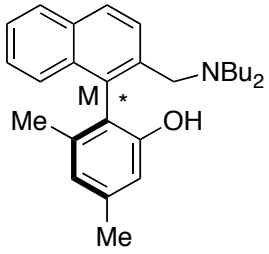

non-C2-symmetric biaryl compound
The tertiary aminophenol

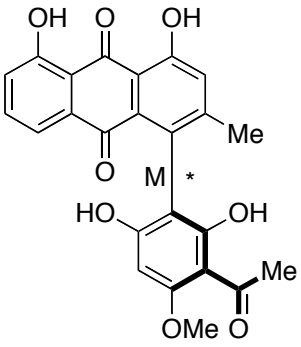

knipholone

Naturally occurring axially chiral biaryl compound

Scheme 4.1 Examples for Axially chiral biaryl compounds

Atropisomers are the stereoisomers resulting from hindered rotation about single bonds where the steric strain barrier to rotation is high enough to allow for the isolation of the conformers.[92] The term "atropisomerism" (from the Greek, **a =** not and **tropos =** turn) was introduced by Kuhn in 1933 and originally referred solely to biaryl compounds.[93] Oki, defined atropisomers as conformers that interconvert with a half-life of more than 1000 seconds at a given temperature.[94] Atropisomers are an important class of compounds because they display axial chirality. In general, there are two necessary preconditions for axial chirality in biaryl molecules: a rotationally stable axis

and the presence of different substituents on both sides of the axis as indicated in **86**, that is, A ≠ B and A' ≠ B'. If A=A' and B=B', the molecule has C_2 symmetry (but is still chiral) as in **87**, **88**, and **89** (Scheme 4.2).

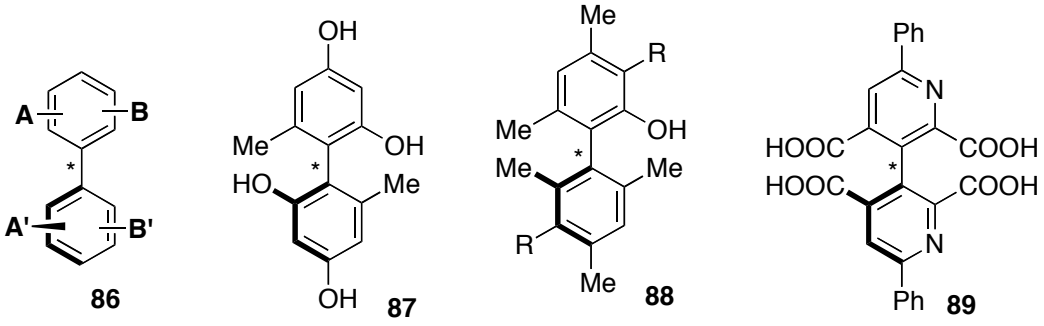

Scheme 4.2 Atropisomerism in biaryl compounds

The configurational stability of axially chiral biaryl compounds is determined by three major factors: 1) the (combined) steric demand of the substituents in proximity to the axis; 2) the existence, length, and rigidity of bridges; and 3) the involvement of atropisomerization mechanisms different from a merely physical rotation about the axis, for example, by photochemically or chemically induced processes. Therefore, atropisomers differ from other chiral compounds in that they can be equilibrated thermally whereas in the other forms of chirality isomerization is usually only possible chemically.

4.2 Thermal Atropisomerism

The other crucial precondition for atropisomerism is the rotational stability of the biaryl axis. The temperature has a profound influence on the one hand, even biaryl compounds with a low degree of steric hindrance will

suffer impeded rotation if sufficiently cooled down and split up into atropo-enantiomers or –diastereomers, if unsymmetrically substituted; on the other hand, biaryl species that are axially chiral at room temperature may start to atropisomerize upon heating, resulting in thermodynamically controlled equilibrium mixtures. As an arbitrary, but useful definition, atropisomers are recognized as physically separable species when, at a given temperature, they have a half-life time of at least 1000 s (16.7 min). Thus the minimum free energy barrier $\Delta G^{\ddagger}$ required varies with temperature (e.g. $\Delta G^{\ddagger}_{200K}$ = 14.7 Kcal mol^{-1}, $\Delta G^{\ddagger}_{300K}$ = 22.3 Kcal mol^{-1}, and $\Delta G^{\ddagger}_{350K}$ = 26.0 Kcal mol^{-1} etc.).

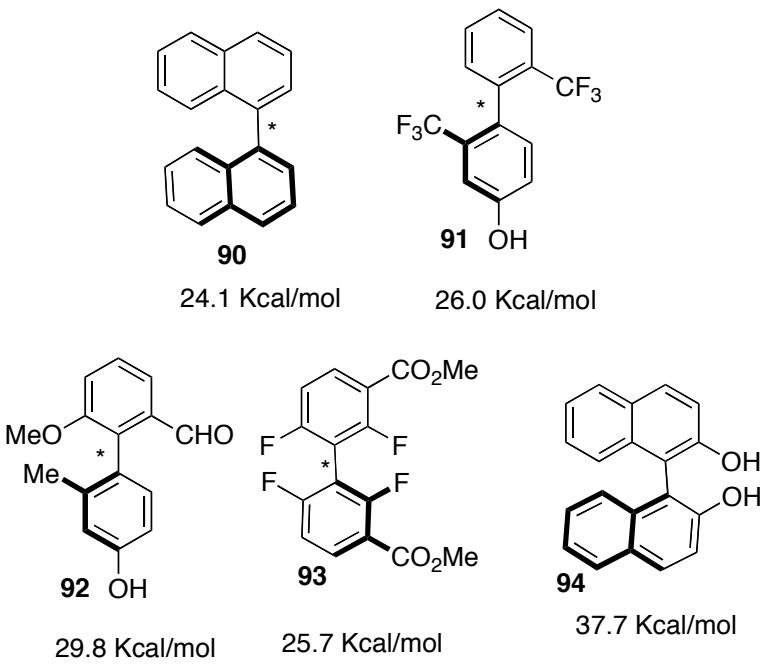

Scheme 4.3 Energy barriers for rotation for substituted biphenyls

In many cases, the barrier to rotation can be rationalized in terms of substituent effects. Ortho Substituents increase the atropisomerization barrier

in nonbridged biaryl compounds by their steric repulsion, corresponding largely to the van der Waals radii of the substituents,[95a] that is, I > Br > Me > Cl > NO_2 > CO_2H > OMe > F > H and some examples of substituted biphenyls and their energy barriers for rotation are given in **Scheme 4.3**, and in the di substituted compounds **90** and **91**, the energy barrier for rotation is 24.1 and 26.0 Kcal/mol at 327 K and 332 K respectively. Where as, in tri and tetra substituted biphenyls, the energy barrier for rotation is 29.8, 25.7 and 37.7 Kcal/mol at 383 K, 358 K and 493 K respectively.

4.3 Atropisomerism in ortho-substituted tetraphenyl porphyrins (TPPs)

The rotation of the phenyl groups in substituted and unsubstituted 5,10,15,20-tetraphenylporphyrins (TPPs) has been known since the 1970s, and within the last 30 years, many other rotational processes in porphyrins have been studied. The rotation of phenyl rings in TPP and substituted derivatives is very similar to the atropisomerism observed in biphenyls and related systems discussed in **section 4.2**. For a phenyl group to rotate it must pass through the plane of the porphyrin, much like two aryl rings in a biphenyl must become coplanar in the transition state (**scheme 4.4**).

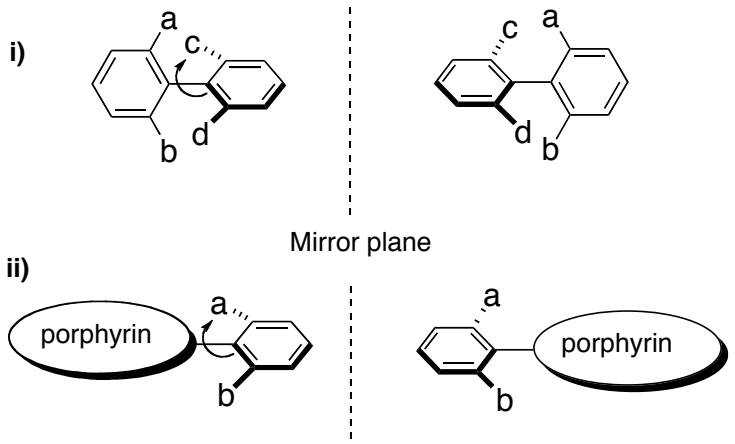

Scheme 4.4 Comparision of atropisomerism in biphenyls (i) *verses* TPPs (ii)

Typically, ortho -substitutedphenyls and some meta-substituted phenyls give rise to atropisomerism observable on the NMR time scale, which has almost solely been used to observe and measure activation barriers for such processes. In a conformationally immobile system, four atropisomers exist for TPPs, differing by the location of the substituent above (**α**) or below (**β**) the porphyrin plane: **αααα**, **ααα**β , **αβαβ** , and **ααββ** (**Scheme 4.5**).

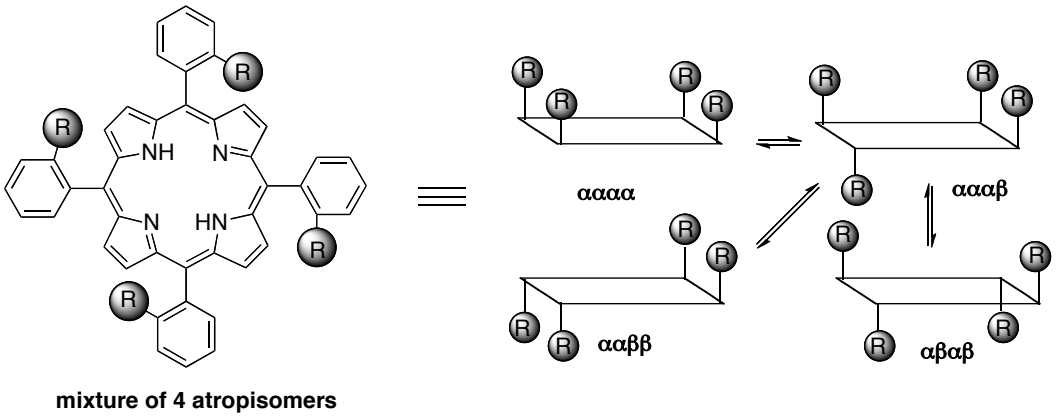

Scheme 4.5 Atropisomeric mixture of substituted TPPs

In 1969, Gottwald and Ullman[95b] were the first to observe rotation of the phenyl rings in TPPs (**Scheme 4.6**) in tetra-*ortho*-hydroxyphenylporphyrin (*o*-OH-TPP; **95**). Due to the relatively large barriers to rotation, they isolated the four isomers on silica gel and studied the isomerization crudely by thin-layer chromatography separation followed by spectroscopic identification. Isomerization at room temperature occurred with a first-order rate constant of $(1.5 \pm 0.5) \times 10^{-5}$ s^{-1}, which corresponds to an activation barrier ($\Delta G^{\ddagger}_{293K}$) of 24.0 kcal mol^{-1}. To test whether distortion from planarity of the porphyrin ring ("ruffling") occurred in the transition state, they made the more rigid copper metalloporphyrin (**96**), but they found that the activation barrier increased only slightly to ($\Delta G^{\ddagger}_{293K}$) 25.4 kcal mol^{-1}. Metalated porphyrins are not as flexible as their free-base congeners and are thus not as susceptible to ruffling. This makes the passage of the sterically demanding phenyl group through the plane of the porphyrin more difficult, and the resulting activation energy for the rotation is thus higher. However, the small change indicated that the ruffling might not be very important.

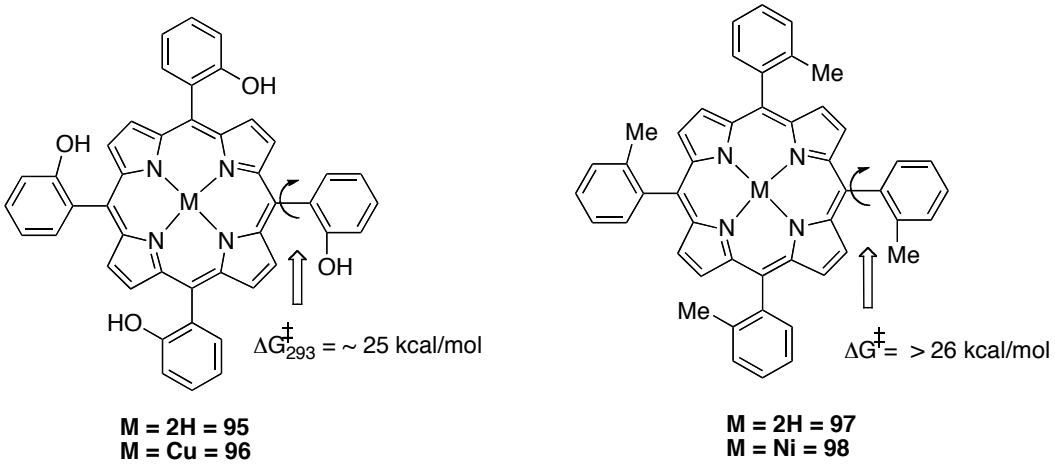

Scheme 4.6 Early tetraphenylporphyrin systems for the study of phenyl ring

rotation.[96]

In 1971, Walker and Avery[97] discovered atropisomerization in nickel(II) tetra-*ortho*-tolylporphyrinate [Ni(*o*-tol-TPP), **98**], and they found the barrier to rotation to be at least (($\Delta G^{\ddagger}$) 26.0 kcal mol^{-1} using DNMR (**Scheme 4.6**). Because of experimental limitations, they could not determine the exact value.

After these initial successes in observing atropisomerism in TPPs, Eaton and Eaton,[98] published a series of papers discussing rotation in substituted metalated TPP complexes of Ru(II), In(III), Ga(III), and Ti(IV) bearing axial ligands. Depending on the metal and the ligand, they found activation energies (ΔG 298) between 13.0 and more than 23 kcal mol-1 using DNMR. In 1979, Gust and co-workers[99] investigated the DNMR of H_2 TPPs and diprotonated H_4 –TPPs (**Scheme 4.7**) They found an activation barrier ($\Delta G^{\ddagger}_{433K}$) of 25.9 kcal mol^{-1} for H_2 (*o*-OMe-TPP, **99**) and 23.0 kcal/mol for dicationic, H_4(*o*-OMe-TPP, **100**). For H_2(di-*o*- OMe-TPP, **101**) the barrier for rotation ($\Delta G^{\ddagger}_{433K}$ = 25.2 kcal/mol) is almost close to the mono methoxy derivatives **99** and **100**, but for H_4(di-*o*- OMe-TPP, **102**) is slightly lower ($\Delta G^{\ddagger}_{388K}$ = 21.8 kcal/mol) than all other derivatives in this series. The diacids are known to be less conformationally rigid than the free-base porphyrins, which are in themselves less rigid than metalated porphyrins, and this accounts for the lower barrier to phenyl rotation. Hatano et al.[100] studied the dynamics of

o-CN-TPP and found an activation energy (***Ea***) of about 21.0 kcal/mol for the rotation of one phenyl group. Medforth and co-workers[101] investigated atropisomerism in TPPs with *o*–carborane appended to the *meta*-position of the phenyl rings and found the barrier ($\Delta G^{\ddagger}_{323K}$ = ~17.0 kcal/mol, and for Zn derivative it was 18.0 -19.0 kcal/mol and for Ni derivative was 13.0 kcal/mol. These results indicate that the barrier is mainly depends on the substitution on the ortho position of the phenyl group in the porphyrin.

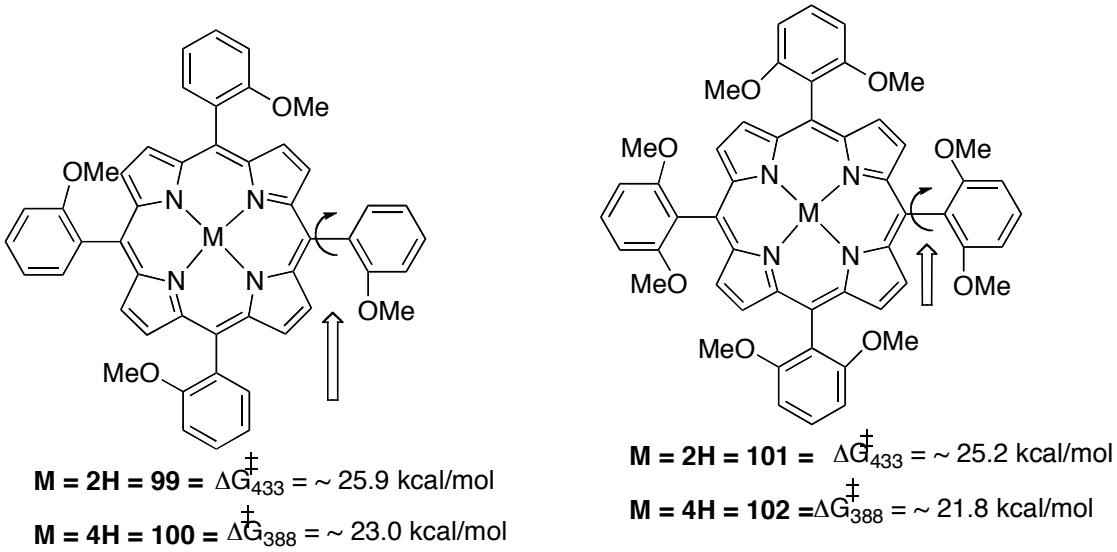

M = 2H = 99 = $\Delta G^{\ddagger}_{433}$ = ~ 25.9 kcal/mol

M = 4H = 100 = $\Delta G^{\ddagger}_{388}$ = ~ 23.0 kcal/mol

M = 2H = 101 = $\Delta G^{\ddagger}_{433}$ = ~ 25.2 kcal/mol

M = 4H = 102 = $\Delta G^{\ddagger}_{388}$ = ~ 21.8 kcal/mol

Scheme 4.7 Energy barriers to rotation in substituted phenylporphyrins

In 1979, Collman and co-workers in their studies on iron porphyrins as mimics for oxymyoglobins and oxyhemoglobins[102] they were interested in the **αααα** -isomers of TPPs, bearing steric groups in the ortho positions of the phenyl rings to form "picket fence" porphyrins. The idea was to create a hydrophobic pocket by placing all the substituents on the same side of the porphyrin ring, which mimics the natural system and allows oxygen to enter

where it is protected from other species by the pickets. In this way, they were able to crystallize the first iron porphyrin complex with bound dioxygen. Whitten and co-workers (**Scheme 4.8**)[103] have studied tetraamido-TPPs similar to those investigated by Collman and collaborators, They performed a detailed study of the activation barriers to rotation both thermally and photochemically, for the free bases, the diprotonated forms, and metal containing complexes of tetra-*o*-propionamido-TPP, *tetra-**o***-hexadecanamido-TPP, and tetra-*o* -pivalamido-TPP. Nickel(II) complexes gave the lowest barriers to rotation in all cases. This is not surprising, since Ni-TPP complexes are nonplanar in the solid state, indicating that deformation ispossible and leads to a pathway for easier phenyl group rotation. As expected, they found that the zinc- (II) comp lexes gave the highest barriers to rotation Zn- TPP complexes are known to be the least deformable planar metal- TPP complexes in the solid state. Although the free-base and diacid compounds gave slightly higher barriers to rotation than the Nickel(II) complexes, they were lower than all the other metals, presumably because they are more easily deformed. The diprotonated forms gave lower values than the free bases. The pivaloyl group gave higher barriers than the other groups, which indicates that the size of the tert -butyl group is more important than the chain length (**Table 4.1**).

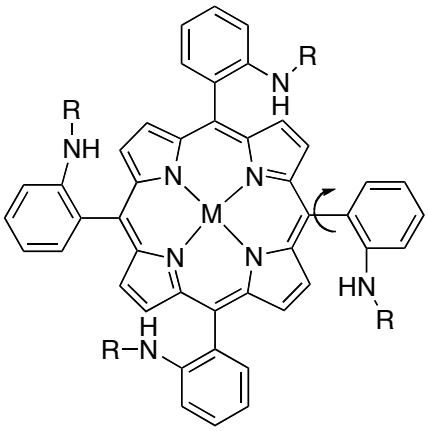

Scheme 4.8 Thermal atropisomerism in amido 'picket fence' porphyrins[104]

Metal (M)	R	(ΔG_{383}) kcal/mol	Compound
2H	$C(O)CH_2CH_3$	29.1	**103**
	$C(O)C(CH_3)_3$	30.6	
4H	$C(O)CH_2CH_3$	26.4	**104**
	$C(O)C(CH_3)_3$	28.3	
Ni(II)	$C(O)CH_2CH_3$	25.8	**105**
	$C(O)C(CH_3)_3$	--	
Cu(II)	$C(O)CH_2CH_3$	29.7	**106**
	$C(O)C(CH_3)_3$	31.4	
Pd(II)	$C(O)CH_2CH_3$	31.0	**107**
	$C(O)C(CH_3)_3$	31.7	
Zn(II)	$C(O)CH_2CH_3$	31.4	**108**
	$C(O)C(CH_3)_3$	32.2	

Table 4.1 Energies for the Rotation of Substituted Phenyl Groups in the Amido "Picket-Fence" Porphyrins

These early results provided the groundwork for understanding the factors that influence the rotation about the C_{porph}- C_{Ph} single bond. The ability of the porphyrin ring to distort from a planar structure lowers the activation barrier to rotation. However, the barrier is tunable, depending on the nature of the substituent on the aryl rings and on the state of the porphyrin ring (free-base, diacid, or metalated form). The choice of the metal serves to further fine-tune the relative energy to rotation of the phenyl rings.

4.4 Thermal Atropisomerization of *meso-tetrakis*[2-(N-neopentylamino or N-benzylamino)phenyl]-porphyrins

4.4.1 tetra(N-alkyl/arylaminophenyl)porphyrins

This work was submitted for full publication for Tetrahedron Letters.[105] Controlling the alignment and rotation of substituted phenyl rings in 5,10,15,20-tetraphenylporphyrins (TPP) is crucial to the design and application of metallotetraphenylporphyrin catalysts.[1] The ability to align all four amino groups above the same porphyrin face through thermal isomerization in the presence of silica gel has enabled facile access to (α,α,α,α)-*tetra*(o-aminophenyl)porphyrin **74**.[106] We now wish to take advantage of this pre-aligned scaffolding to hold amino substituents above a reactive site in metalloporphyrins. Towards this end we describe herein an ability to functionalize (α,α,α,α)-tetra(*o*-aminophenyl)porphyrin **74** with minimal atropisomerization, an ability to purify this atropisomer, the determination of the energy barriers for atropisomerization of substituted tetra(N-

alkyl/arylaminophenyl)porphyrins, and a failure in attempts to interconvert mixtures of substituted tetra(N-alkyl/arylaminophenyl)porphyrin atropisomers into a single atropisomer.

Atropisomerism in tetraarphylporphyrins is similar to that observed in *ortho*-substituted biphenyls in which restricted rotation of the phenyl groups can result in the formation of room temperature stable atropisomers.[107] In atropisomerism of tetraphenylporphyrins, the *ortho* substituents on the phenyl group must pass through the plane of the porphyrin. As a result of the steric repulsion between these groups, rotation about the porphyrin-phenyl bond is hindered to such a degree that the inclusion of even one non-hydrogen ortho substituent per phenyl group is sufficient to enable atropisomers at room temperature.[108] The four atropisomers pictured in **Scheme 4.9** correspond to the possible distributions of the four *ortho*-phenyl substituents between the two sides of the porphyrin plane.[109]

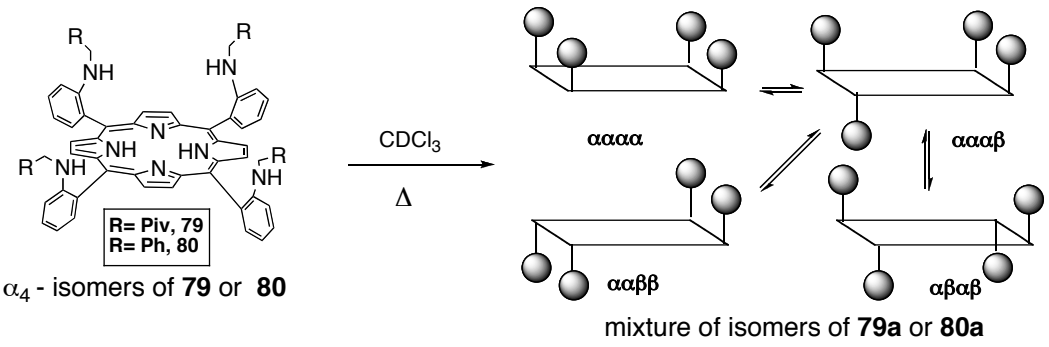

Scheme 4.9. Atropisomerization of *meso*-tetra(*o*-alkyl/arylarylaminophenyl) porphyrins **79** and **80**.

Given a diversity of methods to readily derivatize aminophenyl groups, substituted tetraarylporphyrins containing nitrogen atoms on the *ortho*-phenyl position are particularly promising scaffolds. The barrier for atropisomeriztion of tetra(2-aminophenyl)porphyrin **73** has been determined to be $\Delta G^{\ddagger}_{354}$ = 27.9 kcal/mol,[110] while atropisomerization of tetraamido TPPs, range from $\Delta G^{\ddagger}_{383}$ = 29.1 to 30.6 kcal/mol.[111] Barriers for the atropisomerization of tetra[2-(N-alkyl/arylamino)phenyl]porphyrins have not been previously reported. Herein we report the preparation and activation barriers for the atropisomerization of αααα-*meso*-tetra[2-(N-(neopentylamino)phenyl]porphyrin (TnPAPP, **79**) and αααα - *meso*-tetra[2-(N-benzylamino)phenyl]porphyrin (TBnAPP, **80**).

4.4.2 Results and Discussion

The preparation of predominately the α,α,α,α-atropisomer of the desired substituted tetraphenylporphyrins TnPAPP (**79**) and TBnAPP (**80**) was achieved by adopting a procedure by Lindsey, et al,[112] as shown in **Scheme 3.8 and 3.9**. Isomerically enriched (α,α,α,α)-*meso*-tetra(*o*-aminophenyl)porphyrin (**74**) was prepared by thermal isomerization in the presence of silica gel.[113] Schiff base formation and subsequent reduction by $NaBH_3CN$ provided (α,α,α,α)-isomer **79** (73% yield) and **80** (~75% yield). The long reaction times allowed some isomerization of **74** into other atropisomers during the course of reaction and isomeric enrichment of **79** and **80** by chromatography was not completely effective. The synthesis of compounds **79** and **80** by

Lindsey's reductive amination method[112] gave improved isomeric purity and isolated yields of α,α,α,α-isomer of **79** (up to 93%) and **80** (up to 83%).

Thermal rotation of one substituted phenyl ring about the phenyl-porphyrin bond enables the formation of an equilibrium mixture of atropisomers. The preparation of the equilibrium isomeric mixture of **79a** or **80a** from isomerically mixed TAPP **73** is shown in **Scheme 4.10**. After heating a $CDCl_3$ solution of (α,α,α,α)-**79** or **80** at 90 °C for 24 h, all four isomers were observed in the NMR spectra in ratios similar to those seen in the samples prepared from isomerically mixed TAPP **73**.

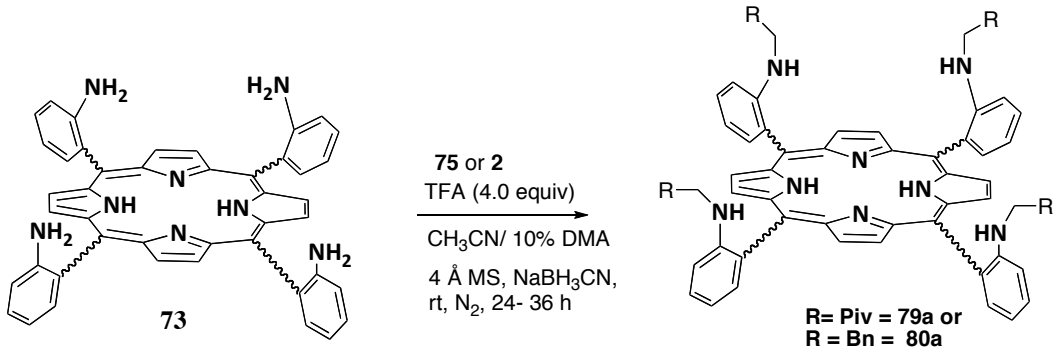

Scheme 4.10. Synthesis of isomeric mixtures **79a** and **80a** by the method of reductive amination.

Monitored thermal atropisomerization reactions of **79** and **80** were conducted in $CDCl_3$ at 70, 80 and 90 °C in a constant temperature water bath. The conversion of (α,α,α,α)-TnPAPP **79** and (α,α,α,α)-TBnAPP **80** into the mixture of isomers (**79a** or **80a**) was monitored by periodically immersing the NMR sample tube in an ice bath prior to NMR spectroscopy at ambient temperature and then immediately returning the sample into the temperature

bath.[113] As shown in **Figure 4.1**, a decrease in the ratio of NMR signals of methylene protons of **79** or **80** was observed as well as a correpsonding increase in the intensity of the other atropisomers. The isomerization process was evidenced by the observation that resulting new NMR signals due to methylene protons were similar to the methylene protons of compounds of **79a** and **80a**, which were synthesized starting with equilibrium mixture of **73** by reductive amination method (**Scheme 4.10**).

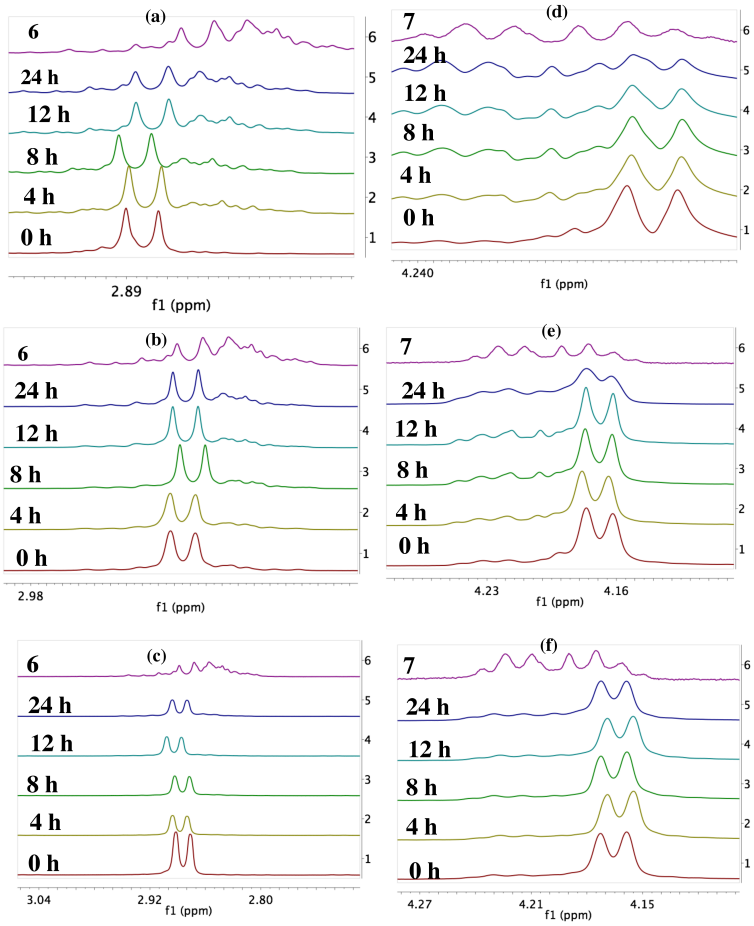

Figure 4.1. VT NMR's (at 0, 4, 8, 12 and 24 hrs) of **TnPAPP (79)** : a) at 90 ºC, b) 80 ºC, c) 70 ºC; **TBnAPP (80)** : d) at 90 ºC, e) 80 ºC, f) 70 ºC.

The NMR signals due to the α,α,α,α-amino methylene hydrogens were sufficiently different in the four atropisomers to enable an unambiguous

assignment for the decay of **79** and **80** and conversion into the other atropisomeric mitures **79a** and **80a**.[114]

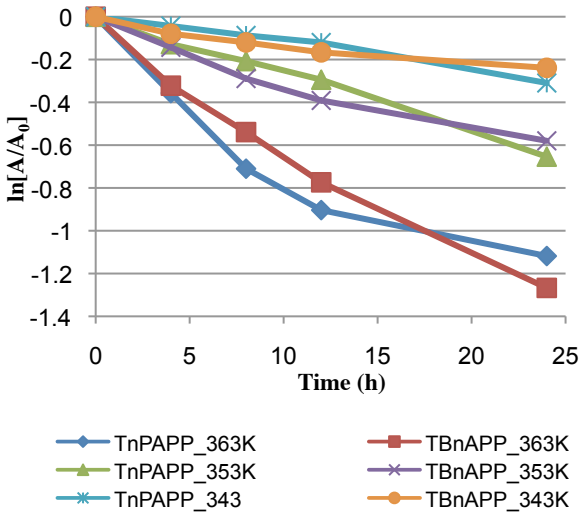

Figure 4.2. Conversion extent: **79 (TnPAPP), 80 (TBnAPP)**

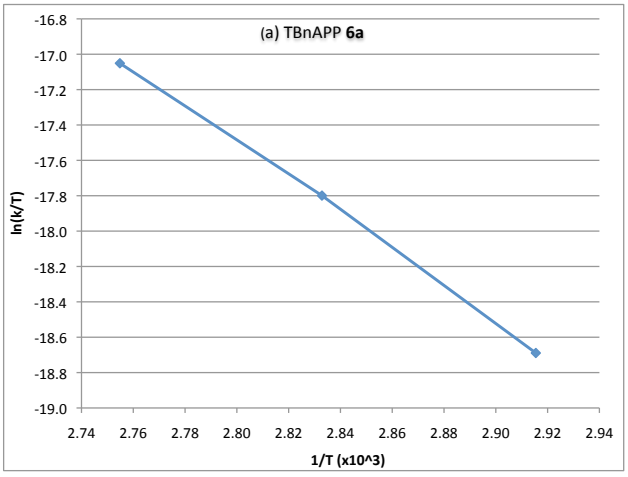

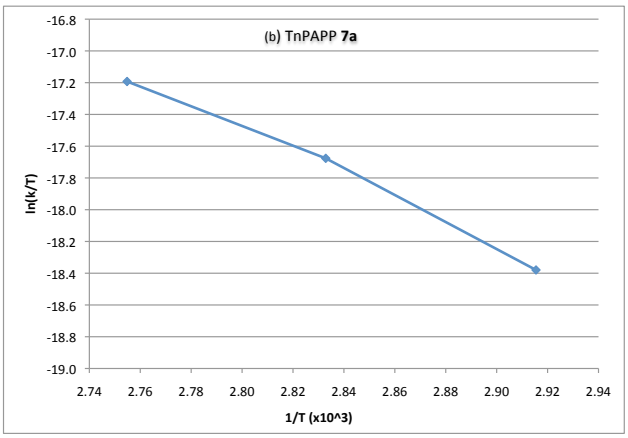

Figure 4.3. Eyring plots for a) **TnPAPP (79 = 6a)** and b) **TBnAPP (80= 7a)**

The initial reduction in the magnitude of the methylene signals for the (α,α,α,α)-atropisomers at the different temperatures was used to obtain the first order kinetic parameters for the atropisomerization. The plots for $\ln(A/A_0)$ *vs* time are shown in Figure 4.2. The initial points (8-12 h) were used to obtain the first order rate constants at each temperature.

The rate constants at 90, 80 and 70 °C and average free energy of activation for atropisomerization of TnPAPP **79** were calculated to be $k = 1.2 \times 10^{-5}$ sec^{-1}, 7.4×10^{-6} sec^{-1}, 3.5×10^{-6} sec^{-1}, with $\Delta G^{\ddagger}_{353}$ = 29.1 kcal/mol and for TBnAPP **80**, $k = 1.4 \times 10^{-5}$ sec^{-1}, 6.5×10^{-6} sec^{-1}, 2.6×10^{-6} sec^{-1} with $\Delta G^{\ddagger}_{353}$ = 29.2 kcal/mol. These $\Delta G^{\ddagger}$ values are very close to those of tetraamido phenylporphyrins reported by Whitten and co-workers.[115]

Eyring plots of the variation of the rate constants (*k*'s) versus 1/T shown in Figure 4.3 were used to separate the entropy and enthalpy

components of the activation barrier. The resulting kinetic parameters for atropisomerization of **79** and **80** are listed in Table 4.2. The average free energy of activation for the previously reported 5,10,15,20-tetrakis(*o*-amidophenyl)porphyrin,[116] of $\Delta G^{\ddagger}_{383}$ = 29.1 kcal/mol is similar to that of **79** and **80**. The amino-substituted tetraphenylporphyrins ($\Delta G^{\ddagger}_{354}$ = 27.9 kcal/mol)[112] and hydroxy-substituted tetraphenylporphyrins ($\Delta G^{\ddagger}_{393}$ = 24.0 kcal/mol)[117] were reported to have average free energy of activations lower than those of the substituted amine derivatives **79** and **80**. While the overall activation barrier was similar for the neopentyl- and benzyl derivatives **79** and **80**, the enthalpy of activation for the neopentyl derivative **79** was over 5 kcal/mol lower than with the benzyl substituent. This decrease in the enthalpy of activation appears to be offset by an increase in the entropic order of the transition state with approximately 16 entropy units more order observed for the neopentyl substituted **79**. A rationalization of these entropic results indicate that the bulkier neopentyl group may require more cooperative rotating of the substituent to enable its passage through the plane of the porphyrin. The decreased enthalpy of activation is harder to rationalize and may be due to some additional ground state destabilization by the bulkier neopentyl groups.

Temp (K)	$\Delta G^{\ddagger}$ (kcal/mol)		$\Delta H^{\ddagger}$ (kcal/mol)		$\Delta S^{\ddagger}$ (cal/mol-K)		Rate Constant (k/sec)	
	79	**80**	**79**	**80**	**79**	**80**	**79**	**80**
363	29.5	29.5	14.6	20.3	-41	-25	1.2×10^{-05}	1.4×10^{-05}
353	29.0	29.1	14.7	20.3	-41	-25	7.4×10^{-06}	6.6×10^{-06}
343	28.7	28.9	14.7	20.3	-41	-25	3.6×10^{-06}	2.6×10^{-06}

Table 4.2: Thermodynamic parameters for thermal atropisomerization of **79** and **80**

4.4.3 Methods to control atropisomesism in *meso*-tetra(N-alkyl/arylaminophenyl)porphyrins

Since the energy barrier for rotation of alkyl/arylaminophenyl groups in **79** is $\Delta G^{\ddagger}_{353}$ = 29.1 kcal/mol and for **80** with $\Delta G^{\ddagger}_{353}$ = 29.2 kcal/mol, these scaffolds can only be used at room temperature or lower temperatures as catalysts. Therefore, advanced methods have to be developed in order for the improvement of (α,α,α,α)-TnPAPP **79** and (α,α,α,α)-TBnAPP **80** isomers from the atropisomeric mixture of **79a** and **80a** respectively (**Scheme 4.11**). Initially we have tried to achieve this goal by Lindsey's atropisomerization method, in which dry toluene (5 mL) was added to a roundbottomed flask with silicagel ~ 3.0 g and refluxed under nitrogen for 2 h, then added ~ 100 mg of **79a** or **80a** and refluxed for additional 20 hrs and the dark slurry was then cooled to room temperature and transferred into a chromatography column and eleted with benzene and acetone. But, there was no isomerization observed for either of compounds and no starting material recovered. Which means the compounds are decomposed on silicagel after refluxing for 20 h. This is evidenced by the fact that the change in the color of crude (black) compared to starting material **79a** or **80a** (brownish red).

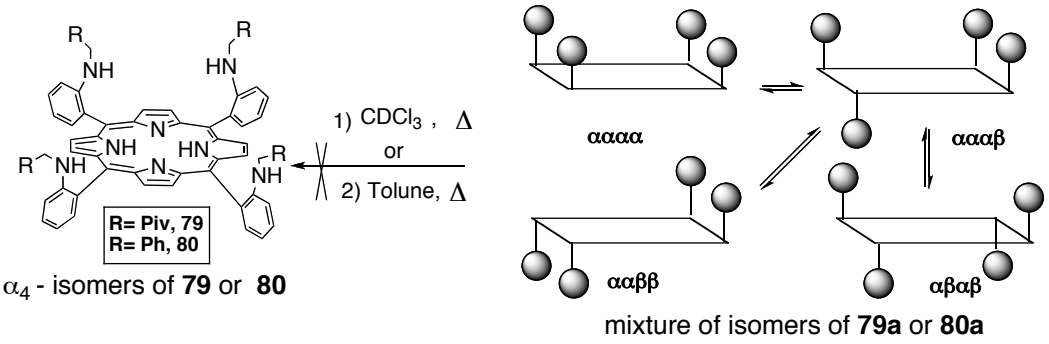

Scheme 4.11 Thermal atropisomerism of **79a** and **80a**

Another attempt by using HPLC method, in which samples of **79a** or **80a** were dissolved in chloroform and heated at high temperature in waterbath for few hrs and immersed in a icebath for few minutes to freeze the equilibration followd by injecting into HPLC column. But, the peaks (retention times) corresponding to **79** and **80** were not observed. It may be due to no isomerization of **79a** or **80a** into **79** or **80**. Final attempts made for the atropisomerization of **79a** or **80a** by the use of non-covalent templating. But, we had some synthetic challenges in template synthesis.

4.4.4 Conclusion

We have synthesized neopentyl- and benzyl substituted tetra(2-aminophenyl)porphyrins as isomeric mixtures (**79a** and **80a**) and as the ($\alpha,\alpha,\alpha,\alpha$)-isomers (**79** and **80**). We have found that the energy barriers for atropisomerization have sizable differences in the enthalpy and entropy of activation, but that the overall energy of activation is too low to maintain isomeric stability in solution at room temperature. Attempts to control isomerization in **79** and **80** were not succeful. In order for compounds of this

type to be used as stereochemically defined scaffolds for catalysts, additional steps to limit atropisomerism must be developed.

4.4.5 Experimental Section:

4.4.5.1 Synthesis of Compounds 79a and 80a by Reductive amination

The αβ-mixture of TAPP **73** (20 mg, 0.0296 mmol) was dissolved in dry acetonitrile/10% DMA (20 mL) to which was added 100.0 equiv of Pivaldehyde **75**, 4.0 equiv of TFA and 5-10 equiv of NBH_3CN periodically at room temperature under nitrogen. After 48 h, the reaction was quenched and evaporated to dryness under vacuum. The resulting material was purified by small silica gel column with 1:3 ($CHCl_3$: Hexane) eluent system to give a dark brown colred compound **79a**. Same method applied for the synthesis of **80a**.

79a. H^1 NMR ($CDCl_3$, 400 MHz): 8.89-8.86 (m, 8h, β-pyrrrole-H), 7.8-7.55 (m, 10H, Ph-H), 7.14-7.0 (m, 8H, Ph-H), 3.36-3.39 (m, 4H, N-H), 2.9-2.8 (M, 8H, CH_2), 0.48 - 0.29 (m, 36H, CH_3). ESI-MS: ($C_{64}H_{74}N_8$), $(M+H)^+$ 958.4889(100%), $(M+Na)^+$ 977.4719, calcd mol wt 954.60

80a. H^1 NMR ($CDCl_3$, 400 MHz): 8.93-8.92 (m, 8H, β-pyrrrole-H), 7.90-7.89 (br d, 2H, Ph-H), 7.83-7.81 (br d, 2H, Ph-H), 7.64-7.61 (br t, 4H, Ph-H), 7.17-6.96 (m, 28H, Ph-H), 4.24-4.15 (m, 8H, CH_2), 3.83-3.65 (m, 4H, N-H).
ESI-MS: ($C_{72}H_{58}N_8$), $(M+H)^+$ 1035.50(30%), $(M+Na)^+$ 1057.50 calcd mol wt 1034.48

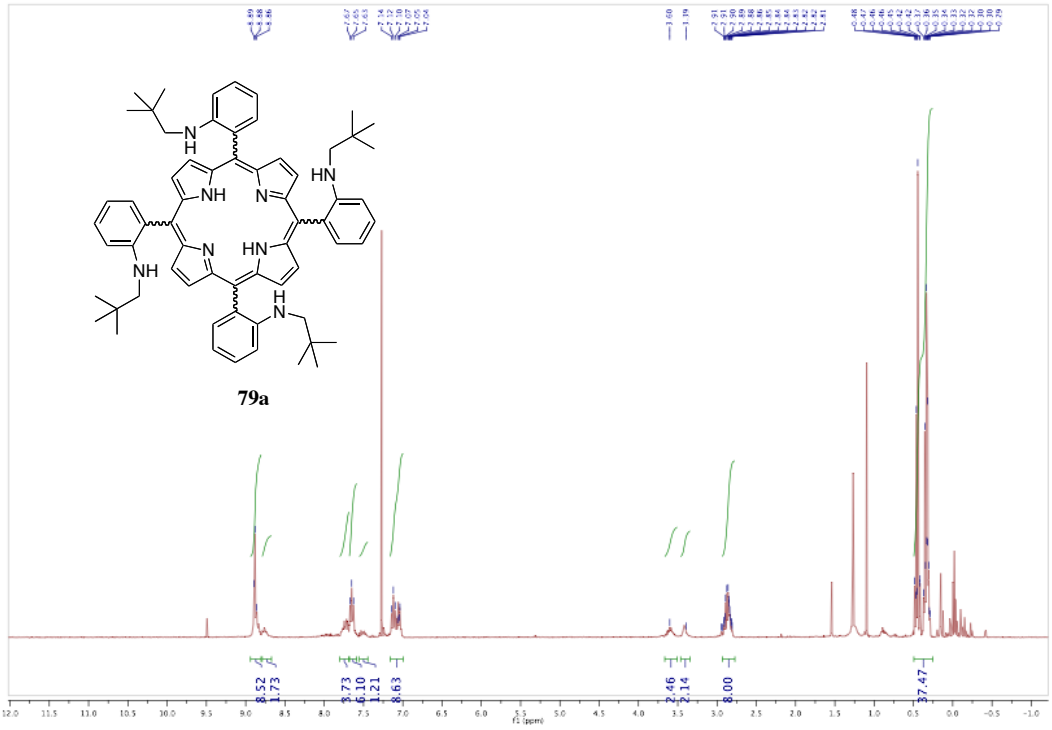

Figure 4.4 ^{1}H NMR of 79a

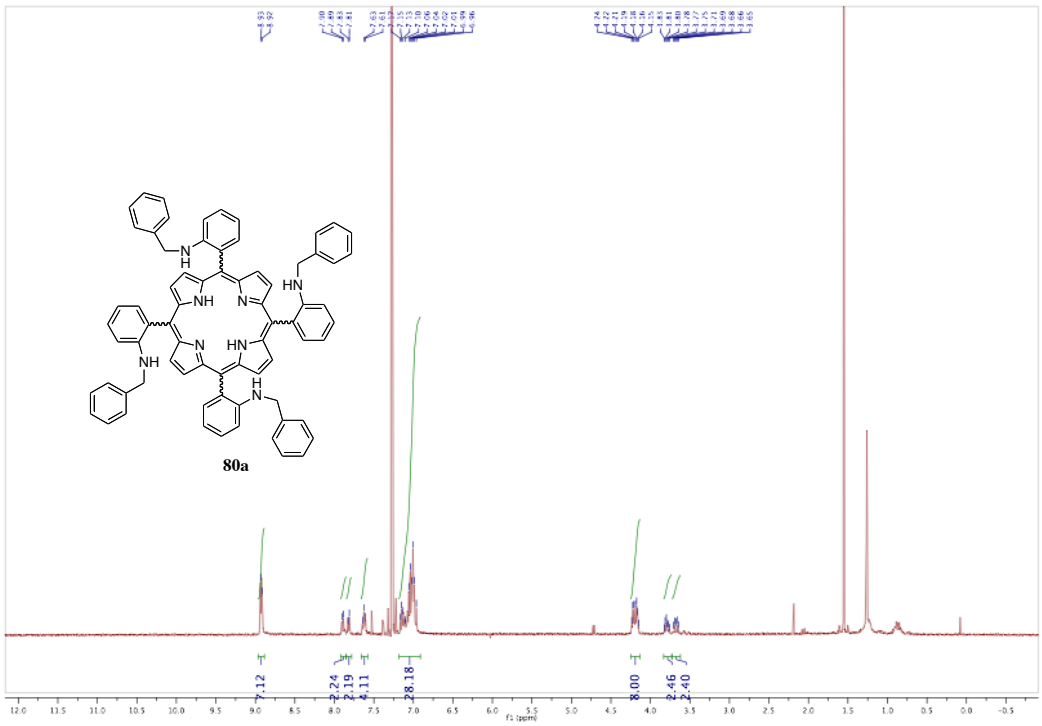

Figure 4.5 ^{1}H NMR of 80a

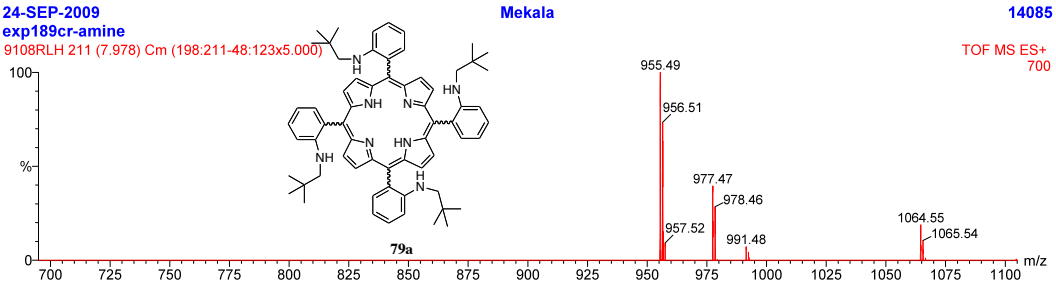

Figure 4.6 ESI-MS of 79a

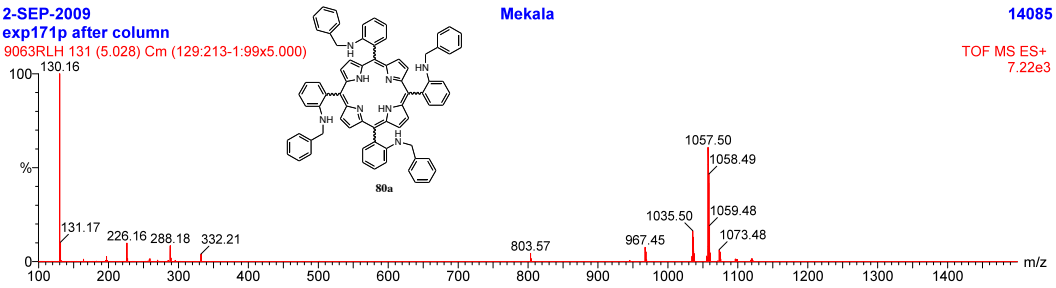

Figure 4.7 ESI-MS of 80a

4.5 Methodology for the Calculation of Energy barrier for rotation of phenyl rings in TnPAPP (79) and TBnAPP (80)

4.5.1 Sample Preparation

TnPAPP (**79**) or TBnAPP (**80**) (~ 10 mg) were dissolved in of dry $CDCl_3$ (0.5 mL) and filtered through a pipette with a plug of cotton and transferred into a NMR sample tube and sealed the NMR tube under vacuum with a screw cap and placed into the constant temperature water bath at desired temperatures (90 or 80 or 70 ºC). Then monitored the atropisomerization of the compound at 0, 4, 8, 12 and 24 hrs of time at constant temperature by placing the 'hot NMR sample tube' into ice bath to freeze the equilibration and quickly

run the ^{1}H NMR spectrum on 400 MHz instrument followed by quickly returning the NMR sample tube back into the constant temperature water bath.

4.5.2 Analysis of Atropisomerization

The change of the concentration of a specific peak in ^{1}H NMR spectrum or the appearance of new signals over time and decrease of initial concentration in a specific peak is the evidence for the atropisomerism in the molecule over time at constant temperature. By comparing the ^{1}H NMR spectra of **79** or **80** at different times (0 – 24 h) at constant temperature with the ^{1}H NMR spectrum of **79a** or **80a**, which is the mixture of all the atropisomers of **79** or **80**. Since the conversion of one isomer into another is the first order rate and the rate constant can be calculated from the known initial concentration (A_o, at t = 0 h) and the final concentration (A, at t = 24 h) of the molecule by ^{1}H NMR integration values. The rate constant '*k*' can be calculated by the first order rate constant equation and the thermodynamic parameters can be calculated by using Eyring plot and equation.

4.5.2.1 Rate constant Equation

Based on the assumption that, the initial rate of atropisomerization (one phenyl ring rotation) is equal to the first order rate of reaction. Therefore, the first order rate equation is:

$$\ln \frac{[A]}{[A_0]} = -k \cdot t \qquad \textbf{(1)}$$

$[A_0]$ = Initial concentration at t = 0 h

$[A]$ = Final concentration at t = 24 h

k = First order rate constant

Linear form of Eyring equation

$$\ln \frac{k}{T} = \frac{-\Delta H^{\ddagger}}{R} \cdot \frac{1}{T} + \ln \frac{k_B}{h} + \frac{\Delta S^{\ddagger}}{R} \qquad \textbf{(2)}$$

k = Reaction rate constant

T = Absolute temperature in K

$\Delta H^{\ddagger}$ = Enthalpy of activation

R = Gas constant (8.3145 J. mol^{-1}. K^{-1})

k_B = Boltzman constant ($1.381*10^{-23}$ J. K^{-1})

h = Planck's constant (6.626*10-34 J.s

$\Delta S^{\ddagger}$ = Entropy of activation

Eyring Plot is $\ln\left(\frac{k}{T}\right)$ *verses* $\frac{1}{T}$

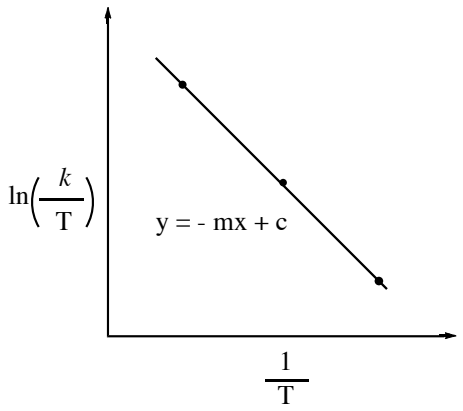

Using Eyring equation, one can calculate rate of the chemical reaction at different temperatures, The plot of $\ln\left(\frac{k}{T}\right)$ *verses* $\frac{1}{T}$ gives a straight line with slope $\frac{-\Delta H^{\ddagger}}{R}$ from wich the entholpy of activation ($\Delta H^{\ddagger}$) can be calculated and with the intercept $\left(\ln\frac{k_B}{h} + \frac{\Delta S^{\ddagger}}{R}\right)$ from which, entropy of activation $\Delta S^{\ddagger}$ can be calculated.

4.5.2.2 Calculation of Thermodynamic paremeters from Eyring plot

a) Slope m = $\frac{-\Delta H^{\ddagger}}{R}$ Therefore, $\Delta H^{\ddagger} = -m*R$

b) Entropy of activation = $\Delta S^{\ddagger}$ = from intercept from Eyring equation

$$\text{intercept} = c = \left(\ln\frac{k_B}{h} + \frac{\Delta S^{\ddagger}}{R}\right)$$

c) Gibb's free energy change = $\Delta G^{\ddagger} = \left(\Delta H^{\ddagger} - T\,\Delta S^{\ddagger}\right)$ **(3)**

4.5.3 Calculation of Energy barrier in TnPAPP (79)

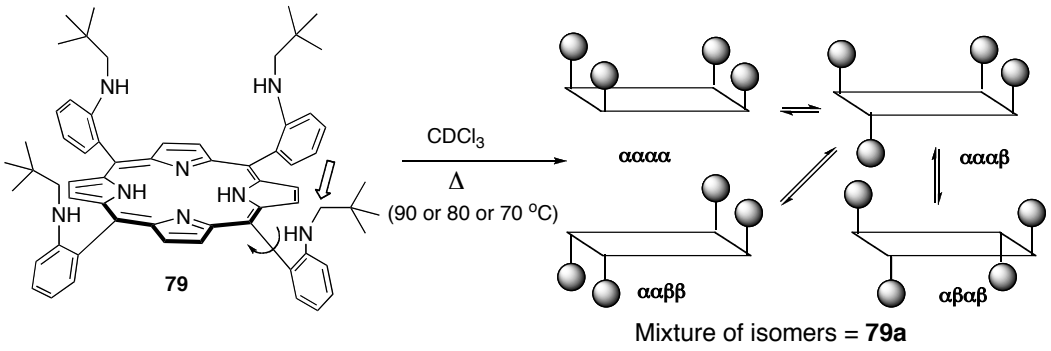

Scheme 4.12 Thermal atropisomerization in TnPAPP (79)

a) @ 90 °C: ^{1}H NMR spectra of 79 at 0, 8, 12, 24 h in $CDCl_3$ on 400 MHz

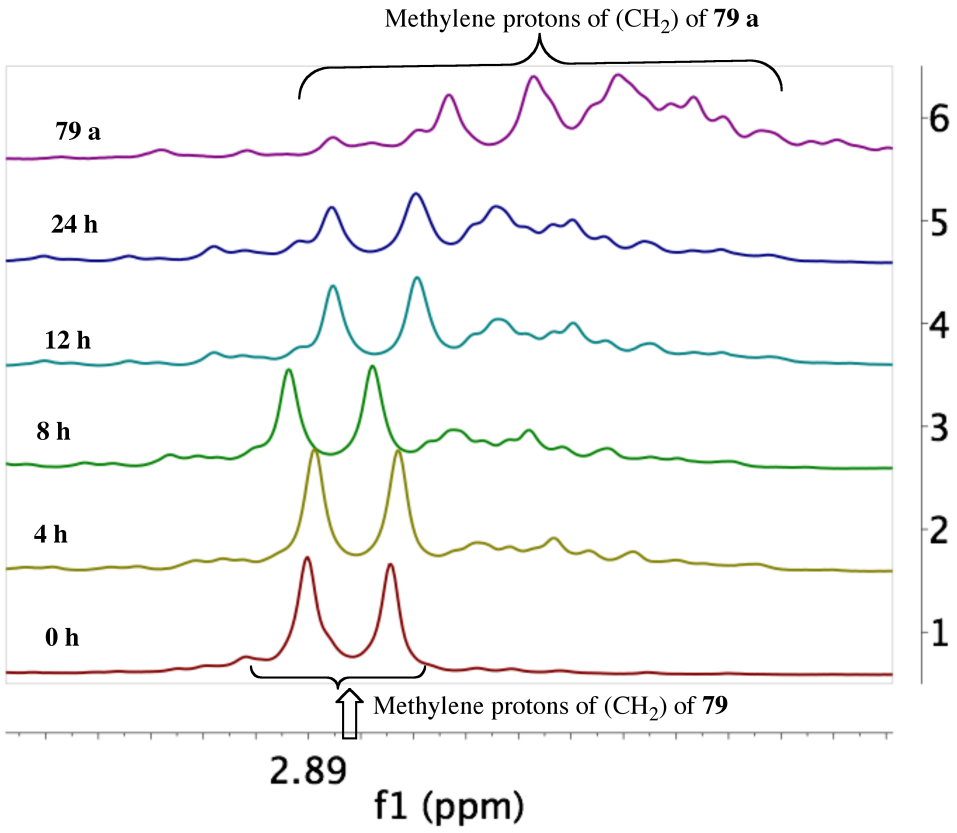

Figure 4.8 a) Stacked ^{1}H NMR spectra (# 1-5) of **79** at 0, 4, 8, 12 and 24 h @ 90 °C, b) ^{1}H NMR spectrum of **79a** (#6).

Time(h)	%TnPAPP(79)	ln[A/A$_0$]
0	78.87	0
4	55.2	-0.356837974
8	38.77	-0.710154176
12	31.95	-0.903628747
24	25.78	-1.11820193

Table 4.3 Rate of atropisomerization of **79** at 90 °C

b) @ 80 °C: ^{1}H NMR spectra of **79** at 0, 8, 12, 24 h in $CDCl_3$ on 400 MH

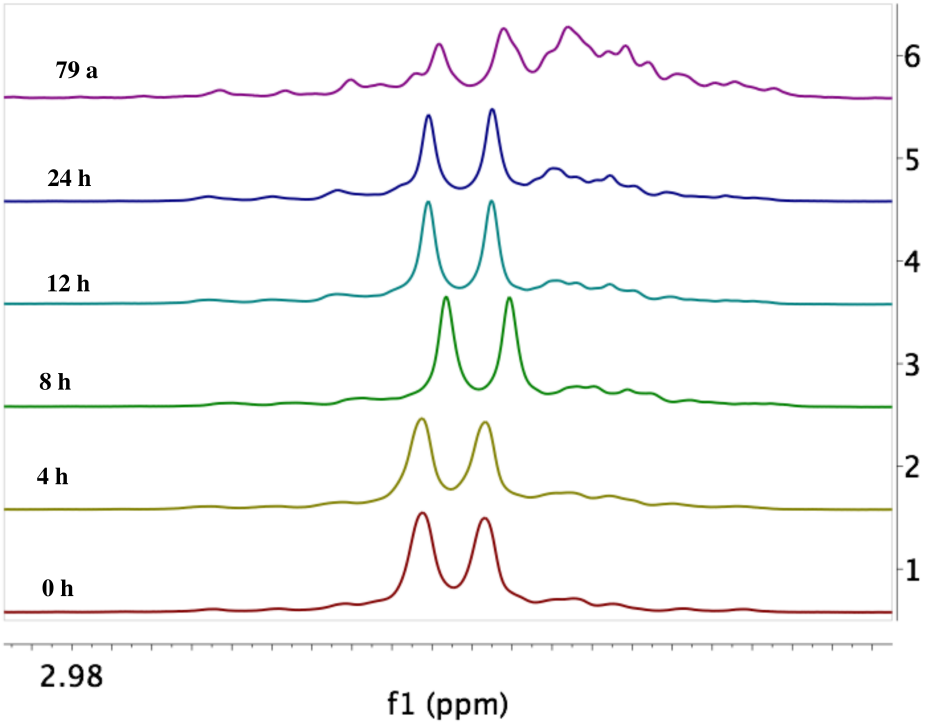

Figure 4. 9 a) Stacked ^{1}H NMR spectra (# 1-5) of **79** at 0, 4, 8, 12 and 24 h @ 80 °C, b) ^{1}H NMR spectrum of **79a** (#6).

Time(h)	%TnPAPP(**79**)	ln[A/A_0]
0	75.87	0
4	66.73	-0.128366722
8	61.66	-0.207385927
12	56.53	-0.294249879
24	39.45	-0.653987302

Table 4.4 Rate of atropisomerization of **79** at 80 ºC

c) @ 70 ºC: ^{1}H NMR spectra of **79** at 0, 8, 12, 24 h in $CDCl_3$ on 400 MHz

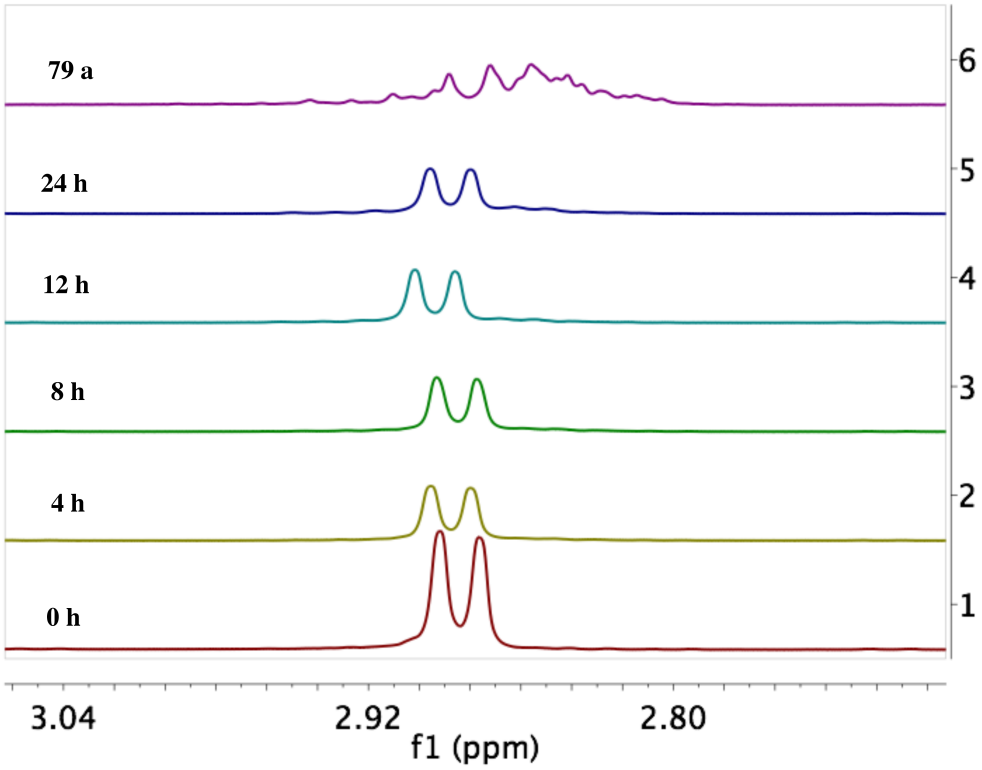

Figure 4.10 a) Stacked 1H NMR spectra (# 1-5) of **79** at 0, 4, 8, 12 and 24 h @ 70 ºC, b) ^{1}H NMR spectrum of **79a** (#6).

Time(h)	% TnPAPP(79)	ln[A/A$_0$]
0	93.13	0
4	89.19	-0.043227441
8	85.36	-0.08711876
12	82.57	-0.120349948
24	68.34	-0.30950112

Table 4.5 Rate of atropisomerization of **79** at 70 ºC

4.5.4 Calculation of energy barrier for TBnAPP (80)

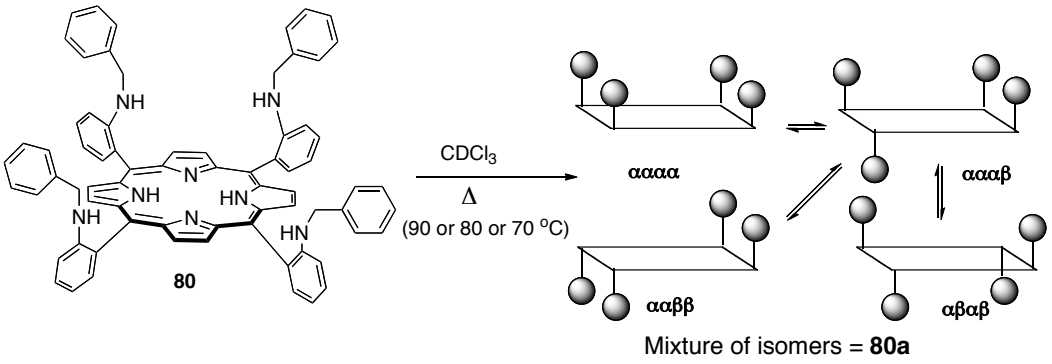

Scheme 4.13 Thermal atropisomerization in TBnAPP (**80**)

a) @ 90 ºC: ^{1}H NMR spectra of TBnAPP(**80**) at 0, 8, 12, 24 h in $CDCl_3$ on 400 MHz

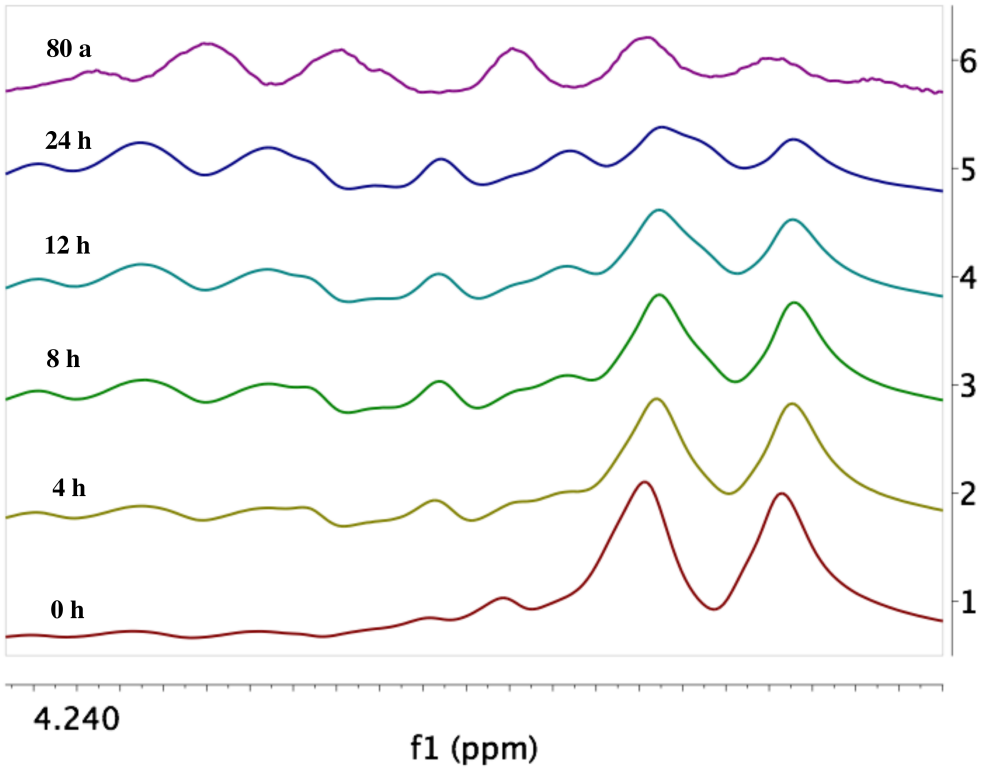

Figure 4.11 a) Stacked 1H NMR spectra (# 1-5) of **80** at 0, 4, 8, 12 and 24 h @ 90 ºC, b) ^{1}H NMR spectrum of **80a** (#6).

Time(h)	%TBnAPP(**80**)	ln[A/A$_0$]
0	73.82	0
4	53.48	-0.322321945
8	43.06	-0.539035206
12	34.05	-0.773799665
24	20.79	-1.267157596

Table 4.6 Rate of atropisomerization of **80** at 90 ºC

b) @ 80 ºC: ^{1}H NMR spectra of **80** at 0, 8, 12, 24 h in $CDCl_3$ on 400 MHz

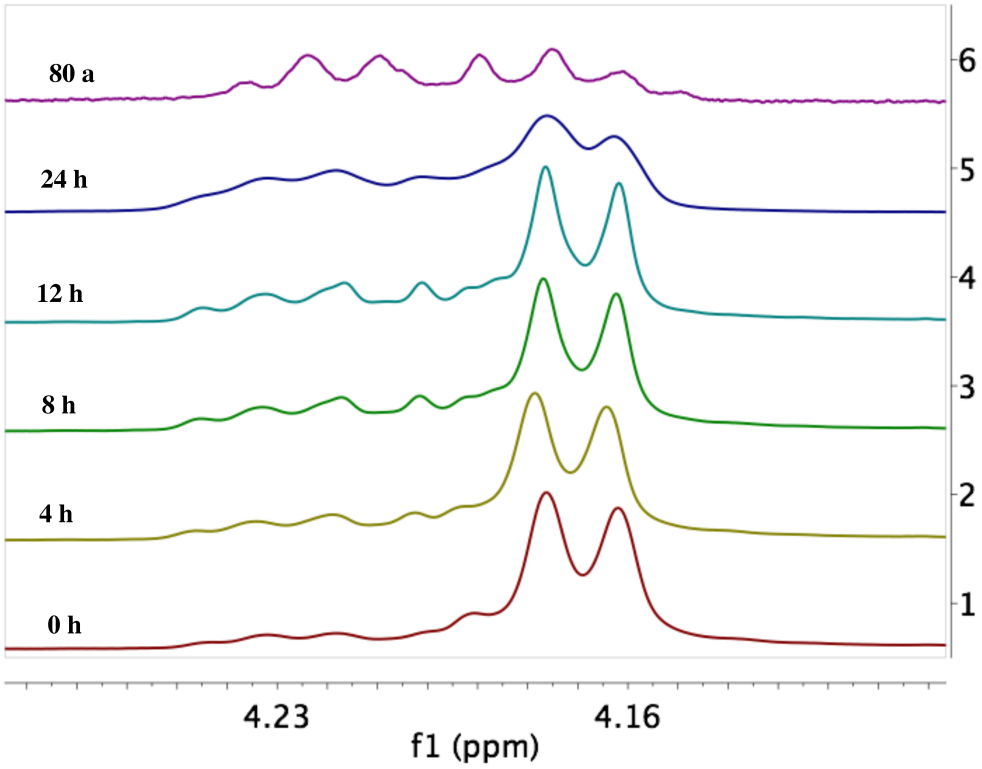

Figure 4.12 a) Stacked 1H NMR spectra (# 1-5) of **80** at 0, 4, 8, 12 and 24 h @ 80 ºC, b) ^{1}H NMR spectrum of **80a** (#6).

Time(h)	%TBnAPP(80)	ln[A/A$_0$]
0	73.82	0
4	63.98	-0.143059163
8	55.29	-0.289037637
12	49.92	-0.391207974
24	41.34	-0.579799143

Table 4.7 Rate of atropisomerization of **80** at 80 ºC

c) @ 70 ºC: ^{1}H NMR spectra of **80** at 0, 8, 12, 24 h in $CDCl_3$ on 400 MHz

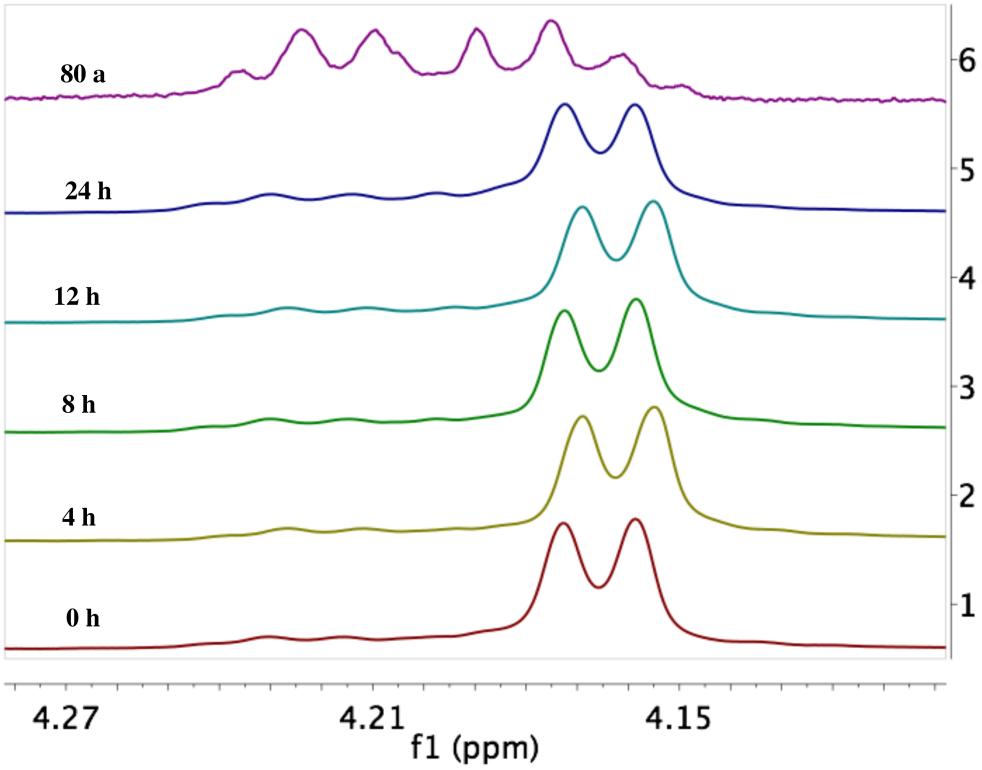

Figure 4.13 a) Stacked 1H NMR spectra (# 1-5) of **80** at 0, 4, 8, 12 and 24 h @ 70 °C, b) ^{1}H NMR spectrum of **80a** (#6).

Time(h)	%TBnAPP(80)	ln[A/A$_0$]
0	82.54	0
4	76.23	-0.079527938
8	73.2	-0.120087603
12	69.88	-0.166503539
24	65	-0.238895754

Table 4.8 Rate of atropisomerization of **80** at 70 °C

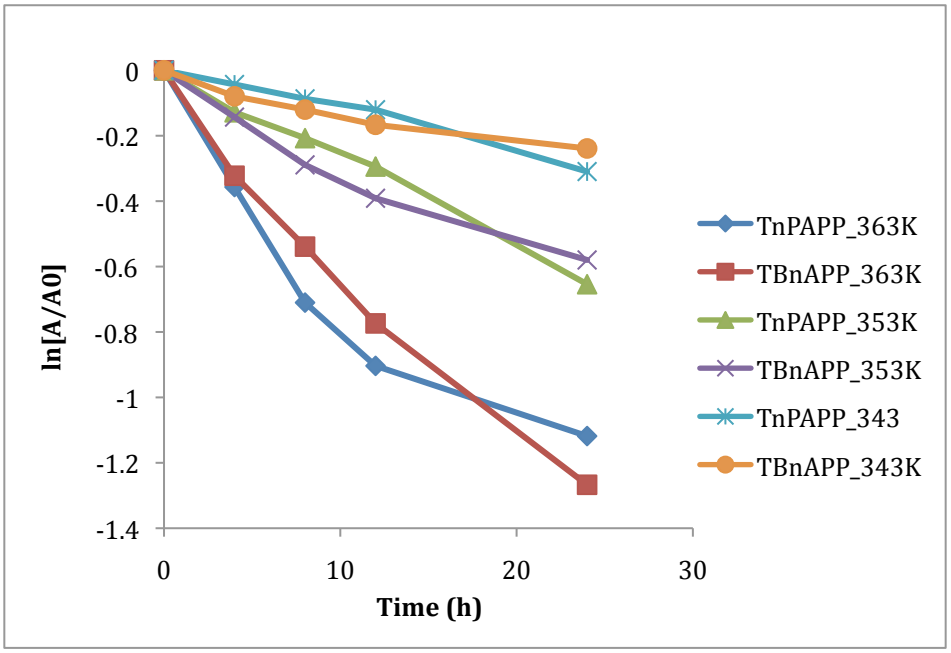

Figure 4.14 Rate of conversion of **79** and **80**

	Slope	*k*/sec
TnPAPP(**79**) @ 90 °C	-0.044623459	1.23954E-05
TnPAPP(**79**) @ 80 °C	-0.026748071	7.43002E-06
TnPAPP(**79**) @ 70 °C	-0.012866133	3.57393E-06
TBnAPP(**80**) @ 90 °C	-0.051405452	1.42793E-05
TBnAPP(**80**) @ 80 °C	-0.023656885	6.57136E-06
TBnAPP(**80**) @ 70 °C	-0.00944048	2.62236E-06

Table 4.9 Rate constants (*k*/sec) at different temperatures

Eyring Plots for TnPAPP(**79**) and TBnAPP(**80**)

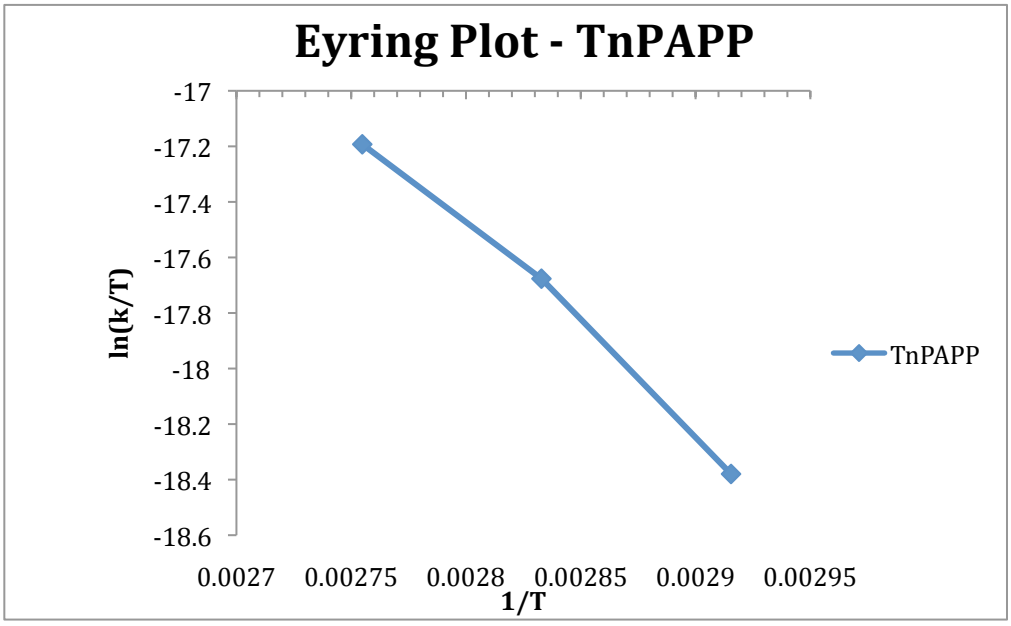

Figure 4.15 Eyring Plots for TnPAPP(**79**)

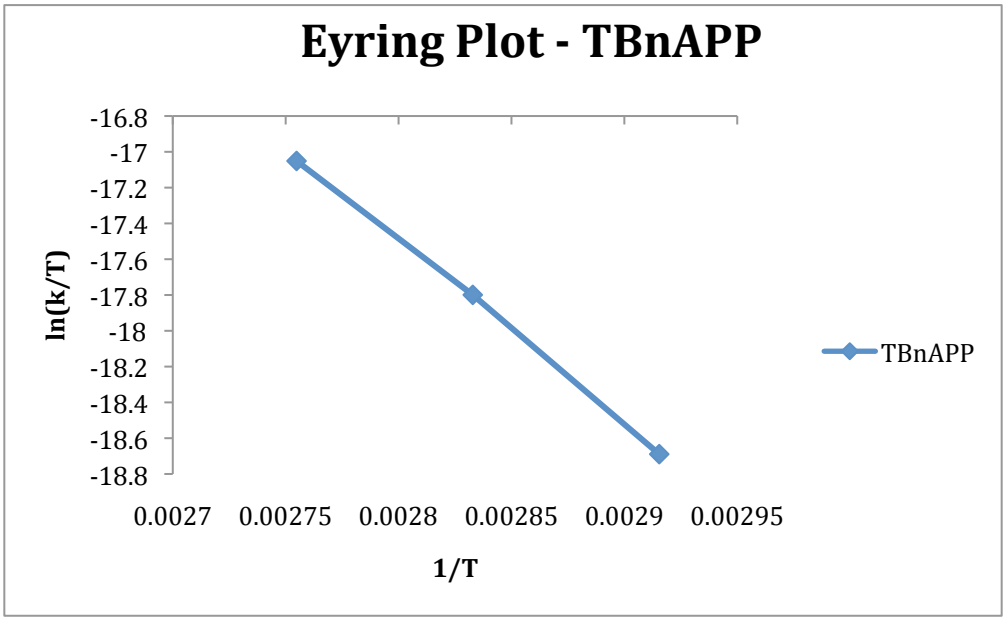

Figure 4.16 Eyring Plots for TBnAPP(**80**)

T °C	T(K)	1/T	ln(*k*/T)
90	363	0.002754821	-17.192587
80	353	0.002832861	-17.676450
70	343	0.002915452	-18.379576
	Slope	-7400.44955	
	ΔH	61531.03786	

Table 4.10 Eyring plot parameters for **79**

T °C	T(K)	1/T	ln(*k*/T)
90	363	0.002754821	-17.051103
80	353	0.002832861	-17.7992582
70	343	0.002915452	-18.6891680
	Slope	-10203.2958	
	ΔH	84835.30329	

Table 4.11 Eyring plot parameters for **80**

4.5.5 Final calculation of thermodynamic parameters using Eyring plot

Step A: Rate constants at different temperatures: Rate constants at different temperatures can be calculated from the plot of $\ln[A]/[A_0]$ *v/s* t.

Step B: $\Delta H^{\ddagger}$ Calculation: Enthalpy change can be calculated from the slope (ln(*k*/T) v/s 1/T) of Eyring plot.

Step C: $\Delta S^{\ddagger}$ Calculation: Entropy change can be calculated from Eyring equation using rate constant from step A and enthalpy from step B.

$$\ln \frac{k}{T} = \frac{-\Delta H^{\ddagger}}{R} \cdot \frac{1}{T} + \ln \frac{k_B}{h} + \frac{\Delta S^{\ddagger}}{R}$$

Step D: $\Delta G^{\ddagger}$ Calculation: Free energy of activation can be calculated from the equation using known enthalpy and entropy values from step B and C.

$$\Delta G^{\ddagger} = \left(\Delta H^{\ddagger} - T\,\Delta S^{\ddagger}\right)$$

Temp (K)	$\Delta G^{\ddagger}$ (kcal/mol)		$\Delta H^{\ddagger}$ (kcal/mol)		$\Delta S^{\ddagger}$ (kcal/mol/K)		Rate Constant (k/sec)	
	79	**80**	**79**	**80**	**79**	**80**	**79**	**80**
363	29.5	29.5	14.6	20.3	-41	-25	1.2×10^{-05}	1.4×10^{-05}
353	29.0	29.1	14.7	20.3	-41	-25	7.4×10^{-06}	6.6×10^{-06}
343	28.7	28.9	14.7	20.3	-41	-25	3.6×10^{-06}	2.6×10^{-06}

Table 4.2: Thermodynamic parameters for thermal atropisomerization of **79** and **80**

4.6 References

89. Kauffman, *G. B.;* R. D. Meyers, R. D. The resolution of racemic acid: A classic stereochemical experiment for the undergraduate laboratory, *J. Chem. Educ*. **1975**, *52,* 777–781.

90. Jacobsen, E. N.; Pfaltz, A.; Yamamoto, H. *Comprehensive Asymmetric Catalysis I–III (Eds), Springer, Berlin,* **2000**.

91. McCarthy, M.*;* Guiry, P. J. Axially chiral bidentate ligands in asymmetric catalysis, *Tetrahedron***, 2001**, *57, 3809–3844*.

92. Bringmann, G.; Motimer, A. J. P.; Keller, P. A.; Gresser, M. J.; Garner, J.; Breuning, M, Atroposelective Synthesis of Axially Chiral Biaryl Compounds, *Angew. Chem. Int. Ed*. **2005**, *44***,** 5384–5427. 93. Sasaki, H.; Irie, R.; Hamada, T.; Suzuki, K.; Katsuki, T. Rational design of Mn-salen catalyst (2): Highly

enantioselective epoxidation of conjugated cis olefins, *Tetrahedron,* **1994***, 50,* 11827–11838.

94. Oki, M. *Topics in Stereochemistry*, **1983**, 1.

95. a) Bott, G.; Field, L. D.; S. Sternhell, S. Steric effects. A study of a rationally designed system, *J. Am. Chem. Soc.* **1980**, *102*, 5618–5626. b) Gottwald, L. K.; Ullman, E. F. Biphenyl-type atropisomerism as a probe for conformational rigidity of α, β, γ, δ-tetraarylporphines *Tetrahedron Lett.* **1969**, *10*, 3071 - 3074.

96. Walker, F. A.; Avery, G. L. An NMR investigation of the atropisomers of meso-o-tolylporphinatonickel (II), *Tetrahedron Lett.* **1971**, *12*, 4949-4952.

97. Walker, F. A.; Avery, G. L. An NMR investigation of the atropisomers of meso-o-tolylporphinatonickel (II), *Tetrahedron Lett.* 1971, *12*, 4949-4952. 98. a) Bonnet, J. J.; Eaton, S. S.; Holm, R. H.; Ibers, J. A. Spectroscopic and structural characterization of ruthenium(II) carbonyl-porphine complexes, *J. Am. Chem. Soc.* 1973, *95*, 2141. b) Eaton, S. S.; Eaton, G. R. Effects of para substituent and metal ion on rates of phenyl ring rotation in ruthenium, indium, and titanium complexes of para-substituted tetraphenylporphyrins, *J. Am. Chem. Soc.* 1977, *99*, 6594. Eaton, S. S.; Fishwild, D. M.; Eaton, G. R. Effect of para substituent on rates of phenyl ring rotation in gallium complexes of para-substituted tetraphenylporphyrins, *Inorg. Chem.* 1978, *17*, 1542.

99. Dirks, J. W.; Underwood, G.; Matheson, J. C.; Gust, D. Conformational dynamics of α,β, γ,δ-tetraarylporphyrins and their dications, *J. Org. Chem.* 1979, *44*, 2551.

100. Hatano, K.; Anzai, K.; Kubo, T.; Tamai, S. Synthesis and Kinetic Investigation of the Atropisomerization of meso-Tetra(2-cyanophenyl)porphine, *Bull. Chem. Soc. Jpn.* **1981**, *54, 3518*.

101. Vicente, A. G. H.; Nurco, D. J.; Shetty, S. J.; Medforth, C. J.; Smith, K. M. First structural characterization of a covalently bonded porphyrin–carborane system, *Chem. Commun.* **2001**, 483.

102. Collman, J. P. Synthetic models for the oxygen-binding hemoproteins, *Acc. Chem. Res.* 1977, *10*, 265, Collman, J. P.; Decréau, R. A.; Zhang, C. Synthesis of Cytochrome *c* Oxidase Models Bearing a Tyr^{244} Mimic, *J. Org. Chem.* 2004, *69*, 3546.

103. Freitag, R. A.; Mercer-Smith, J. A.; Whitten, D. G. Photoatropisomerization of "picket-fence" porphyrins and their metal complexes, *J. Am. Chem. Soc.* 1981, *103*, 1226, Freitag, R. A.; Whitten, D. G. Thermal and photo-induced atropisomerization of picket-fence porphyrins, metalloporphyrins, and diacids: a means for examining porphyrin solution properties, *J. Phys. Chem.* 1983, *87*, 3918.

104. Freitag, R. A.; Mercer-Smith, J. A.; Whitten, D. G. Photoatropisomerization of "picket-fence" porphyrins and their metal complexes, *J. Am. Chem. Soc.* 1981, *103*, 1226.

105. Mekala, S.; Halterman, R. L. Thermal Atropisomerization of *meso*-tetrakis[2-(N-neopentylamino or N-benzylamino)phenyl]-porphyrins, Tetrahedron Letters, submitted.

106. a) Lindsey, J. Increased yield of a desired isomer by equilibriums displacement on binding to silica gel, applied to meso-tetrakis(o-aminophenyl)porphyrin, *J. Org. Chem*, **1980**, *45*, 5215. b) Elliott M. C. *Anal. Chem*, **1980**, *52*, 666–668. c) Gottwald, L. K.; Ullman, E. F. Biphenyl-type atropisomerism as a probe for conformational rigidity of α,β,γ,δ-tetraarylporphines. *Tetrahedron Lett*, **1969**, *10*, 3071-3074.

107. a) Leroux, F. Atropisomerism, Biphenyls, and Fluorine: A Comparison of Rotational Barriers and Twist Angles, *Chem. Bio Chem*, **2004**, *5*, 644-649. b) Paul, L-W.; Ernest, G. Atropisomerism, biphenyls and the Suzuki coupling: peptide antibiotics, *Chem. Soc. Reviews,* **2001**, *30*, 145-157. c) Nobusuke, A.; Masayoshi, O.; Noriko, H.; Isao, K.; Yasuko, K.; Yohko, F. Atropisomerism of biphenyl compounds. An Important role of o-substituted methoxy groups and fluorine atoms, *J. Organic Chem*, **1981**, *46*, 389-92.

108. a) Medforth, C. J. In *The Porphyrin Handbook*; Kadish, K. M., Smith, K. M., Guilard, E., Eds; Academic Press: New York, **2000**; Vol. 5; pp 3–74. b) Scheer, H.; Katz, J. J. In *Porphyrins and Metalloporphyrins*; Smith, K. M., Ed.; Elsevier: Amsterdam, **1975**; p 399.

109. Freitag, R. H.; Whitten, D. G. Thermal and photo-induced atropisomerization of picket-fence porphyrins, metalloporphyrins, and diacids:

a means for examining porphyrin solution properties, *J. Phys. Chem*, **1983**, *87*, 3918–3925.

110. Hatano, K.; Anzai, K.; Nishino, A.; Fujii, K. A Kinetic Study of Thermal Rotational Isomerization of 5,10,15,20-Tetrakis(o-aminophenyl)porphyrin and 5,10,15,20-Tetrakis(o-pivaloylaminophenyl)porphyrin, *Bull. Chem. Soc. Jpn,* **1985**, *58*, 3653-3654.

111. Kottas, G. S.; Clarke, L. L.; Horinek, D.; Michl, J. Artificial Molecular Rotors, *Chem. Rev,* **2005**, *105*, 1281-1376.

112. a) Lindsey, J. S.; Mauzerall, D. C. Synthesis of a cofacial porphyrin-quinone via entropically favored macropolycyclization, *J. Am. Chem. Soc*, **1982**, *104*, 4498–4500. b) Lindsey, J. S.; Chaudhary, T.; Chait, B. T. 252Cf plasma desorption mass spectrometry in the synthesis of porphyrin model system, *Anal. Chem*, **1992**, *64*, 2804–2814. c) Lindsey, J. S.; Delaney, J. K.; Mauzerall, D. C.; Linschitz, H. Photophysics of a cofacial porphyrin-quinone cage molecule and related compounds: fluorescence properties, flash transients, and electron-transfer reactions, J. *Am. Chem. Soc,* **1988**, *110*, 3610-3621. d) Delaney, J. K.; Mauzerall, D. C.; Lindsey, J. S. Electron tunneling in a cofacial zinc porphyrin-quinone cage molecule: novel temperature and solvent dependence, *J. Am. Chem. Soc,* **1990**, *112*, 957-963.

113. The isomerization of **79a** and **80a** were carried out by placing the NMR tubes containing $CDCl_3$ solutions of **79** and **80** into a constant temperature water bath.

114. We have not assigned other isomers in the NMR spectra. 115. a) Freitag, R. A.; Mercer-Smith, J. A.; Whitten, D. G. Photoatropisomerization of "picket-fence" porphyrins and their metal complexes, *J. Am. Chem. Soc,* 1981, *103*, 1226. b) Freitag, R. A.; Whitten, D. G. Thermal and photo-induced atropisomerization of picket-fence porphyrins, metalloporphyrins, and diacids: a means for examining porphyrin solution properties, *J. Phys. Chem.* 1983, *87*, 3918.

116. Hatano, K.; Anzai, K.; Nishino, A.; Fujii, K. A Kinetic Study of Thermal Rotational Isomerization of 5,10,15,20-Tetrakis(o-aminophenyl)porphyrin and 5,10,15,20-Tetrakis(o-pivaloylaminophenyl)porphyrin, *Bull. Chem. Soc. Jpn*, **1985**, *58*, 3653-3654.

117. Gottwald, L. K.; Ullman, E. F. Biphenyl-type atropisomerism as a probe for conformational rigidity of α, β, γ, δ-tetraarylporphines, *Tetrahedron Lett.* **1969**, *10*, 3071 – 3074.

CHAPTER 5

5. Syntheses of 'Novel' Water-Soluble Calix[4]arenes as Supramolecular Scaffolds for Aqueous Molecular Recognition and Catalysis

5.1 Introduction

Calix[4]arenes are one of the most important supramolecular scaffolds in the host-guest chemistry. During the last decade, there have been a variety of sophisticated molecular hosts bearing calix[4]arene skeletons were prepared. Calix[4]arenes are metacyclophanes having a hydrophobic cavity of lower and upper rims, and formed by the phenolic units bridged with methylene units. Calix[4]arenes are easily accessible via a base-catalyzed, single step condensation of phenols with formaldehyde. Calix[4]arenes possesses a hard oxygen cavity formed by the hydroxyl groups at the lower (narrow) rim and the soft π-donar cavity consisting of benzene rings at the upper (wide) rim. Therefore, the hydrophilic narrow rim and the hydrophobic wide rim encompassing a cavity may be functionalized with appropriate groups. One can tune the cavity size as well as confirmation of the calix[4]arenes by changing length of the functional groups at the both ends, and the different conformers have the different capabilities for molecular recognition of neutral, anionic and cationic guest molecules in different solvents ranging from apolar, polar and protic solvents. To improve the properties of calix[4]arens in terms of reactivity, selectivity and solubility, functionalization of lower or upper rim is necessary. The presence of specific functional groups at the mouth of the cavity suggests their role for the accessibility of substrates into the cavity.

Since this dissertation is mainly based on the design and synthesis of novel water soluble calix[4]arenes for aqueous molecular recognition and catalysis, I would discuss few examples on water soluble calix[4]arens and their binding properties toward anions, cations and neutral molecules in aqueous media. By definition, entropy is the thermodynamic measure of disorderness of a system. If, two systems are bound together by intermolecular interactions (non-covalently) such as hydrogen bonding or π-π stacking etc, upon dilution inherently they dissociate for favorable entropy, which intern increases the translational and rotational entropy of the individual components. For example, nature counteracts the unfavorable entropy associated with holding complexes together with weak noncovalent interactions, which are enthalpically favored by low activation energy of formation. Hence, these weak noncovalent interactions required to counteract the unfavorable entropy. But, solvation effects or desolvation effects can give rise to favorable entropy changes, which also counteract the unfavorable change in translational and rotational entropies that result from the association process of the individual components. For example, incorporation of the non polar amino acids at interfaces of the interacting proteins[118] is truly based of the desolvation effect and has significant effect on the overall thermodynamics of association and these desolvation phenomenon is based on the hydrophobic effects[119] of the nonpolar amino acids. Moreover, as the number of components in the supramolecualr system increases, the enthalpy contribtion or desolvation must increase to counteract the inherent negative entropy that drives from association[120].

Therefore, the supramolucular complexes with stoichiometry more that 1:1 is driven by enthalpy or desolvation effect in the system. In 2000, Rekharsky et al,[121] have showed that, solvent release can occur upon complexation thereby giving overall positive entropy and demonstrated experimentally by comparing 1:1 and 1:2 complexes of cyclodextrins with various guest molecules at different reagent concentrations. Schmidtchen[122] et al, have explored the control of solvation/ desolvation processes as a possible strategy to overcome the loss of entropy upon binding, even in systems that do not exploit the hydrophobic effect, such as ion-pairing**.** Although ion pairing may be expected to be associated with negative enthalpy, it has been found that it only sometimes behaves this way and that commonly entropy in part drives the interaction. Therefore, the control of complexation in aqueous media is a truly enthalpy driven in systems that posseses the hydrophobic interactions more predominantly than ion pairing interactions. Hence, to control the complexation/encapsualtion of guests in aqueous media is enthalpycally favored. Since, this dissertation is mainly focused on the design of systems with highly hydrophobic character for dimerization or complexation in aqueous media while the association or desolvation by ionic interactions is the least criteria for complexation.

5.2 Calix[4]arenes and Molecular recognition in aqueous media

In supramolecular chemistry, calix[4]arenes are the most versatile and useful blocks, because of their tunable structure and size. Water soluble calix[4]arenes attracted considerable attention very early on because of their

very well formed hydrophobic cavities make it possible to study molecular recognition in aqueous media. Since the calix[4]arenes are tunable with various functional groups therefore, can be functionalized with variety of water soluble groups such as, sulfonates, phosphates, carboxylates and amines etc. In late 1980s, Shinkai developed water soluble calix[4]arens with sulfonates,[123] and Gutsche developed carboxylates[124], Phosphonates by Arimura et. al,[125] follwed by the development of amino derivatives in late 1990s by, Nagasaki et. al,[126] and Shimizu et. al,[127] showed a tremendous impact on the development of new class of water soluble calix[4]arenes with various functional groups for molecular recognition in aqueous media, more recently, calix[4]arenes have become attractive multivalent scaffolds for making amphiphiles useful in both biological and chemical applications. In 2005, Zhao et. al,[128] have reported the synthesis of new class of calix[4]arenes by 'click chemistry' method.

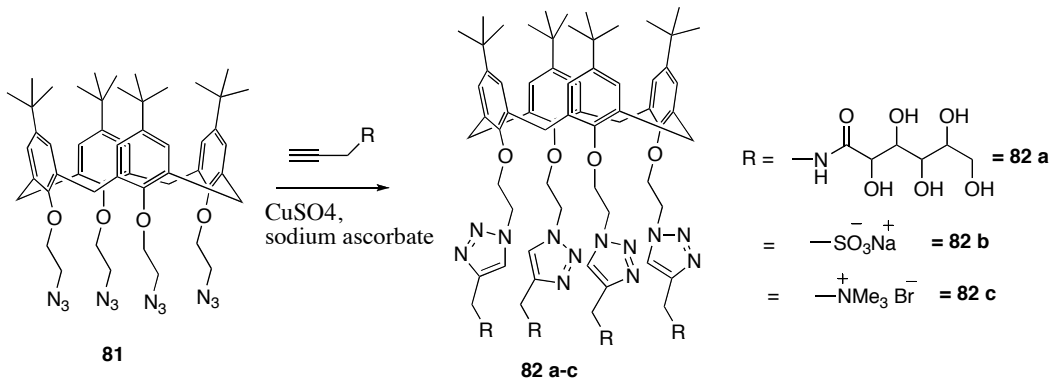

Scheme 5.1 Zhao's Click chemistry method for the synthesis of water soluble calix[4]arenes

Surprisingly, the compound **81a** was not soluble in water but **81b** and **81c** were soluble because of the charge in the molecule, as well as the 'micelle like'

structure formation by solvation effect, but not soluble in any of the organic solvents, but **81c** was soluble in methanol and this was the novel method for the synthesis of water soluble calix[4]arenes, but no studies were done on host-guest complexation. Therefore, it is necessary to derivatize compound **81a** with appropriate functional groups such as ether chains etc. to increase the water solubility.

Since the increasing importance of calix[4]arene derivatives for molecular recognition in water, the use and derivatization of calix[4]arenes are necessary to utilize them in different purposes. In 1997, Tyso et al[129], have reported a diazo-calix[4]arene based scaffolds (**83 a-c**) for the study of interaction with N,N,N-trimethylarylammonium iodides and benzene in water in order to correlate the effect of anilinium salts on the binding properties of cup-shaped hydrophobic cavity with the monolayer spreading behavior of a series of amphiphilic analogs.

Recently, series of papers published by Ak et al,[130] based on the chromogenic azocalix[4]arene derivatives for transition metal extraction for the environmental applications, followed by the work of Zhou et al,[131] published their work to investigate the inclusion behavior of *p*-(*p*-carboxylbenzeneazo) calix[4]arene (CBC4A) with norfloxacin in NaAc-HAc buffer silution at pH ~5.0, and found the decrease in the fluoresent intensity of norfloxacin and this work was used for sensory applications and association constant was found to be $8.21*10^5$ M^{-1} with 1:1 complexation. Recently, new class of water soluble calix[4]arenes were

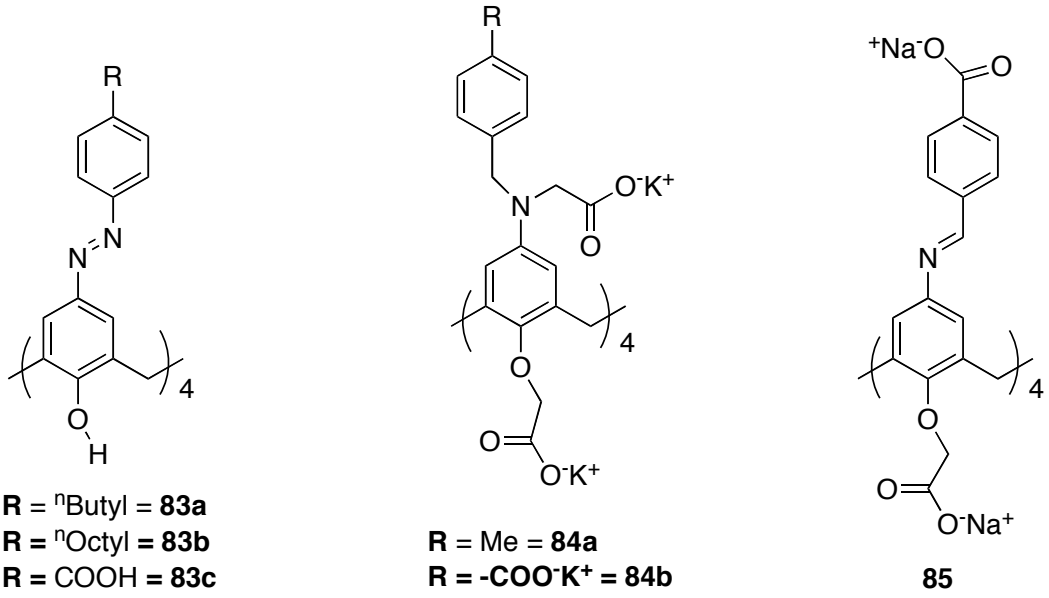

Scheme 5.2 Recently reported water soluble calix[4]arene derivatives for molecular recognition

reported for molecular recognition purposes by Kim et al[132] and these are the new class of water-soluble iminecalix[4]arene based molecular platforms (**85**) for the development of artificial receptors for recognition of neutral and charged species. In 2010, they have reported another paper[133] based on the dual behavior (hydrophobic and hydrophilic) of aminocalix[4]arenes (**84 a,b**) for molecular recognition in aqueous media. In the case of 'imine' calix[4]arens, the inclusion phenomenon is mainly based on the deep hydrophobic cavity of the calix[4]arene, but where as in the case of 'amine' calix[4]arene, the inclusion behaviour was based on hydrophobic as well as hydrophilic character of the calix[4]arene. The hydrophilic character can enhances the binding of neutral or charged species with ionic interactions in addition to hydrophobic attraction by the cavity.

All biological phenomena take place in water and involve reversible

and weak non-covalent interactions between molecular species ranging from simple inorganic slats to organic compounds of widely varying complexity and molecular weight. Therefore, the development of new class of water-soluble synthetic receptors that mimic natural systems in their ability to bind a given substrate is one of the most investigated and emerging fields in the supramolecualr chemistry.[134] To this end, many receptors such as cyclodextrins, cucurbiturils, resorcarenes and calixarenes have been designed and investigated. As i discussed above, the use of calix[4]arene based scaffolds in aqueous media implies the introduction of various polar groups at the lower or upper rim, such as, carboxylates, phosphates, and sulphonates. Derivatives of this type have been synthesized and studied their important properties such as metal complexation and recognition of cationic or anionic or neutral organic molecules. But, there have been no studies done on the design and synthesis of highly water soluble calix[4]arenes for heterodimerization and heterocapsule formation with neutral organic molecules in aqueous media at pH ~ 7.1 buffer to mimic the biological phenomena in physiological conditions as well as for sensory applications. To this end, we have designed and synthesized several novel water soluble calix[4]arene derivatives for heterodimerization studies and hetero capsule formation studies in aqueous media at pH ~ 7.1 phosphate buffer solution at room temperature. In this dissertation, I will be discussing the design and synthesis of novel water soluble calix[4]arens and preliminary studies on binding properties with various guests aqueous media.

5.3 Design and synthesis of water soluble calix[4]arenes

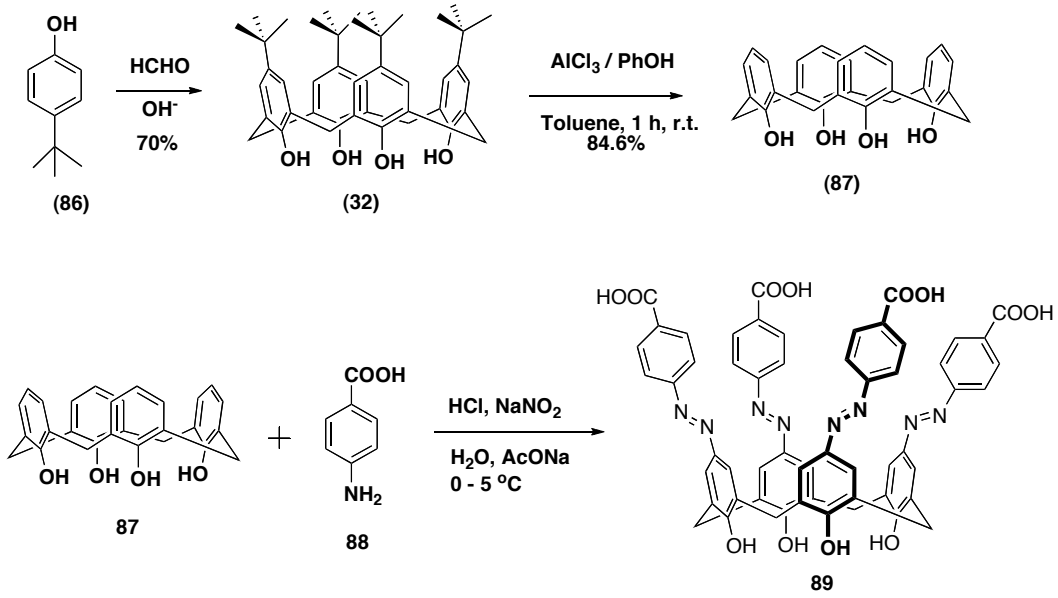

Scheme 5.3 Synthesis of Calix[4]arene **89**

We have synthesized the compound **89** in 4 steps following literature procedure (**Scheme 5.3**). Surprisingly, the diazocalix[4]arene **89** was only soluble in bicarbonate buffer solution at pH ~ 11.0 and the sample solution was bright red in color. The host guest complexation was studied in aqueous media with various guest molecules (**93**, **94** and **95**). The guest 2-Phenylacetophenone **93** was commercially available and partially soluble in water. The other guest molecule [1,1'-Biphenyl]-4-carboxylic acid, [1,1'-biphenyl]-4-yl ester **94** was synthesized in one step from starting with 4-Phenylphenol **98** and 4-Phenylbenzoic acid **99** in presence of phosphorous pentoxide. [1,1'-Biphenyl]-4-carboxylic acid, 4-methoxyphenyl ester **95** was synthesized in two steps starting with **99** as shown in scheme **5.6**. The later two guest molecules were insoluble in water. The ^{1}H NMR titration experiments showed that there was no host-guest complex formation with host **89** and guests **94** and **95**. The

reasons were due to the larger size of these guests, and no solubility in water. Therefore, these guests are not suitable for host-guest complexation, but the guest **93** showed significant binding with the host **89** and association constant K_a was calculated by using curve-fit software and K_a was found to be 4.88 /mM.

5.3.1 ^{1}H NMR titration experiments for calculation of association constant in host-guest complexation of Host-89 and Guest-93

a) Sample preparation: The stock solution of host **89** was prepared by adding 16 mg (0.0157 mmol) of *tetrakis*(4-carboxyphenylazo)calix[4]arene **89** and 6.59 mg (0.0785 mmol) of $NaHCO_3$ in 4 mL of D_2O (Sonicated with heat @ 50 ºC for ~30 min).

The stock solution of guest **93** was prepared by adding 10 μL of 2-phenylacetophenone **93** into 1 mL of methylene chloride in a small vial. Then each NMR tube (#1-8) was charged with 0.0, 0.2, 0.4, 0.6, 0.8, 1.0, 1.5 and 2.0 equiv of **93** in methylene chloride (0.2 equiv = 0.000393 mmol of **93** or 7.14 μL of stock) and evaporated the methylenechloride on rotavap leaving the guest in NMR tubes. Then each of the NMR tube (#1-8) was charged with 0.5 mL (3.94 mM) of stock solution of host **89**. So each NMR tube has the host **89** concentration (3.94 mM) constant while increasing the concentration of guest **93** (shown in the below table).

Then DMSO stock solution was prepared by adding 10 μL of DMSO in 10 mL of D_2O. Then transferred 27.6 μL of stock solution to each NMR tube which is equal to 0.2 equiv of DMSO (0.0003887 mmol) relative to calix[4]arene **89**

concentration and added additional amount of 72.4 µL of D_2O to each NMR tube to make final volume of 0.6 mL. Then ^1H NMR spectrum for each sample was obtained on 400 MHz instrument.

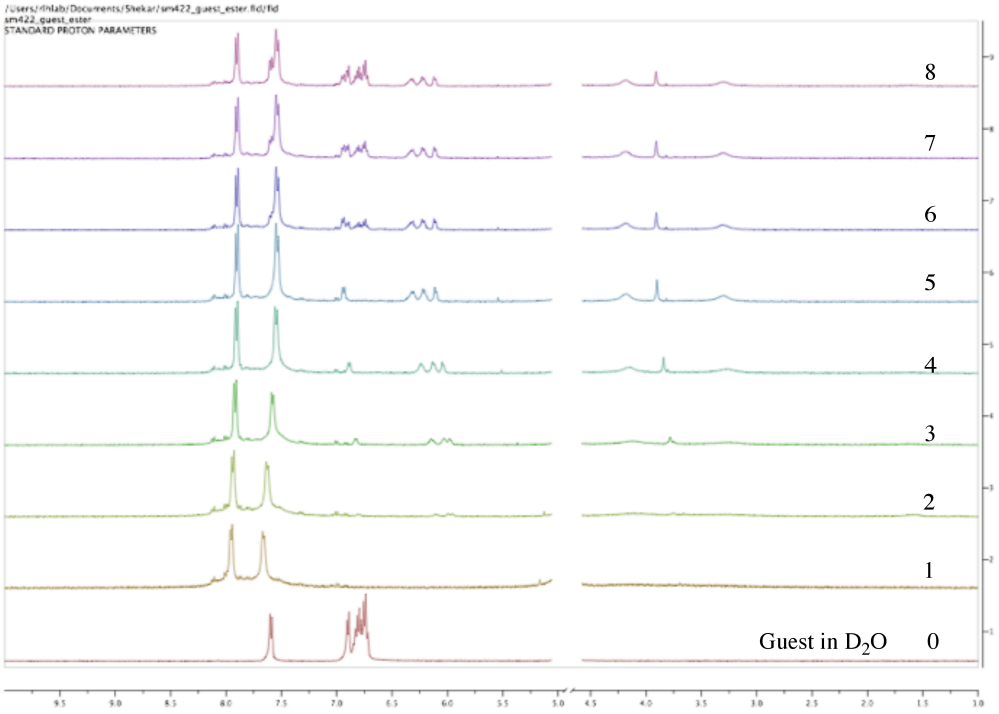

Figure 5.1 Stacked ^1H NMR spectra of titration experiment for host-guest complexation studies between compounds 89 and 93. **H:G ratios added:** NMR# 0 guest in D_2O (no base added), 1(1.0:0.0 equiv), 2(1.0:0.2), 3(1.0:0.4), 4(1.0:0.6), 5(1.0:0.8), 6(1.0:1.0), 7(1.0:1.5), 8(1.0:2.0 equiv).

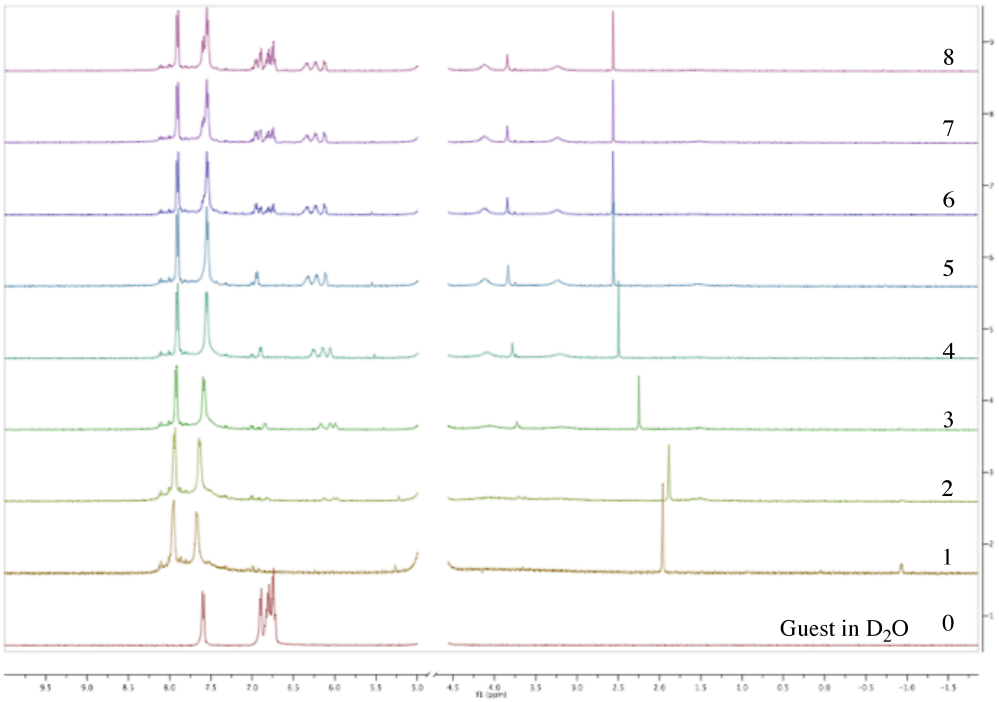

Figure 5.2 Stacked ^{1}H NMR spectra of titration experiment for host-guest complexation studies between compounds **89** and **93** with DMSO as internal standard. **H:G ratios added:** NMR# 0 guest in D_2O (no base added), 1(1.0:0.0 equiv), 2(1.0:0.2), 3(1.0:0.4), 4(1.0:0.6), 5(1.0:0.8), 6(1.0:1.0), 7(1.0:1.5), 8(1.0:2.0 equiv) and 0.2 eqiv of DMSO (relative to the calix[4]arene **1** concentration) added to each NMR tube except NMR#0.

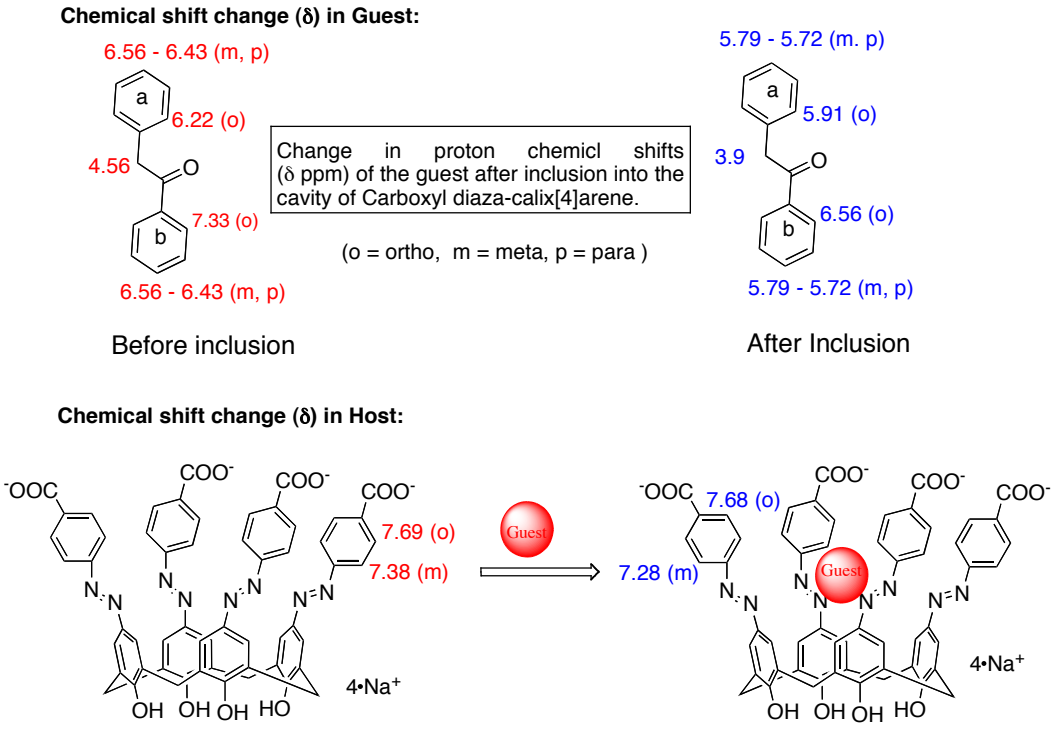

Scheme 5.3a Chemical shift change in host and guest upon complexation

Proton chemical shifts of guest molecule have shifted to up-field upon inclusion into the cavity of the calix[4]arene. Ortho protons of 'b' ring shifted to 6.56 ppm from 7.33 ppm (0.77 ppm up field shift) while the ortho protons of 'a' ring shift is 6.22 to 5.91 ppm (0. 31 ppm up-field shift). The change in the chemical shifts indicate that the 'b' ring is sitting inside the cavity near the calix[4]arene phenyl rings while 'a' ring is at the diazophenyl ring. Because of the pi-stacking and high aromatic ring current from calix[4]arene, the ortho protons of the 'b'ring shifted to more upfield than 'a'ring.

Inclusion of the guest also explained by the up-field shift of the methylene protons of the guest (4.56 to 3.69 ppm). Chemical shifts of

diazophenyl ring also shifted little upfield (0.01 ppm of ortho, 0.1 ppm of meta) compared to guest, because the interaction (π-π stacking) of the diazophenyl ring with guest 'a' ring is very less because of the high flexibility of the the diazophenyl rings than calix[4]arene phenyl groups. Chemical shift change of ortho *vs* meta protons of diazophenyl groups indicate that the guest molecule is inside the cavity and very close to the calix[4]arene phenyl groups and some what close to the meta protons of diazophenyl group. The ratios of initial host, initial guest and bound guest were calculated by the ^{1}H NMR integration with DMSO as internal standard. Upon addition of DMSO, the change in the chemical shift (down field shift) of DMSO indicates the interaction of DMSO with hydroxyl groups of diazocalixarene. The ratios and concentrations are given in the below **Table 5.1**. The association constant (K_a = 3913 M^{-1}) was calculated by the use of spreadsheet software. The association constant indicates the weak binding, which may be due to the high degree of freedom for the phenyl groups in the calix[4]arene and the binding was truly based on the hydrophobic interactions. The main advantage of this diazocalix[4]arene is due to it's larger size, additional π-π interactions with N=N groups may increase the binding ability, but the high flexibility of the phenyl groups may disfavor the association by π-π interactions with guest molecules. Therefore, to improve the binding ability of the diazo carboxycalix[4]arene **89** with various 'neutral' guest molecules, the design with more rigid phenyl groups in the calix[4]arene **89** is necessary.

NMR #	H:G:DMSO equiv	$[H]_0$ mM	$[G]_0$ mM	[DMSO] mM	[BG] mM	[UBG] mM
1	1 : 0.0 : 0.2	3.28	0.0	0.647	0.0	0.0
2	1 : 0.2 : 0.2	3.28	0.654	0.647	0.585	+0.06
3	1 : 0.4 : 0.2	3.28	1.309	0.647	1.326	-0.01
4	1 : 0.6 : 0.2	3.28	1.964	0.647	2.10	-0.1
5	1 : 0.8 : 0.2	3.28	2.618	0.647	2.556	+0.06
6	1 : 1.0 : 0.2	3.28	3.273	0.647	2.680	+0.593
7	1 : 1.5 : 0.2	3.28	4.648	0.647	2.426	+2.21
8	1 : 2.0 : 0.2	3.28	6.547	0.647	2.556	+3.99

NMR#	[H]0 mM in D_2O	[G]0 mM in D_2O	[BG] mM	[UBG] mM	Equiv (H:G)
1	2.58	0	0	0	1:0
2	2.58	0.65	0.65	0	1:0.25
3	2.58	1.38	1.38	0	1:0.53
4	2.58	2.1	2.1	0	1:0.81
5	2.58	2.56	2.56	0	1:0.99
6	2.58	3.43	2.58	0.85	1:1.32
7	2.58	5.0	2.58	2.42	1:1.93
8	2.58	6.67	2.57	4.09	1:2.58

Table 5.1 Ratios of host, guest and complex by ^{1}H NMR titration experiment (top: initial measurements, bottom: calculations based on internal standard DMSO)

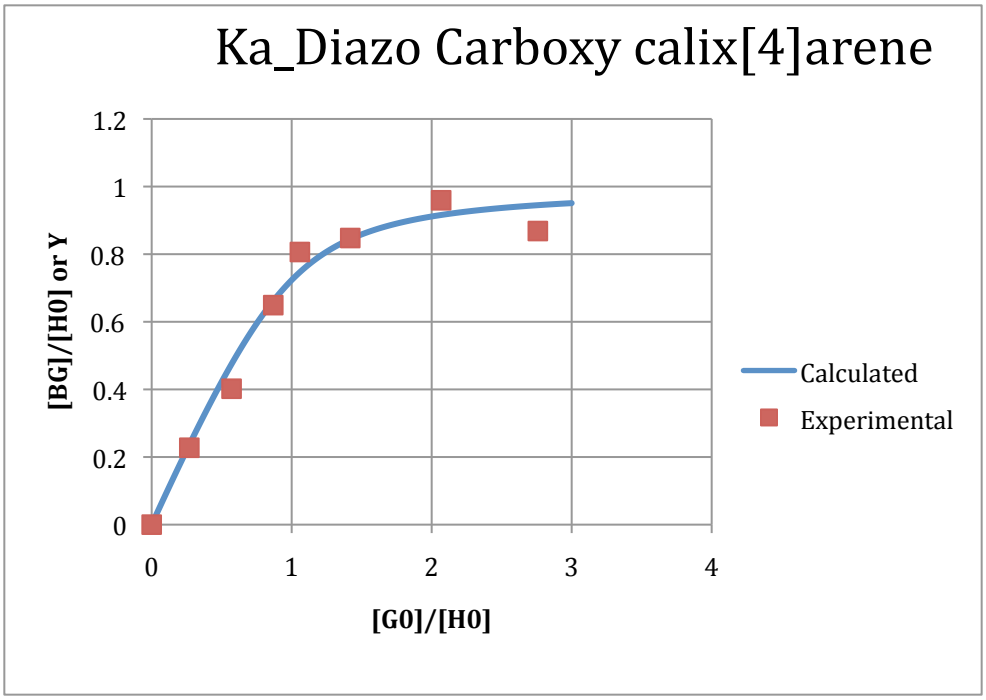

Figure 5.3 Plot of bound guest concentration v/s initial guest concentration

5.3.2 Encapsulation studies

For encapsulation studies in water, we have synthesized diazo-benzylaminocalix[4]arene **92a** in two steps, starting with diazo-coupling reaction of **87** with Boc-protected 4- amino benzyl amine **91** to give Boc-protected diazobenzylamino calix[4]arene **92**, then deprotection of 'Boc' with trifluoroacetic acid in solvent free conditions to give the desired compound **92a** as orange red colored solid. The compound was isolated as salt of CF_3COO^-, therefore, the compound was isolated as super quantitative yield (**Scheme 5.4**). Then, investigated the encapsulated studies by adding host (**89**) and guest (**93**) in 1:1 equivalent in D_2O (bicarbonate buffer) and then added amino counterpart of the diazobenzylamino calix[4]arene **92a** (0.3 -1.0 equiv) and monitored by

^{1}H NMR spectroscopy. Upon addition of **92a**, guest signals were disappeared and precipitate formed after some time. Then the NMR sample was heated, sonicated to dissolve the precipitate and took the 1H NMR. There were no complex induced shifts (CIS) observed in the 1H NMR spectrum. Therefore, upon addition of the 92a, the precipitate formation was due to the insolubility of **92a** in buffer solution and loosing the positive charge because of bicarbonate base. Moreover, the ionic interaction between carboxylate groups of **89** and ammonium groups of **92a** were lost and the resulting neutral compounds were insoluble in bicarbonate buffer. The hydrophobic effects favor the inclusion of the guest **93** in the host **89**, because of large, hydrophobic cavity of **89** in aqueous media. But, as soon as added the amino counterpart for encapsulation, due to the loss of charges in

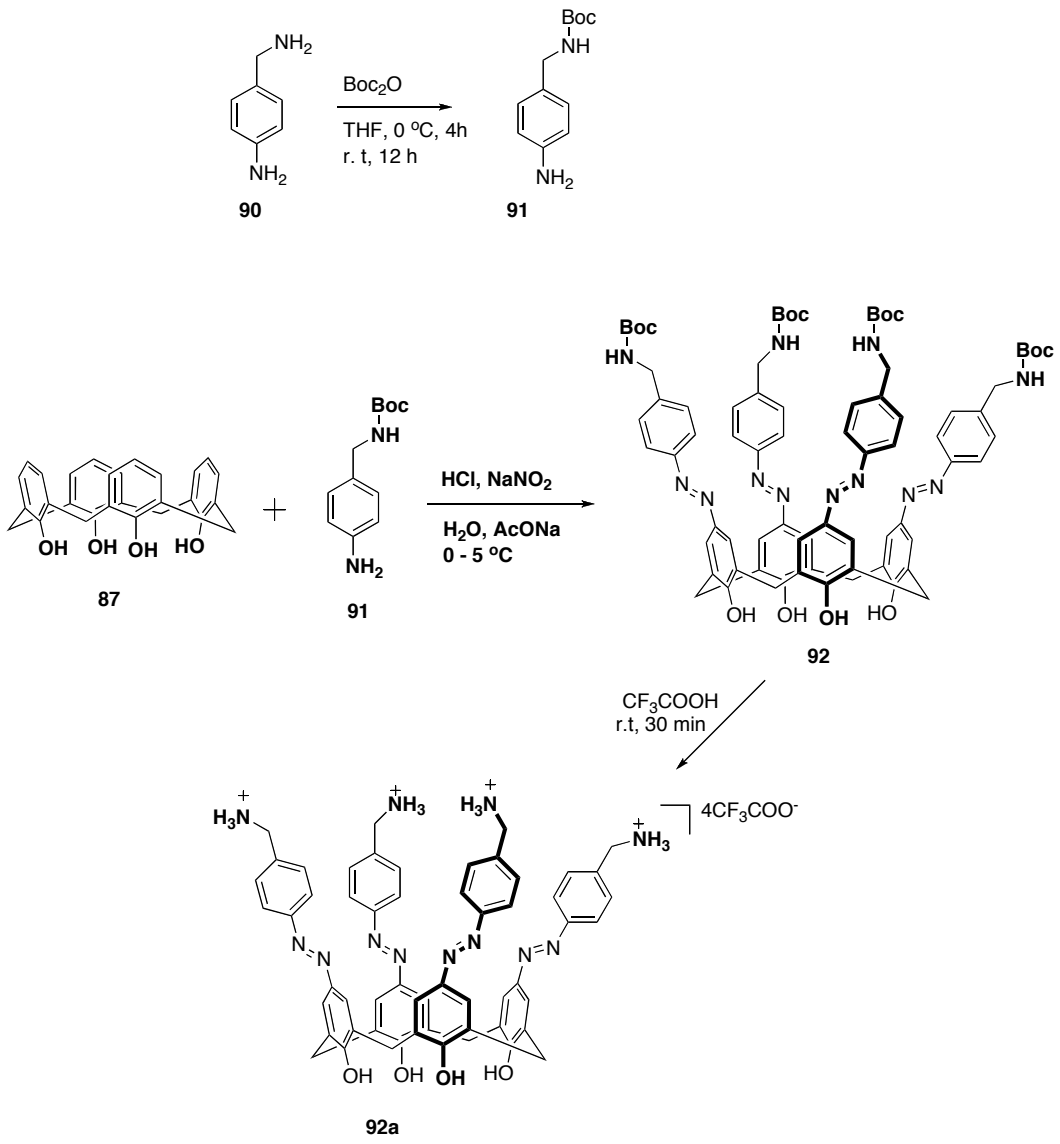

Scheme 5.4 Synthesis of Calix[4]arene **92a**

aqueous media, both calixarenes **89** and **92a** became insoluble in water. In addition to this experiment, there was no binding observed with other guest molecules **94** and **95** (**scheme 5.5**) which may be due to their larger size, which prevents the binding in the cavity, and poor solubility in water (buffer). Therefore we have designed and synthesized new class of novel water soluble

calix[4]arene derivatives for host-guest compelxation and encapsualtion studies in water.

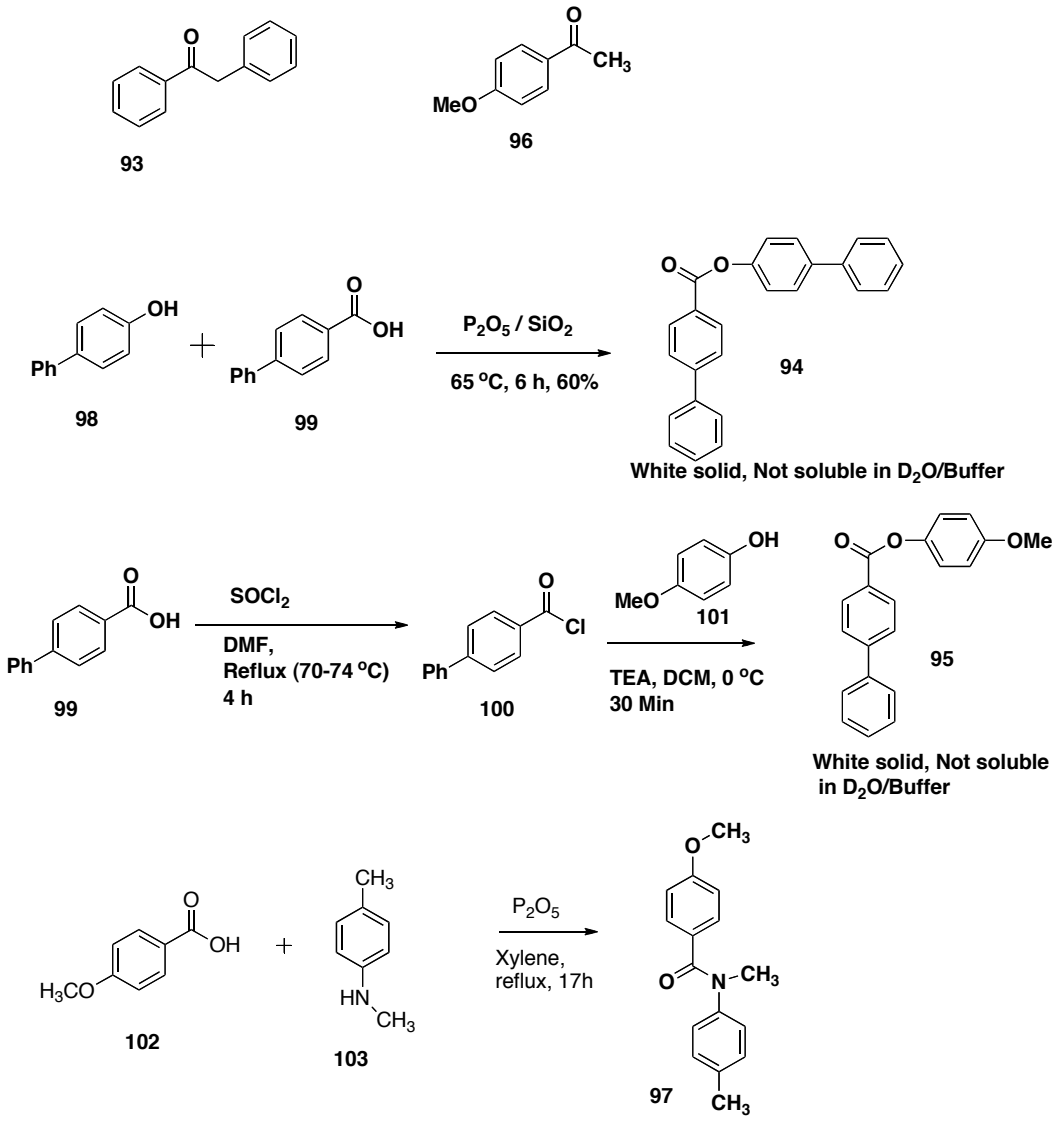

Scheme 5.5 Guests used for the host-guest complexation studies (guests **93** and **96** are commercially available and **94**, **9**5 and **97** were synthesized)

5.4 Design and synthesis of 'novel' water soluble calix[4]arenes for encapsualtion studies in aqueous media at pH 7.1 (Phosphate buffer)

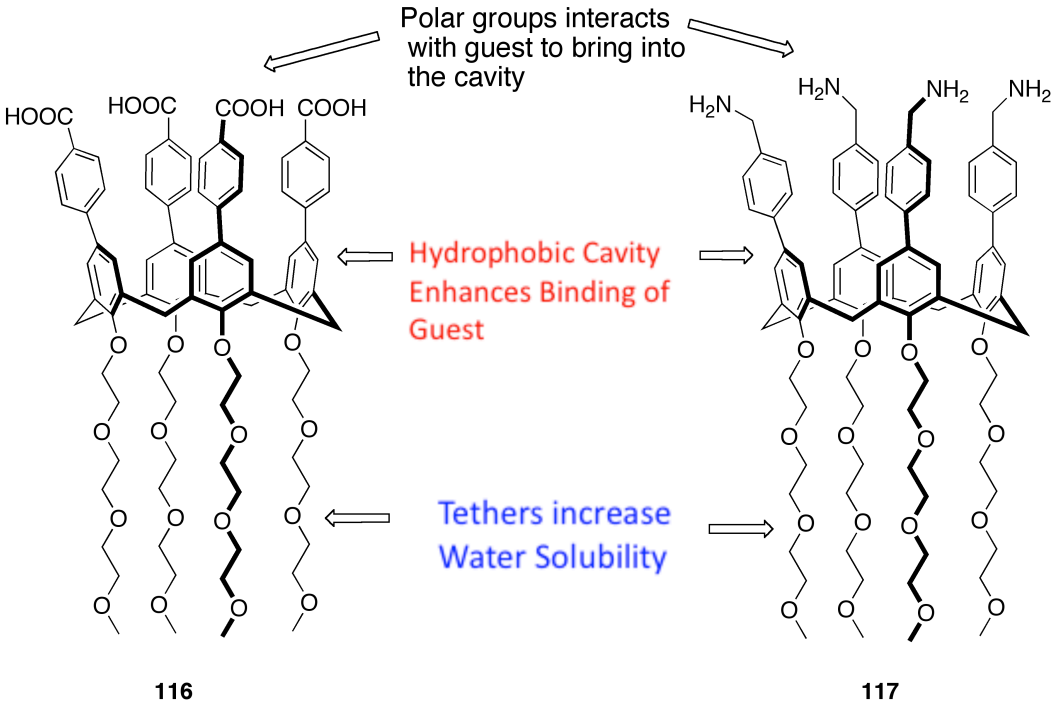

Scheme 5.6 Poperties of 'novel' water soluble calix[4]arene derivatives

To overcome the above problem of solubility, we have designed and synthesized two novel compounds **116** and **117** for encapsulation studies (Scheme 5.6), in which the upper rim of calix[4]arene was functionalized with carboxy phenyl (**116**) and methylamino phenyl (**117**). The polar (carboxylic acid and amine) groups can interact with guest molecules to bring into the cavity and the aromatic phenyl groups forms a deep hydrophobic cavity at the upper rim of the calix[4]arene, which enhances the binding of neutral aromatic guests in aqueous media. The substitution at the lower rim of the calix[4]arene with long chain ether derivatives can enhances the water solubility of the

calix[4]arene derivatives **116** and **117** as shown in **scheme 5.6**.

First, we have synthesized ether derivatives **106** and **110** with known literature procedure (PCT Int. Appl., 2010106341, 23 Sep 2010, J. Am. Chem. Soc, 2005, 127, 373-383) (**scheme 5.7**). But, we have used only **106** for the synthesis of novel derivatives. The advantage of the derivative **110** over **106** would be the more bulky derivative to increase water solubility, the additional π-π interactions from phenyl groups of **110** for binding studies and also makes the calixarene derivative more rigid at the upper rim.

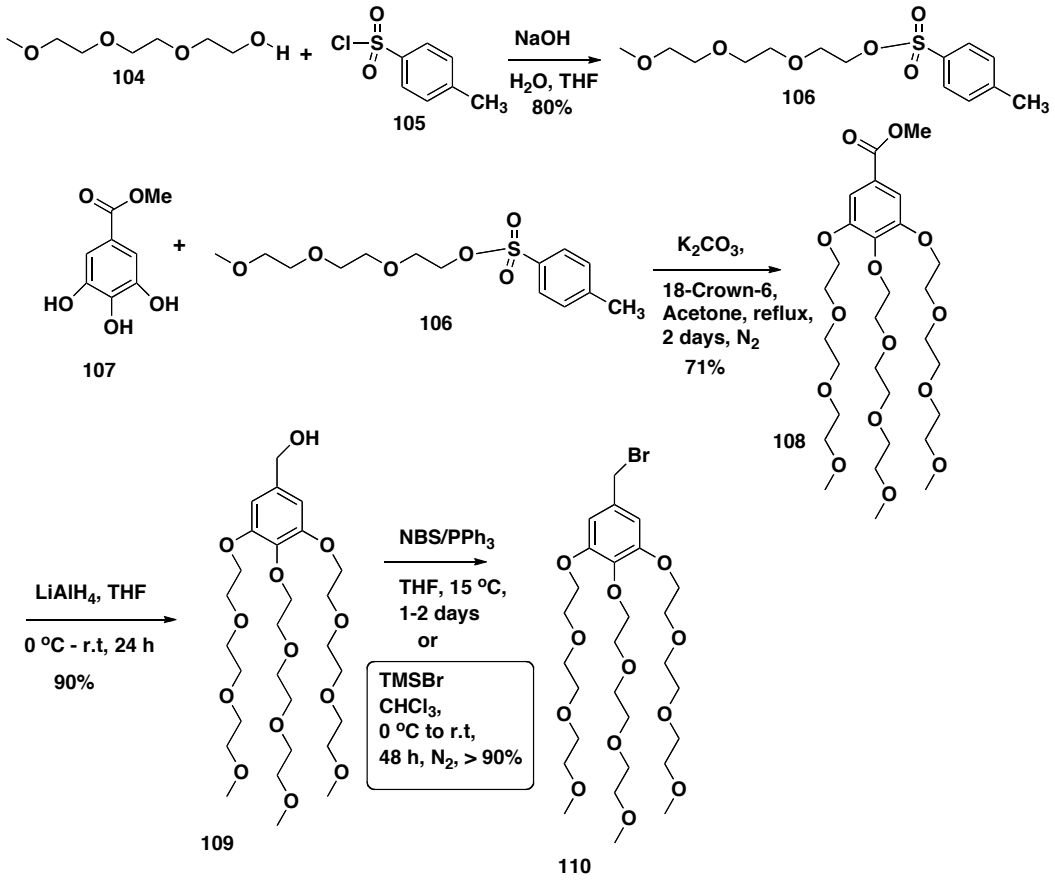

Scheme 5.7 Synthesis of ether derivative **110**

Then, to synthesize desired compounds **116** and **117**, we have first synthesized intermediate bromoderivative **113** in two steps starting from **87** (scheme 5.8). The effective route was the nucleophilic substitution of **87** with **106** in presence of NaH followed by NBS bromination to give compound **113** in 90 % yield. Then we have accessed the compound **115** by Suzuki coupling reaction of **113** by 4-cyanophenyl boronic acid **104** with ~ 24% yield as light brown oily compounds.

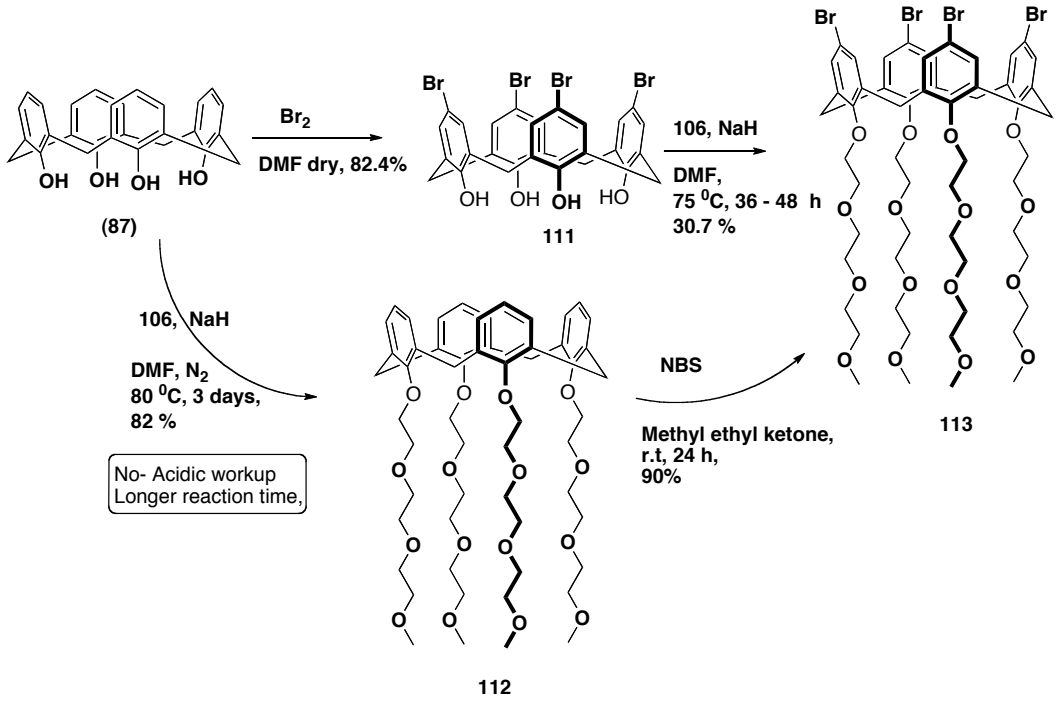

Scheme 5.8 Synthesis of Calix[4]arene derivative **113**

Then, we have synthesized compound **177** by the BH_3 reduction of cyano derivative **115** in THF with quantitative yield. Hydrolysis of compound **115** with KOH, EtOH/H_2O to give carboxyl derivative **116** was unsuccessful in given conditions because of difficulty to isolate the compound **116** from water

in the work up process. Therefore, we have synthesized it by a different route as mentioned in **scheme 5.10**, in which we have synthesized intermediate compound

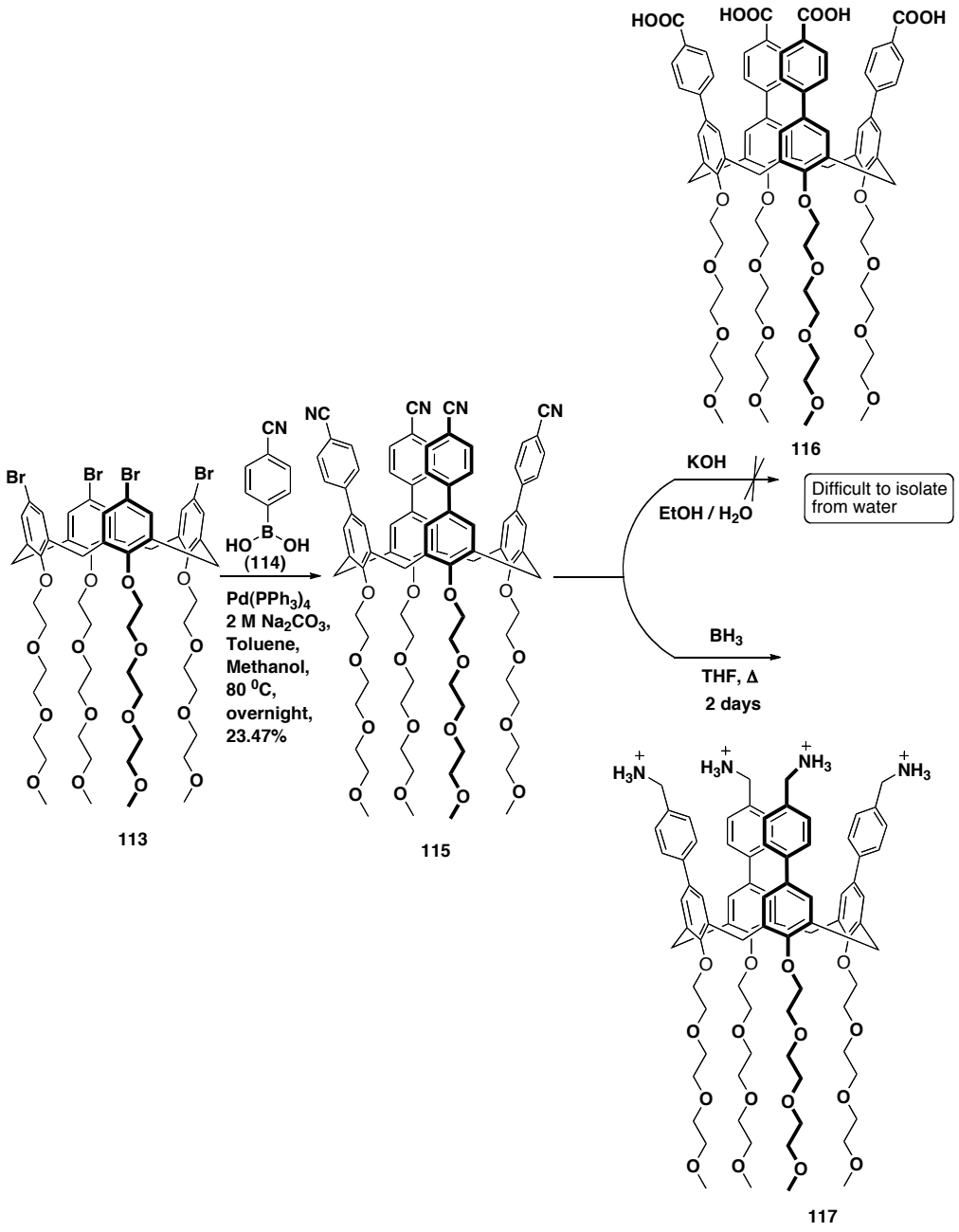

Scheme 5.9 Synthesis of Calix[4]arene derivative **116 and 117.**

119 by Suzuki coupling of **113** and 4-formylphenyl boronic acid **118**, followed by the hydrolysis of **119** with aqueous sulfamic acid and aqueous sodium nitrite in the presence of chlorofom/acetone solvent mixture to give the carboxyl derivative **116** in super quantitative yield as white solid. The superquantitative yield was due to the presence of water and which cannot be removed completely even drying in vacuum oven for 2 days at 80 ^{o}C.

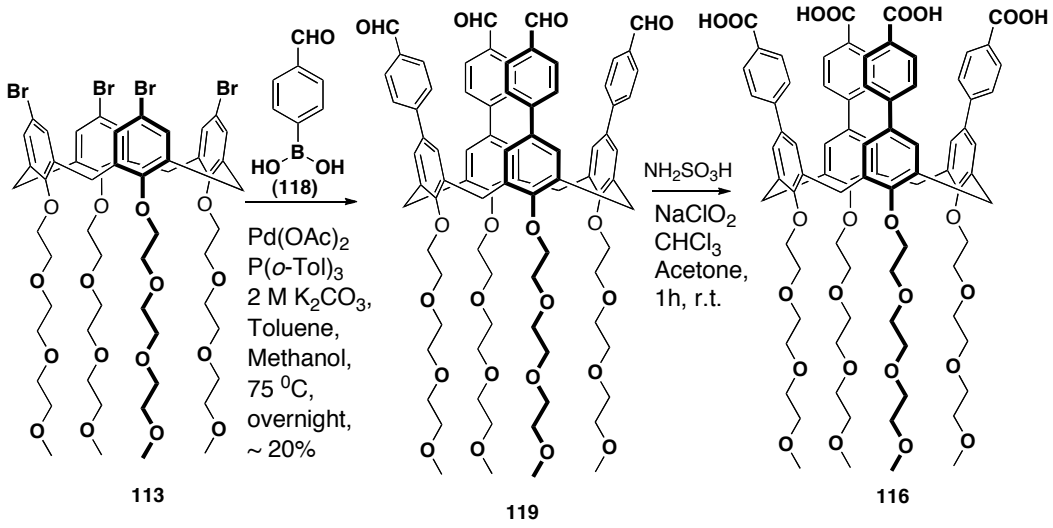

Scheme 5.10 Synthesis of Calix[4]arene derivative **116 (Method B).**

5.5 Results and Discussion

Design of molecular structures that are capable of encapsulating guest molecules in solution is one of the major objectives in supramolecular chemistry. These molecular structures have been investigated for many different purposes such as catalysis, sensoring devises and artificial receptors. Different approaches have been used to obtain capsules via noncovalent interactions, but the hydrogen bonding is the most widely employed tools in

the construction of predefined molecular structures. However many of these systems are used in non polar solvents, but the capsules that can be used in polar protic solvents have been designed by combining hydrogen bond strengths with other weak noncovalent interactions such as π-π stacking and cation-π interactions. However, systems that are capable of binding each other or encapsulating guest molecule in aqueous media are the most emerging fields in organic supramolecular chemistry.

Calix[4]arenes are greatly used as molecular scaffolds in the design of artificial receptors because of its tunable, unique three-dimensional structure and the ease of functionalization at both the rims. The extended, preorganized rigid platform of calix[4]arenes are the most interest in constructing supramolecular systems that are capable to encapsulate larger guests. The extended cavity is not only increases the size, but also acts as a chromophore or fluorophore. By taking advantage of the extended preorganized rigid platform, we envisioned that it could be functionalized at the lower rim with larger ether groups to enhance the water solubility, and introduce appropriate polar functional groups (aminomethy and carboxyl) at the upper rim to interact with guest molecule for encapsulation. Based on these observations we have synthesized two novel calix[4]arene derivatives (**116** and **117**) as a supramolecular scaffolds for encapsulation studies in aqueous media at neutral pH. More interestingly the carboxyl calix[4]arene **116** was completely soluble in D_2O, at pH 7.1 of phopsphate buffer. This is the first water soluble neutral, novel calix[4]arene derivative up to date.

The advantages of these novel calix[4]arenes over previously reported counterparts, are a) preorganization, extended cone conformation due to phenyl-substitution on the upper rim, that also enhances the solubility of the guest based on the fact that the hydrophobic character of the cavity. b) Highly polar groups (carboxy, amino) enhances the hydrogen bonding interactions with guest molecule, and also to form the' hetero-capsule'. c) Ether tethers at lower rim enhances water solubility of the calix[4]arene, guest and the capsule. Based on these facts, we are developing the binding, slectivity, water solubility enhanced, phenyl substituted, and extended novel calix[4]arene hetero capsules for catalytic and material applications.

We have studied the host-guest complex formation between host **116** and the guests **96** and **97** in aqueous media at pH 7.1, phosphate buffer. The main reason of choosing the amide guest **97** was its ability to hydrogen bond with the host carboxylic acid to come to the proximity of the host cavity. In addition to this, the aromatic groups can enhance the binding into the host cavity with strong hydrophobic interactions in aqueous media. To achieve this, the carboxycalix[4]arene **116** was dissolved in aqueous phosphate buffer of pH 7.1. The calix[4]arene **116** was completely dissolved in phosphate buffer at 25 ^{o}C after sonication for 10-15 min. There was no host-guest complex formation observed between **116** and amide guest **97** because of poor solubility of **97** in water and its size was bigger than the cavity size of the calix[4]arene **116**. Moreover, there was no complex induced shift (CIS) observed in the ^{1}H NMR spectrum. Then, added amino counterpart **117** to the sample containing **116**

and **97**, but observed precipitation. Which means that, there was no binding between host and guest rather increased solubility of host (**116**) upon addition of guest.

Then, repeated the ^{1}H NMR titration experiments with a small, water-soluble guest 96 and change in the ^{1}H NMR of host and guests were shown in the **figure 5.4**.

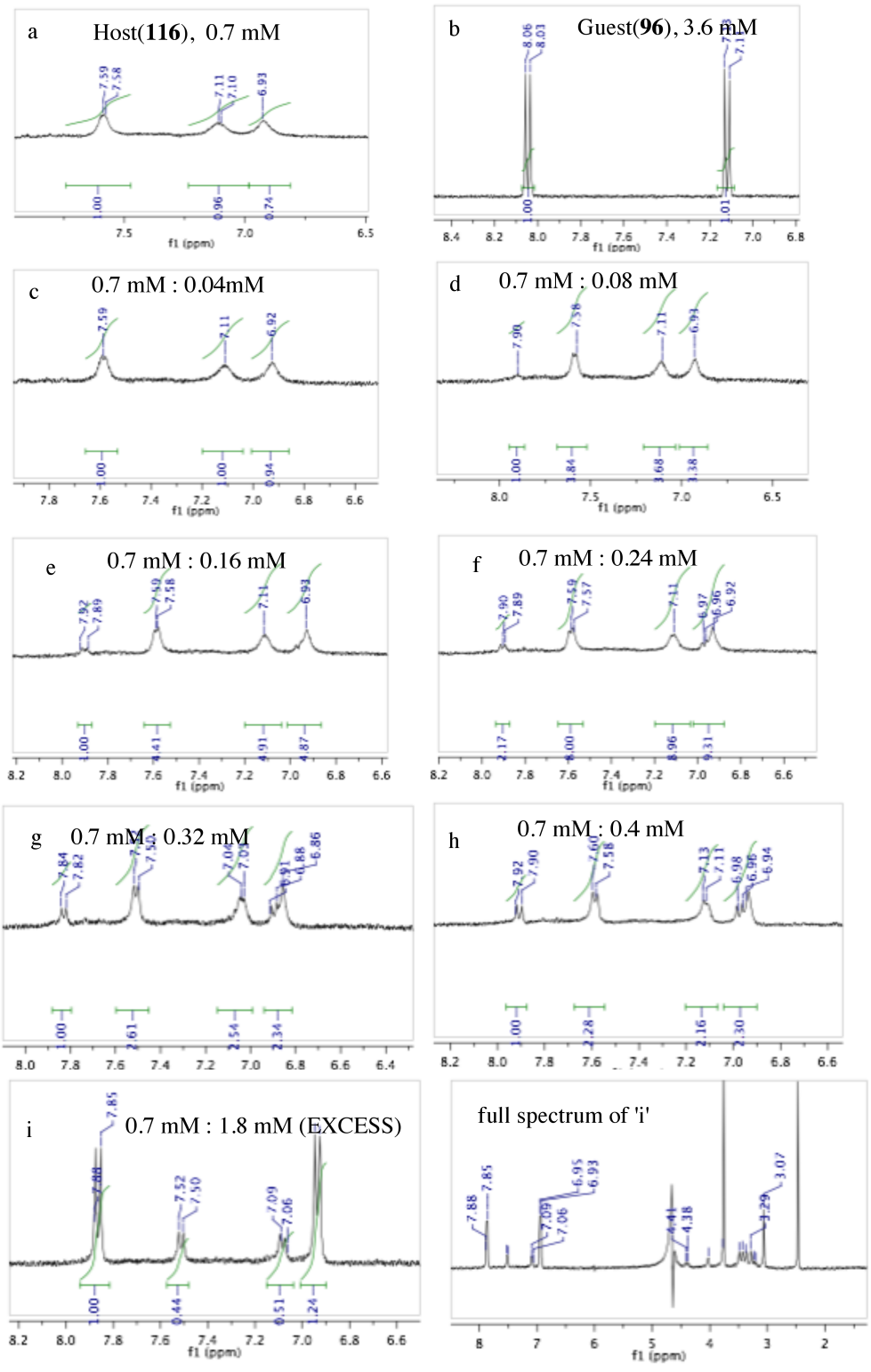

Figure 5.4 ^{1}H NMR spectra of host-guest complex formation between **116** and **96**

Based on the above ^{1}H NMR titration results, I can conclude that, the guest **96** (4-methoxyacetophenone) may not be forming H:G complex with the calix[4]arene **116**, but there were no chemically induced downfield/upfield shifts in the spectra. This is because of a) the weak binding and fast equilibrium between H:G in water, b) there is no complex induced shifts rather only change in the splitting of the phenyl protons of the calix[4]arene A (δ = 7.5ppm, *d* and δ = 7.0ppm *d*), this is because of the π-π interactions of the phenyl rings of the host and guest in the solvent or this may be due to the fixed alignment of phenyl groups of calix[4]arene **116** in presence of guest **96**. Since, the phenyl groups of the calix[4]arene **116** or **117** in the upper rim were not rigid in conformation, but the flexibility leads to the poor association with the guest by hydrophobic interactions was weak and these forces were not enough to host the guest strongly in the hydrophobic cavity. Therefore, surprisingly, there was no binding/encapsulation observed.

5.6 Conclusion and Future directions

Since there was no binding observed in ^{1}H NMR titration experiments, which may be due to the flexible phenyl groups on the upper rim of the calix[4]arene derivarives, which prevents the association with guest. Because of the flexible groups on the upper rim, hydrophobic effects were not strong enough to bring the guest into the cavity. Therefore, to improve the binding affinity of these calix[4]arenes in water, the derivatization at the lower rim with bulky, larger ether chain containing groups such as compound **110 (scheme 5.7)** must be introduced. The high bulkiness groups at the lower rim may

improve the rigidity of the phenyl groups at the upper rim for stable and deep cavity formation. Since, the aminocalix[4]arene **117** was not water soluble at neutral pH, the introduction of more ether chains at the lower rim may improve the water solubility. The other idea is to make the phenyl groups at the upper rim more rigid and this can be achieved by the coupling of phenyl groups together to form a cavitand like structure for encapsulation studies.

5.7 Experimental procedure:

Synthesis of 25,26,27,28-Tetrahydroxycalix[4]arene (32)

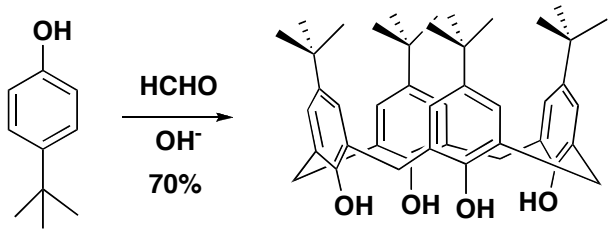

(86) (32)

Proceedure: A. *Preparation of* "*precursor*." A mixture of 20 g (0.133 mol) of *p-tert*-butylphenol, 12.4 mL of 37% formaldehyde solution (0.165 mol of HCHO), and 0.24 g (0.006 mol) of sodium hydroxide (corresponding to 0.045 equiv with respect to phenol) in 0.6 mL of water is placed in a 1-L, two-necked, round-bottomed flask equipped with a magnetic stirrer. The contents of the open flask are allowed to stir for 20 min at room temperature, and then heated for 2 hr at 100—120°C in oil bath. The reaction mixture, which is clear and colorless at the beginning, becomes light yellow after 30 min, a somewhat deeper yellow after 1 hr, and eventually changing to a thick slurry as the water evaporates and finally turning to a deep yellow or brown-yellow very viscous

mass (after 90 min, stirring stopped). During this period there is considerable frothing, and the reaction mixture fills most of the flask before shrinking back to the original volume. After 2 hrs, the reaction vessel is removed from the oil bath, and the reaction mixture is allowed to cool to room temperature. To dissolve the residue, 200 mL of warm diphenyl ether is added to the flask and the contents are stirred, the process generally requiring at least 1 hr.

Comment: After 90 min of the reaction, stirring stopped due to the formation of viscous solid, but continued heating for 30 more minutes (total of 2 hrs at 110-120 ºC).

B. *Pyrolysis of the precursor*. The 1-L, two-necked flask is fitted with a nitrogen inlet. The contents of the flask are stirred and heated (110—120°C) in a oil bath, while a stream of nitrogen is blown rapidly over the reaction mixture to facilitate the removal of the water as it is evolved. During this period the color of the solution changes from yellow to a gray or a light brown. When the evolution of water subsides and a solid starts to form (prior to attaining the reflux temperature) the flask is fitted with a condenser, and the contents of the flask are stirred and heated to ca. 150—160°C for a few minutes (30 min) and then at reflux (260-270 °C) for 3 - 4 hrs under a gentle flow of nitrogen. During this phase of the reaction the solid dissolves, and a clear dark-brown to grayish-black solution is formed. The reaction mixture is cooled to room temperature (some solid separates), and the product is precipitated by the addition of 300 ml of ethyl acetate. The resulting mixture is stirred for 30 min and allowed to stand for at least 30 min (9 hrs). Filtration (Medium pore size,

glass frit filter) yields material that is washed twice with (2*20- mL) portions of ethyl acetate, once with 40 mL of acetic acid, twice with (2*20-mL) portions of water, and twice with (2*10-mL) portions of acetone, then dried for 4-5 hrs on house vcuum to yield ca. 13 g (65%) of crude product. (Lit 66%).

25,26,27,28-Tetrahydroxycalix[4]arene (87): (Gutsche, C. D.; Iqbal. M. *Organic Syntheses, Coll. Vol. 8, p.75* ***(1993)****; Vol. 68, p.234 (1990))*

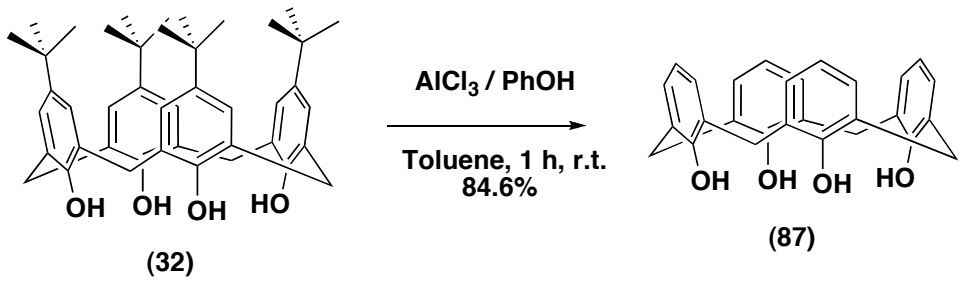

Compound **87** was synthesized by following Gutsche's procedure. A slurry of 4.0 g (6.172 mmol) of *p-t*-Butylcalix[4]arene, 2.788 g (29.625 mmol) of phenol and 4.321 g (32.407 mmol) of $AlCl_3$ was stirred in 50 ml of toluene at room temp for 1 hr in nitrogen atmosphere. Then the mixture was slowly poured into 75 ml of 0.2 N HCl, the organic phase was separated, and the toluene was evaporated on rotavap. Upon addition of MeOH ppt formed, which was collected by filtration. Then recrystallized from MeOH-$CHCl_3$ to give 2.2 g (84.6 %) of white crystals. ^{1}H NMR (400 MHz, $CDCl_3$) δ 10.21 (s, 4H, O-H), 7.06 (d, *J* = 9 Hz, Ar-H), 6.74 (t, *J* = 9 Hz, A r-H), 4.26 (br S, 4H, -CH), 3.56 (br S, 4H, -CH).

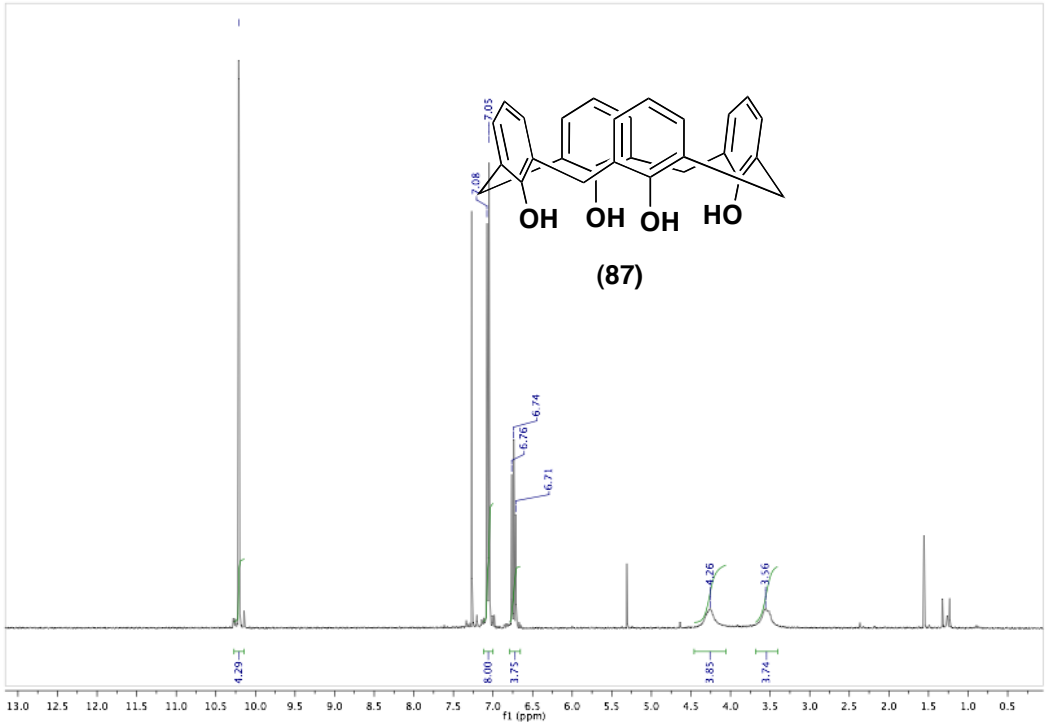

Figure 5.5 1H NMR spectrum of compound 87

Synthesis of Compound **89**:(1.*Tetrahedron*, **1986**, *42*, 1633-1640. 2. *JOC*, **1992**, *57*, 3658-3662)

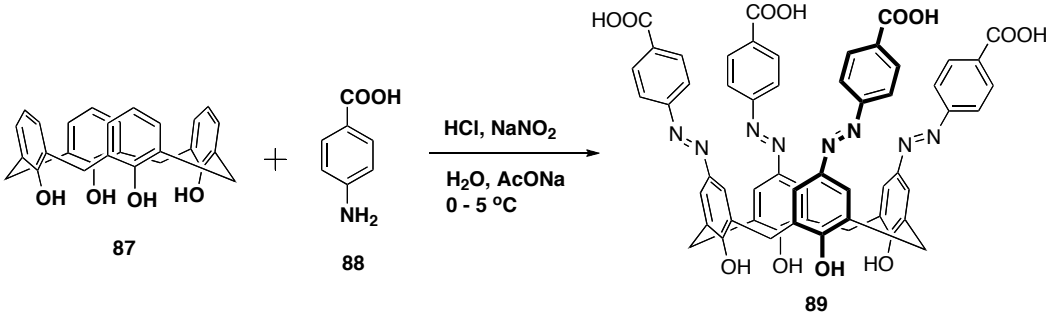

p-Aminobenzoic acid (0.323 g, 2.35 mmol) and 0.145 ml of conc. HCl (4.7 mmol) were added to 3.5 ml of water and the resulting solution was cooled to 2°C. Then, a solution of $NaNO_2$ (0.162 g, 2.35 mmol) in 2 ml of water was added dropwise at such a rate to maintain the temperature below 5°C. The resulting mixture was slowly added to a solution of thiacalixarene 1 (0.100 g,

0.235 mmol) and sodium acetate (0.639 g, 4.7 mmol) in 3.91 ml of dimethylformamide at 5°C. The reaction mixture was stirred for 15 min at the same temperature, allowed to stay at room temperature for 2 h and then heated to 60°C for 30 min. The mixture was acidified with 2 M HCl to pH 5 and the resulting precipitate was filtered off and washed with water and methanol. The resulting red solid was dissolved in a hot solution of sodium hydrogencarbonate (0.420 g in 10 ml of water), added activated charcoal (100 mg), stirred for 15 min and filtered out the charcoal, resulting colored solution was cooled to room temperature and reprecipitated by addition of conc. HCl (1-2 ml). The mixture was stirred at 60°C for 30 min and cooled to room temperature, the red precipitate filtered off, washed with water and methanol and dried overnight at 80°C to yield 0.200g of **89** as a red solid, but the NMR was not good in DMSO-d_6. Then dissolved in THF and let it stand for 1 day at room temperature then filtered off (Medium pore size glass-frit filter) the solid, dried on house vacuum overnight, then at 80 ºC for several hrs (6-8 hrs) to give the red solid, 0.080 g.

^{1}H NMR (DMSO-d_6, 300 MHz): δ 8.0 (d, 8H, J=9.0 Hz, H-arom), 7.83-7.80 (m, 16H, , H-H-arom), 4.30-3.91(br s, 8H, CH_2 -calix).

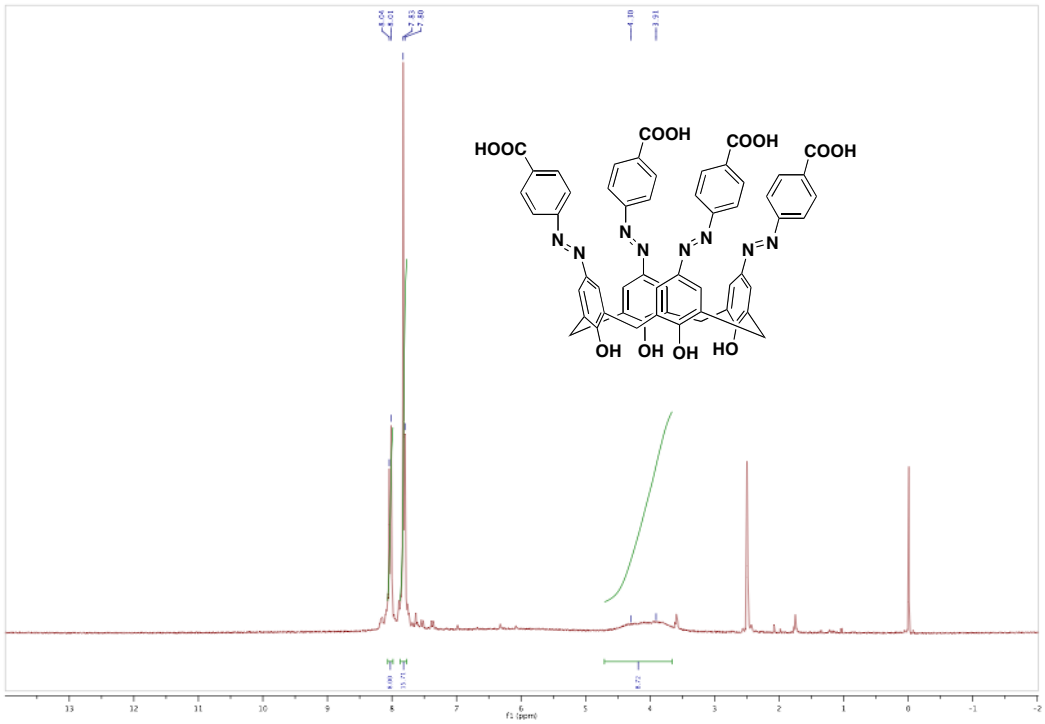

Figure 5.6 ^{1}H NMR spectrum of compound 89

Synthesis of Compound **92**: (*Tetrahedron*, **1986**, *42*, 1633-1640)

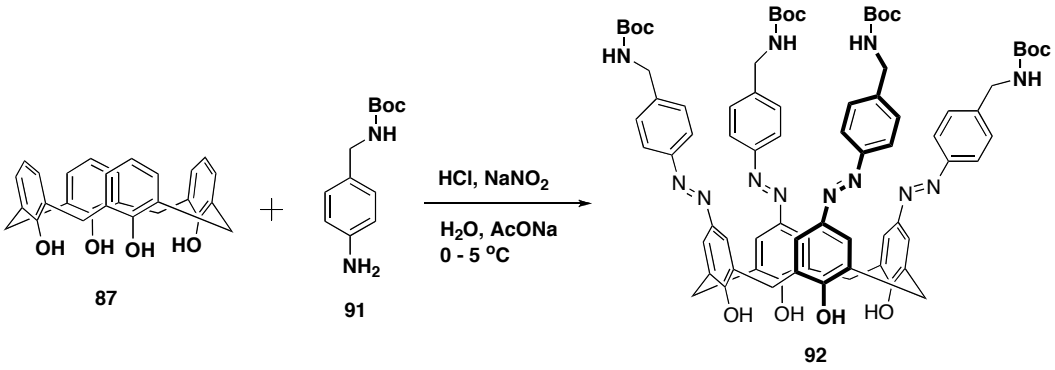

Boc protected *p*-Aminobenzylamine (0.522 g, 2.35 mmol) and 0.145 ml of conc. HCl (4.7 mmol) were added to 3.5 ml of water and the resulting solution was cooled to 2°C. Then, a solution of $NaNO_2$ (0.162 g, 2.35 mmol) in 2 ml of water was added dropwise at such a rate to maintain the temperature below

5°C. The resulting mixture was slowly added to a solution of thiacalixarene 1 (0.100 g, 0.235 mmol) and sodium acetate (0.639 g, 4.7 mmol) in 3.91 ml of dimethylformamide at 5°C. The reaction mixture was stirred for 15 min at the same temperature, allowed to stay at room temperature for 2 h and then heated to 60°C for 30 min. The mixture was acidified with 2 M HCl to pH 5 and the resulting precipitate was filtered off and washed with water and methanol. Dried on house vacuum overnight then in the oven at 80 ºC for 12 hrs to give the orange/red solid. Crude NMR shows lot of starting material/incomplete reaction. Then purified by column chromatography by eluting with EtAc as a solvent, and collected the yellow/light-orange large band in about 4-5 column volumes. Evaporated the solvent to give yellow colored compound. Acetone was added and evaporated the solvent on rotavapor/heated about 1 hr at 60 ºC, to give red solid in the flask.

Comment/Observations: The starting material (mono-protected p-Aminobenzylamine) was not completely soluble in acidic water, before addition of sodium azide, it supposed to be clear and homogenious. Upon addition of insitu generated sodium azide, still lot of unreacted starting material left in addition to lot of orange/red colored solid in the reaction flask.

^{1}H NMR: (Acetone-D_6, 400 MHz): δ 7.8 (s, 8H, Ar-H), 7.6 (d, 8 H, J = 6 Hz, Ar-H), 7.3(d, 8H, J = 6 Hz, Ar-H), 6.4 (t, 4 H, N-H), 4.2-4.1 (m, 16 H, CH_2), 1.3 (s, 36 H, CH_3).

MS: ESI-MS (Chloroform and Acetone solvent): *m/z* 1379.4 (M+Na] indicates the compound **5**. (Top MS is in Chloroform solvent, bottom one is in Acetone solvent)

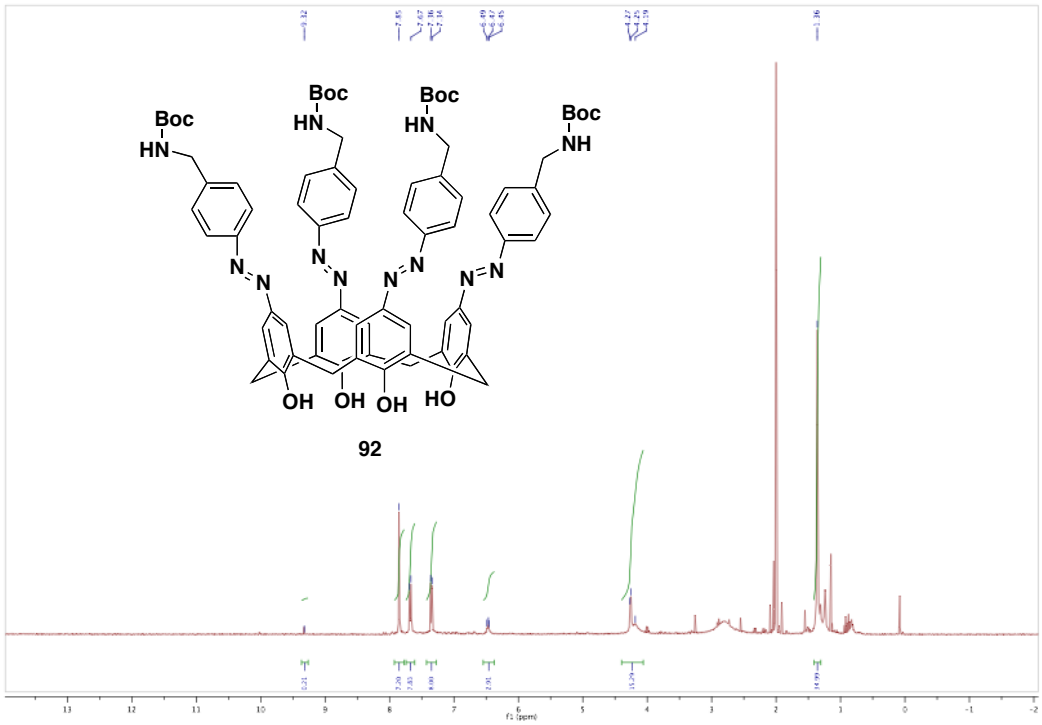

Figure 5.7 ^{1}H NMR spectrum of compound 92

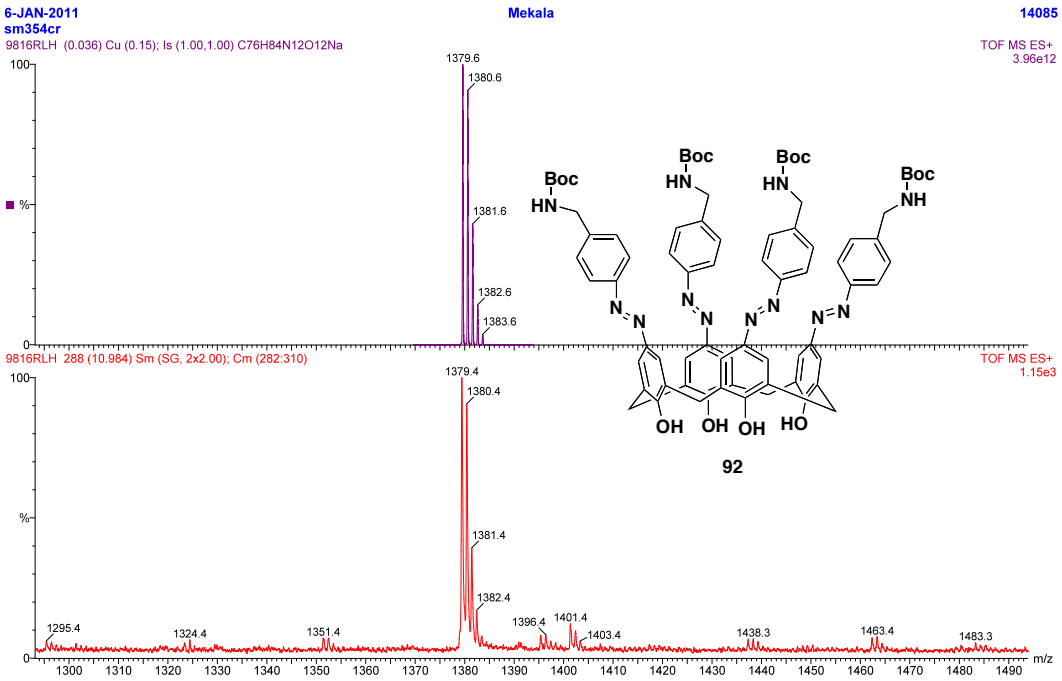

Figure 5.8 ESI-MS spectrum of compound 92

Synthesis of Compound 92a (Boc-deprotection): (*J. Org. Chem.* **2005**, *70*, 7956-7962)

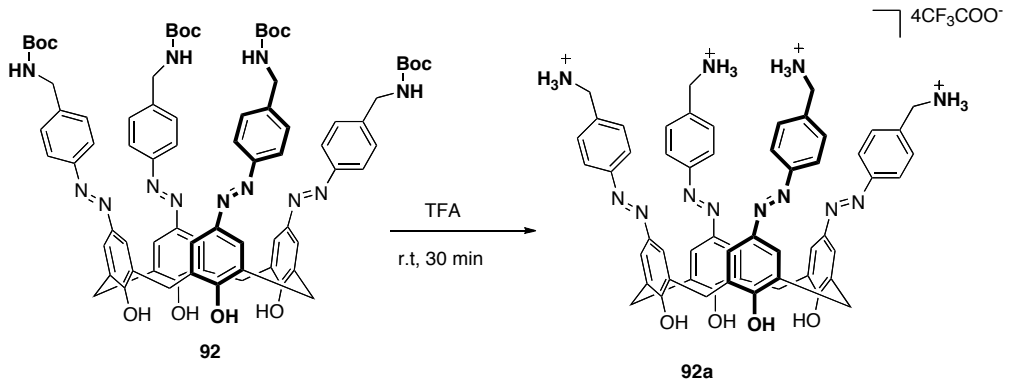

The 'Boc' protecting groups in **1** were removed by the addition of CF_3COOH (2 mL) to solid 1 (32 mg) with stirring at room temperature for 30 min. The reaction mixture was concentrated to dryness, leaving a sticky residue. The

excess of CF_3COOH was removed by 4 repeated additions and removal of MeOH (10 *4 mL) by rotary evaporation under reduced pressure at 50 °C, leaving a red residue. This residue was treated with CH_2Cl_2, (compound is not soluble in DCM, ppt formed) and the solvent was removed by rotary evaporation under reduced pressure at 40 °C until a red solid (20 mg) formed.

^{1}H NMR: CD_3OD, 300MHz:

δ 7.84 (d, 9 Hz, 8 H, Ar), 7.80 (S, 8 H, ArH(Calix)), 7.52 (d, 9 Hz, 8H, ArH), 4.11

(br s, 16 H, CH_2).

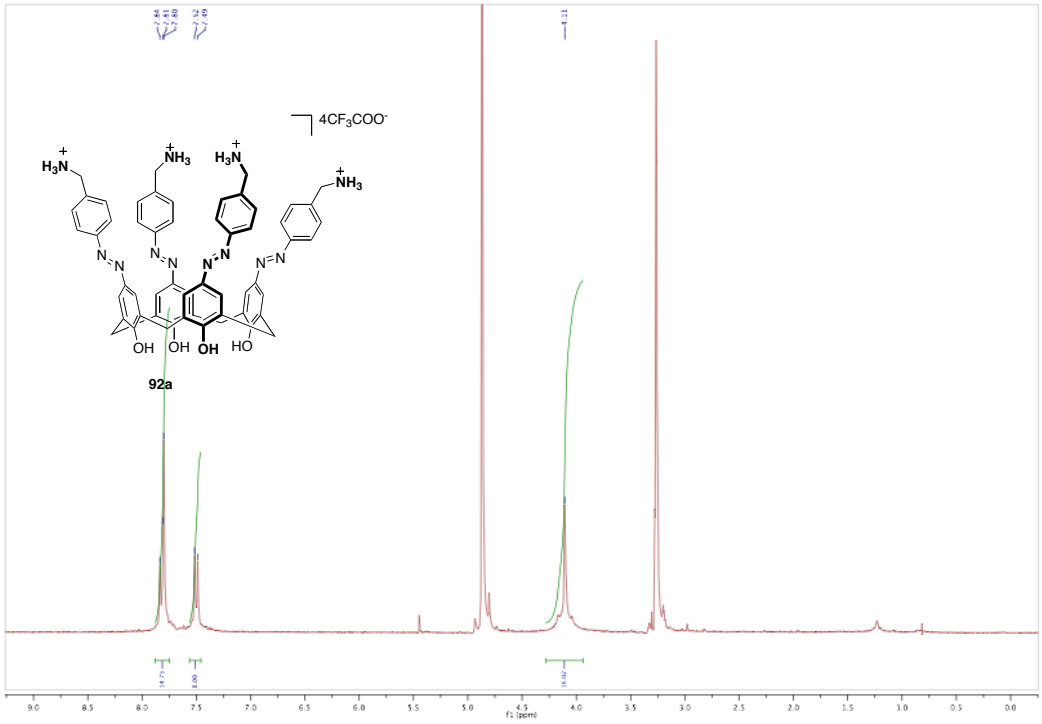

Figure 5.9 ^{1}H NMR spectrum of compound 92a

ESI-MS: *m/z* 957.42 [M+H]

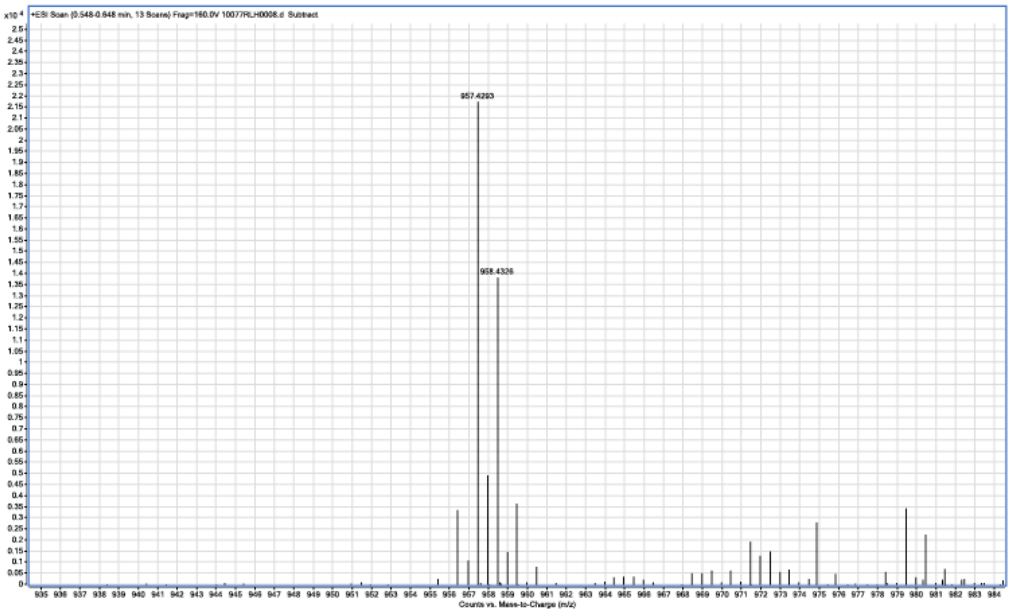

Figure 5.10 ESI-MS spectrum of compound **92a**

Synthesis of Compound 106: (JOC, 2009, 74, 9280-9286) Compound **106** was synthesized following the literature procedure and ^{1}H NMR matches with the literature reported compound.

Toluene-4-sulfonic acid 2-[2-(2-methoxyethoxy)-ethoxy]-ethyl ester (106):

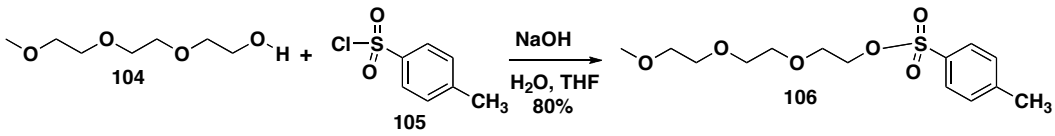

NaOH (8 g, 200 mmol) was dissolved in H_2O (50 ml) and added to solution of 2-[2-(2-methoxyethoxy)- ethoxy]-ethanol (23 g, 100 mmol) in THF (50 ml). The mixture was cooled down to 0-5 oC and the solution of p-toluene sulfonylchloride (25 g, 100 mmol) in THF (50 ml) was added to reaction mixture over 1 hour with addition funnel. The reaction was stirred at 0-5 °C for an additional 45 min-1h. The mixture was poured into the ice cold-water (500

ml) and extracted with CH_2Cl_2. The combined organic layers were washed with H_2O and brine. The organic layer was dried over anhydrous Na_2SO_4 and CH_2Cl_2 was evaporated to give a clear oil. (29 g, 93% yield). ^{1}H NMR (400 MHz, $CDCl_3$) δ 7.8(d, J= 8.0 Hz, 2H, Ar-H), 7.34(d, J= 8.0 Hz, 2H, Ar-H), 4.16(t, J= 4.0 Hz, 2H, -CH2), 3.69(t, J= 4.0 Hz, 2H, -CH2), 3.69-3.62 (m, 6H, -CH2), 3.52-3.54 (m, 2H, -CH2), 3.37 (s, 3H, O-CH3), 2.45 (s, 3H, Ar-CH3).

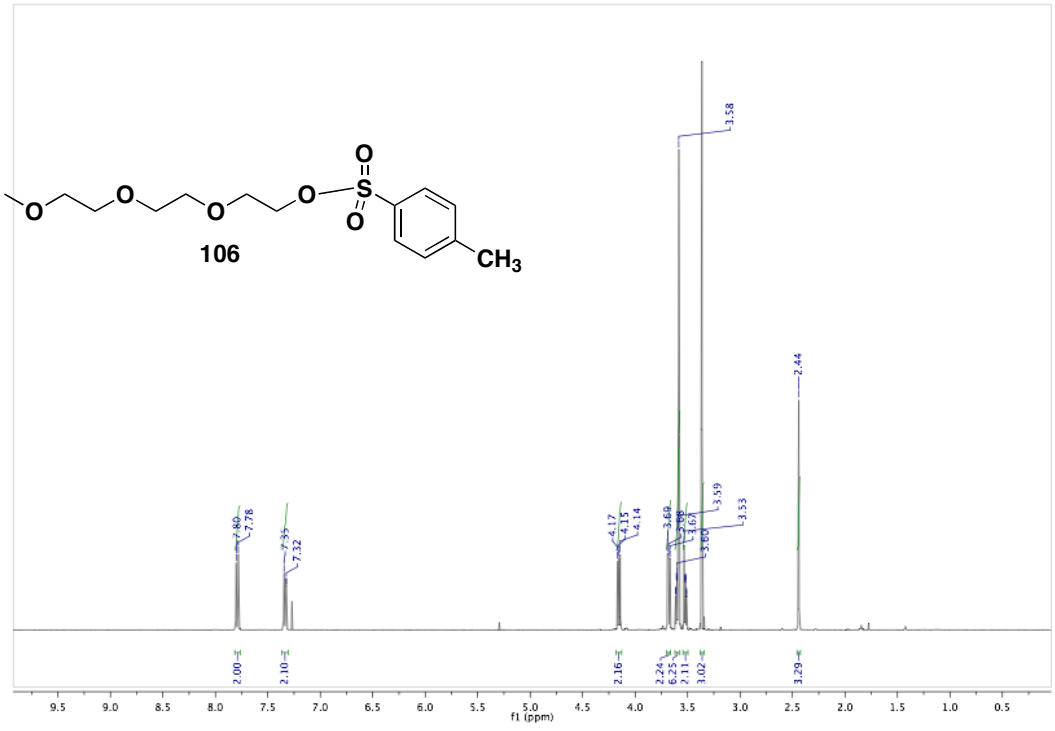

Figure 5.11 ^{1}H NMR of compound **106** in $CDCl_3$, 400 MHz.

Synthesis of Compound 110: (PCT Int. Appl., 2010106341, 23 Sep 2010, J. Am. Chem. Soc, 2005, 127, 373-383) The compound 108 was synthesized following literature procedure in 3 steps with ~90% yield. ^{1}H NMR matches with the literature reported compound.

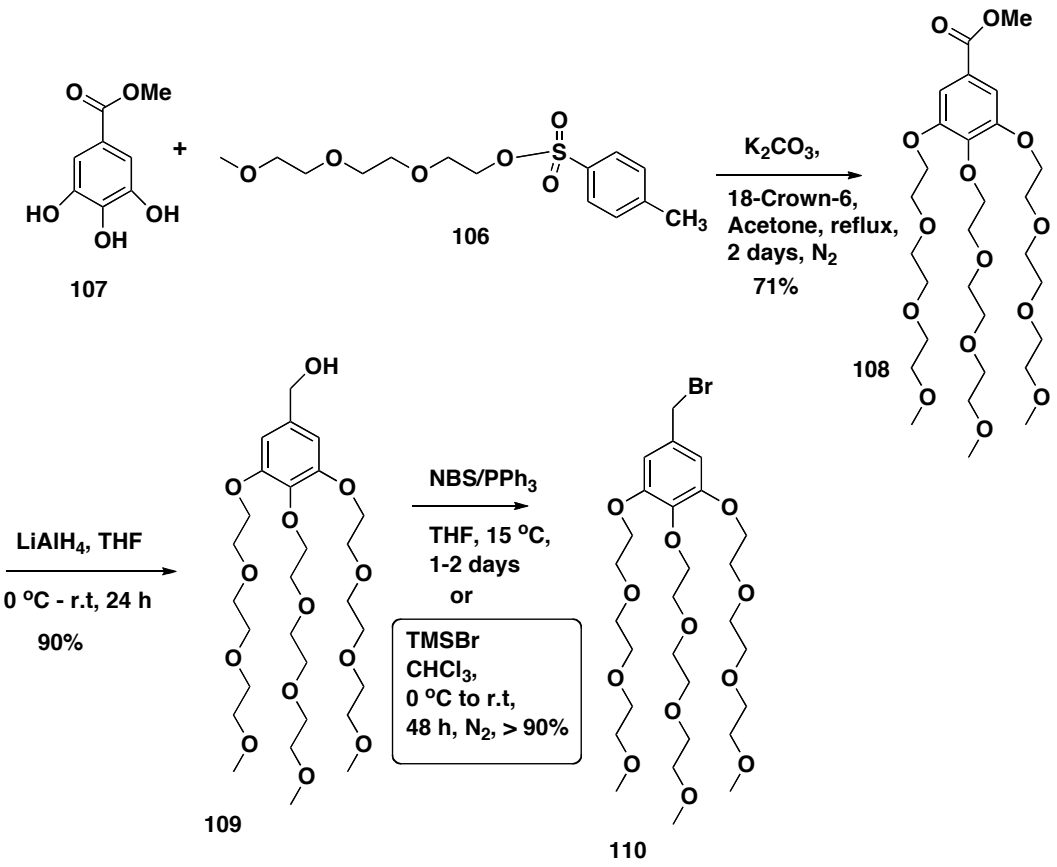

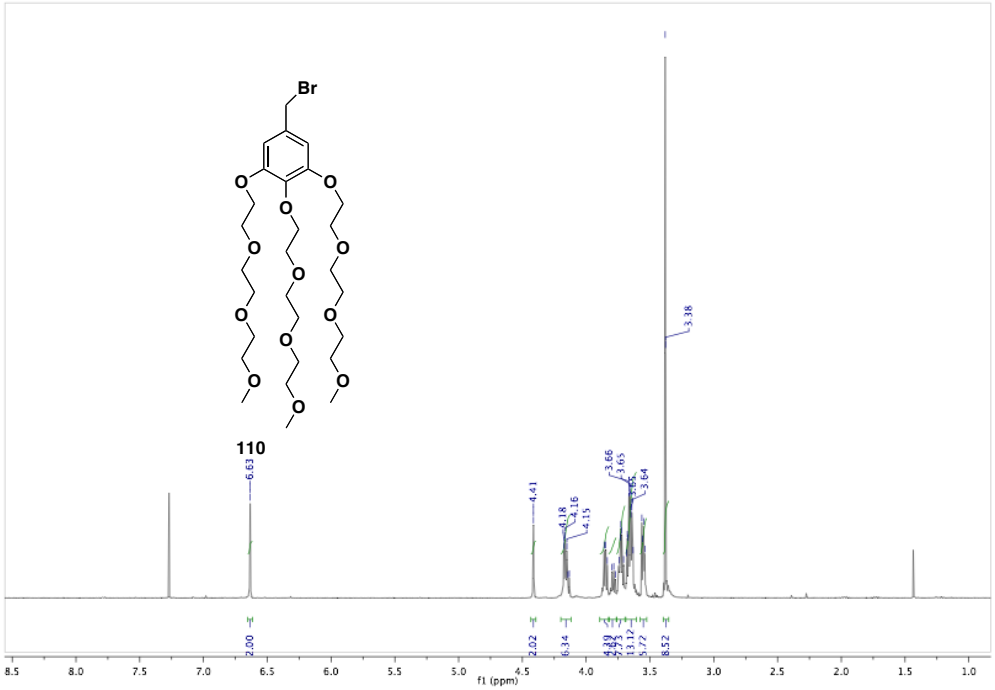

Figure 5.12 ^{1}H NMR of compound **110** in $CDCl_3$, 400 MHz

5,11,17,23-Tetrabromo-25,26,27,28-tetrahydroxycalix[4]arene (111):

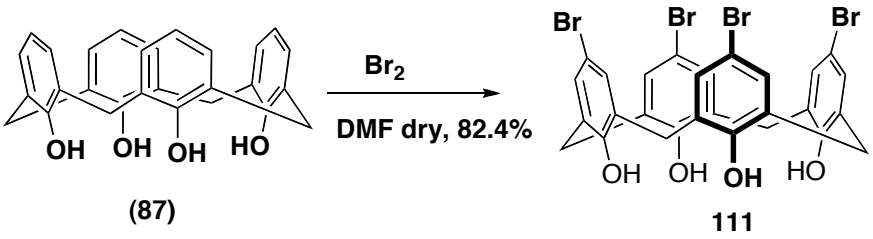

Bromine (0.725 ml, 14.0 mmol) in 10 ml dry DMF was added drop wise with syringe pump (with stirring) to a solution of calix[4]arene (1.0 g, 2.35 mmol) in 40 ml of DMF. The solution was stirred for 4 h (some ppt formed after 0.5 h of stirring). MeOH (40 ml) was added and stirred for another 0.5 h. The precipitate was filtered off and washed with methanol (2 ∗ 20 ml) to yield **111** (1.436 g, 82.4 %) as a white solid. ^{1}H NMR (300 MHz, DMSO-D_6) δ 7.32 (s, 8H, ArH), 3.79 (br s, 8H, $ArCH_2Ar$).

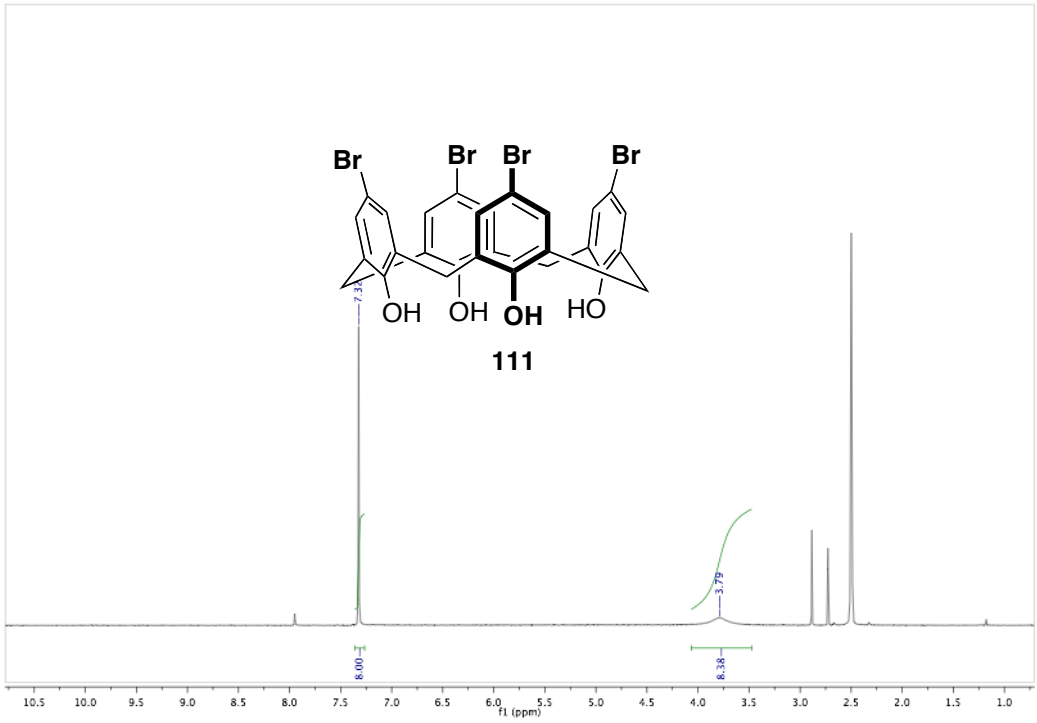

Figure 5.13 ^{1}H NMR spectrum of compound **111** in DMSO-d_6, 400 MHz

25,26,27,28-tetrakis[2-(2-(2methoxyethoxy) ethoxy)ethoxy] -calix[4]arene (112):

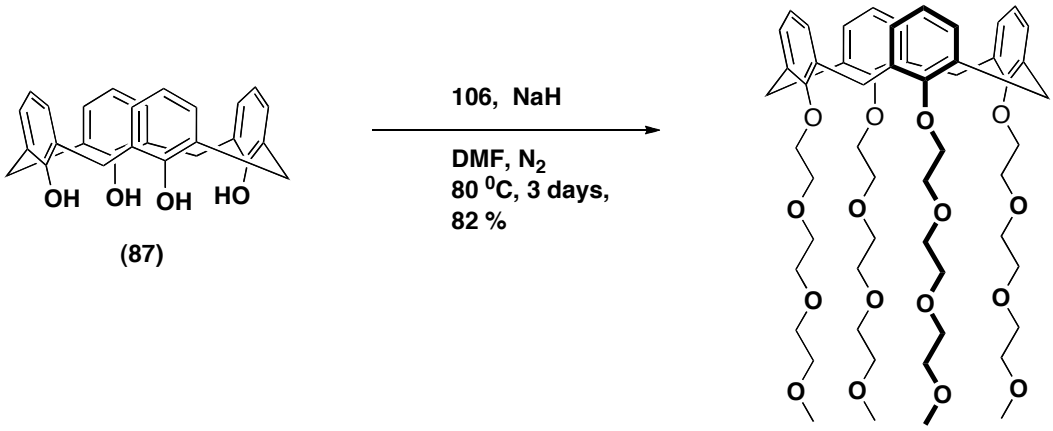

To a 250 mL round bottomed flask, added NaH (60% in mineral oil, 20.0 mmol, 0.480 g) and dry DMF then added calix[4]arene **87**. The resulting slurry was stirred for 10 min at 70 ºC under nitrogen. Then added compound **106** (20.4 mmol, 6.5 g) in 10 mL of DMF and stirred for ~3 days at 75-80 ºC under nitrogen. Then evaporated the solvent on DMF before addition of ~100 mL of water. Aqueous portion was extracted with diethylether (100 mL x 3), and organic phase was dried over anhydrous sodium sulfate for several hrs. Then evaporate the solvent and purify by silica gel column chromatography with 1%MeOH/CH_2Cl_2, 2%MeOH/CH_2Cl_2 and 10%MeOH/CH_2Cl_2 to give the desired compound **112** as thick yellow oily compound with 84.03% yield (2.01 g).

^{1}H NMR, $CDCl_3$, 400 MHz: δ 6.58 (m, 12 H, Ar-H), 4.46 (d, *J* = 13.2 Hz, 4H), 4.10 (t, *J* = 5.6 Hz, 8H), 3.85 (t, *J* = 5.6 Hz, 8H), 3.60 (m, 24 H), 3.51 (m, 8H), 3.36 (S, 12 H), 3.11 (d, *J* = 13.2 Hz, 4 H).

^{13}C NMR, $CDCl_3$, 400 MHz: δ 156.45, 135.15, 128.31, 122.33, 73.07, 72.12, 70.83, 70.74, 70.61, 70.58, 59.17, 31.08.

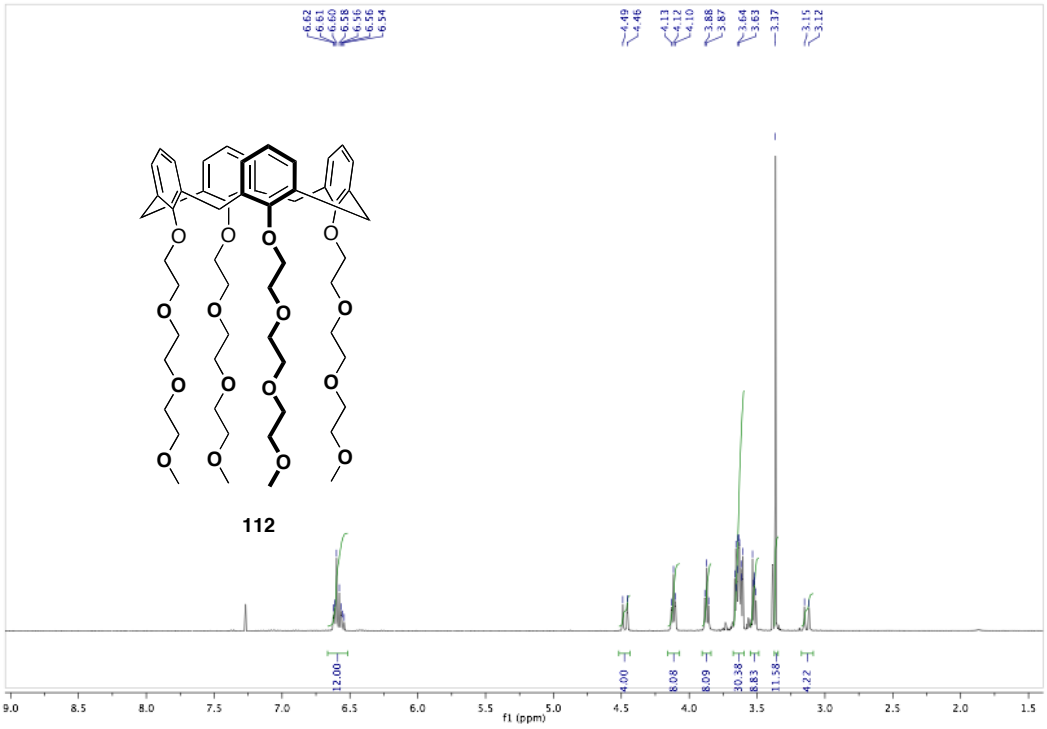

Figure 5.14 ^{1}H NMR spectrum of compound **112**

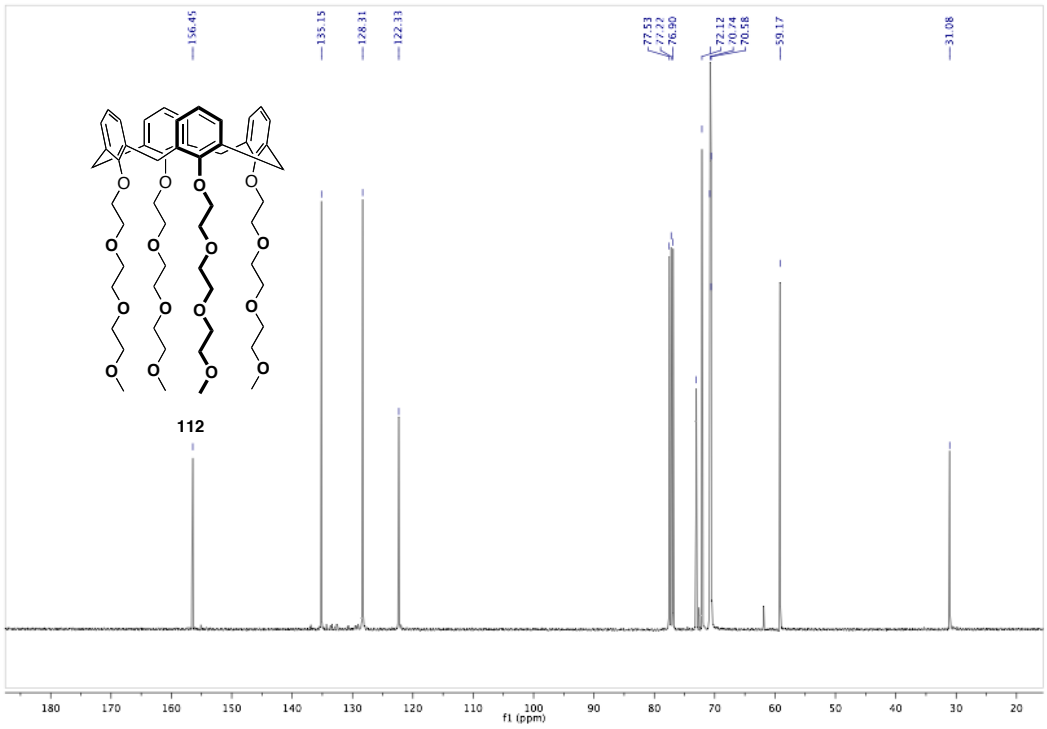

Figure 5.15 ^{13}C NMR spectrum of compound **112**

5,11,17,23-Tetrabromo-25,26,27,28-tetrakis[2-(2-(2methoxyethoxy) ethoxy)ethoxy] -calix[4]arene (113): ***Method A*****:** To a stirred mixture of compound (**7**) 1.0 g (1.351 mmol) and NaH 0.378 g (9.470 mmol) in dry DMF (25 ml) was added tosylate (**3**) (3.016 g, 9.470 mmol) in 5 ml of DMF and the mixture wad heated at 75 ºC for 36 h under nitrogen atmosphere. Then cooled to room temperature and poured into 150 ml of 1 N HCl. The mixture was extracted with CH_2Cl_2. The combined organic phase was washed with water and dried over anhydrous Na_2SO_4, filtered and solvents were removed under vacuum. The compound 8 was purified by column chromatography (EtOAc-MeOH 100:1 and EtOAc-MeOH 1:1) to give a colorless syrup 0.551 g (30.7 %). ^{1}H NMR (400 MHz, $CDCl_3$) δ 6.80 (s, 8H, Ar-H), 4.43 (d, *J* = 13.2 Hz, 4H, Ar-CH2-Ar), 4.09 (t, *J* = 5.2 Hz, 8H, -CH2), 3.80 (t, 5.2 Hz, 8H, -CH2),

3.66 – 3.64 (m, 28H, -CH2), 3.36 (s, 12H, O-CH3), 3.07 (d, J = 13.6 Hz, 4H, Ar-CH2-Ar). ^{13}C NMR ($CDCl_3$, 400 MHz): δ 155.39, 136.45, 130.96, 115.36, 73.30, 71.92, 70.61, 70.59, 70.56, 70.55, 70.50, 70.35, 59.01, 30.68. ESI-MS: Calculated (M+H): m/z = 1325.82, found: (M+Na): m/z = 1347.2.

***Method B*:** (JOC, 1992, 57, 3744-3746, JOC, 1985, 50, 5795-5802).

To a solution of **112** (2.0 g, 1.98 mmol) in 100 mL of methyl ethyl ketone was added freshly recrystallized N-Bromosuccinamide (NBS), (3.176 g, 17.5 mmol) and stirred open flask at room temperature under laboratory light for 24 h. The resulting reaction mixture was added $NaHSO_3$ (75 mL, 10% in water) and stirred for 10 min, then extraction by CH_2Cl_2 (25 mL x 3) and washed organic phase several times with water and dried over anhydrous sodium sulfate. Evaporation of solvent and purification by silica gel column chromatography (95:5 EtAc:MeOH) to give brown oily product with 86.2% yield (2.250g). The crude product can also be recrystallized from CH_2Cl_2/MeOH.

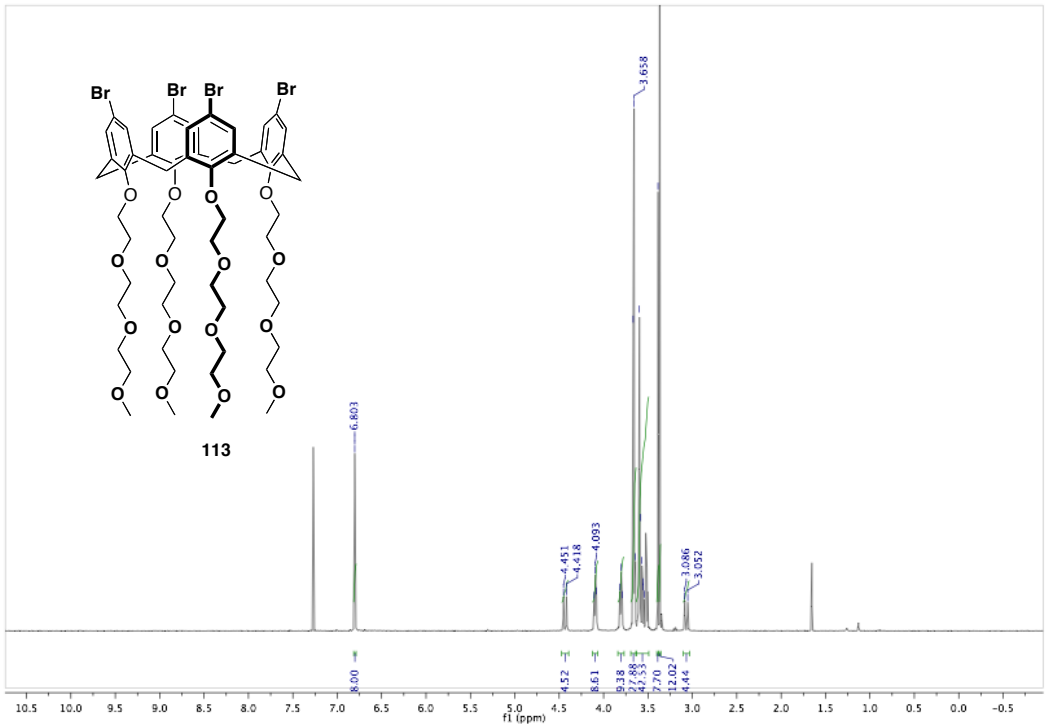

Figure 5.16 ^{1}H NMR spectrum of compound **113**

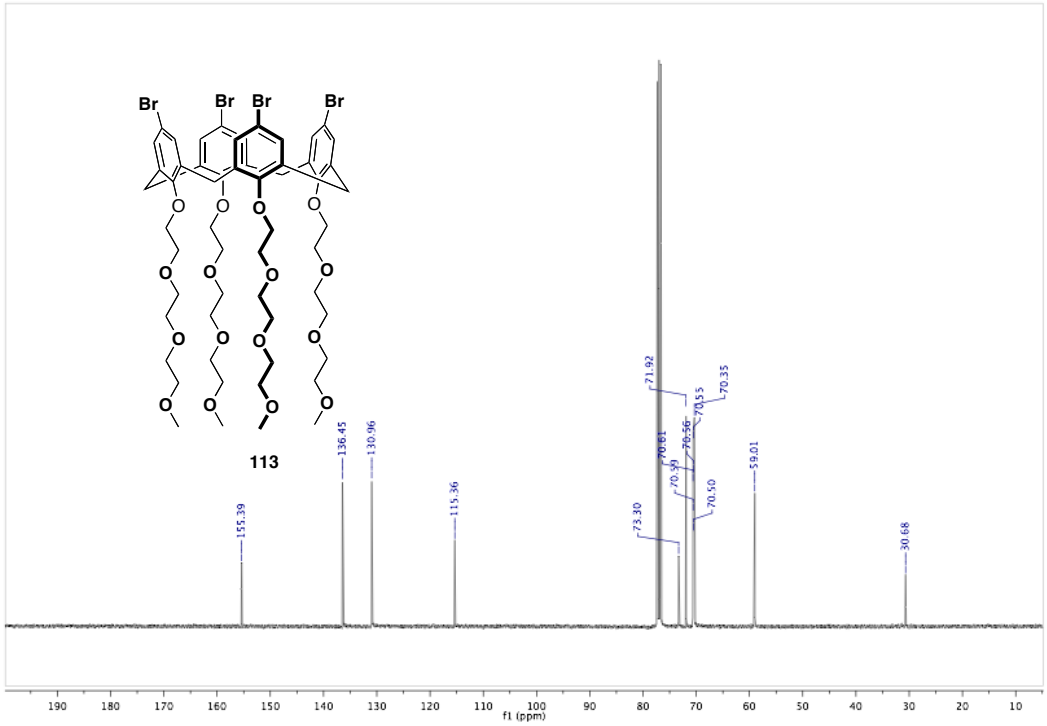

Figure 5.17 ^{13}C NMR spectrum of compound **113**

ESI-MS: m/z 1347.2 [M+H]

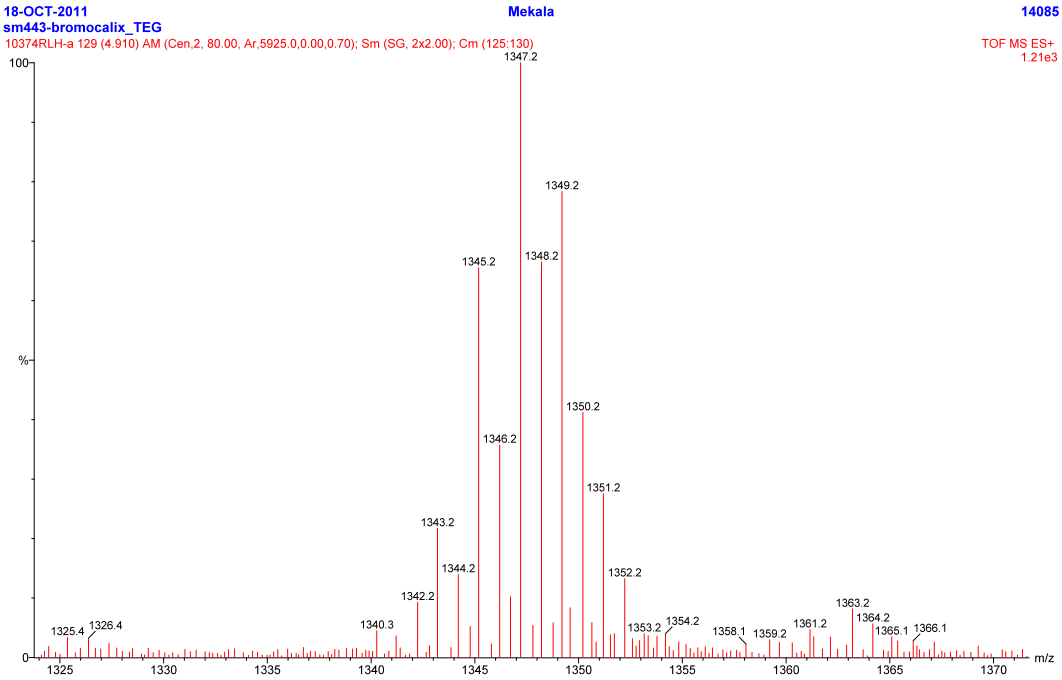

Figure 5.18 ESI-MS spectrum of compound **113**

Tetra(*p*-Cyanophenyl)-25,26,27,28-tetrakis[2-(2-(2methoxyethoxy) ethoxy)ethoxy] -calix[4]arene (115): To a suspension of tetrabromocalix[4]arene **8** (0.200 g, 0.1509 mmol), $Pd(PPh_3)_4$ (0.362 g, 0.3138 mmol), and *p*- cyanophenyl boronic acid 9 (0.110 g, 0.7545 mmol) in toluene (5 ml) were added 2 M aq Na_2CO_3 (2 ml) and methanol (1.5 ml) and the mixture was stirred at 80 ºC for overnight. The reaction mixture was cooled to room temperature and CH_2Cl_2 (10 ml), 2M aq Na_2CO_3 (8 ml), and NH_4OH (1.0 ml) were added. The organic phase was separated and the aqueous phase was extracted with CH_2Cl_2 (2 * 10 ml). The organic phase was combined, washed with water and dried over anhydrous Na_2SO_4. The solvent was evaporated and the product was purified by silica gel column chromatography eluting with EtOAc:MeOH (95 : 5) to give 50 mg (23.47 %) as colorless syrup. ^1H NMR

(400 MHz, $CDCl_3$): δ 7.40 (d, J = 8 Hz, 8H, Ar-H), 7.17 (d, *J* = 8 Hz, 8H, Ar-H), 6.90 (s, 8H, Calix-Ar-H), 4.65 (d, J = 12 Hz, 4H, Ar-CH2-Ar), 4.24 (t, *J* = 4 Hz, 8H, -CH2), 3.91 (t, *J* = 4 Hz, 8H, -CH2), 3.66-3.50 (m, 32H, -CH2), 3.34 (s, 12H, -OCH3), 3.29 (d, *J* = 12 Hz, 4H, Ar-CH2-Ar). ^{13}C NMR (400 MHz, $CDCl_3$): δ 157.41, 145.15, 135.82, 133.40, 132.37, 127.19, 126.98, 118.80, 110.39, 73.67, 72.13, 70.86, 70.80, 70.78, 70.76, 70.71, 70.66, 70.60, 59.22, 31.49. ESI-MS, Calculated (M+H) m/z = 1413.66, found (M+Na) m/z = 1435.9

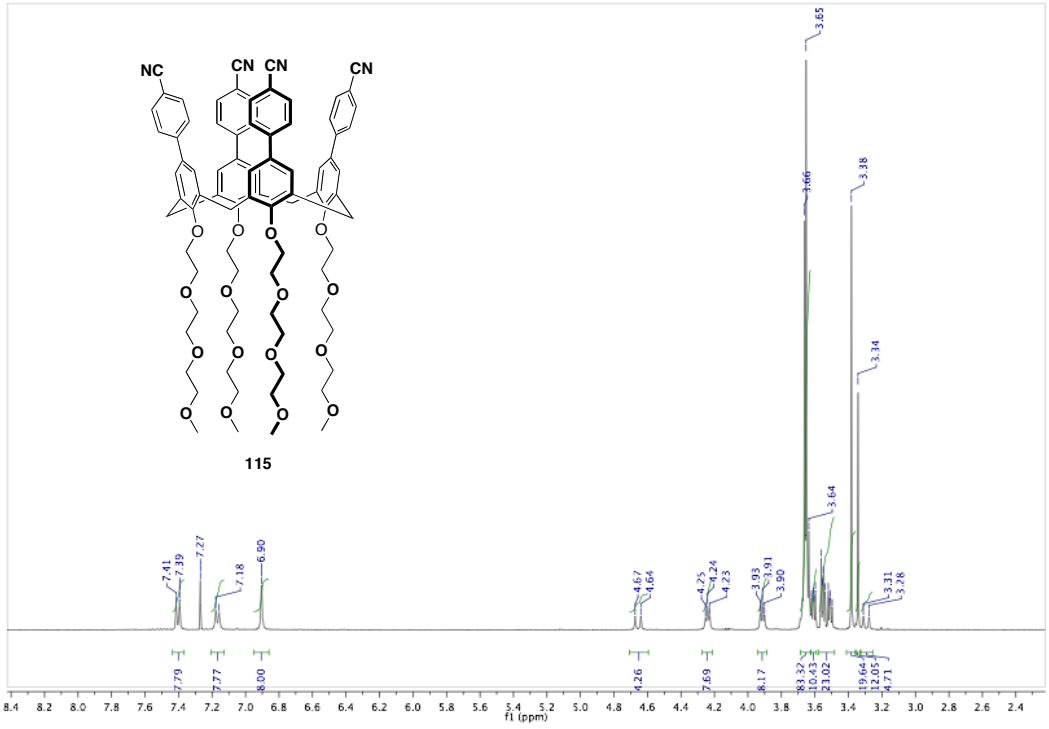

Figure 5.19 ^1H NMR spectrum of compound **115**

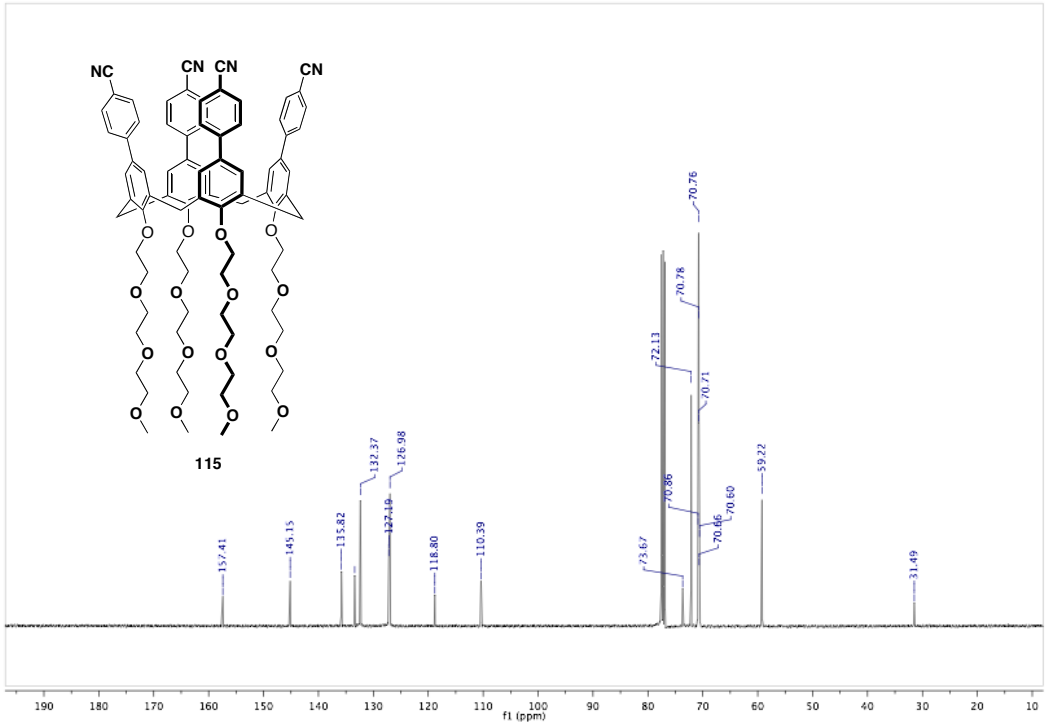

Figure 5.20 ^{13}C NMR spectrum of compound **115**

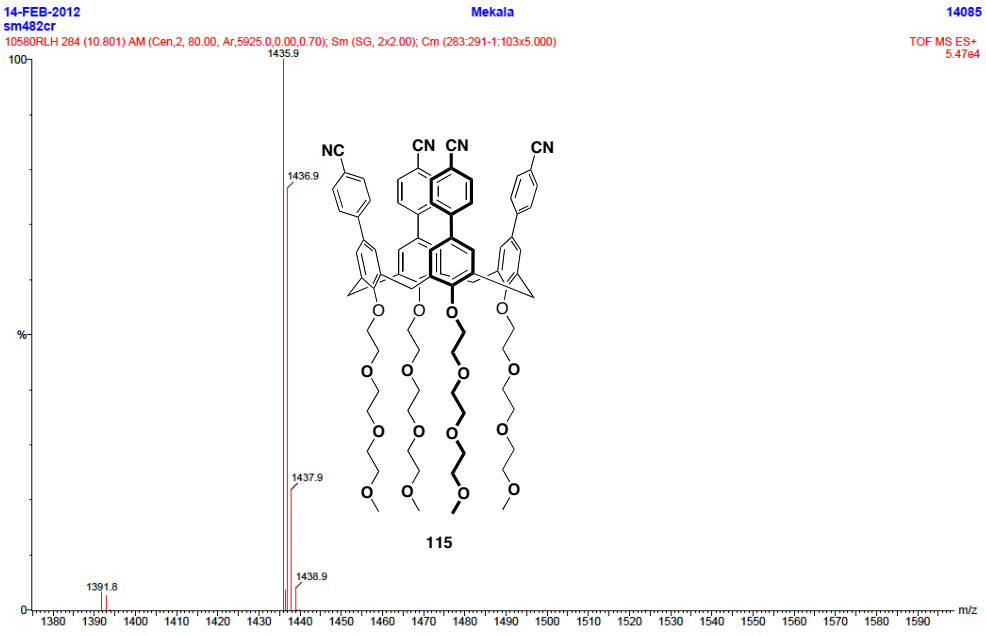

Figure 5.21 ESI-MS spectrum of compound **115**

Tetra(*p*-carboxyphenyl)-25,26,27,28-tetrakis[2-(2-(2methoxyethoxy) ethoxy)ethoxy]-calix[4]arene (116):

Method A: Tetra(*p*-cyanophenyl)-25,26,27,28-tetrakis[2-(2-(2methoxyethoxy) ethoxy)ethoxy]calix[4]arene **10** (20 mg, 0.0141 mmol) was suspended in EtOH (3 mL) in a 25-mL round bottom flask. An aqueous solution of KOH (0.793 g, 14.14 mmol, in 1 ml dH_2O) was added to the stirring suspension, and the flask was fitted with a water-cooled condenser. The mixture was heated to reflux for 4 days, when it was judged complete by TLC (EtOAc : MeOH, 95:5). The cooled reaction mixture was poured into 1N HCl and further acidified with concentrated HCl (to pH1). The Brown suspended solid was removed by filtration on a Buchner funnel and washed with a large amount of water. The solid was dried on the filter paper, and then in vacuo overnight, yielding a dry brown solid, which is insoluble in ($CHCl_3$, CH_2Cl_2, MeOH, H_2O). Therefore half of the solid (~5 mg) dissolved in DMSO-D_6 and took ^1H NMR of 300 MHz instrument. Broad singlet at δ12.4 ppm indicates the presence of carboxylic acid functionality, but the spectrum is very complex in aliphatic region (ether protons of calixarene).

Method B: To a 100 mL round bottomed flask containing **119** (0.150 g, 0.105 mmol) in 15 mL of chloroform and 15 mL of acetone were added mixture of sulfamic acid (0.166 g, 1.71 mmol, dissolved in 1 mL of water) and sodium chlorite (0.154 g, 1.71 mmol, dissolved in 1 mL of water). The reaction mixture was stirred at room temperature for 3 h and then evaporated to dryness. The resulting solid was dried 2 days in the oven ~ 80 ºC, to give white solid with super quantitative yield, which is because of water was not completely removed form the product.

^{1}H NMR, Acetone-d_6, 400 MHz:

δ 7.74 (d, J = 8.4 Hz, 8H), 7.31 (d, J = 8.4 Hz, 8H), 7.17 (S, 8H), 4.77 (d, J = 13.6 Hz, 4H), 4.31 (t, J = 5.2 Hz, 8H), 4.04 (t, J = 5.2 Hz, 8H), 3.72 (m, 8H), 3.65 (m, 8H), 3.59 (m, 8H), 3.46 (m, 12H), 3.27 (m, 12 H).

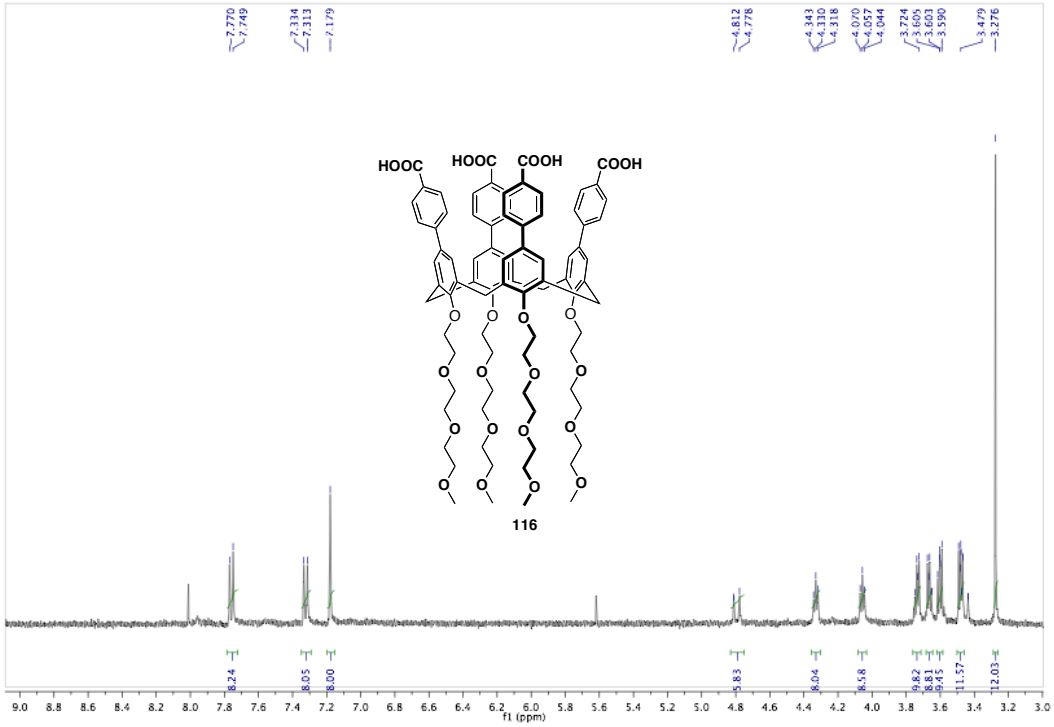

Figure 5.22 ^{1}H NMR spectrum of compound **116**

ESI-MS of **116** in acetone: *m/z* 1511.627 [M+Na]

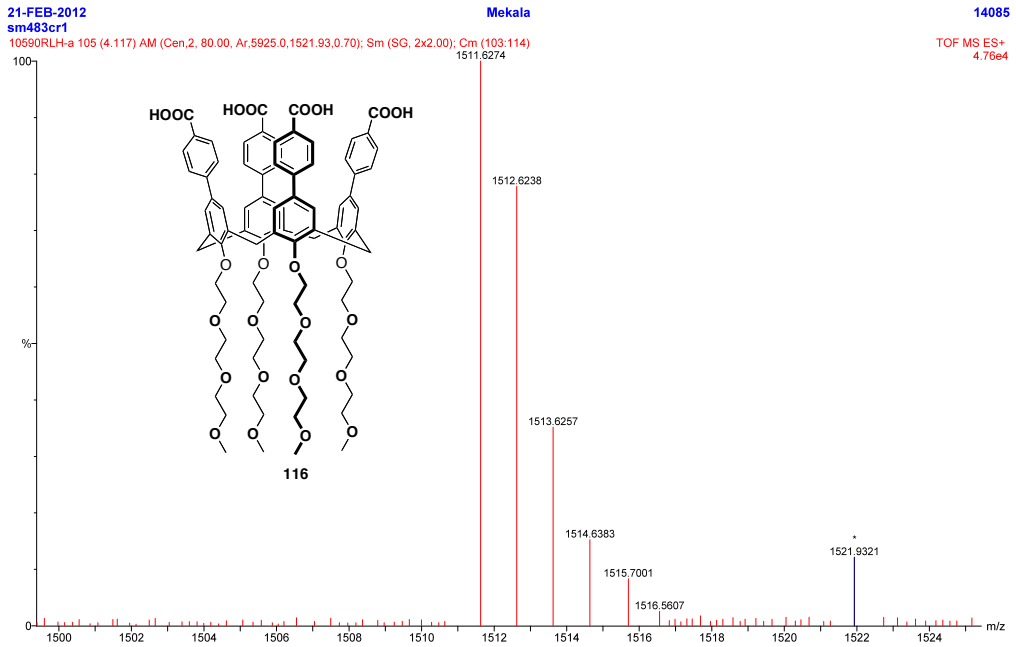

Figure 5.23 ESI-MS spectrum of compound **116**

Tetra(*p*-benzylamino)-25,26,27,28-tetrakis[2-(2-(2methoxyethoxy) ethoxy)ethoxy]-calix[4]arene (117) : *Method A*: To a stirring solution of 10 (0.020 g, 0.01414 mmol) in 5 ml of dry THF at 0 ºC, ~0.5 ml (0.3959 mmol) of a BH_3 solution (1M in dry THF) was added. The reaction mixture was refluxed under nitrogen for 24 h. Then 1 ml of MeOH and 3 ml of 1N HCl was added and the mixture was heated at 50 ºC for additional 0.5 h. THF was removed under reduced pressure and added 10 ml of 1N NaOH solution to get basic form of compound **117**.

NOTE: because of the bad BH_3 solution, this reaction was performed 3 times (a) with BH_3, b) with $LiAlH_4$ c) with new BH_3 solution). But, at the end, I could not recover the final product **117**.

Method B: To a stirring solution of 115 (0.140 g, 0.099 mmol) in dry THF (10 mL) at 0 ºC, was added 2.8 mL of BH_3.THF (1M in dry THF) dropwise and stirred at 0 ºC to room temperature, then reflux for 24 h under nitrogen. 3 mL of methanol and 5 mL of 1N HCl were added and stirred at 50 ºC for 0.5 h and removed THF on rotavap. Then added 5 mL of 1N HCl and extracted with CH_2Cl_2 (15 mL x 3) and dried over anhydrous Na_2SO_4. White solid formed after evaporation of organic solvent with super quantitative yield.

^{1}H NMR Methanol-d_4, 400 MHz:

δ 7.27 (s, 16H), 7.0 (s, 8H), 4.701 (d, J = 13.2 Hz, 6H), 4.258 (t, J = 5.2 Hz, 8H), 4.0 (m, 2H), 3.70 (m, 14H), 3.648 (m, 13H), 3.60 (m, 15H), 3.48 (m, 14H), 3.33 (d, J = 13.2 Hz, 6H).

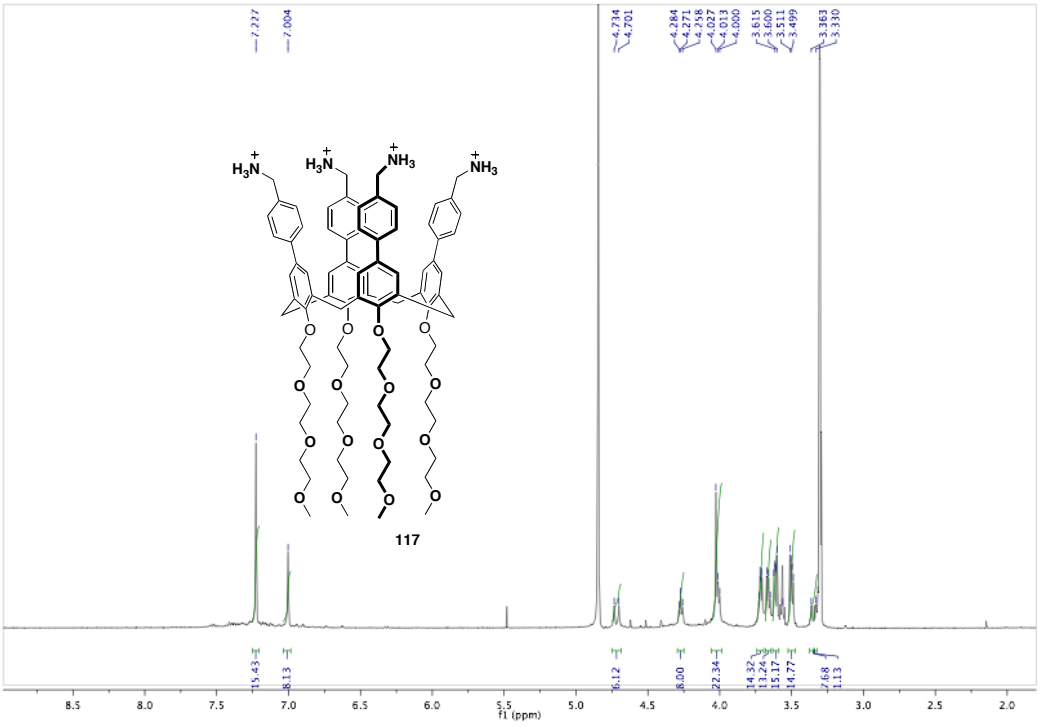

Figure 5.24 ^{1}H NMR spectrum of compound **117**

ESI-MS: MeOD: *m/z* 1451.8 [M+H]

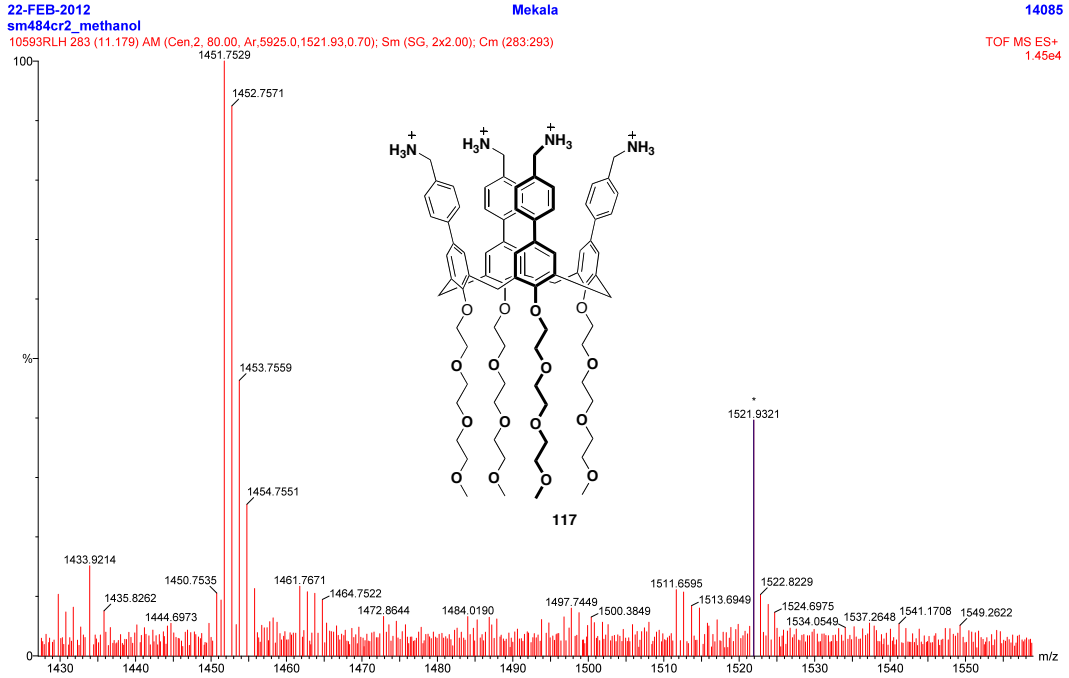

Figure 5.25 ESI-MS spectrum of compound **117**

Tetra(*p*-Formylphenyl)-25,26,27,28-tetrakis[2-(2-(2methoxyethoxy) ethoxy)ethoxy] -calix[4]arene (119):

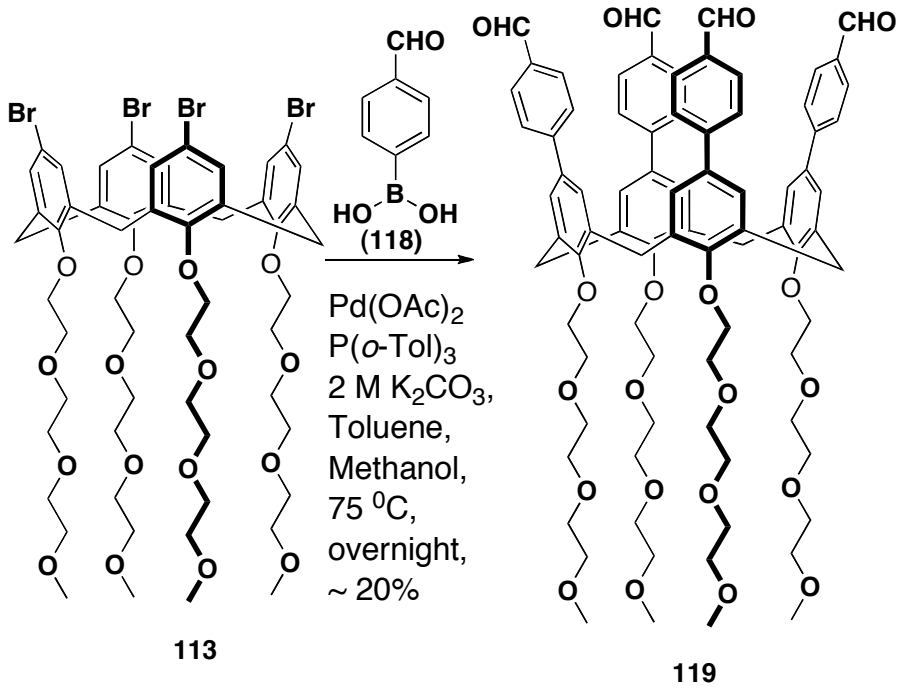

To a 100 mL of round bottomed flask containing **113** (0.6 g, 0.454 mmol) and 20 mol% of $Pd(OAc)_2$ (0.021 g, 0.091 mmol) and 40 mol% of P(*o*-tol)$_3$(0.053 g, 0.182 mmol), (ratio of $Pd(OAc)_2$: P(*o*-tol)$_3$ = 1:2) in 15 mL of dry toluene was added 5 mL of 2M Na_2CO_3 under nitrogen. Then added 6.0 equiv of commercially available 4-formylboronic acid **118** (0.409 g, 2.73 mmol) in 6 mL of MeOH and the resulting reaction mixture was refluxed at ~ 70-75 ºC for 3 h, then added another batch of 20 mol% of $Pd(OAc)_2$ (0.021 g, 0.091 mmol) and 40 mol% of P(*o*-tol)$_3$ (0.053 g, 0.182 mmol), and the reaction mixture was refluxed overnight under nitrogen atmosphere. Then cooled to room temperature and quenched by the addition of 30 mL of water and acidified to pH ~ 3-4 by the addition of Conc. HCl. Then extraction by EtAc (25 mL x 3), and dried over anhydrous Na_2SO_4. Evaporated the solvent and purified the crude by silica gel flash column chromatography using gradient elusion method with EtAc:MeOH (EtAC, EtAc:MeOH 99:1, 98:2, 97:3 and 95:5) to give a colorless oily product of 280 mg with 43.7% yield.

^{1}H NMR in CD_2Cl_2, 400 MHz:

δ 9.83 (s, 4H), 7.55 (d, J = 8.0 Hz, 8H), 7.27 (d, J = 8.0 Hz, 8H), 7.03(s, 8H), 4.66 (d, J = 12 Hz, 4H), 4.25 (t, J = 4.0 Hz, 8H), 3.93 (t, J = 4.0 Hz, 8H), 3.66 (t, J = 4.0 Hz, 8H), 3.59 (t, J = 4.0 Hz, 8H), 3.55 (t, J = 4.0 Hz, 8H), 3.46 (t, J = 4.0 Hz, 8H), 3.34 (d, J = 12 Hz, 4H), 3.29 (s, 12H).

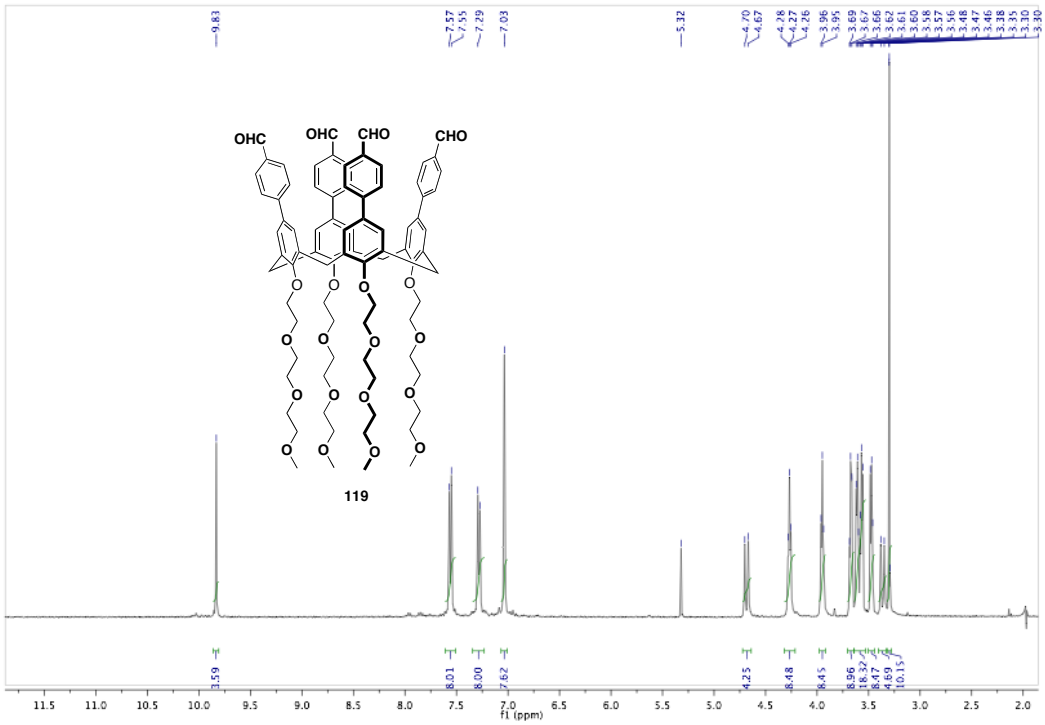

Figure 5.26 ^{1}H NMR spectrum of compound **119**

^{13}C NMR in CD_2Cl_2, 400 MHz: δ 192.11, 157.89, 147.24, 136.18, 135.05, 130.27, 127.79, 127.29, 79.42, 72.48, 71.22, 71.11, 71.04, 71.01, 59.14, 31.80.

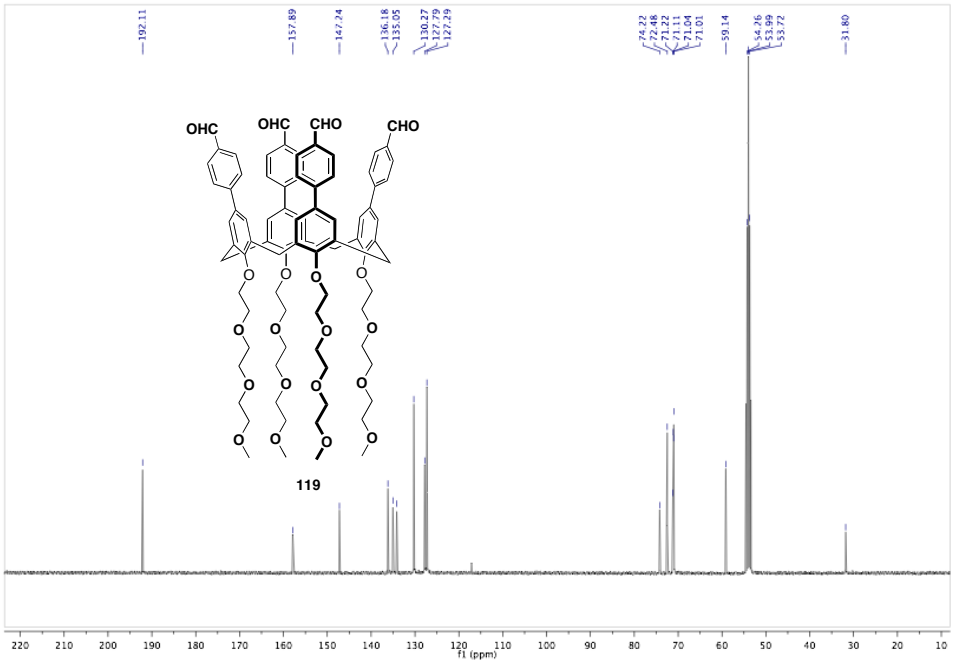

Figure 5.27 ^{13}C NMR spectrum of compound **119**

ESI-MS: *m/z* 1447.9 [M+Na]

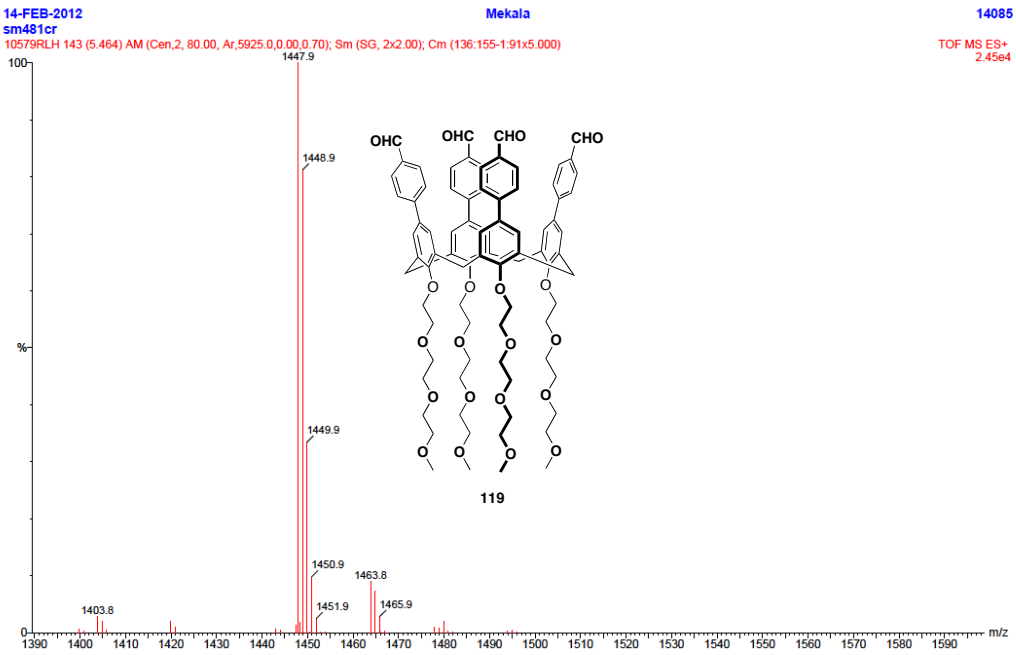

Figure 5.28 ESI-MS spectrum of compound **119**

^{1}H NMR Spectra of Guest Molecule: Guest 93 in D_2O: 400 MHz: δ 7.33 (d, *J* = 8 Hz, 2 H), 6.62 (d, *J* = 8 Hz, 2 H), 6.56 - 6.43 (m, 6 H), 4.56 (s, 2 H, -CH_2)

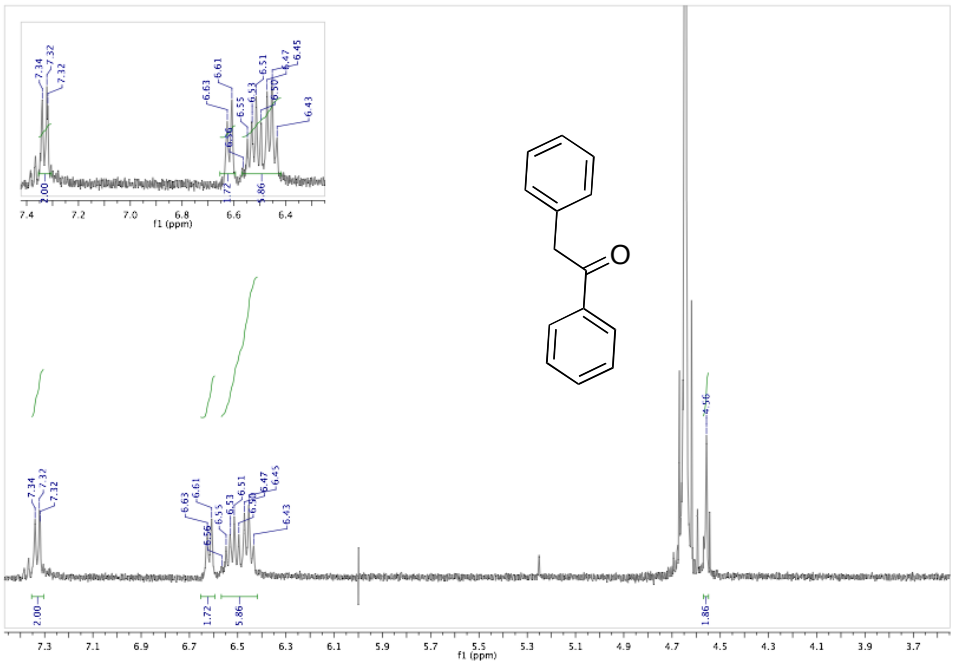

Figure 5.29 ^{1}H NMR spectrum of compound **93 in D_2O**

5.8 References

118. Stites, W. E. Protein–Protein Interactions: Interface Structure, Binding Thermodynamics, and Mutational Analysis, *Chem. Rev.*, **1997**, *97*, 1233–1250.

119. Lazaridis, T. Solvent Size vs Cohesive Energy as the Origin of Hydrophobicity, *Acc. Chem. Res.*, **2001**, *34*, 931–937.

120. Rekharsky, M.; Yoshihisa Inoue, Y.; Tobey. S.; Metzger, A.; Eric Anslyn, E. Ion-Pairing Molecular Recognition in Water: Aggregation at Low Concentrations That Is Entropy-driven, *J. Am. Chem. Soc.* **2002**, *124*, 14959-14967.

121. Rekharsky, M. V.; Inoue, Y. 1:1 and 1:2 Complexation Thermodynamics of γ-Cyclodextrin with *N*-Carbobenzyloxy Aromatic Amino Acids and ω-Phenylalkanoic Acids. *J. Am. Chem. Soc.* **2000**, *122*, 10949-10955.

122. Schmidtchen, F. P. Surprises in the Energetics of Host-Guest Anion Binding to Calix[4]pyrrole, *Org. Lett.* **2002**, *4*, 431.

123. Shinkai, S. Calixarenes as new functionalized host molecules, *Pure Appl. Chem*. **1986**, *58*, 1523-1528. Shinkai, S.; Araki, K.; Tsubaki, T.; Arimura, R.; Manabe, O. New syntheses of calixarene-***p***-sulphonates and ***p***-nitrocalixarenes, *J. Chem. Soc., Perkin Trans*. 1 **1987**, 2297-2299.

124. Gutsche, C. D.; Alam, I. Calixarenes. 23. the complexation and catalytic properties of water soluble calixarenes, *Tetrahedron,* **1988**, *44*, 4689-4694.

125. Arimura, T.; Nagasaki, T.; Shinkai, S.; Matsuda, T. Host-guest properties of new water-soluble calixarenes derived from p-(chloromethyl) calixarenes, *J. Org. Chem*. **1989**, *54*, 3766-3768.

126. Nagasaki, T.; Sisido, K.; Arimura, T.; Shinkai, S. Novel conformational isomerism of water-soluble calix[4]arenes, *Tetrahedron,* **1992**, *48*, 797-804.

127. Shimizu, S.; Kito, K.; Sasaki, Y.; Hirai, C. Water-soluble calixarenes as new inverse phase-transfer catalysts.Nucleophilic substitution of alkyl and arylalkyl halides in aqueousmedia, *Chem. Commun*. **1997,** 1629-1630.

128. Ryu, E.; Zhao Y. Efficient synthesis of water soluble calix[4]arens using click chemistry: *Org. Lett*, **2005**, *7*, 1035-1037.

129. Tyson, J. C.; Collard, D. M.; Huges, K. D. Chromophoric Water-Soluble Tetrakis(4-carboxyphenylazo)-calix[4]arene: Binding of aryl ammonium ions and Benzene, *Journal of Inclusion Phenomenon and molecular recognition in chemistry*, **1997**, *29*, 109-118.

130. Ak, M.; Taban, D.; Deligoz. H. Transition metal cations extraction by ester and ketone derivatives of chromogenic azocalix[4]arene, *Journal of Hazardous Materials*, **2008**, *154*, 51-54.

131. Zhou, Y.; Xu, H.; Yu, H.; Chun, L.; Lu, Q.; Wang, L. Spectrofluorometric study on the inclusion behaviour of *p*-(*p*-carboxylbenzeneazo) calix[4]arene with norfloxacin, *Spectrochimica Acta Part A*, **2008**, *70*, 411-415.

132. Nimse, S. B.; Kim, J.; Ta, V-T.; Kim, H-S.; Song, K-S.; Jung, C-Y.; Nguyen, V-T.; Kim, T. New water-soluble iminecalix[4]arene with a deep hydrophobic cavity, *Tetrahedron Letters*, **2009**, *50*, 7346-7350.

133. Nimse, S. B.; Nguyen, V-T.; Kim, J.; Kim, H-S.; Song, K-S.; Eoum, W-Y.; Jung, C-Y.; Ta, V-H.; Seelam, S. R.; Kim, T. Water soluble aminocalix[4]arene receptors with hydrophobic and hydrophilic mouths, *Tetrahedron Letters*, **2010**, *51*, 2840-2845.

134. Z, Laughrey.; Gibb, B. C. Water-soluble, self-assembling container molecules: an update, *Chem. Soc. Rev*, **2011**, *40*, 363-386, Schneider, H-J.; Binding mechanisms in supramoelcualr complexes, *Angew. Chem. Int. Ed.* **2009**, *135*, 3924-3977, Biros, S. M.; Rebek Jr, J. Structure and binding properties of water-soluble cavitands and capsules, *Chem. Soc. Rev*, **2007**, *36*, 93-104.